MICRO AND NANO PLASTICS IN AGRICULTURE: INTERACTIONS WITH PESTICIDE RESIDUES AND BIOACCUMULATION IN PLANTS

Harshit Sahai

Doctoral Dissertation
Jožef Stefan International Postgraduate School
Ljubljana, Slovenia

Supervisor:
Prof. Dr. María Dolores Hernando Guil, Experimental Station of Arid Zones, The Spanish National Research Council (CSIC-EEZA), Spain

Co-Supervisors:
Prof. Dr. Amadeo R. Fernández-Alba, University of Almería, Spain
Prof. Dr. Ester Heath, IPS and Jožef Stefan Institute, Ljubljana, Slovenia

Evaluation Board:
Prof. Dr. Nives Ogrinc, Chair, IPS and Jožef Stefan Institute, Ljubljana, Slovenia
Prof. Dr. Dimitra Lambropoulou, Member, Environmental Pollution Control Laboratory, Aristotle University of Thessaloniki, Greece
Asst. Prof. Janja Vidmar, Member, IPS and Jožef Stefan Institute, Ljubljana, Slovenia

MEDNARODNA PODIPLOMSKA ŠOLA JOŽEFA STEFANA
JOŽEF STEFAN INTERNATIONAL POSTGRADUATE SCHOOL

Harshit Sahai

MICRO AND NANO PLASTICS IN AGRICULTURE: INTERACTIONS WITH PESTICIDE RESIDUES AND BIOACCUMULATION IN PLANTS

Doctoral Dissertation

MIKRO IN NANO PLASTIKA V KMETIJSTVU: INTERAKCIJE Z OSTANKI PESTICIDOV IN BIOAKUMULACIJA V RASTLINAH

Doktorska disertacija

Supervisor:
Prof. Dr. María Dolores Hernando Guil, Experimental Station of Arid Zones, The Spanish National Research Council (CSIC-EEZA), Spain

Co-Supervisors:
Prof. Dr. Amadeo R. Fernández-Alba, University of Almería, Spain
Prof. Dr. Ester Heath, IPS and Jožef Stefan Institute, Ljubljana, Slovenia

Ljubljana, Slovenia, September 2024

To my readers

"The great aim of education is not knowledge but action."
– Herbert Spencer

Acknowledgments

This PhD thesis would not have been possible without the assistance, guidance, and motivation provided by numerous individuals and institutions. I am sincerely appreciative of all those who have played a role in this significant journey.

Foremost and above all, I wish to convey my deep thanks to my supervisors, Prof. Dr. María Dolores Hernando Guil, Prof. Dr. Amadeo R. Fernández-Alba, and Prof. Dr. Ester Heath for their consistent backing, priceless guidance, and perceptive feedback during the course of my PhD pursuit. Their knowledge and unending patience has played a fundamental role in molding my research and bringing this thesis to its successful completion. Equally important is the contribution of the members of my thesis committee, Prof. Dr. Nives Ogrinc, Prof. Dr. Dimitra Lambropoulou, and Asst. Prof. Janja Vidmar, whose constructive critiques and beneficial recommendations have significantly enhanced my work, motivated me to refine my research even further.

My deep appreciation extends to my colleagues and fellow researchers at the Spanish National Research Council - Experimental Station of Arid Zones (CSIC-EEZA), Josef Stefan International Postgraduate School, and the FoodTraNet project team. The collaborative atmosphere, engaging discussions, and camaraderie I experienced during my time there have left an indelible mark on me. A special acknowledgment goes to Prof. Dr. María Jesús Martínez Bueno, Prof. Dr. Ana M. Aguilera del Real, Prof. Dr. David Heath, Maria Antonietta Carrera and the research group at the European Union Reference Lab for Pesticide Residues in Fruits and Vegetables (EURL-FV) at the University of Almeria for their guidance, backing, and camaraderie, which have been invaluable.

I am greatly beholden to the European Union's Horizon 2020 research and innovation program through the Marie Sklodowska-Curie grant agreement no. 956265 for providing the financial backing for my research.

My gratitude also extends to my family for their unwavering love and support. From my parents, Dr. Anshu Srivastava and Dr. Sulabh Sahai, to my grandmother Sudha Sahai, and my brother, Garvit Sahai, their belief in me and encouragement to pursue my aspirations have been a constant source of strength. Moreover, none of this would have been possible without the love and support of my wife, Isabel Lopez Echanove, who has been a steadfast companion throughout this journey.

Lastly, I am thankful to my friends, both near and far, whose continuous motivation and joy have been a cornerstone in keeping me focused and optimistic. Their encouragement and empathy have played a crucial role in my journey.

To all those who have supported me along this journey, this thesis is dedicated to you. Your contributions have been indispensable in the realization of this work, and I will forever be grateful for your presence in my life. Thank you all.

Harshit Sahai

Abstract

A large body of data now exists demonstrating the influence of micro and nano plastics (MNPs) on living systems, and their detection has been documented across various ecosystems, including organisms that form part of the human diet. Nevertheless, up till now, a substantial portion of that research has been confined to aquatic environments. This limitation underscores the necessity for more comprehensive studies to elucidate the full extent of the implications of MNPs across diverse ecological settings. In this context, the widespread presence of MNPs in the terrestrial domain has been observed, specifically in the agricultural ecosystem, raising concerns regarding their impact on crops.

This study investigates the interactions between microplastics generated from commercial nonbiodegradable polyethylene (PE) and biodegradable polybutylene adipate terephthalate (PBAT) agricultural mulch films and common agricultural pesticide residues. It also investigates the sorption/desorption process on microplastics and the factors influencing this complex phenomenon and the uptake, bioaccumulation, and translocation of 100 nm polystyrene (PS) nanoplastics within the edible herb *Lepidium sativum* to address concerns regarding their entry into the human food chain and impact on crop health. Moreover, a novel approach for quantifying bioaccumulated nanoplastics is introduced, utilizing confocal laser scanning microscopy (CLSM) in conjunction with image analysis.

The study findings show that sorption levels were up to 90% higher when considering microplastics originating from PE mulch films than pure PE microspheres. In PE microplastics sourced from mulch films, the percentages of sorption for pesticides in solutions containing $CaCl_2$ were as follows: for pyridate, 76% and 52%; for fenazaquin, 48% and 32%; for pyridaben, 45% and 56%; for bifenthrin, 74% and 25%; for etofenprox, 82% and 54% and pyridalyl, 97% and 29% at concentrations of 5µg/L and 200µg/L, respectively. The process of sorption was notably impacted by the octanol-water partition coefficient (log K_{ow}) as well as the ionic strength of the medium. Sorption on PE microplastics followed a pseudo-first-order kinetic model, with R^2 values between 0.90 and 0.98, while the best-fit isotherm model was the Dubinin-Radushkevich model, with R^2 values between 0.92 and 0.99. The findings suggest physisorption on the surface through the filling of micropores, highlighting the significant role of hydrophobic and electrostatic forces.

The study found that PE mulch films exhibited lower levels of pesticide residue retention and displayed a higher desorption/release rate [with a median desorption of 71.86 µg/L, approximately 50%] compared to PBAT mulch films. Conversely, PBAT mulch films retained higher quantities of pesticide residues on their surface and exhibited a significantly lower desorption rate [median desorption = 24.27 µg/L, around 17%] after application. The impact of elevated ambient temperatures did not show any notable impact on the final desorption levels from both PE [median = 65.27 µg/L at 20°C and 74.23 µg/L at 40°C] and PBAT [median = 24.26 µg/L at 20°C and 24.78 µg/L at 40°C] mulch films. Nonetheless, it did promote a faster desorption rate in PE films. The desorption process in PBAT and PE plastic categories exhibited a strong correlation with the logarithm of the

octanol-water partition coefficient (log K_{ow}) value [Spearman's correlation: 0.857 and 0.837, respectively, $p < 0.05$]. Conversely, only a moderate correlation with the acid dissociation constant (pKa) was noted for PBAT [Spearman's correlation: 0.478, $p < 0.05$], with no significant correlation observed for PE. The adsorption of pesticides onto biodegradable PBAT microplastics was most effectively described by Elovich [R^2: 0.937–0.959] and pseudo-second-order kinetics [R^2: 0.942–0.987], indicating the presence of chemisorption. Moreover, Weber Morris plots indicated a multi-step process, while Boyd plots suggest that film diffusion or chemical bond formation represents the rate-limiting step governing this phenomenon.

This thesis also confirmed the uptake, translocation, and bioaccumulation of PS nanoplastics (100 nm) within various parts of the plant *Lepidium sativum*. The exposure concentrations ranged from 10 µg/L, considered environmentally realistic, to 100 mg/L. The accumulation pattern observed in the plant tissues was characterized by the aggregation of nanoplastics within the intercellular spaces, leading to a heterogeneous distribution throughout the plant. Nanoplastics were detected in multiple plant regions, including the root tips, root surface, stele, lateral roots, root hairs, stem vascular bundles, leaf veins, mesophyll, and even the leaf epidermis, including stomatal sites. Analysis of the quantification data revealed that most of the nanoplastic particles were retained within the plant roots, with the accumulation in stems and leaves representing only 13% to 18% of the median value observed in roots. The study findings also indicated a significant reduction in various plant parameters under higher exposure concentrations (≥ 50 mg/L), including a decrease in the germination rate (38%), fresh weight (55%), root weight (80%), root length (60%), shoot weight (51% and 78%), and in the number of lateral roots (28%). Conversely, exposure to lower environmental concentrations did not significantly impact plant health.

Povzetek

Številne znanstvene objave so pokazale vpliv mikro- in nanoplastike (MNP) na žive sisteme in njihovo prisotnost v različnih ekosistemih, vključno z organizmi, ki so sestavni del prehranjevalne verige. Kljub temu je bil do nedavnega precejšen del teh znanstvenih raziskav omejen na vodna okolja, kar nakazuje potrebo po obsežnejših študijah, ki bodo prispevale k celostnemu razumevanju posledic MNP v različnih okoljih. Nedavno so raziskave pokazale razširjenost MNP v kopenskem okolju, zlasti v kmetijskih ekosistemih, kar povzroča zaskrbljenost glede njihovih interakcij in potencialnih vplivov na pridelke.

Predloženo doktorsko delo preučuje interakcije med mikroplastiko, ki izvira iz komercialnih zastirnih folij za uporabo v kmetijski pridelavi, vključno s konvencionalnimi polietilenskimi (PE) in biološko razgradljivimi polibutilen adipat tereftalatnimi (PBAT) folijami, ter ostanki pesticidov iz kmetijske uporabe. Študija raziskuje proces sorpcije/desorpcije ostankov pesticidov na mikroplastiko in se poglablja v dejavnike, ki vplivajo na ta kompleksen pojav. Poleg tega študija preučuje tudi absorpcijo, bioakumulacijo in translokacijo 100 nm polistirenske nanoplastike v užitnem zelišču *Lepidium sativum*, kar vzbuja zaskrbljenost glede potencialnega vstopa nanoplastike v človeško prehranjevalno verigo ter vpliva na zdravje pridelkov. V okviru doktorskega dela smo na tem področju uvedli nov pristop za kvantifikacijo bioakumulirane nanoplastike na osnovi konfokalne laserske vrstične mikroskopije v kombinaciji z analizo slik.

Ugotovitve raziskave kažejo, da je bila sorpcija do 90 % višja v primeru mikroplastike, ki izvira iz PE zastirnih folij, v primerjavi s čistimi polietilenskimi mikrokroglicami. V primeru PE mikroplastike iz zastirne folije so bili odstotki sorpcije pesticidov pri koncentracijah 5 µg/L in 200 µg/L v raztopini $CaCl_2$ sledeči: piridat: 76 % in 52 %, fenazakin: 49 % in 32 %, piridaben: 45 % in 57 %, bifentrin: 74 % in 26 %, etofenproks: 82 % in 54 % in piridalil: 97 % ter 30 %. Na proces sorpcije je vidno vplival porazdelitveni koeficient oktanol-voda (log Kow) kot tudi ionska moč medija. PE mikroplastika je sledila kinetičnemu modelu psevdo prvega reda z vrednostmi R^2 med 0,90 in 0,98, medtem ko je bil model izoterme, ki se najbolje prilega, model Dubinin-Radushkevich z vrednostmi R^2 med 0,92 in 0,99. Ugotovitve kažejo na fiziosorpcijo na površini s polnjenjem mikropor, kar poudarja pomen hidrofobnih in elektrostatičnih sil v procesu.

PE zastirne folije so pokazale nižjo stopnjo zadrževanja ostankov pesticidov in višjo stopnjo desorpcije/sproščanja pesticidov [z mediano desorpcije 71,86 µg/L, približno 50 %] v primerjavi s PBAT folijami. Nasprotno pa so PBAT zastirne folije zadržale večje količine ostankov pesticidov na površini in pokazale znatno nižjo stopnjo desorpcije [mediana desorpcije = 24,27 µg/L, približno 17 %]. Vpliv povišane temperature ni pokazal opaznega vpliva na končne ravni desorpcije pri PE [mediana = 65,27 µg/L pri 20 °C in 74,23 µg/L pri 40 °C] in PBAT [mediana = 24,26 µg/L pri 20 °C in 24,78 µg/L pri 40 °C] zastirnih folijah. Kljub temu smo opazili hitrejšo stopnjo desorpcije pesticidov iz PE filmov. Postopek desorpcije je v obeh primerih plastike, PBAT in PE, pokazal močno korelacijo z logaritemskimi vrednostmi porazdelitvenega koeficienta oktanol-voda (log Kow) [Spearmanova korelacija: 0,857 oziroma 0,837, $p < 0,05$]. Nasprotno pa je bila za PBAT opažena zmerna korelacija z disociacijsko konstanto kisline (pKa) [Spearmanova korelacija:

0,478, p <0,05], pri PE pa ni bilo pomembne korelacije. Adsorpcijo pesticidov na biorazgradljivo mikroplastiko PBAT najbolj učinkovito opiše model Elovich [R2: 0,937–0,959] in kinetika psevdodrugega reda [R2: 0,942–0,987], kar kaže na prisotnost kemisorpcije. Poleg tega model Weber Morris nakazuje večstopenjski proces, medtem ko model Boyd kaže na to, da difuzija filma ali tvorba kemične vezi predstavlja stopnjo, ki omejuje hitrost tega pojava.

V predloženem doktorskem delu smo tudi potrdili privzem, translokacijo in bioakumulacijo delcev (100 nm) polistirenske nanoplastike v različnih delih rastline *Lepidium sativum*, pri čemer so se koncentracije izpostavljenosti gibale od 10 µg/L, kar velja za okoljsko relevantne koncentracije, do 100 mg/L. Pri kopičenju le-te v rastlinskih tkivih smo opazili vzorec združevanja nanoplastike v medceličnih prostorih, ki vodi do heterogene porazdelitve po rastlini. Nanoplastiko smo dokazali v različnih delih rastlin, v notranjosti in površini korenin, prevodnem celičju korenin in stebel, stranskih koreninah in koreninskih laskih, listnih žilah, povrhnjici listov, vključno z listnimi režami. Raziskava je pokazala, da se večina delcev nanoplastike zadrži v rastlinskih koreninah, pri čemer kopičenje v steblih in listih predstavlja le del (13 % do 18 %) mediane, določene v koreninah. Ugotovitve so tudi pokazale znatno zmanjšanje različnih parametrov rastline pri višjih koncentracijah izpostavljenosti (≥ 50 mg/L), vključno z zmanjšanjem stopnje kalivosti (≈38 %), celokupne teže (≈55 %) in teže korenin (≈80 %), dolžine korenin (≈60 %), teže poganjkov (≈51 % in 78 %) ter števila stranskih korenin (≈28 %), v primeru izpostavljenosti nižjim okoljskim koncentracijam pa nismo opazili vplivov na zdravje rastlin.

Contents

List of Figures

List of Tables

Abbreviations

PVC	...	Polyvinyl chloride
CAGR	...	Compound Annual Growth Rate
GDP	...	Gross Domestic Product
PE	...	Polyethylene
PP	...	Polypropylene
PET	...	Polyethylene Terephthalate
PS	...	Polystyrene
PA	...	Polyamide
PUR	...	Polyurethane
NAFTA	...	North America Free Trade Agreement
OECD	...	Organization for Economic Cooperation and Development
Mt	...	Metric tons
MPs	...	Microplastics
MNPs	...	Micro and nano plastics
BALF	...	Bronchoalveolar lavage fluid
TSNA	...	Tobacco-Specific Nitrosamines
EVA	...	Ethylene-vinyl acetate
PC	...	Polycarbonate
PMMA	...	Poly-methyl-methacrylate
PLA	...	Polylactic acid
PHA	...	Polyhydroxyalkanoates
PBS	...	Polybutylene succinate
PBAT	...	Polybutylene adipate terephthalate
PCL	...	Polycaprolactone
EPS	...	Expanded polystyrene
TPU	...	Thermoplastic polyurethane
ABS	...	Acrylonitrile butadiene styrene
LDPE	...	Low density polyethylene
HDPE	...	High density polyethylene
EU	...	European Union
ha	...	Hectare
FAO	...	Food and Agriculture Organization

UN	...	United Nations
RAG	...	Red-Amber-Green
EPDM	...	Ethylene propylene diene monomer
BMF	...	Black mulch films
CA	...	Cellulose acetate
SBR	...	Styrene-butadiene rubber
SIS	...	Styrene isoprene styrene
WWTPs	...	Wastewater treatment plants
CPANs	...	Chlorophenylacetonitriles
NPAHs	...	Nitro polycyclic aromatic hydrocarbons
BaA	...	Benzo [a] anthracene
BaP	...	Benzo [a] pyrene
PSMP	...	Polystyrene Microplastics
PTFE	...	Polytetrafluoroethylene
PSO	...	Pseudo-second order
PFBA	...	Perfluorobutanoic acid
PFAS	...	Perfluoroalkyl substances
PFPeA	...	Perfluoropentanoic acid
PFHxA	...	Perfluorohexanoic acid
PFHpA	...	Perfluoroheptanoic acid
PFOA	...	Perfluorooctanoic acid
PFNA	...	Perfluorononanoic acid
PFDA	...	Perfluorodecanoic acid
PFUdA	...	Perfluoroundecanoic acid
PFDoA	...	Perfluorododecanoic acid
PFTrA	...	Perfluorotridecanoic acid
PFTeA	...	Perfluorotetradecanoic acid
PFHxDA	...	Perfluorohexadecanoic acid
PFODA	...	Perfluorooctadecanoic acid
PFBS	...	Perfluorobutanesulfonate
PFHxS	...	Perfluorohexasulfonate
E2	...	17β-estradiol
EE2	...	17α-ethynylestradiol
PFOS	...	Perfluorooctanesulfonate
PFDS	...	Perfluorodecanesulfonate
PFOSA	...	Perfluorooctanesulphonamide
PeCB	...	Pentachlorobenzene
HeCB	...	Hexachlorobenzene

TFL	...	Trifluralin
SDZ	...	Sulfadiazine
AMX	...	Amoxicillin
TC	...	Tetracycline
CIP	...	Ciprofloxacin
TMP	...	Trimethoprim
CAT	...	Catalase
SOD	...	Superoxide dismutase
POD	...	Peroxidase
AM	...	Arbuscular mycorrhizal
PES	...	Polyester
MDA	...	Malondialdehyde
PSNPs	...	Polystyrene nanoplastics
Bio-MP	...	Biodegradable microplastic
BM	...	Black mulch
PS-Eu	...	Polystyrene nanoplastics doped with europium chelate
SELs	...	Size exclusion limits
SMA	...	Styrene-co-maleic anhydride
PS-COOH	...	Carboxyl-modified polystyrene nanoplastics
PS-NH2	...	Amino-modified polystyrene nanoplastics
CLSM	...	Confocal laser scanning microscopy
nano-CT	...	X-Ray computed nano-tomography
DF-HIS	...	Dark-field hyperspectral imaging
TEM	...	Transmission electron microscopy
SEM	...	Scanning electron microscopy
GC-MS	...	Gas chromatography-mass spectrometry
FTIR	...	Fourier-transform infrared spectroscopy
µ-XRF	...	Micro X-ray fluorescence
QA/QC	...	Quality assurance/quality control
DLS	...	Dynamic light scattering
NTA	...	Nanoparticle tracking analysis
TRPS	...	Tunable resistive pulse sensing
CLS	...	Centrifugal liquid sedimentation
FFF	...	Field-flow fractionation
MALS	...	Multi-angle light scattering
Py-GC/MS	...	Pyrolysis-gas chromatography-mass spectrometry
MALDI–TOF MS	...	Matrix-assisted laser desorption/ionization–time-of-flight mass spectrometry
TGA-MS	...	Thermal-Gravimetric Analysis with Mass Spectrometry

TED-GC-MS	...	Thermal extraction desorption-gas chromatography/mass spectrometry
ICP-MS	...	Inductively coupled plasma mass spectrometry
CLSM	...	Confocal Laser Scanning Microscopy

Symbols

ng/m^3	...	Nanogram per cubic meter
CO_2	...	Carbon dioxide
H_2O	...	Water
CO	...	Carbon monoxide
NO_X	...	Nitrogen oxides
Pb	...	Lead
Cd	...	Cadmium
Cr	...	Chromium
SO_2	...	Sulfur dioxide
As	...	Arsenic
Au	...	Gold
N_2O	...	Nitrous oxide
Q_t	...	The concentration (µg/g) of the pesticide adsorbed onto the unit mass of microplastics at time t
Q_e	...	The concentration (µg/g) of the pesticide adsorbed onto the unit mass of MP at equilibrium
k_1 (h^{-1})	...	Pseudo-first-order reaction rate constant
t	...	Time
k_2 (g μg^{-1} h^{-1})	...	Pseudo-second-order rate constant
α (µg g^{-1} h^{-1})	...	Initial sorption rate
β (g μg^{-1})	...	Desorption constant
k_i (µg g^{-1} $h^{-1/2}$)	...	Intra-particle diffusion rate constant
C_i (µg g^{-1})	...	Intra-particle diffusion constant, which is dependent upon the thickness of the boundary layer
C_e (µg/L)	...	The concentration of the pesticide in the aqueous phase at equilibrium
B (L/µg)	...	The Langmuir constant
Q_{max} (µg/g)	...	Maximum sorption capacity
k_f	...	Freundlich rate coefficient
n	...	Freundlich isotherm exponent
ε (kJ/mol)	...	Sorption potential or Polanyi potential

β	...	Constant related to the free energy of sorption
R	...	Universal gas constant (8.314 $Jmol^{-1}K^{-1}$)
T	...	Absolute temperature (K)
k_t	...	Temkin rate coefficient
b	...	Temkin constant
k_{rp} (L/µg)	...	Redlich-Peterson rate constant
a	...	Redlich-Peterson parameter
n	...	Exponential factor
Fe	...	Iron
Mn	...	Manganese
Cu	...	Copper
Zn	...	Zinc
Ni	...	Nickel
Hg	...	Mercury
Ti	...	Titanium
Mg	...	Magnesium
Ca	...	Calcium

Chapter 1

Introduction

1.1 Plastic Waste Production Trends and Mismanagement

1.1.1 A brief history of plastic production

The history of plastic production is a narrative of exponential growth and widespread application, beginning modestly before becoming a cornerstone of modern industry and daily life. Plastic has been a part of our existence since the Olmecs of Mexico utilized plant sap to create materials like latex more than 3500 years ago. The modern forms of plastics were first developed in the late 1800s and early 1900s as an affordable alternative to expensive natural materials like ivory. Alexander Parkes created and displayed the first plastic alternative, Parkesine, in 1862. The subsequent significant development in the field of plastics was the nitrated cellulose compound known as "Celluloid", developed in 1867 by John Wesley Hyatt for the pool/billiards business. The first modern polymer developed was Polyvinyl chloride (PVC), inadvertently discovered by German chemist Eugen Baumann in 1872[1], while the first fully synthetic plastic, known as "Bakelite," was created in New York in 1907 by Leo Baekeland. Another milestone was in the early 1920s when Hermann Staudinger formulated the macromolecular theory of polymers, a feat that led to him winning the Nobel Prize in Chemistry. His theory formed the basis for numerous modern developments in materials science and biosciences, thereby leading to the rapid growth of the plastics industry. At this point, plastic stopped being a natural product with synthetic ingredients and became wholly synthetic.

The next significant innovation in plastics was in the 1920s with the addition of plasticizers, making the final product softer and more flexible than the pure polymer. During World War 2, the plastic industry flourished, and plastic was used to make everything from light aircraft components to parachutes, from helmets to gun parts. In the years following the war, the industry experienced a decline in demand, which compelled it to promote the use of plastic in everyday household items. Ultimately, it contributed to the emergence of "disposable culture" and "single-use culture". The post-war period's unparalleled economic expansion and the rise of contemporary consumerism resulted in a swift and steady increase in the world's plastic output and consumption [1]. The compound annual growth rate (CAGR) of the world's yearly plastic manufacturing for the two decades after 1950 was approximately 15% [1]. During the 1950–2017 period, this remained at 8.3% overall, more than 2.5 times the global gross domestic product (GDP) for the same period [2].

The number of polymers and additives in plastics today is substantial and still increasing. Broadly, they have been defined into two categories based on their melting property. The most well-known and frequently used plastic varieties, such as polyethylene

(PE), polypropylene (PP), PVC, polyethylene terephthalate (PET), polystyrene (PS), and polyamide (PA), are categorized as thermoplastics since they melt upon heating. Such polymers have the potential to be recyclable since they can melt, solidify, and re-melt. The other category is thermosets, which do not melt upon heating since they comprise 3-dimensional networks instead of linear, branching chains. Polyurethanes (PUR), unsaturated polyester, silicone, epoxy, melamine, phenolic, and acrylic resins are common thermoset polymers [1].

1.1.2 Current plastic production stats

Plastics are utilized in various sectors, with packaging being the largest consumer, accounting for 36% of global demand, followed by building and construction at 16%, textiles at 14%, and consumer products at 10% [2], [3]. Different regions exhibit varying per capita plastic consumption levels, with estimates ranging from 16 kg in the Middle East and Africa to almost 140 kg in NAFTA and Western Europe [3]. According to the most recent figures by the OECD, global plastic production grew steadily between 2018 and 2022, with the latest production numbers standing at an estimated 400.3 million metric tons (Mt) in 2022 [4]. Of this, about 362.3 Mt were fossil-based polymers, approximately 35.5 Mt were mechanically recycled post-consumer plastics, about 2.3 Mt were bio-based plastics, 0.1 Mt were chemically recycled post-consumer plastics, and <0.1 Mt were produced using carbon capture [4]. In Europe, production was an estimated 58.7 Mt in 2022, out of which about 47.2 Mt were fossil-based plastics, 7.6 Mt were mechanically recycled post-consumer plastics, 3.2 Mt were mechanically recycled pre-consumer plastics, 0.7 Mt were bio-based plastics and <0.1 Mt were chemically recycled post-consumer plastics [4]. This estimate for Europe, however, suggests a slight decline in plastic production from 62.3 Mt in 2018 to 58.8 Mt in 2022 (about -5.6%) [5]. At the same time, global plastic use is estimated to reach 1231 Mt by 2060 [6].

1.1.3 Global trend of plastic waste generation

Plastic waste worldwide has increased significantly, becoming a serious environmental issue. According to recent OECD estimates, plastic waste is projected to increase almost three-fold from 353 Mt in 2019 to about 1014 Mt in 2060 [6]. Of this, a large percentage is expected to be generated in non-OECD countries (65%), especially economies in Asia and Africa [6]. Of the total plastic production globally, 10% is recycled, and 14% is incinerated. Unfortunately, the remaining 76% is in landfills or the environment [7]. In the case of Europe, of the approximately 25.8 million tons of plastic waste generated annually, less than 30% is collected for recycling, about 39% is incinerated, and about 31% ends up in landfills [8].

The mismanagement of plastic waste in the environment further exacerbates the situation. It is estimated that about 79 million metric tons of mismanaged plastic waste was produced globally in 2019, with projections suggesting this could reach up to 153 Mt by 2060 [6]. In addition, the cumulative plastic waste in the environment is expected to grow to 12 billion metric tons by 2050 [9]. Between 2019 and 2026, the amount of plastic waste recycled is expected to grow from 9% to 17%. The incinerated component is expected to be stable at around 18%. The portion of plastic sent to landfills is expected to stay at 50%, while the overall mismanaged plastic waste is expected to decrease from 22% to about 15% [6]. Since plastic was not found in sediment layers before 1950 but became more prevalent after that, it has lately been suggested that plastic can serve as a geological indicator of the Anthropocene [10].

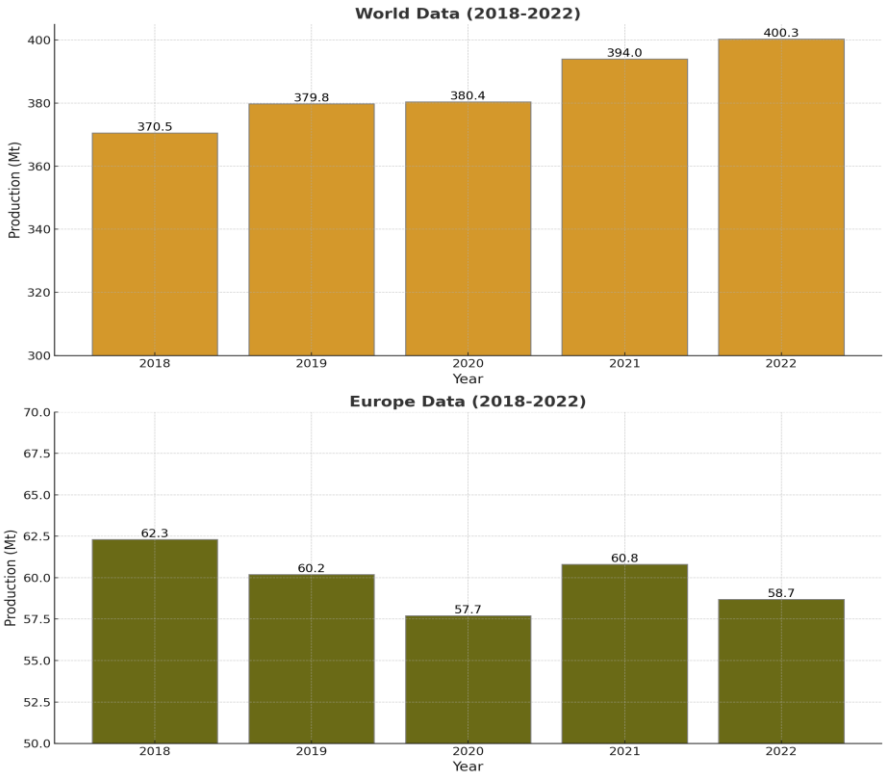

Figure 1: Plastic production over the years. Figure adapted from [4].

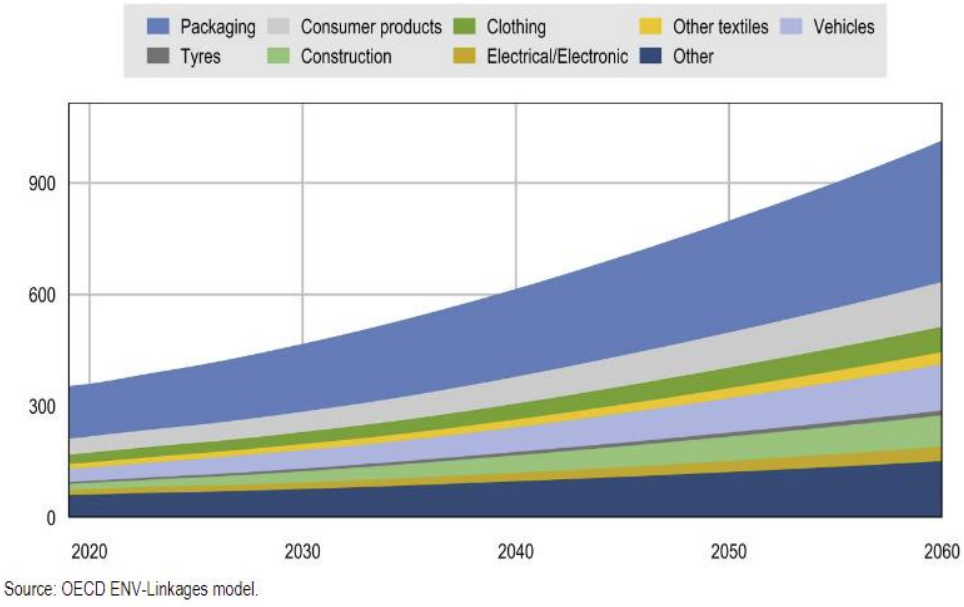

Figure 2: Plastic waste generation projection (2060) by category in millions of tons (Mt). Figure reproduced from [6]. Copyright: OECD.

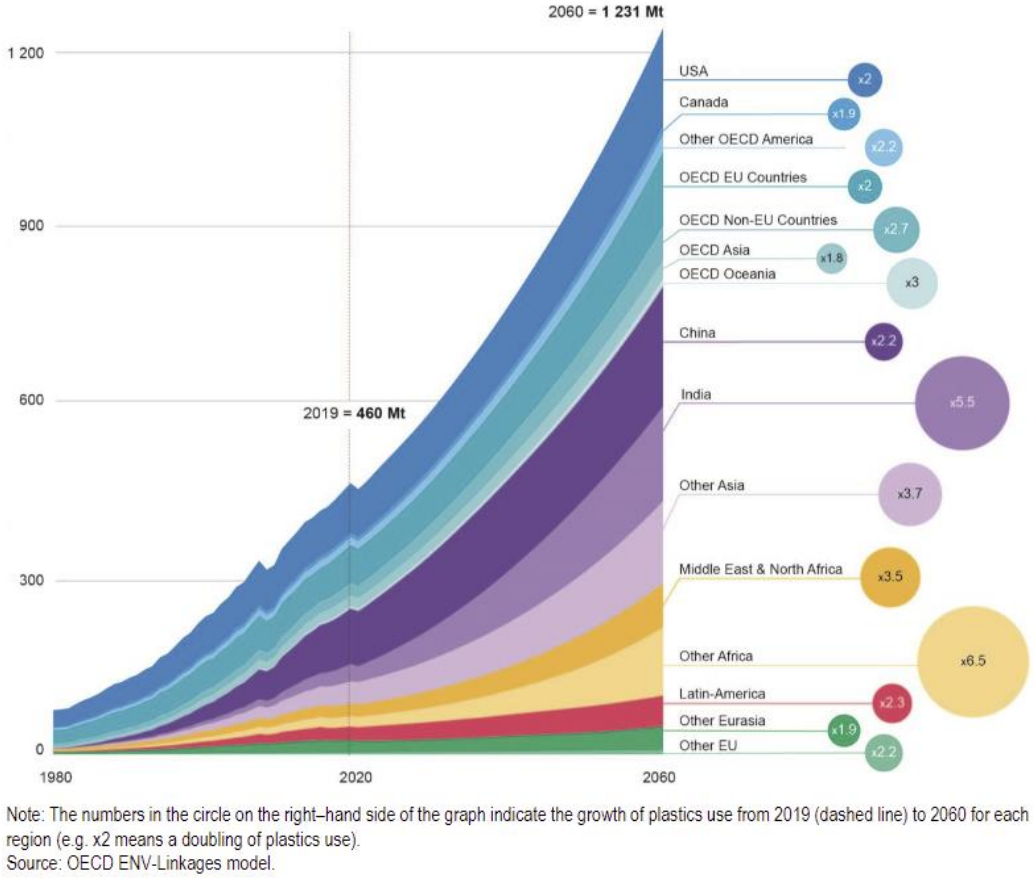

Note: The numbers in the circle on the right–hand side of the graph indicate the growth of plastics use from 2019 (dashed line) to 2060 for each region (e.g. x2 means a doubling of plastics use).
Source: OECD ENV-Linkages model.

Figure 3: Projections for plastic use by 2060 in millions of tons (Mt). Figure reproduced from [6]. Copyright: OECD.

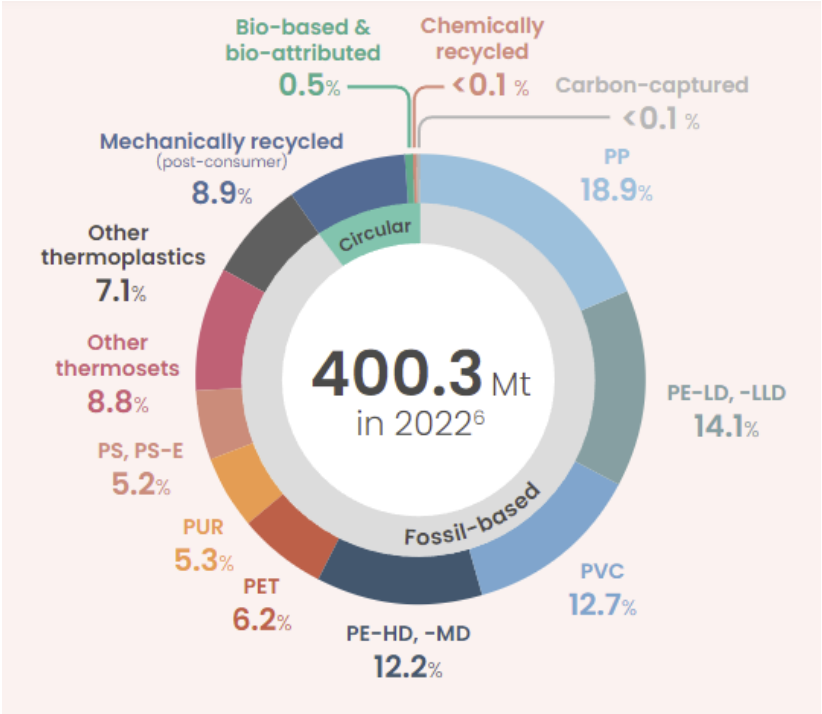

Figure 4: Global plastic production by polymer (reproduced from [4]).

Illustration generated using DALL-E. Copyright: Harshit Sahai

1.2 Microplastics

1.2.1 What are microplastics?

Microplastics are plastic particles that range in size from 5 millimeters down to 1 micrometer in their largest dimension. In contrast, nanoplastics are particles that fall in the sub-micron range or below 1000 nm. They may be characterized into primary and secondary types [11]. Primary micro and nano plastics (MNPs) are intentionally manufactured in microscopic sizes for various commercial and industrial applications. They are primarily used in paints, cosmetics, personal care products, and other products. Alternatively, secondary MNPs are particles produced from the environmental degradation of larger plastic particles by various physical, chemical, and biological degradative forces that act upon them.

1.2.2 Research history of microplastics

The first reported evidence for the presence of plastic particles dates back to 1969 when plastics were found in the gut of the Laysan Albatrosses from the Hawaiian Islands National Wildlife Refuge [12]. During the 1970s, plastics were found in marine waters, with their presence reported in surface waters and surface-dwelling plankton [13], [14]. During the 1980s, marine plastic litter was identified as having a wide-scale impact on the marine environment [15]. The word “microplastics” started to garner interest in the early 2000s. Initial research on this problem focused on marine and aquatic ecosystems, where microplastics were first identified as a threat [16]. However, with increasing awareness about the issue, the line of investigation broadened to include aspects such as distribution, pollution, impacts, and remediation strategies. According to a recent study, research on microplastics has gone through three distinct stages of development: the nascent stage (before 2015), a slow rise (2016–2018), and rapid development (2019–2022). During this time, the focus has shifted from initial topics such as surface, effect, presence, and tributary to current concerns, including toxicity, species, organism, threat, risk, and ingestion [16][17].

1.2.3 Presence of micro and nano plastics in the environment

Research regarding the presence and distribution of MNPs in the environment has garnered significant attention, with studies reporting their presence across different regions of the globe and different environmental compartments, including the aquatic [18], terrestrial [17], [19], as well as aerial compartments [20]. Their presence has also been detected in remote regions of the world such as the Arctic [21][22][23], Antarctica [24], [25] and other polar locations [26], remote offshore environments [27], rural and remote surface waters [28], high altitude locations including mountains and foothills [29], [30], mountainous lakes [31], deep-sea sediments [21] and protected areas [32], [33]. While most studies have reported their presence in the aquatic environment, more recent investigations have highlighted their presence in terrestrial ecosystems, including agricultural soils [34]. Moreover, if we include aquaculture, mariculture, and poultry, we find microplastics in various food products across several regions, particularly fish and shellfish.

The sources of microplastics fall into two general categories: primary and secondary. Plastic pellets, beauty product beads, and other small-sized industrial items are examples of primary microplastics directly released into the environment. Conversely, secondary microplastics come from the breakdown of larger plastic materials due to chemical, biological, and physical degradation processes. This group derives from the wear and tear of regular-use plastics, fibers released from laundering textiles and clothing, and the remnants from the breakdown of plastic waste in undesignated areas such as coastal shorelines.

In aquatic environments, microplastics have been shown to affect organisms across various trophic levels and different aquatic environments, including marine, freshwater, and estuarine. Microplastics impact marine life by causing toxic effects, reduced food intake, delayed growth, oxidative damage, abnormal behavior, and genetic damage at the molecular level, significantly affecting aquatic biodiversity [18]. Furthermore, they have been shown to impact marine microalgae through growth inhibition, reactive oxygen species production, chlorophyll reduction, internalization, impacts on photosynthesis, direct physical damage, nutrient depletion, increased osmotic pressure, the release of toxic chemicals, resulting in morphological changes and impacts on populations [35]. Their presence has also been verified in marine and freshwater fishes, turtles, whales, seals and seabirds, and other organisms such as chicken and worms, fungi and commercial fishes, and seafood for human consumption [18], [36]. Of major concern is their direct ingestion by these organisms, leading to effects such as foraging, mobility, and reproductive disorders, inflammatory response, embryonic defects, sub-lethal and lethal effects, bioaccumulation at lower trophic levels, and subsequent transfer and biomagnification at higher trophic levels [18]. Other reported effects of MNPs on organisms include particle toxicity through accumulation and bio-persistence in the tissues, immune-toxic responses or immune suppression, disruptions to endocrine systems, crossing the cell membranes and accumulation in organs, changes to energy and lipid metabolism, oxidative stress and cytotoxicity as well as genotoxicity [37], [38], [39].

In addition, MNPs have been reported in the air as well. Studies in many parts of the world, both urban and rural, have verified that microplastics in the air are widely dispersed. A study conducted in Zhuhai City, China, revealed the presence of microplastics in the bronchoalveolar lavage fluid (BALF) of both nonsmokers and smokers, suggesting that these particles were inhaled from the air [40], [41]. Another recent study provided evidence of microplastics in the marine atmosphere, including tire wear particles, with concentrations up to 37.5 ng/m^3, indicating their transport and widespread presence in the North Atlantic air [42]. Similarly, microplastics from airborne sources were found in atmospheric deposition tests conducted in Auckland, New Zealand, where deposition rates

were found to be correlated with wind speed [43]. The proven existence of suspended air microplastics in Manila, Philippines, suggests the possibility of both local and long-distance movement [44]. Studies have discovered microplastics in snow samples throughout the Ross Island region, indicating local and long-distance contamination. Even Antarctica, one of the most remote places on Earth, has not been immune to the problem with MPs detected there [24]. Furthermore, studies have also reported the presence of MNPs in indoor air environments, with reports suggesting the possibility of constant inhalation of these particles from breathing [45].

Recent studies have also reported the presence of MNPs in terrestrial environments across the globe and have shown that they affect the soil's bio-physical parameters, including water retention capacity, structural properties, soil microbiota, and soil flora and fauna. Some recent studies have even predicted that terrestrial environments are a bigger sink of MNPs than aquatic ecosystems [46]. This topic is dealt with in detail in the subsequent sections.

1.3 Plastics in the Agricultural Environment

1.3.1 Plastic usage statistics for the agricultural sector

The widespread application of plastics in the agricultural sector has led to the evolution of the term “plasticulture”. The term "plasticulture" describes the use of plastic materials in agricultural activities to improve the quality and efficiency of crop production. The development and study of PE polymer in the late 1930s served as the basis for this technique, which saw the commercialization of plastic films, mulches, drip irrigation tubes, and other related goods in the early 1950s and 1960s. The use of plastics in agriculture further increased with the discovery of various polymers, such as polyesters, polyvinyl chloride, and polypropylene, used in pipes, fittings, fertilizer application tools, and row covers. Plasticulture significantly increases agricultural output by increasing crop quality and quantity and reducing environmental impact by reducing the demand for water, fertilizer, and pesticides. It encompasses various applications, including drip irrigation, plastic mulches, packaging, storage, and post-harvest management, significantly advancing horticulture by providing structural integrity, chemical resistance, and versatility [47], [48].

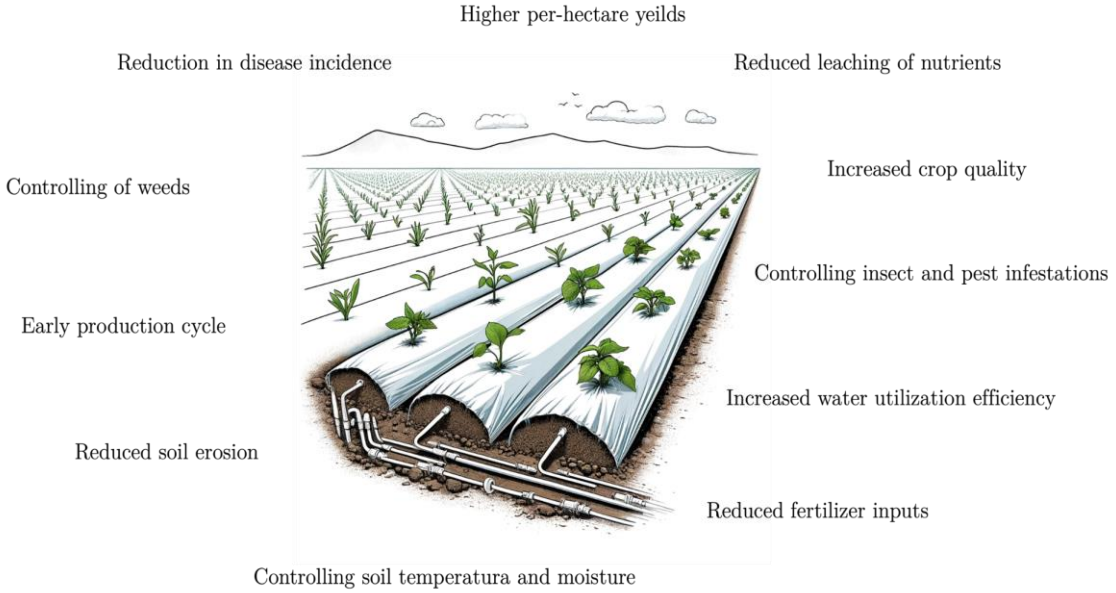

Figure 5: Possible advantages of plasticulture. Adapted from [47].

One of the primary advantages of plasticulture is the significant improvement in water use efficiency, mainly through the adoption of drip irrigation systems, which directly deliver water to plant roots, minimizing waste and optimizing plant growth conditions. Additionally, plasticulture facilitates the use of raised beds and plastic mulches, which have been shown to increase yields in crops such as watermelons by improving the root environment and reducing the impact of pests like the root-knot nematode [49]. Furthermore, using plastic mulches and coverings improves weed control and fruit quality, as demonstrated in strawberry production, where plasticulture systems have yielded superior fruit quality and higher yields than traditional methods[50]. It also benefits strawberry production under cold climatic conditions [51], management of root-knot nematodes and Fusarium wilt through supplemental fumigant placement in tomato production [52], increased yield and quality, and reduced TSNA (Tobacco-Specific Nitrosamines) formation in Burley Tobacco [53], increased production and enhanced nutrient and water use efficiency for example for watermelon [54] and okra [55].

Several studies have estimated the predicted amounts of plastics utilized in the agricultural sector. According to one estimate, approximately 6.7 million tons of plastic are used annually for “plasticulture”, or in agricultural applications. This amount accounts for roughly 2% of the world's annual production of plastics [48]. According to a more recent estimate, the global annual use of plastic films alone was estimated at 7.4 million tons [56]. Including other applications such as irrigation infrastructure, twines, nets, and pipes, the overall plastic use was 10 million tons annually for terrestrial crop and livestock production and 12.5 million tons for overall agricultural production. Of this, films for mulch, silage, and greenhouses represent up to 60% [56]. This use amounts to about 3.5% of the global plastic production [56]. To meet the rising needs of an expanding population, horticulture alone would require eight million tons of plastic worldwide by 2030 [57]. Due to contamination by sand, soil, water, and organic materials, agri-plastic waste will amount to 17 metric tons by the year 2030, which will need to be managed [57].

Types of plastics used in the agricultural industry include a wide range of PE, polypropylene (PP), ethylene-vinyl acetate (EVA) copolymer, as well as poly-vinyl chloride

(PVC), polycarbonate (PC), and poly-methyl-methacrylate (PMMA) amongst others [58]. Additionally, biodegradable and bio-based polymers frequently used in the agricultural sector include Polylactic acid (PLA), Polyhydroxyalkanoates (PHA), Polybutylene succinate (PBS), Polybutylene adipate terephthalate (PBAT), Polycaprolactone (PCL) and starch blends [56]. Their applications include greenhouses, low tunnels, mulching, reservoir and irrigation systems, silage storage, and miscellaneous applications such as packaging, collection and transport, and shading nets [58].

However, notwithstanding its advantages, the adverse environmental effects of plasticulture, particularly the difficulty in managing plastic trash, are concerning. The main concern is the impact of plasticulture on local environmental stress, as evidenced by the significant environmental footprint of the industry and its extensive growth in Shandong province, China, to an area of 156,900 hectares [59]. Agricultural soil is the principal absorber of agri-plastic pollution, making the environmental cost of plastic production and contamination a generational burden. These agricultural techniques produce microplastics, which have the potential to harm human health when they end up in the soil and water sources. They can also lower crop yield and quality. Since plastics are composed of chemicals that are not biodegradable, they do not break down over time but build up in the environment, contaminating the land and water. Burning PE bags releases dangerous chemicals into agricultural areas, such as carbon monoxide (CO), nitrogen oxides (NO_X), lead (Pb), cadmium (Cd), and sulfur dioxide (SO_2). These chemicals pose a risk to the health of humans and animals. Moreover, the complete plastics life cycle—from production to waste—is linked to unsustainable resource use, greenhouse gas emissions, hazardous chemicals, and unparalleled environmental pollution. This issue underscores the necessity of interventions throughout the plastics value chain to lessen these effects.

Figure 6: Satellite image of Poniente Almeriense, highlighting the extent of plastic greenhouse cover in the Almería region of Spain. Sometimes also referred to as the "Mar de plástico" or the "sea of plastic". Source: Google Earth, 2024.

Table 1: Types of plastic polymers used in agriculture.

Conventional non-degradable polymers				**Biodegradable polymers**	
Frequently used polymer	**Usage examples**	**Less frequently used polymers**	**Usage examples**	**Frequently used**	**Usage examples**
PE - Low Density Polyethylene (LDPE) - High Density Polyethylene (HDPE)	Thin films Rigid/semi-rigid products, thick films, protective nets, bale nets	PC	Thermoplastic materials	PLA	Mulching films, twines, nets, fishing lines
PP	Films and bags, rigid crates	PMMA	Lightweight and shatter-resistant sheets	PHA	Potential substitute for polyolefins, PET, PS, and PVC
Expanded polystyrene (EPS)	Packaging and produce insulation	Thermoplastic polyurethane (TPU)	Traceability tags	PBS	Potential substitute for PP
EVA	Stress-resistant materials, UV-resistant materials, Temperature resistant materials	Polyamide (Nylon)	Monofilament fishing lines. Gill nets, Pesticide containers	Starch blends	Films
PVC	Mulching films, Greenhouse films, Irrigation drip tapes	Acrylonitrile butadiene styrene (ABS)	Rigid products, Fishing net floats	PBAT	Mulching films, sheets

PET	Thermoplastic fibers, Containers for liquids and foods	PCL	Added as a blend to starch-based biodegradable plastics

Data adapted from the report Assessment of Agricultural Plastics And Their Sustainability: A Call For Action (FAO) [56]

Table 2: Examples of plastic applications in the agricultural ecosystem and types of polymers used.

Crop production		**Forestry**		**Livestock production**		**Fisheries and aquaculture**	
Use case	**Polymer used**	**Use case**	**Polymer used**	**Use case**	**Polymer used**	**Use case**	**Polymer used**
Polymer coated fertilizer	- PE - EVA - LDPE - Cellulose	Tree guards	- PP	Ear tags	- Thermoplastic PU	Insulating crates	- EPS - Expanded PE - PP
Fertilizer sacks	- PP	Fuel containers	- HDPE - PP	Bunker covers	- HDPE	Ropes	- PE - PP
Bulk containers	- PP	Tree labels and support ties	- PVC - Synthetic rubber	Bale nets and twines	- HDPE - PP	Fishing nets	- PE - Nylon
Seedling plug trays	- PP - PE - EPS			Silage tubes	- LDPE		
Nursery pot trays	- PE - PP			Bale twines	- PP		
Mulching films	- LDPE - PVC - PLA - PHA			Film-wrapped silage bales	- LDPE		
Non-woven textile protection	- PP - Polyester						
Greenhouses and low tunnels	- Multilayer LDPE - Multilayer EVA						

	- Rigid PC			
Shade and protective nets	- HDPE			
Irrigation drip tapes	- HDPE - LDPE - PVC			
Irrigation pipes	- PE - PVC			
Support ties and clips	- HDPE - PVC - Synthetic rubber			
Hermetic storage bags	- LDPE			
Pesticide containers	- HDPE - PET - Co-extruded /mixed polymers			
Reusable crates	- HDPE			

Data adapted from the report Assessment of Agricultural Plastics And Their Sustainability: A Call For Action (FAO) [56]

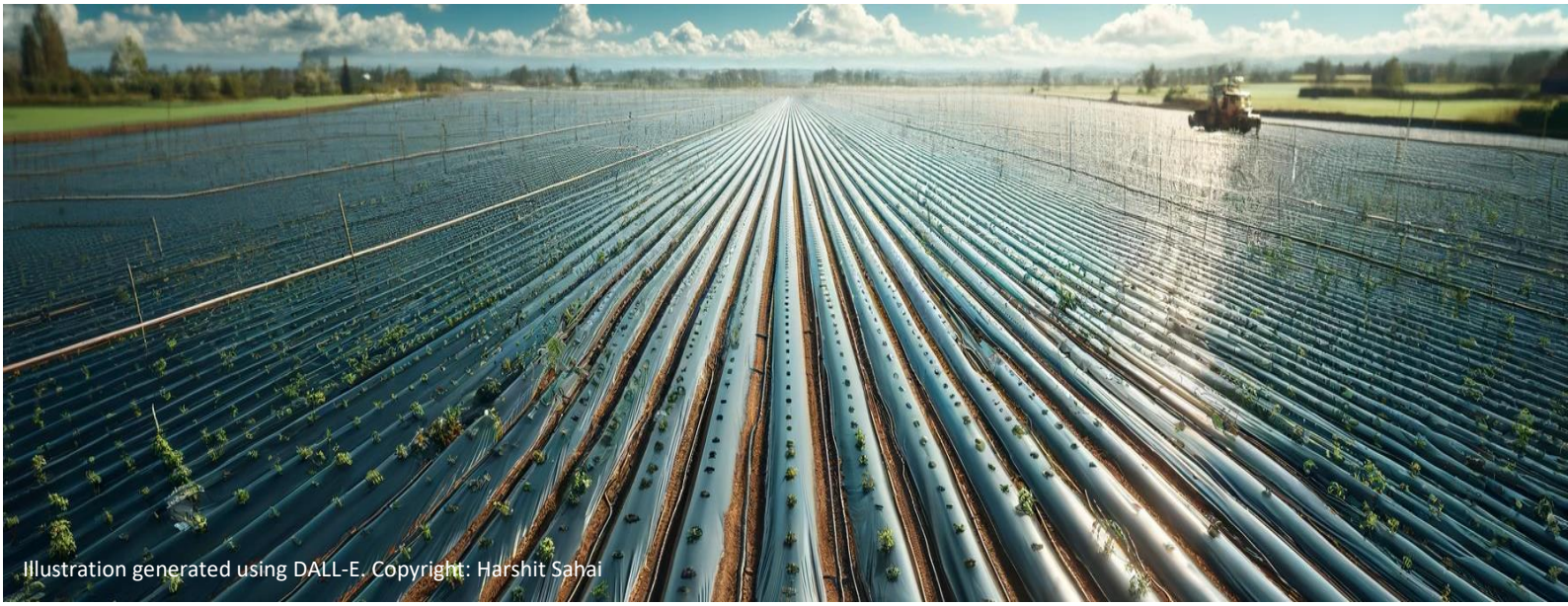

1.3.2 Mulch films in the agricultural environment

The global market for agricultural films is expected to grow by 50% between 2018 and 2030, from 6.1 million tons to 9.5 million tons [60]. Mulch films account for the second largest component of agricultural films after greenhouses. In this category, LDPE is the most prominent [56]. In 2012, plastic mulch film accounted for approximately 40% of the total plastic application in the agricultural sector, while global usage was predicted to reach 7.4 million tons by 2019 [61]. Out of this, greenhouse films accounted for 3.5 million tons, mulch films accounted for 2.5 million tons, and silage films accounted for 1.4 million tons [56]. According to estimates, South and North America and Africa account for the lowest demands, while Asia, Europe, and Australia account for the highest global demands [56]. Black plastic and straw remain the most used mulch films in agricultural production globally [62]. Intensively farmed regions such as Almeria, the southern agricultural province of Spain, use about 31,000 hectares of mulch film and greenhouse films. The use of mulch films amounts to approximately 250 kg/ha, which results in 250 to 500 kg/ha of waste annually [56].

Plastic mulch films offer numerous benefits to the agricultural production system, such as weed and insect control, soil temperature and moisture conservation, protection against harsh climatic conditions, pesticide and fertilizer usage reduction, and increased crop productivity. They are known to raise soil temperature, retain moisture, lessen weed pressure, increase crop yields, and more effectively utilize soil nutrients [63]. Furthermore, different colored plastic mulches have been created to alter the radiation budget, which can improve plant development, production, and quality by controlling soil moisture and temperature [64]. In the case of cotton cultivation, they have been shown to increase the crop yield by up to 28% and the net profit of cultivation by 33% [65]. Similarly, it helped increase potato yield by about 27% [66].

Similarly, mulching, with legume rotation, can alleviate the adverse effects of continuous cropping on potatoes by enhancing soil fertility and regulating soil microbial communities [67]. Another crop that gains from plastic film mulches is lettuce, which has better nitrogen use efficiency, higher soil mineral nitrogen concentrations, and higher yields when organic fertilizers are used [68]. When covered with plastic mulch film, Miscanthus,

a high-yielding C4 crop, shows quicker maturation and decreased plant losses in biomass production, suggesting its usefulness in temperate climes [69].

1.3.2.1 Usage of conventional films

Conventional mulch films are regulated according to the CSN EN 13655 specifications [70]. Polyethylene is the most frequently used polymer in this category, comprising fossil-based, non-degradable plastics. Furthermore, PVC is the second most used polymer for agricultural mulching films globally; its use, however, in Europe, is not reported [56]. In the case of PE, both LDPE and HDPE are utilized for mulch film applications. Low density polyethylene is the dominant type and is favored on most occasions due to its flexibility, ease of production, and ease of application. Alternatively, HDPE is used in certain situations due to its strength and durability where the film is expected to be subject to higher levels of environmental stress or for long term soil coverage.

There are barriers to collecting and removing the conventional mulch films used at the end of their life. These include improper removal leading to the tearing of the films and subsequent production of residual fragments on the field, insufficient economic/regulatory incentives for their removal, and insufficient awareness amongst farmers and stakeholders [71]. The amount of film left on the field ranges from 5-25%; however, the lack of data makes this estimation difficult [71]. A recent report by the European Commission DG Environment suggests that if the average amount of mulch film left in the EU is between 5 and 25%, the 83,000 tons of mulch film used annually would leave 4,750–20,750 tons of conventional plastic on agricultural land annually [71].

1.3.2.2 Biodegradable or bio-based films

Bio-based plastics are polymers derived from plant-based raw materials. However, not all bio-based polymers are biodegradable or compostable, and they are often blended with fossil-based polymers and additives to produce usable plastic products. On the other hand, biodegradable plastics can be broken down into constituent monomers through metabolism by microorganisms such as bacteria and fungi into substances such as water, carbon dioxide, and biomass and can be produced from bio-based and fossil-based precursors. The current global production of bioplastics stands at 2.42 million tons in 2021, with Asia being the largest producer (≈50%), Europe at the second spot (≈24%), and North America at the third spot (≈17%). However, this production capacity is projected to reach 7.59 million tons by 2026 (European Bioplastics, 2021). Of these, the top three materials currently employed for bioplastics are PBAT (19.2%), PLA (18.9%), and starch blends (16.4%). At the same time, an estimated 14% of the total biodegradable plastic production is used by the agricultural and horticultural markets (European Bioplastics, 2021).

In the European Union, biodegradable mulch films are regulated per the specifications mentioned in the EN 17033 guidelines, which state that films labeled as biodegradable should achieve at least 90% biodegradation under ambient soil conditions within two years [72]. Any such polymer used as a mulch film must meet the specification requirements outlined by this guideline and the ISO 23517:2021 standards [73]. Biodegradable films can also be produced using fossil fuel-based precursors as well as bio-based polymers. Common biodegradable polymers in the fossil fuel-based category include PBAT, poly ε-caprolactone or PCL, and PBS. Alternatively, biodegradable polymers from the bio-based category include PLA, Polyhydroxyalkanoates (PHA), Chitin, Alginate, Starch, and Cellulose [73]. Polymers such as PBAT, PLA, and other starch-based bioplastics are widely used in commercial agricultural mulch films and other agricultural practices.

1.3.2.3 Concerns regarding mulch films

Despite the numerous benefits that mulch films provide to modern agricultural production systems, concerns have emerged regarding the environmental impact of their widespread application. Conventional mulch films are also subject to economic constraints. For instance, removing plastic mulch films from the ground at the end of the growing season takes roughly 42 hours per hectare (ha) [74]. The final disposal costs of PE film are 176.5 €/ha for removal, 186 €/ha for landfilling, and 192 €/ha for recycling [75]. These financial drawbacks cause PE mulch film wastes to build up or be tilled on the field; some growers even leave them abandoned near rivers or rural areas [76]. In certain instances, these wastes are even burned under uncontrolled and open-air conditions [76].

According to recent estimates, depending on the type of polymer, 147 to 475 microplastic particles could be produced on average per cm^2 of the mulch film due to various degradative forces in the environment [77]. When these films are used over an extended period, particularly if composed of non-biodegradable materials like LDPE, microplastic residues can build up in the soil, harming crop quality and soil health [78]. Moreover, the degradation and distribution of plastic mulch films also release those additives used in their manufacture. These additives—plasticizers, lubricants, and antioxidants—are not chemically bonded to the polymeric matrix, which permits their gradual release into soil and water, whereupon they can affect the soil characteristics, its microbiota, and the actions of other chemicals within it [79]. PE mulching films leach plasticizers like phthalates, and acetyl tributyl citrate into the soil, posing a potential environmental and human health risk [80].

Bioplastics have been marketed as more environmentally friendly and sustainable than traditional, non-biodegradable plastics because they can naturally break down into end products like carbon dioxide (CO_2), water (H_2O), and biomass. As a result, they are much less persistent in the environment than non-biodegradable plastic waste. However, even these bioplastics are often modified using several compounds (additives) that provide chemical, physical, and structural properties to the polymer, making them commercially useable. These modifications can affect the degradability of bioplastics [81] and can also lead to the addition of micro-bioplastics to agricultural ecosystems owing to incomplete degradation [77], [82], [83]. Some reports suggest that these biodegradable films could produce even higher amounts of microplastics in agricultural soils [77]. A recent risk assessment of agricultural plastics conducted by the FAO of the UN, using a RAG rating approach, attributed a very high degree of risk priority to agricultural mulch films, second only to polymer-coated slow-release fertilizers [56].

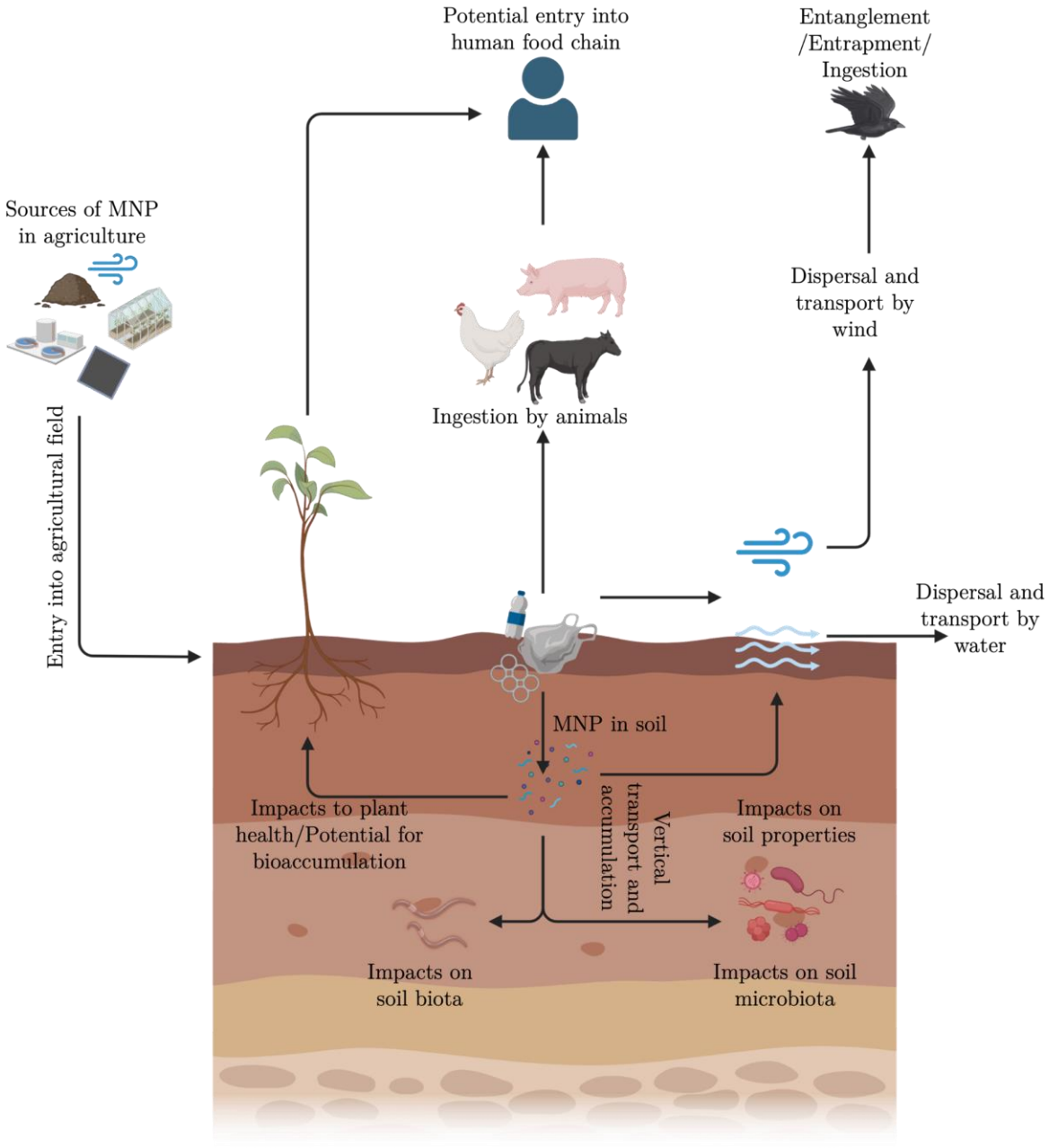

Figure 7: Flow of plastics in the terrestrial environment. Figure adapted from FAO. 2021. Assessment of agricultural plastics and their sustainability. A call for action. Rome. [56] Illustration created using BioRender.


Illustration generated using DALL-E. Copyright: Harshit Sahai

1.4 Microplastics in the Agricultural Ecosystem

1.4.1 Global presence of micro and nano plastics in the agricultural ecosystem

Micro and nano plastics have been reported in agricultural fields from across the globe [34]. The amount of MNPs reported in fields globally varies based upon factors such as agricultural practices, soil management, land use, proximity to industrial or urban areas, proximity to roads and highways, use of soil amendments such as biosolids or sludge and history of plastic use in the area. Other factors affecting the presence and concentration of MNPs in agricultural soils include plastic mulching and wastewater irrigation, plowing frequency, farm management, meteorological conditions, proximity to roads and highways, and population density. According to recent estimates, the input of MNPs in agricultural soils in the US alone amounts to 70 kilotons annually, while the global input could be as high as 0.5 megatons annually [84]. Recent studies have speculated that soil could be an even larger sink or pool of micro and nanoplastics than aquatic ecosystems [85].

In intensively farmed soils, the load of MNPs could be as high as 43,000 particles/kg [86]. For instance, in Xinjiang, China, fields with different years of mulching history showed an apparent increase in MP abundance, ranging from 538 to 9708 particles/kg soil, with the size of MPs decreasing as the mulching history increased. In this study, microplastic concentrations in agricultural fields varied based on mulching history: <5 years (538 particles/kg), 5–10 years (1484), 10–20 years (5812), and >20 years (9708) [87]. High amounts of MPs (874 particles/kg in treated vs. 664 particles/kg in untreated areas) were found in agricultural soils treated with biosolids in the southeast of England, suggesting that while biosolids contribute to MP pollution, they are not the only cause [88]. In South Korea, the number of MPs was estimated to be between 195 and 306 particles/kg of dry soil across various land uses, and mainly comprised PE, PP and PET [89]. These findings point towards the widespread presence of MNPs in agricultural soils with varying concentrations, encompassing a broad range of sizes, dependent upon a complex mix of factors.

The levels of microplastics in European soils also vary widely. In the urban soils of Coimbra City, Portugal, microplastic concentrations ranged from 5×10^3 to 571×10^3

particles/kg, with an average concentration of 106×10^3 particles/kg, highlighting the significant impact of urbanization on microplastic pollution [90]. The application of biosolids to agricultural land in southeast England resulted in high microplastic numbers, with concentrations in biosolid-treated fields reaching 874 particles/kg [88]. A recent review of published studies on microplastics in European soils revealed an average of 2914 particles/kg or 8.9 $mg\,kg^{-1}$, twice that of China [34]. The same study estimated the average concentration of MNPs in East Asian soils to be about 1076 particles/kg, 1190 particles/kg in American soils, $205 \pm 186\,mg\,kg^{-1}$ in the Middle Eastern soils and an average of 2400 $mg\,kg^{-1}$ MNP in Australian soils to be [34]. Another study from Canada estimated the annual MNP introduction to agricultural soils in Ontario to be about 4.1×10^{11} and 1.3×10^{12} particles [91].

Numerous types (in terms of polymer composition) and shapes of MNPs have been identified in agricultural soils. Common types of polymers identified include PE, PP, PS, PET, and PBT), synthetic rubbers, EPDMs, and common thermoplastic polymers [92], [93]. Commonly found shapes include fibers, films, fragments, granules, and spheres. Of these, the most common are fibers. Other less frequently occurring polymers include nylon, latex, and PVC. In terms of size, the most common size range for reported MNPs is 20 to 5000 µm [85]. However, detecting and characterizing nanoplastic particles in soil is extremely difficult, leading to a lack of reporting regarding their types and size ranges.

Possible sources for the entry of MNPs into agricultural soils include agricultural practices such as plastic film usage for mulching, greenhouses and other on-field infrastructure containing plastics, repurposed wastewater for irrigation, repurposed sewage sludge, composts and manure as amendments, fertilizers as well as atmospheric deposition. Furthermore, possible impacts include effects on soil physicochemical and biological properties, soil flora and fauna, microbiota, plant health, bioaccumulation in plants and crops, and possible entry into the human food chain. These topics are dealt with in detail in the upcoming sections.

Table 3: Overview of MNPs in agricultural fields.

Location	**Dominant polymer type reported**	**MNP concentration reported**	**Dominant MNP size range reported**	**Reference**
Republic of Korea	PE, PP, PET	195–306 particles/kg	20-2,000 µm	[89]
Germany	PE, chlorinated-PE, rubbers	0.00 to 56.18 particles/kg	0.4–57.5 mm	[94]
China	PE	538 to 9708 particles/kg	578 to 1523 µm	[87]
China	PP, PE, ethylene-propylene copolymer and PS	2462 ± 3767 particles/kg on average.	Mostly between 200–500 µm	[95]
Greece	PE from black mulch films (BMF)	69 ± 38 particles/kg to 301 ± 140 particles/kg	N/A	[96]
Iran	PET, PS, and nylon	Up to 1.1 particles/g	N/A	[97]
Bangladesh	PS, EVA, latex, HDPE, PVC, ABS, CA, LDPE, PP.	$2.13 \times 10^4 \pm 0.13 \times 10^4$ particles/kg	0.02-1.5 mm	[98]
China	PP and PET	85, 109 and 150 particles/kg in different land-use types	$<$ 2000 µm were 77.3 % and $>$ 3000 µm accounted for 9.25 %	[99]
Germany	PE, PP, PS	0.34 ± 0.36 microplastic particles/kg	N/A	[100]
Taiwan	LDPE	12–117 particles/m^2	Average of 2.56 mm and 1.43 mm in the upper and lower soil layers	[101]
Spain	N/A	2243 ± 983 particles/kg	N/A	[102]
Netherlands	N/A	888 ± 500 particles/kg	N/A	[102]
China	PE from mulch film	40.22±5.53 kg/ha after 5 years of mulching to	N/A	[103]

		164.08±8.31 kg/ha after 30 years,		
China	PE from mulch film	538, 1484, 5812, and 9708 particles/kg, depending on mulching history	1000–5000 and 200–500 µm	[87]
Portugal	PP and PE	$104 \times 10^3 \pm 111 \times 10^3$ particles/kg	< 50–250 µm	[90]
Tunisia	PP and PE	50 to 880 particles/kg	<1 mm	[104]
Canada	PP, PE, Polyester and Acrylic	541 particles/kg	N/A	[91]
Chile	Acrylates, PVS, PE, PP, nitrile rubber, PS	306 ± 360 particles/kg	0.076 ± 0.292 m m^2 particle area	[105]
Republic of Korea	SBR, SIS, PP, PE, EPS, PS, PET	664 particles/kg	1-5 mm	[106]

1.4.2 Sources of micro and nano plastics in agriculture

The sources of microplastics in agriculture are numerous and varied, reflecting both the environmental problems caused by plastic waste and the pervasive use of plastics in contemporary agricultural practices. Plastic films, which are widely used for mulching, are a key source of soil contamination because they break down into smaller fragments over time as a result of exposure to environmental variables such as mechanical stress and UV radiation [87], [103], [107]. Furthermore, the introduction of microplastics into agricultural soils is also facilitated by the use of organic fertilizers, such as sewage sludge, manure, and composts [108], [109], [110], [111]. Irrigation techniques that use wastewater or recycled water, in particular, have the potential to introduce microplastics onto agricultural fields because these waters may contain microplastics from industrial and urban sources [112]. Another factor is atmospheric deposition; microplastics are dispersed over agricultural landscapes by wind and rain from sources including cities, landfills, and roadways where tire wear particles are produced [111]. Utilizing fertilizers and pesticides in composite forms, which could include binders or carriers of microplastics for the slow release of nutrients, increases the complexity of the sources by applying these contaminants directly to crops and soils [56].

The degradation of plastic mulch films, primarily composed of LDPE, leads to the formation of MPs through processes like photodegradation, chemical degradation, and microbial activity. Research has demonstrated that the number of MPs in soils increases with mulch film usage over time, suggesting a direct relationship between the history of mulching and MP pollution levels. In Xinjiang, China, agricultural fields with different years of mulching history showed an increasing trend in microplastic abundance, ranging from 538 to 9708 particles/kg of soil, indicating that the longer the soil has been mulched, the higher the microplastic content [87]. Another similar study of cotton fields in Xinjiang mulched for 5–30 years revealed that microplastics, identified as PE materials, were present at an abundance of 78.51±2.57 particles/(100 g) across different soil depths [103]. In Sichuan Province, China, the abundance of plastic fragments in mulched agricultural farmlands varied widely, with some areas reaching 1158.33 ± 52.04 particles/kg [113]. In another study, the authors focused on introducing low density microplastics from compost and mulch film application in two vegetable production systems in southeast Spain and the Netherlands. They found that both Spanish and Dutch soils were contaminated by microplastic, containing 2242 ± 984 MPs/kg and 888 ± 500 MPs/kg, respectively [102].

Another source of microplastics in agricultural land is the application of repurposed sewage sludge from wastewater treatment plants as an amendment. An estimated 99% of the MPs are retained in the sewage sludge in the wastewater treatment plants [108]. A recent study from Spain that compared treated and untreated soils revealed that MP concentrations were 2.3-2.8 times higher in soils amended with sewage sludge with an average of 5190 particles/kg as opposed to 2030 particles/kg in untreated soils [109]. According to recent estimates, from the 10 million tons of sludge produced yearly in the EU, agricultural areas may receive 7.2×10^{12} to 1.5×10^{14} MP particles annually [112]. Another study reports this input to be between 63 000 to 430 000 metric tons annually [108].

Reusing wastewater in farming can also release MPs into the soil, negatively affecting the environment and agricultural health. A sink for MPs is treated wastewater from wastewater treatment plants (WWTPs) [114]. For example, areas irrigated with wastewater in Iran displayed a heterogeneous distribution of MPs, with concentrations as high as 1.1 MP particles/g and a notable contribution of spherules most likely derived from

the wastewater. The different degrees of weathering of these MPs, which included nylon and PET, indicate that agricultural soil functions as both transient sinks and dynamic secondary sources of MPs, with wind erosion playing a further role in their dissemination [97].

Similarly, composite or polymer-coated fertilizers or slow-release fertilizers are also a significant direct source of MNPs in agricultural soils [56]. Agricultural soils are also further burdened by MPs transported via the atmosphere. The aerodynamic properties of MPs facilitate their long-distance transport, allowing them to be deposited in areas far from their source, including agricultural fields [20], [111]. Additionally, microplastics generated from the wearing of vehicle tires also contribute to this issue. In a recent study, soil samples were found to contain 372 ± 50 fragments/kg of dry weight, and subsequent analysis revealed that more than 90% of these particles were tire-derived synthetic rubber [115]. In addition to these factors, numerous other sources, such as silage films, nets, tubing, greenhouses, packaging, and transportation materials, also add to the problem [56].

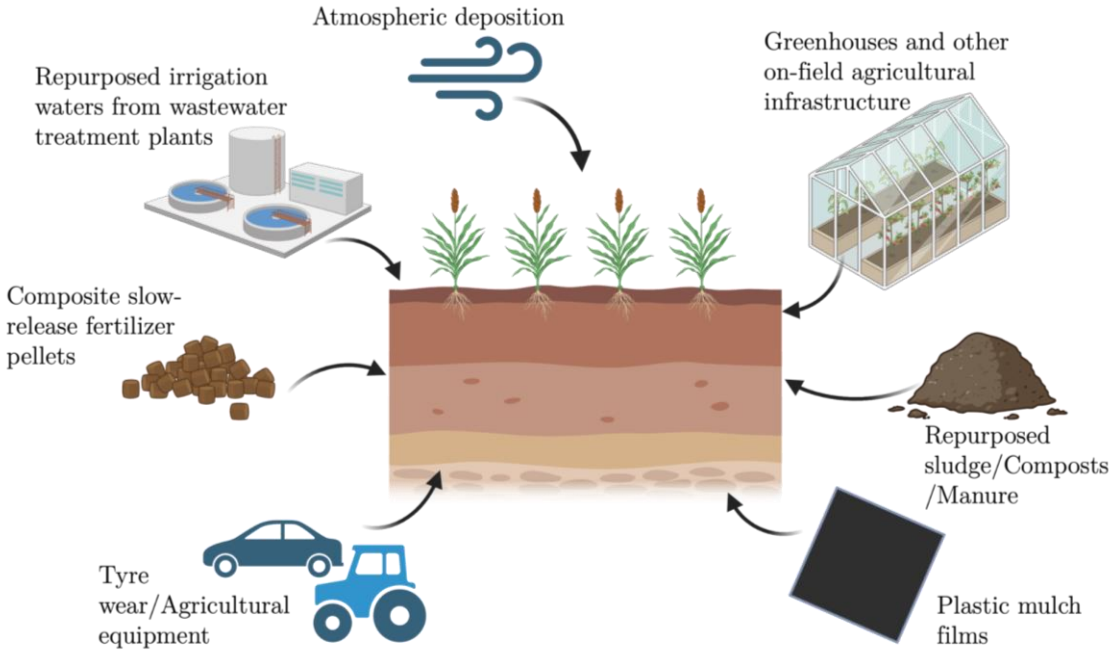

Figure 8: Sources for the introduction of MNPs in the agricultural ecosystem. Illustration created using BioRender.

1.4.3 Impacts of micro and nano plastics on the agricultural ecosystem

1.4.3.1 Effects on abiotic factors

The effects of MNPs on soil properties depend on the properties of the polymer in question, such as its type, size, shape, degradability, and the amounts present [116]. Microplastics have been shown to affect the biophysical parameters of soil, such as water retention capacity, bulk density, hydraulic conductivity, and particle composition [117], [118]. Furthermore, MNPs have been shown to affect the wetting/drying cycle of silt-loam soils by altering their structural properties [117]. They can also be responsible for altering soil

compaction, aggregation, and porosity [118] and increasing CO_2 emissions from soil and humification [119]. They have been shown to reduce soil nitrous oxide (N_2O) emissions and fertilizer-derived nitrogen loss [120]. Polyester fibers have also been shown to reduce sediment concentration and soil loss due to erosion in erodible soils [121]. In soil-plant systems, MPs/NPs can affect the amount and cycle of several macro- and micronutrients, including carbon (C), nitrogen (N), and phosphorus (P) [122]. According to Zang et al., [123] MPs had a major impact on important pools and fluxes within the C cycle, including CO_2 emission and the allocation of absorbed 14C. However, it has been shown that the effects of micro- and nano-plastics on the physical properties of soil are minimal at environmentally relevant concentrations [124] and that effects were only significant at high concentrations of 2% (w/w) [125].

1.4.3.2 Effects on soil flora and fauna

Micro and nano plastics have been well documented to impact the soil microfauna and mesofauna [126]. These include protists, tardigrades, soil rotifers, nematodes, collembola, mites, springtails, and earthworms [126], [127]. The impacts depend on the type and concentration of the particle in the soil [128], [129]. For instance, microplastics obtained from disposable medical masks did not induce severe adverse effects on the survival or reproduction of certain soil invertebrates but did cause a transient immune response in woodlice and altered energy-related traits in mealworm larvae [130]. While larger microplastics have a varied effect on earthworm reproduction, smaller microplastics often have more detrimental effects on the diversity of soil bacteria and the growth and reproduction of nematodes [127]. The physiological effects of microplastics on insects, a key group of soil arthropods, are dose-dependent and can negatively impact their survival, reproduction, and development [131]. The ingestion of microplastics by earthworms can lead to histopathological damage and oxidative stress and serve as carriers for other pollutants, thereby exacerbating ecological harm [132]. Co-exposure to microplastics and heavy metals has been shown to increase earthworm mortality, suggesting a compounded negative effect when multiple pollutants are present [122].

In one study, PE microplastics at 0.5% concentration caused a ≥70% reduction in earthworm reproduction, DNA damage, and phthalate accumulation, highlighting significant adverse chronic and transgenerational effects on earthworms [133]. They have also been shown to impact the microbial community of the earthworm gut, affecting the abundance of various bacterial genera [134]. Studies have shown that while some microplastics, such as PBAT, degrade to some extent in the earthworm gut, others, like LDPE, remain unchanged, indicating a selective impact on earthworms based on the microplastic type [135]. Microplastics significantly impact soil microbial biomass, decrease bacterial diversity, and alter microbial community structure, affecting soil flora [127]. For instance, microplastics, mainly PVC, have been shown to cause variations in soil chemical parameters and significantly alter the abundances of specific bacterial and fungal taxa, including *Acidobacteria, Actinobacteria, Bacteroides, Candidatus, Saccharibacteria, Proteobacteria, Ascomycota, Basidiomycota*, and *Mortierellomycota*, suggesting a taxa-dependent impact of these pollutants on soil microbiomes [136]. According to a global meta-analysis, the effects of microplastics varied depending on the types, sizes, concentrations, and exposure times of the particles. Microplastics were found to considerably increase soil microbial biomass, decrease soil bacterial diversity, and change the organization of microbial communities [127]. A recent study comparing various microplastic materials discovered that they can create new microbial niches in soil, with particular community compositions depending on the materials employed, which could ultimately affect the overall microbiota of the soil [137].

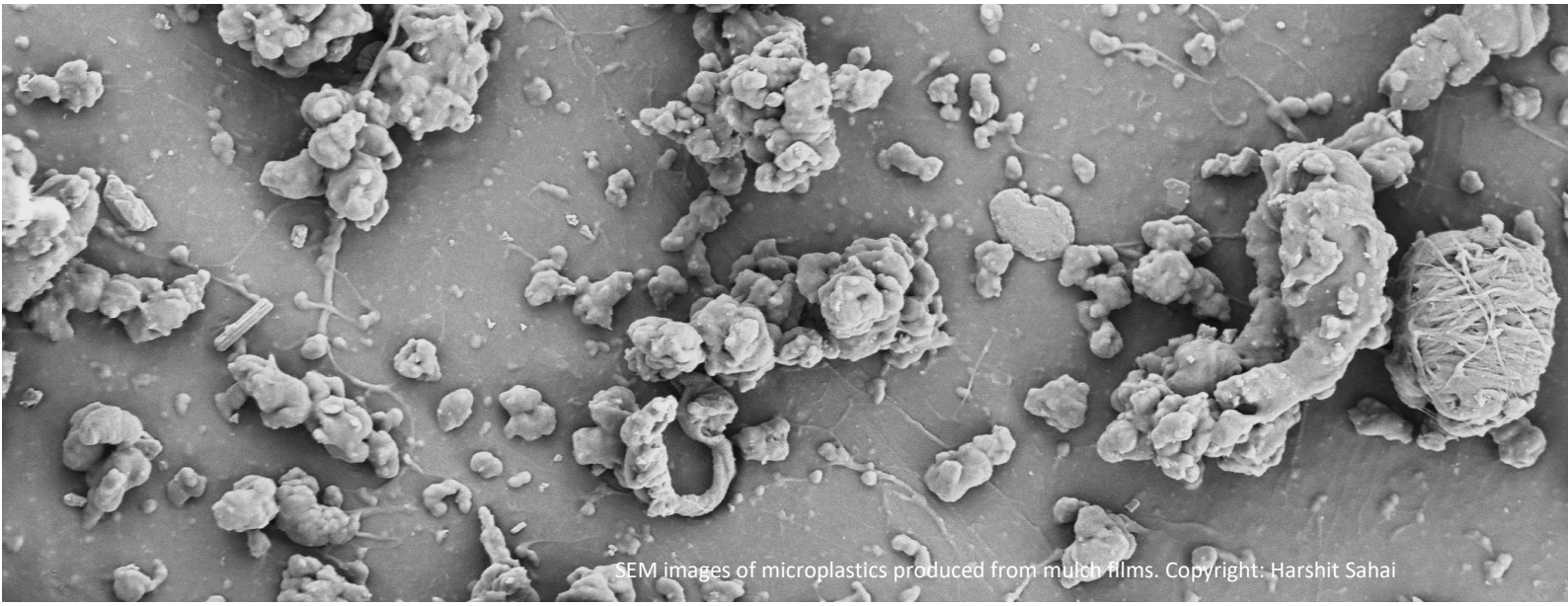

1.5 Interaction of Microplastics with Other Contaminants

Microplastics can operate as vectors for transmitting hydrophobic organic pollutants in terrestrial and marine settings because of their high surface area-to-volume ratio and increased affinity for these contaminants in aquatic circumstances. Chemical adsorption on MNPs in aquatic settings is well documented and is a complicated process that is impacted by several variables, such as their chemical properties and environment. Hydrophobicity, Van der Waals forces, π–π bond, electrostatic, and hydrogen bond interactions are polymeric sorption mechanisms that affect a MNP's capacity for adsorbing chemical pollutants [138]. In addition, the adsorption process is greatly influenced by environmental variables such as temperature, pH, and ionic strength, as well as MNP parameters (particle size, surface area, shape, and dosage) and the characteristics of the pollutants (ionic properties, hydrophobicity, molecular dimensions) [138]. This interaction significantly impacts the transportation, fate, bioavailability, and ecotoxicity of the adsorbed chemicals and the plastic particles in the environment.

In the case of aquatic environments, numerous studies have reported this phenomenon on the surface of MNPs. For instance, the adsorption of trace metals (Ag, Cd, Co, Cr, Cu, Hg, Ni, Pb, Zn) to new (virgin) and aged (beached) plastic production pellets suspended in river water was demonstrated with beached pellets showing increased adsorption compared to virgin pellets [139]. Another study reported the adsorption of antibiotics (sulfadiazine, amoxicillin, tetracycline, ciprofloxacin, and trimethoprim) on MP in both freshwater and seawater, with freshwater conditions reporting increased adsorption than in seawater [140]. Similarly, other chemicals that have been shown to react and adsorb on MNP surfaces include estrogens [141], Chlorophenylacetonitriles (CPANs) [142], Nitro polycyclic aromatic hydrocarbons (NPAHs) [143], heavy metals [144], dyes [144], Perfluoroalkyl substances (PFAS) [145] and oil [146]. A list of studies reporting this phenomenon is given in Table 4: Interactions of MNPs with pollutants in the aquatic environment.

Table 4: Interactions of MNPs with pollutants in the aquatic environment.

MNP type	**Pollutant Category**	**Pollutant**	**Reaction condition**	**Reference**
PE PP	Alkylphenols and Estrogens	4-t-butylphenol, 4-t-octylphenol, 4-n-octylphenol, 4-n-nonylphenol, 17β-estradiol, and 17α-ethinylestradiol	Seawater	[141]
PS PET PE	Chlorophenylacetonitriles (CPANs)	2-chlorophenylacetonitrile, 3-chlorophenylacetonitrile, 4-chlorophenylacetonitrile, 2,6-dichlorophenylacetonitrile, 3,4-dichlorophenylacetonitrile, 2,3-dichlorophenylacetonitrile, 2,4-dichlorophenylacetonitrile, 2,5-dichlorophenylacetonitrile	Wastewater	[142]
PE PS PP	Nitro polycyclic aromatic hydrocarbons (N PAHs)	2-Nflu, 9-Nant and 1-Npyr	Ultrapure water	[143]
PS, PET, HDPE, LDPE	Dyes	BB9 and RR120	Ultrapure water	[144]
PS, PET, HDPE, LDPE	Heavy metals	Cd(II), Pb(II), arsenic (As(III)), and As(V)	Ultrapure water	[144]
PP, PS, and PVC	Trace heavy metals	Pb, Cu, Cr, and Cd	River water	[147]
PVC, PP, and PE	Steroid hormones	17β-estradiol (E2) and 17α-ethynylestradiol (EE2)	Seawater	[148]
PP and PET	Oil	Red palm cooking oil	Seawater	[146]
PS and HDPE	Perfluoroalkyl substances (PFAS)	Perfluorobutanoic (PFBA), Perfluoropentanoic (PFPeA), Perfluorohexanoic (PFHxA), Perfluoroheptanoic (PFHpA), Perfluorooctanoic (PFOA), Perfluorononanoic (PFNA),	River water Seawater	[145]

		Perfluorodecanoic (PFDA), Perfluoroundecanoic (PFUdA), Perfluorododecanoic (PFDoA), Perfluorotridecanoic (PFTrA), Perfluorotetradecanoic (PFTeA), Perfluorohexadecanoic (PFHxDA) and Perfluorooctadecanoic (PFODA) acids; and ii) Perfluorobutanesulfonate (PFBS), Perfluorohexasulfonate (PFHxS), Perfluorooctanesulfonate (PFOS) and Perfluorodecanesulfonate (PFDS), was mixed with the sulfonamide Perfluorooctanesulphonamide (PFOSA)		
PVC, PS, PE, and PP	Fluoroquinolone Antibiotics	Norfloxacin	Simulated natural water and actual surface water	[149]
PE	Chlorobenzene and Trifluralin	Trichlorobenzenes (1,2,3-TeCB, 1,3,5-TeCB, 1,2,4-TeCB), Pentachlorobenzene (PeCB), Hexachlorobenzene (HeCB), and Trifluralin (TFL)	River water and synthetic water	[150]
PVC, aged PVC, PS, and aged PS	Metalloid	Boron	Distilled water	[151]
Virgin and beached PE pellets	Trace metals	Ag, Cd, Co, Cr, Cu, Hg, Ni, Pb, Zn		[139]
PE, PS, PP, and PVC	Antibiotics	Sulfadiazine (SDZ), Amoxicillin (AMX), Tetracycline (TC), Ciprofloxacin (CIP), and Trimethoprim (TMP)	Freshwater and Seawater	[140]

1.5.1 Interactions of MNPs with pollutants in the terrestrial/agricultural environment

Several chemicals are intentionally added to plastics during manufacturing to improve their flexibility, stability, and functionality. These chemicals include plasticizers, surfactants, flame retardants, stabilizers, color pigments, antioxidants, solvents, and biocides. These chemicals can leach out of the plastic under certain conditions and contaminate the surrounding environment. Phthalate-based plasticizers, such as ethylhexyl phthalate, dimethyl phthalate, diethyl phthalate, di-n-butyl phthalate, benzyl butyl phthalate, bis-2-ethylhexyl adipate, and di-n-octyl phthalate, are frequently found in soil, sediment, water, and sludge that has been contaminated with microplastics [152]. Besides this, microplastics can also adsorb surrounding pollutants onto their surface through various adsorption processes. The number of studies reporting the interaction of MNPs with agricultural contaminants is relatively low compared to those focused on aquatic environments.

Microplastics in terrestrial environments have been identified as specific chemical vectors owing to their high surface area-to-volume ratio and various adsorption mechanisms. These chemicals include hydrophobic organic contaminants such as benzo[a]anthracene (BaA) and benzo[a]pyrene (BaP), which have been shown to adsorb onto PE and PS microplastics through mechanisms like electrostatic interaction, π–π interactions, and hydrophobic interaction [153]. In another study, the adsorption and partitioning of triclosan between PE and PS microplastics and soil particles was demonstrated by triclosan preferentially adsorbing over MP surface than soil [154]. Similarly, 17β-estradiol (E2) showed preferential adsorption over MP surfaces in a soil-MP solution matrix [155]. In addition, several polymer types, including PE, PP, PS, PET, PVC, PA, and nylon, have been shown to adsorb heavy metals (As, Cd, chromium (Cr), copper (Cu), Pb, zinc (Zn), nickel (Ni), mercury (Hg), titanium (Ti), manganese (Mn) and Fe) onto their surface in the terrestrial environments [156].

These interactions could affect the fate, transport, bioavailability, and co-toxicity of MNP particles and adsorbed chemicals to soil biota, including plants. For example, Wang et al., in a recent study, demonstrated the co-toxicity of HDPE and PE microplastics along with Cd to maize plants and observed that while HDPE alone did not impact plant health, co-exposure of PS and HDPE with Cd resulted in a higher accumulation of Cd in plants and increased Cd toxicity causing impacts on plant growth [157]. In another study, PS and PTFE microplastics reduced the As uptake by plants. The soluble starch synthase and pyrophosphorylase activities in rice grains were also shown to be suppressed by PSMP, PTFE, and As, resulting in decreased starch accumulation and subsequent rice biomass and yield [158]. Furthermore, PE, PS, PA, PLA, PBS, and polyhydroxybutyrate (PHB) in Pb-Zn-contaminated soil altered the soil properties. It decreased the richness and diversity of bacterial communities and altered microbial community composition, causing the enrichment of specific taxa due to alterations in heavy metal bioavailability [159].

1.5.2 MNP sorption mechanisms

The sorption process onto MNP surfaces can be broadly categorized into physisorption and chemisorption. Whereas chemisorption uses valence forces and chemical bond formation between adsorbate and adsorbent, physisorption is an adsorption process in which the molecular interactions between the adsorbate molecules and the adsorbent are controlled mainly by van der Waals forces [138]. Physisorption is a weak, reversible process that occurs at varying speeds on the heterogeneous surface of microplastics. It is characterized

by competitive adsorption and desorption and is non-specific. Conversely, chemisorption relies mainly on the surface area's proportionality and is highly selective and irreversible [138]. In general, there are four steps in the sorption process: (1) sorbate migration from bulk solution to sorbent surface (bulk diffusion); (2) sorbate diffusion through boundary layer to sorbent surface (film diffusion); (3) sorbate diffusion from surface to interior pores (intraparticle diffusion or pore diffusion); and (4) adsorption at an active site on sorbent surface through chemical reaction [160].

One of the predominant sorption mechanisms is hydrophobic interaction. It is defined as the behavior of nonpolar molecules or groups that exhibit low solubility in water, leading to interactions that minimize their contact with water molecules. These hydrophobic interactions increase as the sorbate's organic pollutant-water partition coefficient increases. Other reported mechanisms for the adsorption of contaminants onto MNP surfaces include Van der Waals forces, π–π bond, electrostatic, and hydrogen bond interactions [138]. It has been shown that the adsorption capacity of microplastics for different pollutants, such as dyes and heavy metals, depends on the physical and chemical adsorption mechanisms. These mechanisms are regulated by the environment and the specific kind of microplastic particle in question. Studies have demonstrated that chemical adsorption and hydrophobic partitioning regulate the adsorption behavior of nitro-polycyclic aromatic hydrocarbons (NPAHs), with the hydrophobicity of NPAHs playing a significant role in adsorption capacity [143]. Furthermore, saltwater conditions decreased the adsorption of polyfluoroalkyl substances (PFAS) onto microplastics, demonstrating the impact of water chemistry on the adsorption process [145].

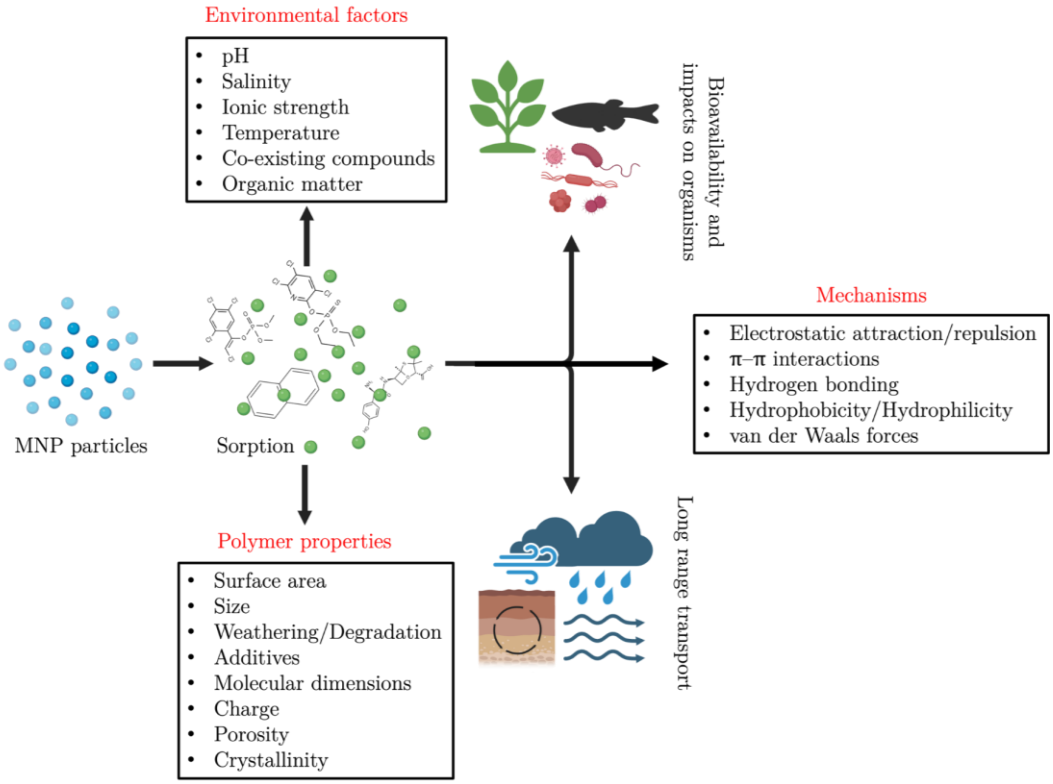

Figure 9: Sorption of contaminants onto MNP surfaces; mechanisms and factors. Illustration created using BioRender.

1.5.3 Modeling of the adsorption process on MNPs

In numerous investigations, the kinetic and isothermal models have proven to be useful instruments for comprehending the dynamics of desorption and adsorption of sorbates, primarily chemical pollutants, concerning the rate constant's order. The most common adsorption kinetic models used to investigate the sorption of pollutants onto MNPs include the pseudo-first-order kinetic model, pseudo-second-order kinetic model, intraparticle diffusion model, and the Elovich kinetic model. The most commonly employed isotherm models include the Langmuir isotherm, Freundlich isotherm, Dubinin-Radushkevich Isotherm, Temkin isotherm, and Redlich-Peterson isotherm model [138].

Pseudo-first order: The pseudo-first-order kinetic model, a cornerstone in the study of adsorption kinetics, has a rich history that traces back to the late 19th century. Initially proposed by Lagergren in 1898, this model was designed to describe the adsorption of oxalic acid and malonic acid onto the charcoal, marking the first instance of a rate equation for adsorption processes. It is assumed that one of the reactants is present in such excess that its concentration does not significantly change throughout the reaction, allowing the reaction to be treated as if it were first-order with respect to the other reactant [161]. Other assumptions include reaction nearing equilibrium, spatially non-uniform diffusion, reaction dependent upon the concentration of a single reactant, and negligible reverse reaction [162]. The non-linear form of this model is defined by the rate equation as follows:

$$Q_t = Q_e(1 - e^{-k_1 t})$$

Where Q_t and Q_e represent the concentration (µg/g) of the pesticide sorbed onto the unit mass of MP at time t and at equilibrium, respectively. The term k_1 (h^{-1}) is the rate constant of the first-order reaction.

Pseudo-second order: This model explains how adsorbates adsorb onto adsorbents, with the adsorption capacity of the adsorbent being determined by the chemical bonding (interaction) between adsorbates and functional groups on the surface of adsorbents. The concept relies on equilibrium adsorption, which is determined by the quantity of adsorbate adsorbed onto the adsorbent's surface and the quantity of adsorbate adsorbed at equilibrium [163]. The fundamental assumption is that the adsorption rate is proportional to the square of the number of unoccupied sites, implying that the adsorption process is more dependent on the availability of sites than on the concentration of the adsorbate in the solution. This model presupposes that adsorption kinetics are controlled by chemisorption, involving valence forces through the sharing or exchange of electrons between adsorbent and adsorbate. The PSO model also assumes that the adsorption capacity is time-dependent and that the rate of adsorption decreases as the number of unoccupied sites decreases.

$$Q_t = \frac{{Q_e}^2 \times k_2 t}{1 + (Q_e \times k_2 t)}$$

Where Q_t is the amount of pesticide sorbed (µg/g) at time t, Q_e is the amount sorbed (µg/g) at equilibrium, t is the time, and k_2 (g μg^{-1} h^{-1}) is the rate constant for the second order kinetic model.

Elovich kinetic model: The Elovich kinetic model assumes that sorption occurs on localized sites, that there is an interaction between the sorbed ions, and that adsorption

energy increases linearly with the surface coverage [164]. It also assumes that adsorption kinetics are controlled by chemisorption, involving the formation of a chemical bond between the adsorbate and the surface, which is inherently a heterogeneous process due to the non-uniform nature of solid surfaces. This heterogeneity is further emphasized by the model's consideration of the varying activation energies for adsorption across different sites on the adsorbent's surface, suggesting that the adsorption rate decreases as the surface becomes increasingly covered.

$$Q_t = \frac{1}{\beta} \ln(\alpha\beta t)$$

Where Q_t (µg/g) is the amount sorbed at time t, α (µg g^{-1} h^{-1}) is the initial sorption rate, and β (g μg^{-1}) is the desorption constant.

Intra-particle diffusion model: According to this hypothesis, adsorbate molecules diffuse into the pores of polymer adsorbents, resulting in the physisorption mechanism [165].

$$Q_t = k_i \times t^{\frac{1}{2}} + C_i$$

Where k_i (µg g^{-1} $h^{-1/2}$) is the intra-particle diffusion rate constant, t is time, and C_i (µg g^{-1}) is the intra-particle diffusion constant, which depends on the thickness of the boundary layer.

Sorption isotherms are obtained by plotting Q_e (µg/g), which is the amount of pesticide sorbed onto the unit mass of the MP at equilibrium, against C_e (µg/L), which is the concentration of the pesticide in the aqueous phase at equilibrium.

Langmuir Isotherm: According to Langmuir's 1916 postulation, the Langmuir adsorption model explains sorption related to homogeneous surfaces where micropollutants will exhibit a strong sorption affinity and form monolayers with particular MNP sorption sites [138]. The Langmuir isotherm model is a fundamental approach to describing adsorption, emphasizing the formation of a monolayer of adsorbate molecules on the adsorbent surface, where each adsorption site binds a single adsorbate molecule. This model assumes a uniform surface with identical sites and no interactions between adsorbed molecules, leading to a saturation point where no further adsorption can occur due to all sites being occupied [166]. Another fundamental assumption is the uniformity of adsorption energies across all adsorption sites, indicating that each adsorption event occurs with the same affinity and energy, irrespective of the surface coverage. This uniformity is critical for simplifying the model but is often challenged by the heterogeneity of the actual adsorbent surfaces.

$$Q_e = \frac{Q_{max} \times b \times C_e}{1 + (b \times C_e)}$$

Where Q_e (µg/g) is the amount sorbed onto microplastic at equilibrium, C_e (µg/L) is the concentration of pesticide in the aqueous phase at equilibrium, b is the Langmuir constant (L/µg), and Q_{max} (µg/g) is the maximum sorption capacity.

Freundlich Isotherm: An empirical adsorption model, the Freundlich isotherm model applies to both mono- and multilayer sorption and assumes the initial occupation of high-

energy sites and is used to investigate the adsorption or equilibrium data into heterogeneous surfaces [138]. It assumes that the adsorption process occurs on a heterogeneous surface, where the adsorbent possesses a spectrum of binding energies rather than a single uniform energy level. This heterogeneity is fundamental to the model's ability to describe adsorption equilibria for a wide range of adsorbates on various adsorbents [167].

$$Q_e = k_f \times C_e^{\frac{1}{n}}$$

Where k_f is the Freundlich rate coefficient, and n is the Freundlich isotherm exponent.

Dubinin-Radushkevich Isotherm: The physicochemical properties of the sorption process can be effectively explained by the Dubinin-Radushkevich (D-R) adsorption model, which estimates the free energy of sorption on heterogeneous surfaces. It is a popular model for explaining the adsorption of single solutes and accounting for the impact of porosity on heterogeneous adsorbent surfaces [138]. It assumes that adsorption occurs through a micropore-filling mechanism, where the adsorbate molecules are adsorbed into the micropores of the adsorbent material. This model contrasts surface adsorption models like Langmuir, which assume adsorption occurs on a homogeneous surface.

$$Q_e = Q_{max} exp^{-(\beta\varepsilon^2)}$$

Where Q_{max} is the maximum sorption capacity (µg/g), ε (kJ/mol) is the sorption potential or Polanyi potential, and β is a constant related to the free energy of sorption.

In this equation, ε is calculated as follows:

$$\varepsilon = RT \times \ln(1 + \frac{1}{C_e})$$

Where R = 8.314 $Jmol^{-1}K^{-1}$ is the universal gas constant, T = absolute temperature (K), and C_e (µg/L) is the sorbate concentration in the aqueous phase at equilibrium.

Temkin Isotherm: It presupposes that the heat of adsorption of all the molecules in the layer decreases linearly with coverage due to adsorbate-adsorbate interactions rather than remaining constant, as in the Langmuir model. Another fundamental assumption of the Temkin isotherm model is that it does not adhere to the ideal assumption of all sites possessing equal energy for adsorption. Instead, it accounts for the distribution of energies across the adsorption sites, reflecting a more realistic scenario where surface heterogeneity plays a significant role.

$$Q_e = \frac{RT}{b} \times ln(k_t C_e)$$

Where R = 8.314 $Jmol^{-1}K^{-1}$ is the universal gas constant, T = absolute temperature (K), C_e (µg/L) is the concentration of sorbate in the aqueous phase at equilibrium, k_t is the Temkin rate coefficient, and b is the Temkin constant.

Redlich-Peterson Isotherm: The Redlich-Peterson isotherm model is a flexible adsorption model that describes adsorption equilibria over a broad range of concentrations by combining important assumptions from both the Langmuir and Freundlich isotherms.

One of the fundamental assumptions of the Redlich-Peterson model is that it does not strictly adhere to the monolayer adsorption limitation of the Langmuir model, thereby allowing for the description of adsorption phenomena that may extend beyond monolayer coverage. The model assumes that the adsorption process is homogeneous or heterogeneous, with a finite number of sites that can follow a Langmuir or Freundlich adsorption mechanism.

$$Q_e = \frac{k_{rp} \times C_e}{1 + (a \times {C_e}^n)}$$

Where k_{rp} (L/µg) is the Redlich-Peterson rate constant, a is the Redlich-Peterson parameter, and n is the exponential factor.

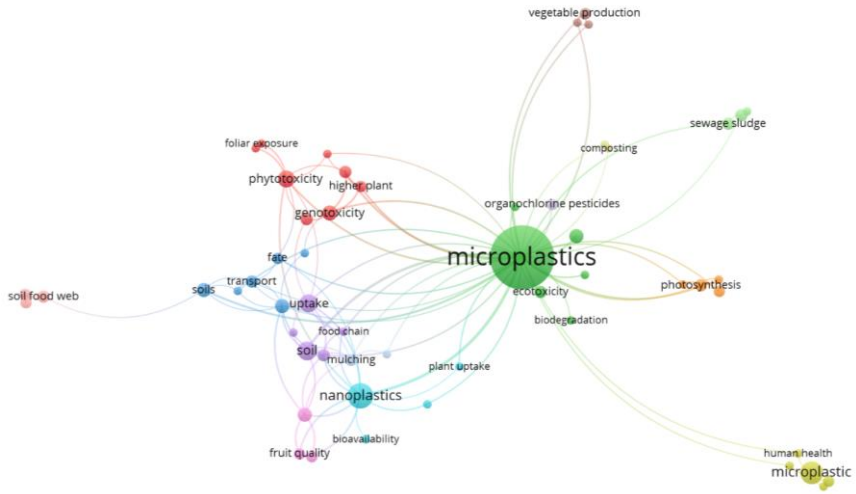

Figure 10: Hot topics in the field of microplastics and agriculture. Generated using VOS Viewer

1.6 Effects of Microplastics on Plants

The effect of MNPs on plant health has garnered attention due to the widespread presence and reporting of MNPs in agricultural fields across the globe and their proximity to the human food chain. The effects of MNP exposure to plants seem to be type and concentration-dependent and could lead to multiple impacts on plant health, productivity, germination, and metabolism. Studies have shown that MNPs can adhere to the surfaces of seeds and roots, inhibiting seed germination, root elongation, and water and nutrient absorption, ultimately restricting plant growth. Furthermore, MNPs have been found to induce oxidative stress, cytotoxicity, and genotoxicity in plants, leading to alterations in plant growth, mineral nutrition, photosynthesis, and metabolite profiles in plant tissues. Nanoplastics have been shown to penetrate plants more easily than larger plastic particles, causing more severe phytotoxic effects due to their ability to permeate through biological membranes. This penetration can lead to oxidative damage, pore space blockages on root surfaces, and decreased nutrient and water uptake, negatively affecting plant health and productivity.

The presence of MNPs in agricultural soils has raised concerns about their impact on crop productivity and food safety. Studies have demonstrated that MNPs can be taken up by crops, accumulate in grains, and adversely affect crop yield and the nutritional quality of grains, including a decrease in the content of mineral elements, amino acids, and unsaturated fatty acids, directly threatening food safety and human health. For instance, research has demonstrated that *Allium sativum L.* exposed to PS nanoplastics substantially reduces chlorophyll content, indicating reduced chlorophyll production and changes in antioxidant enzyme activity, indicating a complicated oxidative stress response [168]. By negatively affecting spindle formation and causing micro-nucleated cells in *Allium cepa* root tip cells, PS microplastics (Ps-MPs) of various sizes and concentrations can induce cytotoxic and nuclear damage, suggesting direct DNA damage to plant cells [169].

The buildup of PS MPs in the *V. faba* root can affect the flow of nutrients and water by obstructing cell wall pores or connections. According to Urbina et al. [170], PE particles

may build up in the rhizosphere of maize, hindering the plant's ability to absorb nutrients. The bioaccumulation of PE also reduces the nitrogen in hydroponically grown maize. Isotopic research revealed that around 30% of the carbon in the maize rhizosphere came from PE. Wheat exposed to PS had a significantly higher C and N content but absorbed and accumulated fewer micronutrients (Fe, Mn, Cu, Zn) [171]. Exposure to foliar-sprayed PS resulted in a loss of micronutrients (Mn, Cu) and critical amino acids in lettuce and a considerable decline in the leaf C:N ratio as PS concentration increased [172]. Polystyrene MNPs have also been shown to induce size-dependent effects on *Lepidium sativum* [173], while other types, including PP, PE, and PVC, have been shown to induce oxidative stress, impact biomass production, germination inhibition, and chlorophyll [174]. They have been reported to impact root and shoot growth, leaf size, and chlorophyll in pumpkin plants [175].

In the case of the fava bean plant, MNPs have been reported to produce concentration and size-dependent reduction or increase in biomass and catalase (CAT) enzyme activity, increase in superoxide dismutase (SOD), and peroxidase (POD) and genotoxic and oxidative damage [176]. A study on PVC MNP exposure to lettuce reported effects on the total length, surface area, volume, and diameter of roots and increased SOD activity [177], while PS MPs led to a reduction in dry weight, plant height, photosynthetic pigment content, plant nutritional quality, and increased oxidative stress [172]. They also affect arbuscular mycorrhizal fungi, increasing aboveground biomass in onion plants [178]. Exposure of wheat to PS MPs led to enhanced wheat seedling growth, increased root elongation, increased carbon, nitrogen content, plant biomass, and a reduction in the shoot-to-root biomass ratio [171]; exposure to LDPE and biodegradable MPs affected plant height, root and shoot biomass and fruit count, fruit biomass, root/shoot ratio, leaf area, chlorophyll content, and stem diameter [179]. Exposure of rice plants to PS MNPs led to various physiological and biochemical changes. These included reduced shoot biomass, impacts on antioxidant enzyme activity, and reduced amino acid content, saccharides, organic acids, lipids, and polyol metabolites in plant leaves [180]. Additionally, there was an increase in antioxidant enzyme activity, a reduction in root length, an increase in lateral roots, enhanced carbon metabolism, and inhibition of jasmonic acid and lignin biosynthesis [181]. Other studies reporting the impacts of MNP exposure on plant and crop health have been detailed in Table 5.

Notable is that most studies were conducted using regularly shaped, spherical, primary MNPs (manufactured in specific sizes), which might not be a realistic scenario. Furthermore, the exposure concentrations used in most of these studies are very high and might not be environmentally relevant. Nevertheless, these findings underscore the urgent need for further research to fully understand the implications of MNP pollution on agricultural systems, crop plants, and human health.

Table 5: Reported effects of MNP exposure on plant health.

Plant Species	Common name	MP polymer type	MP particle size studied	MP concentration	Reported effects	Reference
Lepidium sativum L.	Garden cress	PS	50, 500, 4800 nm	10^3–10^7 particles/mL	Reduction in seed germination. Root growth increased due to exposure to 50 nm particles, whereas it was reduced when exposed to 500 nm particles.	[173]
		PP, PE, PVC, PE+PVC	<0.125 mm	184 mg/kg	Oxidative stress, including effects on H_2O_2, ascorbic acid, and glutathione production. Reduction/Increase in biomass, dependent upon polymer type. Germination inhibition. Effect on shoot height. Impacts on chlorophyll a, chlorophyll b, carotenoid, and aminolaevulinic acid levels.	[174]
Cucurbita pepo L.	Pumpkin	PE, PVC, PP, PET	40–50 µm	0.02%, 0.10%, 0.20% (w/w)	Impacts on root and shoot growth, leaf size, chlorophyll content, and photosynthetic efficiency.	[175]
Vicia faba L.	Fava bean	PS	100 nm, 5 µm	10, 50, 100 mg/L	Reduction in root length with concentration. Size-dependent reduction or increase in biomass and catalase (CAT) enzyme activity, increase in superoxide dismutase (SOD) and peroxidase (POD), and genotoxic and oxidative damage.	[176]
Allium cepa L.	Onion	PES	1.70 µm	0.4% (w/w)	A combined effect of PES fibers and arbuscular mycorrhizal (AM) fungi increases aboveground biomass.	[178]

Lactuca sativa L.	Lettuce	PVC-a and PVC-b	100 nm–18 µm and 18–150 µm	0.5%, 1%, 2% (w/w)	Concentration and type-dependent effects on total length, surface area, volume, and diameter of roots and increased SOD activity. Size and type dependent effects on chlorophyll and carotenoid content.	[177]
		PS	93.6 nm	0, 0.1 and 1 mg/L	Reduction in dry weight, plant height, photosynthetic pigment content, and nutritional quality. Increase in oxidative stress.	[172]
Glycine max (L.) Merr.	Soybean	PE, (Bio) mulch film	2 × 2 cm,1 × 1 cm and 0.5 × 0.5 cm debris	0%, 0.1%, 0.5%, 1% (w/w)	Reduction in plant height, culm diameter, leaf area, and root/shoot ratio due to PE and impacts on germination viability and root biomass due to bio mulch films.	[182]
		PE	6.5 and 13 µm	0, 10, 50, 100, 200, and 500 mg/L	Size and concentration-dependent effects on plant dry weight and root length. Impact on germination parameters.	[183]
Vigna radiata	Mung bean	PE	6.5 and 13 µm	0, 10, 50, 100, 200, and 500 mg/L	Size and concentration-dependent effects on plant dry weight and root length. Impact on germination parameters.	[183]
Cucumis sativus L.	Cucumber	PS	100, 300, 500, 700 nm	50 mg/L	Size-dependent effect on root activity, MDA content, and proline content. Increase in soluble protein content and size-dependent reduction in Mg, Ca, and Fe content.	[184]
		PS	100, 300, 500, 700 nm	50 mg/L	Decrease in plant biomass, chlorophyll a, chlorophyll b, soluble sugar, carotenoid, and proline content. The fluorescence of cucumber leaves was significantly reduced in the presence of 100 nm PSNPs. Malondialdehyde, proline, peroxidase gene expression, enzyme activity, and hydrogen peroxide content significantly increased in cucumber leaves exposed to 700 nm PSNPs. Furthermore, increasing PSNP particle size	[185]

					decreased relative expression levels and activities of the major antioxidant enzymes superoxide dismutase and catalase, while vitamin C and soluble protein content significantly increased.	
Triticum aestivum L.	Wheat	PS	100 nm	0.01–10 mg/L	Enhanced wheat seedling growth, increased root elongation, Increased carbon and nitrogen content, Increased plant biomass, reduced shoot-to-root biomass ratio	[171]
		Macro LDPE: Macro Bio: Micro:	6.92 × 6.10 mm 6.98 mm × 6.01 mm 50 µm–1 mm	1% (w/w)	Type-dependent effect on plant height, root and shoot biomass and fruit count, fruit biomass, root/shoot ratio, leaf area, chlorophyll content, and stem diameter.	[179]
		PS	40 nm, 1 µm	0, 10 mg/L	Reduction of Cd contents in leaves and alleviation of Cd toxicity to wheat. Reduction in superoxide dismutase (SOD) activity. Formation of long-lived radicals in leaves after exposure to Cd and elevated carbohydrate and amino acid metabolisms.	[186]
Allium fistulosum L.	Spring onion	PA beads: PES fibers: HDPE, PP: PS, PET:	15–20 µm 5000 µm length, 8 µm diameter 2–3 mm spheres 2–3 mm cylinders	PES: 0.2% Others: 2.0% (w/w)	Type and concentration-dependent effects on plant biomass, tissue elemental composition, root traits, and soil microbial activities.	[187]
Phaseolus vulgaris L.	Common bean	LDPE, Bio	250–500 µm, 500–1000 µm	0.5%, 1.0%, 1.5%, 2.0%, 2.5% (w/w)	Concentration-dependent effects on specific root nodules, specific root length, leaf area, and chlorophyll content in LDPE plastic-type and	[188]

					concentration-dependent effects on specific root length, root nodules, reduction in root, shoot, and fruit biomass in Bio-MP type.	
Brassica rapa L.	Chinese cabbage	PS	70 nm, 5 µm	10 mg/kg	Potential size-dependent changes to plant growth and photosynthetic parameters.	[189]
Lycopersicon esculentum L.	Tomato	PS, PP, PE	52–368 µm	10, 100, 500, 1000 mg/L	Concentration-dependent inhibitory effects on seed germination and growth.	[190]
Zea mays L.	Maize	PE	3 µm	0.0125 mg/L 100 mg/L	Accumulation in the rhizosphere, decreased transpiration, nitrogen content, and plant growth. Impaired water and nutrient uptake.	[170]
Oryza sativa L.	Rice	BM and PE	50 µm	1% (w/w)	Reduction in dry weight and height of the plant, oxidative stress, and effects on nitrogen metabolism and photosynthesis.	[191]
		PS	8.5 – 30.7 µm	50 mg/L and 250 mg/L	Reduction in shoot biomass impacts antioxidant enzyme activity and reduces amino acid, saccharide, organic acid, lipid, and polyol metabolites in plant leaves.	[180]
		PS	19 ± 0.16 nm	0, 10, 50, and 100 mg/L	Significant increase in antioxidant enzyme activity, reduction in root length, increase in lateral root number, increase in carbon metabolism, and inhibition of jasmonic acid and lignin biosynthesis.	[181]
A. thaliana L		PS-SO_3H: PS-NH_2:	55 nm 71 nm	0.3,1.0 g/kg 10, 50, 100 µg/mL	Reduction in above-ground biomass, seedling growth, and root elongation.	[192]

Data partially adapted from [193]

1.7 Bioaccumulation of Micro and Nano Plastics in Plants

Research regarding the uptake and bioaccumulation of MNPs in plants and crops is still in its infancy. However, MNPs, ranging from about <100 nm to about 1 micron, have been speculated to penetrate plant roots and accumulate in various plant parts. Studies have demonstrated that submicrometric PS and PMMA particles can enter the stele of crop plants like wheat and lettuce, primarily through a crack-entry mode at lateral root emergence sites [194]. Other such studies have looked at cress (*Arabidopsis thaliana*), pea (*Pisum sativum*), rice (*Oryza sativa*), carrot (*Daucus carota*), orange jasmine (*Murraya exotica*), radish (*Raphanus sativus*), maize (*Zea mays*), onion (*Allium cepa*) seeds, cucumber (*Cucumis sativum*), and fava bean (*Vicia faba*). For example, PS and PMMA NPs were found to accumulate wheat and lettuce roots and were speculated to reach the above-ground parts through the transpiration stream [194]. Also, 20 nm PS nanoparticles were reported to accumulate in the pea plant [195]. In another study of wheat, 200 nm PS-Eu (PS nanoplastics doped with europium chelate) were found to accumulate in the plant roots with minimal presence in the plant shoot [196]. In the case of Italian lettuce, radish, wheat, and corn, NPs were uptaken after a short exposure period of just seven days; however, their presence in the above-ground parts was not confirmed [197]. A detailed description of all such studies and their observations regarding uptake and bioaccumulation is provided in Table 6.

Based on current knowledge, the absorption of MNPs in crops is complicated and influenced by various elements, including the structure of the plant, the charge and other properties of the plastic polymer such as shape, size, and type, and the features of the surrounding media, such soil/water. To be taken up and translocated by the plants, MNPs must pass a series of physiological, chemical, and physical barriers that constitute the size exclusion limits (SELs). In general, absorption could occur by a crack entrance method in the roots, and the transpiration stream through intercellular spaces or the apoplastic pathway could aid its upward translocation. It has also been suggested that one potential uptake route is the symplastic pathway, which entails endocytosis via plasmodesmata apertures and the subsequent passage of nanoparticles across cell membranes. In addition to entering through the roots, it has been demonstrated that nanoplastics can also be absorbed through the stomatal entry pathway, followed by a downward translocation from the leaf to the root.

The possible implications of this phenomenon are grave. The impact of accumulation and toxic effects on plant health could result in changes to plant health, including nutritional quality, biomass production, and decreased crop production. Furthermore, the accumulation of MNPs in crops could open another pathway for MNPs to enter the food chain, affecting food safety and human health. Studies have shown that nanoplastics can enter crops like peanuts and rice grains, affecting the yield and nutritional quality by decreasing the content of mineral elements, amino acids, and unsaturated fatty acids. In order to create viable remediation strategies that would guarantee food safety and security, more research is required to fill in the knowledge gaps about how nanoplastics enter plants and the variables that affect phytotoxicity levels. Although plants have strong cell walls to defend them from nanoplastics, they can still absorb them from soil and water. The amount of nanoplastics that plants absorb is inversely correlated with the size of the nanoparticles. The urgency of developing measures to reduce nanoplastic contamination and protect food quality and agricultural output is highlighted by this thorough understanding.

Table 6: Studies reporting the accumulation of MNPs in plant samples.

Plant species	Common name	Particle type	Particle size used	Exposure concentration	Observations	Reference
Triticum aestivum and *Lactuca sativa*	Wheat, Lettuce	PS PMMA	0.2 µm and 2, 5, 7 and 10 µm	50 mg/L in hydroponic and 150 mg/kg in sand	The transpiration stream transported 0.2 µm and 2 µm plastic beads from roots to shoots. No uptake of larger-sized beads was observed. Accumulation was also observed in the plant roots grown in sandy soil but less than in hydroponic media. Higher uptake was observed in higher transpiration conditions.	[194]
Lepidium sativum	Garden cress	PS	50, 500, and 4800 nm	103 to 107 particles/mL.	Plastic particles accumulate in seed pores. The germination rate was significantly reduced after eight hours of exposure for all three sizes of plastics, with increased adverse effects with increasing plastic sizes. Impacts on germination are likely due to the physical blockage of the pores in the seed capsule.	[173]
Arabidopsis thaliana	Thale cress or mouse-ear cress	Negatively and positively charged gold (Au) NPs	13.4 ± 1.3 nm, and 12.1 ± 0.8 nm, respectively	10 mg/L	The root cap's border cells exhibited charge-specific behavior: positively charged NPs increased mucilage synthesis and adhered to it, preventing transfer into the root tissue. Negatively charged NPs	[198]

					could move into the apoplast but could not bind to the mucilage.	
Pisum sativum	Pea	PS	20 nm	40 and 20 mg/kg in soil	MPs moved onto aerial sections via the apoplast pathway along the vascular bundle's cell walls after infiltrating into partially formed Casparian strips during root formation.	[195]
Oryza sativa	Rice	PS	80 nm and 1 µm	40 mg/L	Roots, stems, and leaves of rice seedlings contained both nano- and micro-sized PS microspheres.	[199]
Daucus carota	Carrot	PS	0.1–1 µm (small-sized PS) and 5 µm (large-sized PS)	0 and 20 mg/L	While 0.2 µm PS beads reached the leaves, 1 µm microplastics only entered the intercellular layer of carrot roots and accumulated there. However, its frequency of occurrence was low. Small-sized PS in carrot roots was 50–150 nm, and its frequency of occurrence was higher than that of large-sized PS; small-sized PS was also found in the leaves. PS was mainly found in the pectin of the intercellular space and intercellular layer.	[200]
Murraya exotica	Orange jasmine	poly(styrene-co-maleic anhydride) (SMA)	12 ± 4.5 nm	55 µg/mL	Uptake and translocation were confirmed in the plant stem. Particles were trapped along the lignified cell walls.	[201]
Triticum aestivum and	Wheat and Lettuce	PS-Eu	200 nm	0 - 50,000 µg/L	PS-Eu particles accumulated mainly in the roots, while transport to the shoots was limited.	[196]

Lactuca sativa)						
	Italian lettuce, radish, wheat and corn	PS	100 nm and 5 µm	1 mg/L and 5 mg/L	Uptake only confirmed for 100 nm particles. Uptake was observed in plant roots only in the case of lettuce and radish. In the case of wheat and corn, accumulation was observed in seedling root and seed germ. Translocation to root and aerial parts was not observed in any tested sample. Nanoplastics were taken up by plant seeds even at a very early growth stage (< 7 days after sowing).	[197]
Zea mays	Maize/corn	Carboxyl-modified polystyrene nanoplastics (PS-COOH) and Amino-modified polystyrene nanoplastics (PS-NH_2)	22.0 ± 1.5 nm and 24.0 ± 2.2 nm respectively	0, 10, 50, 100, 200, 400 and 500 ng/spot	The vascular bundle was the main pathway for the leaf-to-root translocation of nanoplastics. Aggregation limits the nanoplastic translocation to roots over a prolonged period. The impacts of differently charged nanoplastics on plant physiology were evaluated. Due to electrostatic attraction to the negatively charged cell wall, positively charged PS-NH2 association with the leaf surfaces was significantly more than negatively charged PS-COOH.	[202]
Arabidopsis thaliana	Thale cress or	Functionalized polystyrene:	200 nm	10 and 50 µg/ml	Arabidopsis can uptake and transport nanoplastics of less than	[192]

	mouse-ear cress	PS-SO_3H and PS-NH_2 for biological effects and PS-COOH for uptake visualization			200 nm regardless of the surface charge. The pathway of uptake and transport of nanoplastics in root tissues differ between differentially charged nanoplastics. Although positively charged nanoplastics (PS-NH2) had a more substantial effect on the roots, their uptake and internalization were lower than those of negatively charged nanoplastics. PS-NH2 stimulated the roots to produce high levels of exudates, which influenced the stability of PS-NH2 and limited its uptake.	
Cucumis sativus	Cucumber	PS	100, 300, 500, and 700 nm	50 mg/L	PSNPs initially accumulated in the root system before being transported to aboveground parts. Finally, they were distributed in the leaves, flowers, and fruits through the stems.	[184]
Lactuca sativa	Lettuce	PS	93.6 nm	1 mg/L	Accumulation was observed in the leaf, phloem, and roots—internalization in the cytoplasm (inside the cell) and aggregation in the stoma.	[171]
Oryza sativa	Rice	PS	20 nm	10 mg/L	PS-NPs entered the rice roots and were distributed in the intercellular spaces. Aquaporins played a role in the uptake of PS-NPs by rice roots.	[181]

Vicia faba	Fava bean	PS	5 µm and 100 nm	10, 50, and 100 mg/L	A significant number of 100 nm PS-NPs entered the root tips.	[176]


Illustration generated using DALL-E. Copyright: Harshit Sahal

1.8 Detection of Micro and Nano Plastics in Plants

The selection and improvement of detection techniques are critical to precisely identifying micro/nanoplastic absorption and translocation in plants. The fact that micro/nanoplastics vary widely in size, shape, and chemical makeup makes it difficult to standardize detection techniques, which is one of the main problems [203]. Since there are currently no widely accepted standard procedures and protocols for effectively extracting micro/nanoplastics from plant tissues, scientists are looking into several approaches, including chemical digestion, density separation, and enzymatic digestion, to solve the difficulties [203]. Multiple analytical techniques are currently being explored for this purpose, including confocal laser scanning microscopy (CLSM)[173], [176], [181], [184], [192], [194], [197], [204], [205], [206], [207], X-Ray computed nano-tomography (nano-CT) clubbed with dark-field hyperspectral imaging (DF-HIS) [198], transmission electron microscopy (TEM) [208], time-resolved optical imaging/fluorescence imaging and scanning electron microscopy (SEM) [196]. Often, the tiny size, erratic shape, and varied polymeric composition of MNPs pose difficulties for these techniques, making it difficult to identify them in complex matrices [203]. The potential for micro-spectroscopic techniques to detect nanoplastics (NPs), which are particularly difficult to identify since their size is smaller than the spatial detection limit of most conventional analytical instruments, is also being investigated. While traditional microscopic techniques, such as light and electron microscopy, have been applied to detect micro/nanoplastics in tissues, they may lack the necessary resolution to differentiate between micro/nanoplastics and similar cell components [203].

The presence of cellulose, lignin, and other bioactive molecules in plant tissues can create background “noise” during analysis, making it difficult to differentiate between the MNPs and other organic matter [203]. For instance, a recent study that aimed at quantifying NPs using py-GC/MS in wheat and Arabidopsis roots was unsuccessful due to the presence of styrene peaks (monomers of polystyrene) in negative control samples due to the degradation of plant material during pyrolysis [209]. Due to its capacity to deliver quick, non-destructive, high-throughput examination, spectroscopic techniques—most

notably Fourier-transform infrared spectroscopy (FTIR) and Raman spectroscopy—have also found increasing application [203]. However, although FTIR has been widely applied for detecting and identifying MNPs in various environmental samples, its application for detecting MNPs in plant samples remains limited. On the other hand, Raman spectroscopy has been highlighted for its utility in the facile detection of MNPs, offering early diagnosis of potential risks to environmental matrices. As a distinct analytical method for examining the interactions between plants and nanomaterials, μ-XRF has also been explored with its ability to identify several elements with lateral resolution, and it provides a significant understanding of the fundamental processes involved in the absorption, movement, and build-up of MNPs in plant systems [210].

Scanning Electron Microscopy (SEM) is also essential in analyzing and identifying micro and nanoplastics, offering detailed insights into their accumulation in various environments. One of the primary advantages of SEM is its ability to provide high-resolution images, enabling the detailed visualization of nanoparticles [211]. However, it has not been explored as a suitable technique for quantitative analysis, but it has been employed as a complementary analytical approach in tandem with other approaches [172].

The need to investigate the bioaccumulation of MNPs in plants and crops and their proximity to the human food chain has led scientists to explore the above-mentioned analytical techniques, and it necessitated the formulation of a standardized analytical approach. In this context, CLSM emerges as one of the most widely utilized approaches and could help explore the trends and mechanisms behind this phenomenon in the natural environment. Confocal Laser Scanning Microscopy is a sophisticated imaging technique capable of producing high-resolution 3-dimensional images of structures within tissues, non-invasively, offering significant advantages over conventional microscopy methods by allowing for the detailed real-time observation of cellular and subcellular processes.

The technology operates by scanning a sample sequentially, point by point, and layer by layer, with a focused laser beam, which is then detected through a pinhole to ensure that only light from the focal plane is captured. This method has several benefits and has been widely utilized for detecting and localizing MNPs in complex biological matrices, including plant tissues. First, CLSM has a high spatial resolution that makes it possible to image samples in 3 dimensions with great detail at the micrometer and nanometer levels. Furthermore, because CLSM is non-destructive, it enables in situ chemical analysis of plants without requiring significant sample preparation or staining. Moreover, CLSM enables depth profiling of samples, providing information on deep structures and composition gradients. These benefits make CLSM an essential technique for high spatial resolution and thorough structural information studies of biological tissues and multilayer systems. It has been widely used to identify ingested MNPs in various organisms and has been found widely successful. It has also been adapted to study the uptake of MNPs by plants (Table 7).

Although CLSM is a powerful tool in biological and biomedical research, offering 3-dimensional, high-resolution imaging capabilities, there are certain limitations associated with its use. The spatial resolution is restricted by diffraction to approximately half the light's wavelength, which is one of the main drawbacks; however, methods such as structured illumination have been devised to improve this feature [212]. Sample preparation presents difficulties in controlling compound diffusion during the preparation and observation procedures, which can impact the imaging's accuracy, mainly when dealing with turgid plant organs [213]. However, this can be minimized through careful sample handling, preparation, and incorporation of QA/QC procedures. Although improvements in scanning techniques address these limitations, scanning speed—especially with galvanometric scanning mechanisms—can severely limit image speed and quality [214]. Moreover, several factors, such as pinhole diameter, detector gain, laser intensity, and

scanning speed, affect the quality of confocal imaging and must be carefully optimized to provide high-quality images.

In the specific case of detection of fluorescently labeled MNPs in plant tissues, CLSM and acquired image quality can also be limited by other factors, such as the presence of pigments and metabolites in the plant tissue that could result in autofluorescence from the plant tissue [215]. This autofluorescence signal originating from the plant tissue makes it harder to differentiate and isolate the fluorescence signal from the accumulated MNPs. If not appropriately controlled during image acquisition or processing, this could lead to over or underestimation of accumulated MNPs and inaccurate localization. However, some steps could be followed to deal with this issue. During image acquisition, the autofluorescence of the plant sample can be eliminated or minimized using a time-gated acquisition, which selectively acquires the fluorescence signal during a specific period corresponding to the fluorescence of MNPs and eliminates the autofluorescence signal [216]. Even after the optimization of the acquisition step and minimization of background autofluorescence collection, some residual background or autofluorescence is expected when analyzing plant samples using fluorescence-based CLSM. However, this can be dealt with later during image processing, whereby the mean background or autofluorescence from the control samples can be subtracted from individual sample images using the data from control sample images where MNPs would not be present. These steps have been detailed and described in Publication 3.

Table 7: Techniques utilized for the qualitative detection/localization of MNPs in plant samples.

Primary technique utilized	**Plant species investigated**	**Polymer detected**	**Particle size investigated**	**Complementary technique used**	**Reference**
Confocal laser scanning microscopy (CLSM)	Wheat and Lettuce	PS	0.2 µm and 2, 5, 7 and 10 µm	SEM and X-ray computed microtomography	[194]
	Lepidium sativum or Garden cress	PS	50, 500, and 4800 nm	N/A	[173]
	Pisum sativum or Pea	PS	20 nm	N/A	[204]
	Oryza sativa or Rice	PS	80 nm and 1 µm	N/A	[205]
	BY-2 cells	PS	20 nm, 40 nm, 100 nm, 1000 nm	N/A	[207]
	Italian lettuce, radish, wheat and corn	PS	100 nm and 5 µm	N/A	[197]
	Thale cress (*Arabidopsis thaliana*) and wheat (*Triticum aestivum*)	Negatively charged PS (carboxylate-modified)	40 nm and 1 µm	Pyrolysis gas chromatography-mass spectrometry (GC/MS)	[206]

	Arabidopsis thaliana	PS-COOH	200 nm	TEM and SEM	[192]
	Cucumber (*Cucumis sativus*)	PS	100, 300, 500, and 700 nm	SEM	[184]
	Rice (*Oryza sativa L.*)	PS	20 nm	N/A	[181]
	Vicia faba or fava bean/broad bean	PS	5 µm and 100 nm	N/A	[176]
Scanning electron microscopy (SEM)	Lettuce (*Lactuca sativa L.*)	PS	93.6 nm	TEM	[172]
Transmission electron microscopy (TEM)	Onion seeds and root (*Allium cepa*)	PS	50 nm	N/A	[208]
	Carrot (*Daucus carota L.*)	PS	0.1–1 µm (small-sized PS) and 5 µm (large-sized PS)	N/A	[200]
Fiber optic fluorimetry	Maize (*Zea mays L.*)	Carboxyl-modified poly styrene nanop lastics (PS-COOH) and amino-modified polystyrene nanoplastics (PS-NH2)	22.0 ± 1.5 nm and 24.0 ± 2.2 nm	Fluorescence microscopy imaging	[202]
Time-gated luminescence	Wheat (*Triticum aestivum*) and	PS	200 nm	SEM	[196]

through the time-resolved fluorescence of the Eu chelate	lettuce (*Lactuca sativa*)				
Two-photon excitation and time-resolved (TPE-TR) optical imaging	*Murraya exotica* or orange jasmine	Poly(styrene-co-maleic anhydride) (SMA)	12 ± 4.5 nm	Optical microscopy and TEM	[201]
Enhanced dark-field microscopy combined with hyperspectral imaging (DF-HSI)	*Arabidopsis thaliana*	Negatively or positively charged gold NPs	13.4 ± 1.3 nm, and 12.1 ± 0.8 nm, respectively	X-ray computed nano-tomography (nano-CT)	[198]

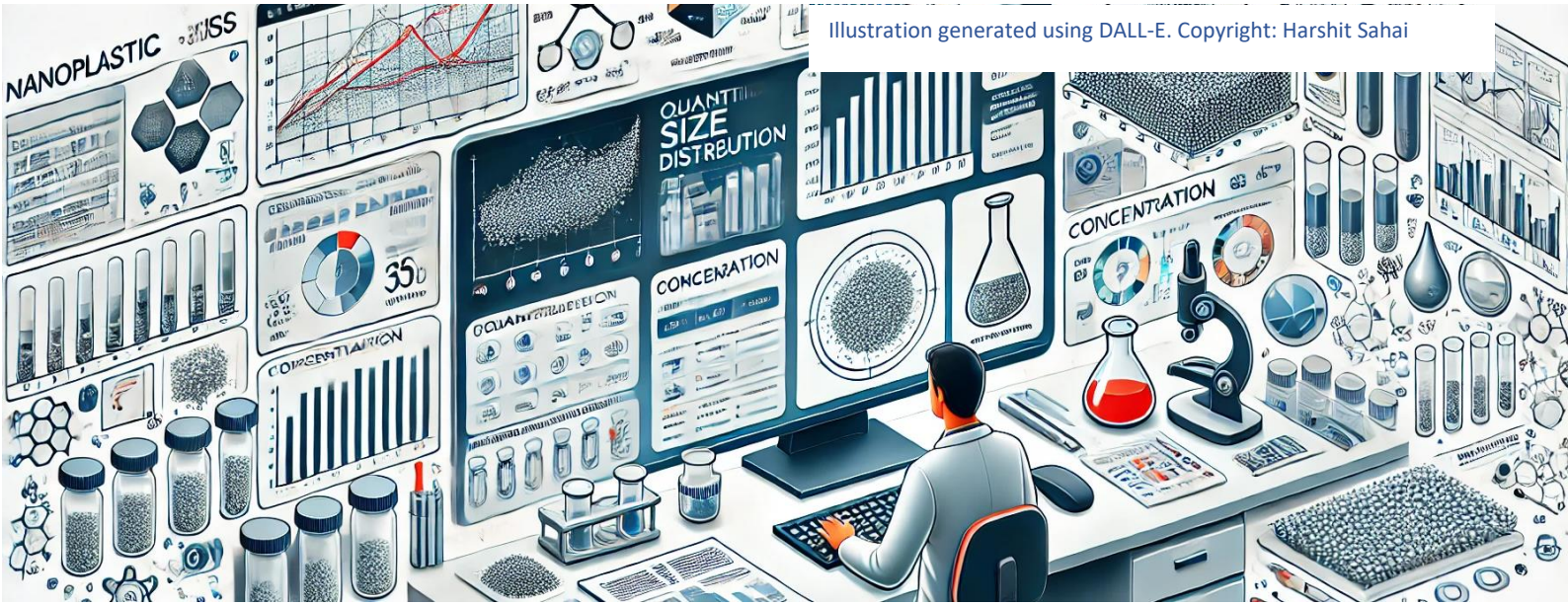

Illustration generated using DALL-E. Copyright: Harshit Sahai

1.9 Quantification of Micro and Nano Plastics in Plants

The quantification of MNPs in various environments employs diverse analytical techniques, each with unique advantages and limitations. Several techniques, including dynamic light scattering (DLS), nanoparticle tracking analysis (NTA), tunable resistive pulse sensing (TRPS), transmission electron microscopy (TEM), and scanning electron microscopy (SEM), as well as separation/fractionation methods such as centrifugal liquid sedimentation (CLS) and field-flow fractionation (FFF)–multi-angle light scattering (MALS) combined with pyrolysis gas chromatography-mass spectrometry (py-GC/MS) or Micro-Raman spectroscopy are being explored for the physiochemical characterization and quantification of nanoplastic particles [217]. In addition, UV-Vis spectrophotometry, chromatography, total organic carbon analysis, and qualitative methods like FTIR and Raman spectroscopy play significant roles in determining the number, amount, type, and specifications of MNPs [218]. For example, Keys et al. demonstrated the usefulness of flow cytometry coupled with FTIR analysis for the qualitative and quantitative assessment of MNPs ingested by seabirds [219]. In another study by Wu et al., the authors demonstrated the applicability of matrix-assisted laser desorption/ionization–time-of-flight mass spectrometry (MALDI–TOF MS) for MNP identification/quantification in environmental samples [220]. Other approaches include thermo-analytical methods coupled with mass spectrometry, such as (Py)-GC-MS, TGA-MS, and TED-GC-MS [221], as well as single particle tracking [222]. However, most previously reported analytical techniques involve long, complex sample preparation and extraction procedures.

Only a few studies have proposed specific analytical methods for quantifying accumulated MNPs in plant samples. For example, Luo et al. utilized ICP-MS in order to identify lanthanide Eu chelates incorporated into 200 nm PS NPs that were accumulated in wheat and lettuce plant tissues, and subsequently, the Eu concentration was used to estimate the amount of NPs [196]. Single-particle ICP-MS has been employed previously for detecting and quantifying gold nanoparticles in the 50 – 1200 nm range in environmental waters and has proven successful [223]. This technique has also been employed to detect and quantify gold nanoparticles in tomato tissues after sample digestion using Macerozyme R-10 [224]. Another study demonstrated its potential in quantifying

copper nanoparticles in lettuce, kale, and collard leaves [225]. The last two studies, however, utilized sample pre-treatment steps and enzymatic digestion and were not explicitly focused on plastic polymers.

Another recent analytical approach highlighted in recent years is py-GC/MS. The method involves the breakdown of a sample at high temperatures, followed by separating components by GC/MS analysis. One study, for example, aimed to quantify the uptake of PS NPs using py-GC/MS in wheat and Arabidopsis roots grown in the presence of 40 nm and the 1 µm PS spheres. However, the study was unsuccessful due to styrene peaks (PS monomers) in negative control samples formed due to the degradation of plant material during pyrolysis [209]. Although not focused on plant samples, another study utilized this approach to detect and quantify PS and PMMA nanoparticles in aquatic animals [226]. The protocol utilized alkaline digestion and protein precipitation to extract nanoplastics from tissues, and the procedure exhibited good reproducibility and high sensitivity with the respective detection limits of 0.03 µg/g for PS NPs and 0.09 µg/g for PMMA NPs. However, results strongly depend on sample preparation, pyrolysis type, and pyrolysate transfer, making inter-lab repeatability and comparison difficult [227].

A significant obstacle to accurately quantifying and identifying micro/nanoplastics in plant tissues is their low levels. Standardized procedures for collecting, fractionating, characterizing, and quantifying small plastic particles in terrestrial systems are lacking, leading to underestimation, especially for smaller particle sizes. It has been observed that the detection limit for PS using py-GC/MS is 0.003 µg per pyrolysis analysis cup. This amount equals 5450 PS particles at 1 µm or 8.5 × 107 PS particles at 40 nm. Only a large number of PS particles inside plant roots may be detected using the py-GC/MS approach [209]. In contrast, confocal microscopy has substantially lower detection limits since it can identify a single 1 µm PS particle or several 40 nm PS particles in an aggregate [209]. Furthermore, confocal microscopy allows spatial resolution and 3D reconstruction of internalized MNPs and can help visualize the localization of plastic beads in plants, providing valuable insights into their distribution.

Confocal laser scanning microscopy has been used in various studies to analyze MNP uptake by plants (Table 7) qualitatively. However, although it provides 3-dimensional, high-resolution imaging capabilities, specific issues must be overcome. When working with turgid plant organs, sample preparation can be challenging in controlling chemical diffusion during the preparation and observation operations, affecting imaging accuracy [213]. Furthermore, several variables that must be adjusted correctly to produce high-quality images include pinhole diameter, detector gain, laser intensity, and scanning speed. Another critical factor that affects this technique is the presence of autofluorescence in plant tissues. Ways to minimize or eliminate this have been detailed in section 1.8. However, CLSM by itself is insufficient for quantifying MNPs in plant tissues. Here, image analysis can be helpful if fluorescence signal detection and estimation of fluorescence intensity are relied on using image analysis software to estimate the number/amount of accumulated MNPs.

Fiji-ImageJ is a widely used, open-source software used in scientific imaging and has been used in numerous studies to study the accumulation of compounds such as dyes, proteins, pharmaceuticals, and particles in plant cells and tissues [228]. For example, immunofluorescence probes can quantify the relative protein expression in tissues by measuring the mean fluorescence intensity throughout a region of interest. Output images from the microscope comprise multiple layers of individual 2-dimensional slice-by-slice images stacked on top of each other to produce a 3-dimensional stack. Each of these constituent layers comprises individual pixels containing information on the detected fluorescence intensity in that region of the sample. The z-project option in Fiji can be utilized to convert this 3-dimensional stack of images from the confocal microscope into a

single 2-dimensional image where each pixel is made up of the sum of the fluorescence intensities recorded for that particular pixel in each constituent layer of the z-stack. Subsequently, the analyzed particle function in Fiji can be used to quantify the fluorescence intensity captured in each pixel, which can then be used to estimate the number of MNPs present in the sample. An advantage of using this approach is that Fiji-ImageJ can quantify fluorescence intensity through automated procedures and allows standardization for accurate and reliable fluorescence measurements [229].

Owing to the lack of current methodologies, the possibility of bioaccumulation of MNPs in crops, its proximity to the food chain, and the lack of understanding of the underlying trends and mechanisms governing this phenomenon, there seems to be an urgent need to develop an analytical approach that could help in the quantification of MNPs in plant samples.

Chapter 2

Aims and Hypothesis

The presence and impacts of micro and nano plastic have been widely studied in varied environmental compartments such as marine, freshwater, and groundwater, but their interactions and impacts in the agricultural environment remain largely underexplored. While some reports suggest that terrestrial soils could be a more significant sink for MNPs than aquatic environments, research regarding MNPs in this domain remains in its infancy. Numerous studies have reported the direct introduction of MNPs to agricultural soils by applying plastic mulch films, which remain one of the largest components of agricultural plastics. The large-scale application of plastic mulch films globally and the ubiquitous presence of MNPs in agricultural farmlands across the globe calls for an urgent investigation into the interactions of these particles with residual contaminants such as pesticides. Recently, the focus has shifted towards using biodegradable polymers, and numerous polymer types (made from fossil-fuel-based precursors and bio-based precursors) are being explored for such applications. However, most biodegradable polymers are either blended with conventional polymers or modified using numerous additives to enhance their chemical and mechanical properties, thereby increasing their suitability for producing mulch films. More often than not, these modifications decrease their biodegradability, leading to incomplete degradation under environmental conditions and the production of MNPs. Few recent studies have reported the production of higher amounts of MNPs from biodegradable mulch films than conventional non-degradable plastic types. These MNPs produced from biodegradable mulch films can interact with agricultural pesticide residues. What remains to be investigated is the extent of this interaction compared to MNPs from conventional non-degradable mulch films.

Furthermore, the introduction of MNPs into the agricultural environment raises concerns regarding their interactions with plants and crops grown in contaminated soils, potentially leading to adverse effects on plant health and bioaccumulation. Previous studies have shown that nanoplastics can accumulate in plant samples, yet the underlying trends and mechanisms have not been thoroughly investigated. Despite qualitative attempts in prior research to explore this phenomenon, the quantitative aspect remains a significant challenge that requires further examination. The quantification of bioaccumulated MNPs in plant tissues can shed light on the patterns governing this process and pinpoint associated risks to different plant parts, specifically those consumed by humans. Additionally, such quantification could establish a baseline for MNPs in plants and crops, paving the way for developing monitoring programs, field surveys, and risk assessment protocols. Delving deeper into the bioaccumulation of MNPs in plants enhances our understanding of the issue and provides valuable insights for implementing proactive measures to address potential environmental risks.

This thesis is directed towards comprehending the intricate relationships between MNPs within the agricultural setting, emphasising the sorption and desorption dynamics exhibited by plastic mulch films and microplastics derived from agricultural mulch films when in contact with residues of commonly employed agricultural pesticides. Furthermore, the study seeks to explore the uptake, accumulation, and distribution of nanoplastics within plants while applying an innovative methodology for quantifying the accumulated nanoplastics within plant tissues by utilizing CLSM with advanced image analysis.

The overarching objective of this thesis is to advance the current understanding of the impact of plastic pollution on agricultural ecosystems by highlighting the intricate processes governing the interactions between plastics and agricultural elements, thus contributing to the development of more effective strategies for mitigating the adverse effects of nanoplastics in agricultural environments.

The specific aims are the following:

A) To understand the sorption and desorption behavior of agricultural pesticide residues on microplastics produced from mulch films:
   - Investigate the interaction of microplastics derived from commercial agricultural mulch films with agricultural pesticide residues, primarily focusing on the sorption of these pesticides onto the microplastic particles, factors that influence the process and model the process;
   - Investigate the retention and desorption of agricultural pesticide residues onto the surface of conventional PE and biodegradable PBAT mulch films and the factors that influence it;
   - Understand the differences in the sorption mechanism between PE and PBAT microplastic types and the retention/desorption of pesticides on/from PE and PBAT mulch films.

B) To understand the bioaccumulation of nanoplastics in crop plants:
   - Investigate the uptake, bioaccumulation, and translocation of nanoplastics in model plants and provide detailed visual evidence;
   - Highlight the trends and mechanisms behind this process of bioaccumulation of nanoplastics in plants;
   - Propose a methodology for quantifying bioaccumulated nanoplastics in plant tissues using CLSM and image analysis.

The thesis sets out to test the following hypotheses:

H1: Microplastics derived from mulch films can be shown to adsorb agricultural pesticide residues.
H2: The sorption mechanism of pesticides on conventional petroleum-based PE microplastic particles differs from that on biodegradable PBAT microplastic particles.
H3: Biodegradable PBAT mulch films exhibit a higher pesticide adsorption capacity, with a higher retention and reduced desorption rate than conventional PE mulch films.
H4: Nanoplastics can bioaccumulate in the model crop *Lepidium sativum* and translocate from the roots to aerial/edible parts.
H5: Fluorescence-based confocal laser-scanning microscopy with image analysis can quantify nanoplastics uptake and bioaccumulation in plants

Chapter 3

Publications

3.1 Publication 1

Title: Exploring sorption of pesticides and PAHs in microplastics derived from plastic mulch films used in modern agriculture

Harshit Sahai[a,b,c], Mar García Valverde[b], María Murcia Morales[b], María Dolores Hernando[a], Ana M. Aguilera del Real[b,*], A.R. Fern´ andez- Alba[b]

a) Experimental Station of Arid Zones, The Spanish National Research Council (CSIC-EEZA), Ctra. de Sacramento S/n, La Cañada de San Urbano, 04120, Almería, Spain
b) Department of Chemistry and Physics. University of Almería. Agrifood Campus of International Excellence (ceiA3). Ctra Sacramento S/n La Ca˜ nada de San Urbano, 04120, Almería, Spain
c) Jožef Stefan International Postgraduate School, Jamova 39, 1000, Ljubljana, Slovenia

The application of plastic mulch films in agricultural production is extensively emphasized in the background data, highlighting their role in facilitating various functions such as safeguarding crops, regulating soil temperatures, retaining moisture, and increasing crop yield. Nevertheless, these benefits come at a cost. As these films gradually deteriorate, they generate minuscule plastic particles, leading to MNPs buildup in agricultural soils. The presence of these particles has sparked significant concerns due to their ability to adsorb and transport a broad spectrum of contaminants in aquatic settings. Nonetheless, their interactions within the agricultural domain are still largely unexplored and inadequately researched.

This paper addresses the gap in the existing literature by investigating the sorption attributes of pesticide residues onto microplastics sourced from traditional non-biodegradable PE agricultural mulch films. The study comprised sorption experiments and the study of sorption kinetics and isotherms to gain insights into the fundamental mechanisms at play. The results revealed that the pseudo-first-order and Dubinin-Radushkevich models best elucidated the sorption process, focusing on concentrations of contaminants that mirror real-world environmental scenarios. The significance of this work lies in its potential ramifications for environmental governance and agricultural methodologies. By illustrating that microplastics from agricultural mulch films can serve as carriers for contaminant residues, notably pesticide residues, the study emphasizes the need for enhanced plastic waste management within the agricultural sector.

Chemosphere 333 (2023) 138959

Contents lists available at ScienceDirect

Chemosphere

journal homepage: www.elsevier.com/locate/chemosphere

Exploring sorption of pesticides and PAHs in microplastics derived from plastic mulch films used in modern agriculture

Harshit Sahai [a,b,c], Mar García Valverde [b], María Murcia Morales [b], María Dolores Hernando [a], Ana M. Aguilera del Real [b,*], A.R. Fernández- Alba [b]

[a] Experimental Station of Arid Zones, The Spanish National Research Council (CSIC-EEZA), Ctra. de Sacramento S/n, La Cañada de San Urbano, 04120, Almería, Spain
[b] Department of Chemistry and Physics. University of Almería. Agrifood Campus of International Excellence (ceiA3). Ctra Sacramento S/n La Cañada de San Urbano, 04120, Almería, Spain
[c] Jozef Stefan International Postgraduate School, Jamova 39, 1000, Ljubljana, Slovenia

HIGHLIGHTS

- MPs from mulch films showed up to 90% higher sorption than pure polyethylene MP.
- Compounds with log K_{ow} value below cutoff (around 3) were not sorbed/retained.
- Pseudo-first order was the best fitting kinetic model suggesting physisorption.
- Dubinin-Radushkevich, the best fitting isotherm suggested micropore volume filling.
- Compounds with lower log K_{ow} values were rapidly desorbed from mulch films.

GRAPHICAL ABSTRACT

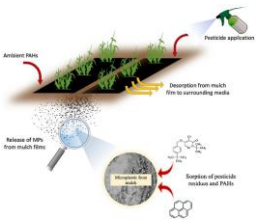

ARTICLE INFO

Handling Editor: Michael Bank

Keywords:
Microplastics
Mulch films
Sorption
Pesticides
PAHs
Agriculture

ABSTRACT

The sorption and vector effect of microplastics on the transfer of pesticides and polycyclic aromatic hydrocarbons (PAHs), as well as its impact on agriculture remain largely unexplored. This comparative study is first to investigate the sorption behavior of different pesticides and PAHs at environmentally realistic concentrations by model microplastics and microplastics derived from polyethylene mulch films. Sorption was found to be up to 90% higher in the case of microplastics derived from mulch films as opposed to pure polyethylene microspheres. For microplastics from mulch films, the sorption percentages for pesticides in media containing $CaCl_2$ were reported to be: pyridate (75.68% and 52.44%), fenazaquin (48.54% and 32.02%), pyridaben (45.04% and 56.70%), bifenthrin (74.27% and 25.88%), etofenprox (82.16% and 54.16%) and pyridalyl (97.00% and 29.74%) at 5 μg/L and 200 μg/L pesticide concentration levels respectively. For PAHs, the sorption amounts were: naphthalene (22.03% and 48.00%), fluorene (38.99% and 39.00%), anthracene (64.62% and 68.02%) and pyrene (75.65% and 86.38%) at 5 μg/L and 200 μg/L PAH concentration levels respectively. Sorption was influenced by the octanol-water partition coefficient (log K_{ow}) and ionic strength. Kinetics of the process in the case of sorption of pesticides were best explained by pseudo-first order kinetic model (R^2 between 0.90 and 0.98) while the best fitting isotherm model was Dubinin-Radushkevich (R^2 between 0.92 and 0.99). Results suggest the presence of surface level physi-sorption through a micropore volume filling mechanism and the role of hydrophobic and electrostatic forces. Pesticide desorption data in polyethylene mulch films indicate that pesticides

* Corresponding author.
E-mail address: aaguiler@ual.es (A.M. Aguilera del Real).

https://doi.org/10.1016/j.chemosphere.2023.138959
Received 9 February 2023; Received in revised form 25 April 2023; Accepted 15 May 2023
Available online 18 May 2023

with high log K_{ow} were almost completely retained in mulch films, while those with lower log K_{ow} were desorbed rapidly into the surrounding media. Our study highlights the role of microplastics from plastic mulch films as vectors for pesticide and PAH transport at environmentally realistic concentrations and the factors that influence it.

1. Introduction

Because of the widespread use of plastics, they are now produced at an astonishing 367 million tonnes per year, up from just 1.5 million tonnes in the 1950s (PlasticsEurope, 2021). The amount of mismanaged plastic waste entering the environment is predicted to reach 230 million tonnes by 2025, and 380 million tonnes by the year 2060, while at the same time, the global recycling rate of plastic waste remains abysmally low at just 9% (Brooks et al., 2018). Almost 11 billion tonnes of plastic waste is expected to accumulate in the environment by 2025 (Brahney et al., 2020).

Microplastics are tiny plastic particles that are ≤5 mm in size in their largest dimension. They are intentionally manufactured in microscopic sizes for various commercial applications (known as primary microplastics) but also formed in the environment by the breakdown of larger plastics (known as secondary microplastics) due to biological, chemical or physical degradation processes (Cole et al., 2011). To date, most scientific research on their presence and negative impacts have been mainly directed at limited environments, especially marine or freshwater. However, the 2021 FAO report titled "Assessment of agricultural plastics and their sustainability: A call for action" indicates that of the approximate 12.5 million tonnes of agricultural plastics generated annually, the amounts that leak into the environment are largely unknown (FAO, 2021). There is still a great deal of unexplored research regarding their impacts on the agricultural ecology (Ng et al., 2018).

The principal sources of microplastics in agricultural ecosystem identified so far, are the application of contaminated sewage sludge or repurposed wastewater from treatment plants (WWTPs) (Nizzetto et al., 2016; Steinmetz et al., 2016; van den Berg et al., 2020). However, plastics are also directly used for agricultural applications such as surface mulch films that provide benefits such as protection from harsh climatic conditions, suppression of weeds, increased soil temperatures, reduced moisture loss from surface evaporation, and reduced nutrient runoff due to heavy rains (Scarascia-Mugnozza et al., 2011). The use of plastic mulching is suspected to be a significant source of microplastics owing to its intensive application in modern agriculture (Huang et al., 2020). Indeed, mulch films represent the second largest use of plastic films in agriculture by volume, exceeding 2 million tonnes globally (FAO, 2021), with low density polyethylene (LDPE) being the dominant plastic type in mulch film applications (Sarkar et al., 2018). During their application life cycle, these films are exposed to various environmental factors that facilitate degradation, with UV radiations being one of the prominent contributing factors along with mechanical weathering (Astner et al., 2019; Sorasan et al., 2022). Additionally, the removal of mulch films after use is a laborious and time-consuming process which further disincentivizes their proper collection and disposal from the fields (Huang et al., 2020). Such films that are often left on the fields without subsequent collection for separate recycling or formal disposal may release micro and nano sized particles into the agricultural fields over time (Astner et al., 2019; Sorasan et al., 2021). According to a recent study, depending on the type of polymer utilized, 147 to 475 microplastic particles could be produced on average per cm^2 of the mulch film in the environment (Yang et al., 2022).

Because of their microscopic sizes and a very high specific surface area, these microplastics can interact with contaminants in the surrounding environment that may get sorbed onto the particle, thus constituting the external load. This could have implications for the eventual fate and bioavailability of these pollutants. In the marine environment, these might include banned or restricted persistent organic pollutants (POPs) such as DDT, polybrominated diphenyl ethers (PBDEs), pesticides such as chlorpyrifos (Camacho et al., 2019; De-la-Torre, 2020), PAHs, heavy metals (Brennecke et al., 2016), pharmaceutical compounds (Atugoda et al., 2021; C. Wu et al., 2016), or polychlorinated biphenyls (PCBs) (Velzebovder et al., 2014). To the best of our knowledge, few studies have documented empirical evidence about the interaction of contaminants with microplastics derived from agricultural plastic films. A recent study has compared the adsorption behavior of pesticides (carbendazim, diflubenzuron, malathion, difenoconazole) by pristine and aged microplastics from agricultural polyethylene soil films. In this case, aged microplastics appear to be better vector of most hydrophobic pesticides than pristine MPs in the agricultural field (Lan et al., 2021). Adsorption of pesticides (carbendazim, dipterex, diflubenzuron, malathion, difenoconazole) was also found on microplastics from agricultural polyethylene films (Wang et al., 2020). Another study dealt with the interaction of banned organochlorine pesticides (HCH and DDT), but on pure polyethylene microplastics in the form of powders and pellets (Zhang et al., 2021). The results of this study indicated that MPs with small size could absorb more pollutants than those with large size, and suggested that MPs could enrich low-concentration pollutants in soil (Zhang et al., 2021).

Sorption of contaminants onto microplastics is affected by the physicochemical properties of the microplastic, the sorbate and the environment or matrix in which the interaction takes place. Also, additives such as plasticizers, pigments, UV-stabilizers, and other compounds (constituting the internal load of chemicals) that impart different physical, chemical and structural properties to the polymer depending on its intended use, can affect sorption behavior of contaminants from the environment. On the other hand, the properties of the sorbate such as the octanol-water partition coefficient (log K_{ow}), molecular dimensions, presence of functional groups and environmental factors such as ambient pH, temperature, ionic strength or other competing/co-existing compounds could also affect the dynamics of this interaction.

The purpose of this study is to explore the sorption behavior of contaminants on microplastics derived from plastic mulch films under environmentally relevant conditions. The study focuses on pesticides as the representative substance used in agriculture as well as on PAHs as the representative contaminant group from diffuse pollution. Both the groups of pesticides and PAHs have varied physicochemical properties covering a wide range of log K_{ow} (Supplementary material, Table S (1)). This study addresses fundamentals of contaminant sorption onto microplastics through sorption kinetics and isotherm models. Here, for the first time, pure PE microspheres were selected against microplastics produced from mulch films containing additives. The effects of different conditions (ionic strength and concentration of pesticides and PAHs) on sorption were tested. In addition, this study also looks into the desorption of certain pesticides from plastic mulch films in order to explore the process as it would happen in the environment after a spraying event in the agricultural field.

2. Materials and methodology

2.1. Analytical standards

Analytical standards for the pesticides bifenthrin, pyridate, fenazaquin and acetamiprid were obtained from Dr. Ehrenstorfer GmbH (Germany), while pyridaben, pyridalyl, etofenprox, carbendazim, azoxystrobin and fluxapyroxad were obtained from Sigma-Aldrich

(United States). All PAH analytical standards, including naphthalene, fluorene, anthracene and pyrene were obtained from Sigma-Aldrich (United States).

2.2. Microplastic samples

Pure polyethylene microspheres (Sample: Pure-PE) of size range 125–150 μm were purchased from CoSpheric (United States), while PE mulch film samples (thickness: 15 μm) were sourced from a local vendor (Almeria, Spain). This mulch film was further cut into small pieces and exposed to liquid nitrogen for freezing. Subsequently, microplastics (Sample: Agri-PE) were produced from these frozen pieces using a grinder (Retsch GM 200, Retsch GmbH, Germany) at 10,000 rpm and multiple repetitions of grinding cycles of 30 s each. The time of each grinding cycle was kept short so as to avoid heating of the plastic film which would reduce its brittleness and in turn the formation of microplastics. The obtained particles were then sieved through a stainless-steel mesh to obtain particles of 50–200 μm size range.

2.3. Experimental design

2.3.1. Sorption experiments

Sorption experiments were conducted in glass Erlenmeyer flasks using 100 mL spiked solutions of pesticides/PAHs with spike concentrations of 5 μg/L and 200 μg/L and distilled water (Milli-Q) as the interaction media. 10 mg microplastics were added to this 100 mL spiked solution and set up on a rotary shaker at 120 rpm. And in a dark environment (to prevent photolysis) with ambient temperature of 25 °C. The Erlenmeyer flask tops were sealed with aluminum foil. 1 mL samples were drawn from this solution every hour, until 4 h, and preserved in glass vials until further analysis. The batches were differentiated on the basis of the type of microplastics (MP) added (Pure-PE and Agri-PE) and on the basis of concentration levels of 5 μg/L and 200 μg/L. In order to study the effect of ionic strength of the interaction media over the sorption process, 0.003 mol/L of NaCl (equivalent to 200 ppm of Cl^-) and 0.002 mol/L of $CaCl_2$ (equivalent to 200 ppm of Cl^-) were added to the spiked solutions in separate batches. All experiments were conducted in triplicates and all replicates fall below a coefficient of variation of 20%.

In the case of pesticides, samples were directly analyzed using LC-MS/MS. In the case of PAHs, the samples were subjected to liquid-liquid extraction in n-hexane. For this, the samples were transferred into a separation funnel and shaken vigorously with 10 mL n-hexane for 1 min. The top layer was extracted from the funnel and sent for GC-MS/MS analysis.

2.3.2. Study of kinetics and isotherms

Since this work was mainly focused on the agricultural ecosystem and considering the fact that pesticides are indeed intentionally used in agriculture (as opposed to PAHs that are un-intentional residues in the environment), only the sorption process of pesticides onto Agri-PE samples was investigated in detail.

2.3.2.1. Kinetic studies. Batch sorption experiments were carried out in glass Erlenmeyer flasks using 100 mL solutions spiked with 5 μg/L and 200 μg/L initial pesticide concentrations and 0.0018 mol/L of $CaCl_2$. 10 mg of Agri-PE MP sample was added to this solution and placed on a rotary shaker in dark environment at 120 rpm. And T = 25 °C. Subsequently, 1 mL samples were taken from this solution at 0.25, 0.5, 1, 1.5, 2, 3, 4, 5, 6, 7, 10, 24, 30 and 48 h and sent for LC-MS/MS analysis. All experiments were conducted in triplicates and all replicates fall below a coefficient of variation of 20%.

2.3.2.2. Isotherm studies. For this, batch sorption experiments (in triplicates) were conducted in the same manner as discussed above in five different initial pesticide concentrations of 5 μg/L, 25 μg/L, 100 μg/L, 150 μg/L and 200 μg/L and a constant ambient temperature of 25 °C with distilled water containing 0.0018 mol/L of $CaCl_2$ as the interaction media. Pesticide analysis was made using LC-MS/MS. Q_e (amount of pesticide sorbed onto unit mass of MP at equilibrium) and C_e (concentration of pesticide in aqueous phase at equilibrium) values were calculated. Non-linear forms of Langmuir, Freundlich, Dubinin-Radushkevich, Temkin and Redlich-Peterson isotherm models were used to fit the experimental data. Each of these models were used due to their specific characteristics: The Langmuir model assumes that the binding sites over the homogenous adsorbent as well as the process of binding of each adsorbate to the binding sites is identical and this results in a monolayer coverage (Sohn and Kim, 2005). The Freudlich isotherm assumes surface heterogeneity of the adsorbent and the role of lateral interactions between the adsorbed molecules (Yang, 1998). The Dubinin-Radushkevich isotherm is based on the theory of micropore volume filling over heterogenous surfaces (Dada et al., 2012) and involvement of van der Waals forces in the interaction (Chen and Yang, 1994). The Temkin isotherm accounts for the influence of adsorbate-adsorbent interaction over the heat of adsorption which decreases linearly as the surface coverage increases. While on the other hand, the Redlich-Peterson model which is the only three parameter model out of all five selected, includes the properties of both the Langmuir and Freundlich models (Brdar et al., 2012). The equations of all selected models and their parameters are detailed in the supplementary information.

2.3.3. Pesticide desorption experiments

In this section of our work, the desorption of only the selected pesticides was studied due to their intentional use in agriculture. Desorption experiments were conducted in triplicates, based on the Commission Regulation (EU) No October 2011 of January 14, 2011 on plastic materials and articles intended to come into contact with food and methodology described elsewhere (Díaz-Galiano et al., 2023). 2 mL spike solution containing all pesticides (acetamiprid, azoxystrobin, bifenthrin, carbendazim, etofenprox, fenazaquin, pyridaben, pyridalyl, pyridate) was sprayed onto a 10 × 10 cm piece of Agri-PE mulch film, using a spray bottle to mimic the spraying of pesticides in the agricultural fields and then left overnight to completely dry at room temperatures. The spike concentration over the plastic films was calculated to be 142 μg/L. Thereafter, the films were carefully transferred into polytetrafluoroethylene (PTFE) tubes and 35 mL of 10% ethanol solution was added to it and incubated at 20 °C. 1 mL samples were extracted from these bottles at 2, 6, and 10 days and analyzed using LC-MS/MS. The 10th day of sampling was chosen based on the previously reported methodology (Díaz-Galiano et al., 2023) and the Commission Regulation (EU) No October 2011. The 2nd day of sampling was chosen since in our preliminary experiments we find that all of the compounds studied, reached their sorption equilibrium within 48 h, while the 6th day of sampling was chosen as a mid-point between 2 and 10 days.

2.4. Analytical methods

2.4.1. LC-MS/MS analysis

Pesticide concentrations were analyzed using Sciex Exion HP-LC coupled to Sciex 6500+ triple quad-LC-MS/MS equipped with a Zorbax Eclipse Plus C8 column (1.8 μm × 2.1 mm x 100 mm) at T = 35 °C. Two mobile phases used were as follows: (A) 0.1% formic acid and 5 mM formate ammonium in MeOH/water (98/2 v/v) and (B) 0.1% formic acid and 5 mM formate ammonium in water/MeOH (98/2 v/v). The gradient program used was as follows: (0–1min)- 100% A; 0% B, (1–2min)- 100% A to 70% A; 0% B to 30% B, (2–3min)- 70% A to 50% A; 30% B to 50% B, (3–11min)- 50% A to 0% A; 50% B to 100% B, (11–14min)-100% B; 0% A, (14-14,1min)- 0% A to 100% A and (14.1–17min)- 100% A. Flow rate was set at 0.3 mL/min and injection volume at 5 μL. Ionization temperature was set at 300 °C and ion spray

voltages of 5550 V positive mode and −4500 V negative mode. Total run time was 17 min for each sample. Method validation was carried out following quality control standards (SANTE/11312/2021). In order to control the performance of sample injection, 10 μg/L solution of dimethoate-d6 was used as internal injection standard and the subsequent analysis monitored.

2.4.2. GC-MS/MS analysis

The analysis was carried out based on a methodology described elsewhere (Trouvé et al., 2022). PAH levels were analyzed using Agilent Intuvo 9000 GC system (Agilent Technologies, Palo Alto, CA, USA) equipped with an Agilent 7693 autosampler and an Agilent 7010 B GC-MS/MS triple quadrupole with two planar columns (Agilent), HP-5MS UI 15 m long, 0.25 mm i. d. and 0.25 μm film thickness. Injection volume was set at 1 μL with injector temperature of 80 °C for 0.1 min which was elevated to 300 °C for 5 min at 600 °C/min. and then back to 250 °C at 100 °C/min. The flow rate was set at 1.317 mL/min For the first column and 1.517 mL/min For the second column. The oven was set at 60 °C for 0.5 min and then ramped to 170 °C at 80 °C/min. and to 310 °C at 20 °C/min. The total run time was 15.37 min for each sample. In order to control and monitor the performance of the analytical procedure, blank samples were injected during the analysis. Additionally, malathion-d10 and triphenyl phosphate (TPP) were used as internal standards for the extraction step while lindane-d6 was utilized as the internal standard during vial preparation and injection and the subsequent analysis monitored.

2.5. Characterization of microplastics

Analytical pyrolysis (Py-GC/MS) was performed using 0.1 mg of sample at 400 °C (1 min) in a micro furnace pyrolysis system (Frontier Lab. Model 3030D, Fukushima, Japan) as described elsewhere (Jiménez-Morillo et al., 2020). In short, the pyrolizer was coupled with a GC/MS system (Agilent 6890) equipped with a low polar-fused silica capillary column (HP 5MS-UI; 30 m × 250 μm × 0.25 μm). The GC was fitted with a mass selective detector (Agilent 5973 MSD) and mass spectra acquired at 70 eV. The following chromatographic conditions were used: the carrier gas was He (flow rate 1 mL/min); the oven was preheated to 50 °C for 1 min and then increased to 100 °C at 30 °C min^{-1}, from 100 to 300 °C at 10 °C min^{-1}, and then constant at 300 °C for the last 10 min. The identification of compounds was achieved by single-ion monitoring (SIM) and by comparison with mass spectra libraries (NIST11 and Wiley7) and published spectra databases.

The microplastic particles were also studied using electron microscopy (Zeiss Sigma 300 VP Field Emission High Resolution Scanning Electron Microscope) to analyze the differences in the surface characteristics of the different types of microplastics used in this study. In order to observe the aggregation behavior of the microplastics in solution, MP were also observed under a microscope (Stereoscopic Microscope LEICA S9i) during the analysis.

2.6. Sorption models

Kinetics of the sorption process were described using non-linear forms of the mathematical models namely: pseudo-first order, pseudo-second order, Elovich and intra-particle diffusion model. Kinetic plots were generated by plotting Q_t (μg/g) (amount of pesticide sorbed onto unit mass of MP at time t) against time (t). Non-linear isotherm models that were used to describe the process were namely: Langmuir, Freundlich, Dubinin-Radushkevich, Temkin and Redlich-Peterson model. Sorption isotherms were obtained by plotting Q_e (μg/g), which is the amount of pesticide sorbed onto unit mass of the MP at equilibrium, against C_e (μg/L), which is the concentration of the pesticide in aqueous phase at equilibrium, for five different initial concentrations of the pesticides. All kinetic and isotherm models were fitted onto the experimental data using the Solver tool in MS Excel by changing the model parameters with the aim of achieving the least SSR (sum of square of residues). The best fit models were chosen on the basis of goodness of fit parameter (R^2) and chi-square parameter (χ^2). All the models used in this study have been described in the supplementary material.

2.7. Data analysis

Data were statistically processed using SPSS (Statistical Package for the Social Sciences) Statistical software for Windows, IBM Corp, 2016. Versión 22.0. IBM Corp, Armonk, NY, US. All the variables available were tested to check whether data trespassing the assumptions for regular parametric tests to report valid results. Parametric statistics were applied when possible. When the data was non-normally distributed, or there was no variance of homogeneity (heteroscedastidity), non-parametric statistics were used. The tests are specified in the results.

3. Results and discussions

3.1. Characterization of microplastics

Agricultural mulch film microplastic samples (Agri-PE) were found to have an irregular, rough surface that is flaked and cracked and having particles of various shapes and sizes, as opposed to Pure-PE microplastics, which had a reasonably smooth and spherical appearance (Fig. S (1)). This surface irregularity has the potential to increase the specific surface area, which would increase the sorption capacity (Lan et al., 2021). Due to the physical, chemical, and biological processes that operate upon microplastics in the environment, it is expected that they will have a variety of shapes and sizes as well as irregular, rough surfaces in the agricultural environment. Therefore, compared to the manufactured virgin PE microspheres that are frequently utilized in most research, the Agri-PE samples employed in our study would be a more realistic model to explore the environmental phenomenon.

In addition, Pyrolysis-GC-MS analysis revealed the presence of 2,4-Di-*tert*-butylphenol (Antioxidant No. 33) in Agri-PE samples (Fig. S (2)), a compound added to commercial plastic films as an intermediate to provide resistance against oxidation. The presence of coatings, additives and functional groups can affect the electrostatic, steric and hydrophilic/hydrophobic behavior of the MP and alter its interactions with surrounding sorbates (Wang et al., 2021). 2,4-Di-*tert*-butylphenol contains a phenolic functional group with a lone pair of electrons and capable of forming hydrogen bonds with the sorbate molecule and interact with π-bonds of the benzene rings of the sorbate.

As observed under the microscope, both Pure-PE and Agri-PE samples formed aggregates in solution (Fig. 1). The aggregates were much more prominent in the case of Agri-PE sample and also increased upon adding $CaCl_2$ to the solution possibly due to the increased ionic strength of the solution (Fig. 1(B) and (D)). An increase in ionic strength of the surrounding media results in a decrease in the electrical double layer on the surface of MP particles and the charge shielding. This affects the particle-particle attachment efficiency (α_{pp}) and in turn the aggregation rate (Alimi et al., 2018).

3.2. Sorption experiments

Out of the ten pesticides and four PAHs investigated for sorption, acetamiprid, azoxystrobin, carbendazim, and fluxapyroxad did not show any significant sorption onto any microplastic sample at both 5 μg/L and 200 μg/L initial concentration levels in distilled water. It is interesting to note that in some previous studies, sorption was observed in the case of azoxystrobin (Wang et al., 2020) and carbendazim (Mo et al., 2021; Wang et al., 2020). However, in these studies, different plastic types, relatively higher concentrations of pesticides and higher amounts of microplastics were used for the investigation, which are factors that could affect the dynamics of the process. It is important to take into account the fact that the concentration of pesticide residues to be

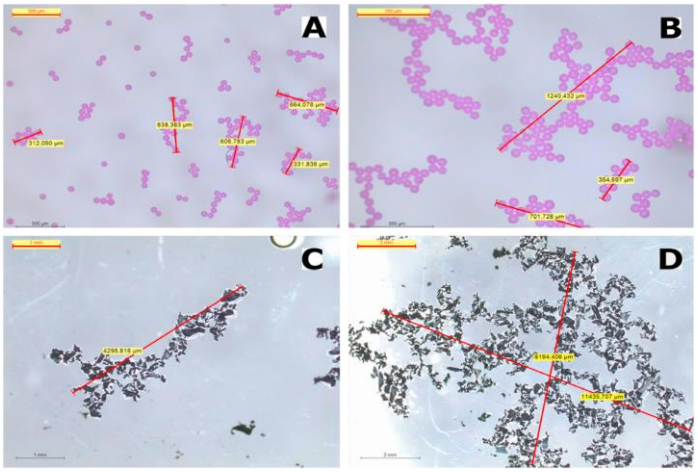

Fig. 1. Microscopic images showing aggregation in Pure-PE in distilled water (A) and $CaCl_2$ (B) and aggregation in Agri-PE in distilled water (C) and $CaCl_2$ (D).

expected in treated wastewater is in the range of ng/L to a few μg/L (Bueno et al., 2012) and that of microplastics in treated wastewater would be a few μg/L (Simon et al., 2018). Furthermore, it is much more realistic to assume the presence of multiple co-existing compounds in the environmental scenarios as opposed to a single target compound because sorption can also be affected by the presence of coexisting compounds in the solution (Bakir et al., 2012; Tourinho et al., 2019). On the other hand, pyridate, fenazaquin, pyridaben, bifenthrin, etofenprox and pyridalyl showed moderate sorption at both concentration levels only in the case of Agri-PE samples.

The data for Pure-PE did not confirm to normal distribution (Kolmogorov-Smirnov, $p \leq 0.05$) and therefore, non-parametric analysis was

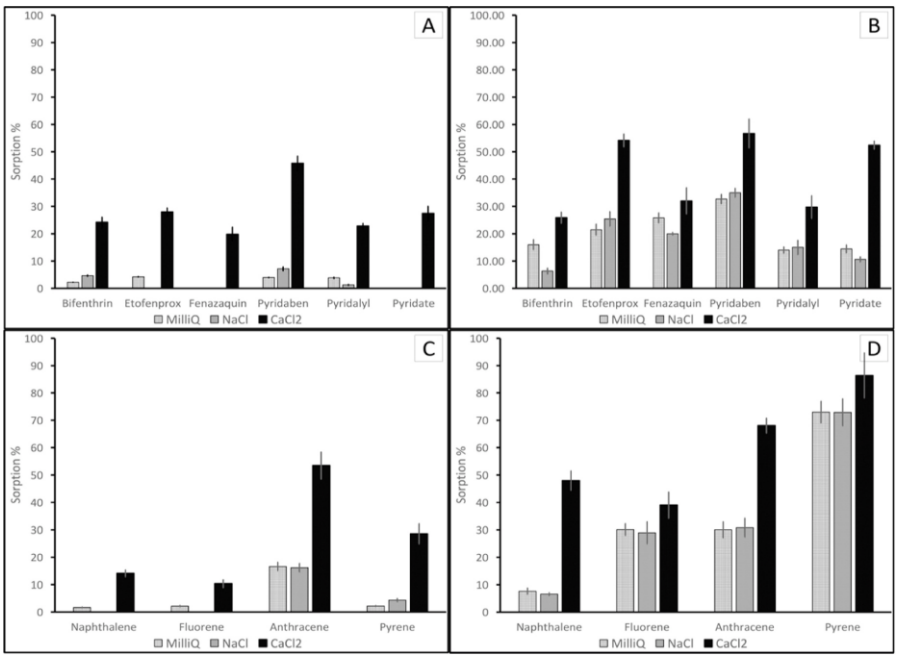

Fig. 2. Sorption of pesticides in distilled water, NaCl and $CaCl_2$ in Pure-PE (A) and in Agri-PE (B) and sorption of PAHs in distilled water, NaCl and $CaCl_2$ in Pure-PE (C) and in Agri-PE (D); initial concentration 200 μg/L.

conducted. For this microplastic type, sorption obtained with $CaCl_2$ medium was significantly superior to the other two mediums (distilled water and NaCl) for all the pesticides studied. In addition, the values obtained with distilled water were significantly higher than those obtained with the NaCl medium for the pesticides pyridaben, pyridalyl, and etofenprox. For etofenprox, no sorption was detected when NaCl was used. Finally, no significant differences in sorption of the pesticides fenazaquin and pyridate were observed when distilled water and NaCl media were used (Kruskal-Wallis $p \leq 0.05$, Mann-Whitney *U* test $p \leq 0.05$). When we consider Agri-PE plastic, parametric statistic was followed since Kolmogorov-Smirnov test for normality and Levene's test for homoscedasticity reported non-significant results ($p > 0.05$). The results again showed that sorption for all the pesticides studied was significantly higher when $CaCl_2$ was used compared to the other two mediums, except for the pesticide fenazaquin, in which case no significant differences were detected between $CaCl_2$ and distilled water. In addition, significantly higher sorption of the pesticides bifenthrin and pyridate was observed in distilled water than in the NaCl medium (One-way ANOVA $p \leq 0.05$, HSD Tukey $p \leq 0.05$). Upon comparing between plastics types, significantly more sorption was detected from all the pesticides studied in the Agri-PE than in the Pure-PE, except for the pesticide bifenthrin, for which the difference was not significant (Mann-Whitney *U* test $p \leq 0.05$). The values are demonstrated in Fig. 2. The difference in size ranges of the two samples could also have contributed to the differences in the sorption capacities to a certain extent. As previously reported, microplastics with smaller size ranges are expected to have greater sorption capacities due to a higher specific surface area (Zhang et al., 2021). However, this case cannot always be true as the smaller sized particles also have a greater tendency to form compact aggregates, thereby limiting the internalized particles of the aggregate from interacting with the contaminant molecules, thus in turn decreasing the overall sorption capacity (Wang et al., 2019). Since, the effect of size was not studied in detail in this work, we must take these facts into account while extrapolating our findings.

In the case of PAHs, the data did not confirm to normal distribution for both plastic types (Kolmogorov-Smirnov, $p \leq 0.05$; Shapiro-Wilk, $p \leq 0.05$) and therefore, non-parametric tests were conducted. When all the results were considered, without differentiating between the two types of plastics, the $CaCl_2$ medium showed a significantly higher amount of sorption than distilled water and NaCl media for naphthalene and anthracene. In contrast, the differences were visible but not significant for the other two PAHs, fluorene and pyrene (Kruskal-Wallis $p \leq 0.05$, Mann-Whitney *U* test $p \leq 0.05$). Upon comparing the sorption between the two types of microplastics, the results again showed a significantly higher amount of sorption of all PAHs in Agri-PE than in Pure-PE. The values are demonstrated in Fig. 2.

These trends can be explained by the fact that microplastics tend to have a net negative surface charge if the pH of the surrounding environment is higher than their point of zero charge (pH_{pzc}) (Li et al., 2021; Xu et al., 2018). Therefore, MP naturally attract positively charged species and repel negatively charged ones due to electrostatic repulsion. However, the presence of bivalent Ca^{2+} cations in the solution, provides a bridging effect between the charged surface of the MP and the sorbate molecule thereby facilitating sorption (Tourinho et al., 2019). Furthermore, adding $CaCl_2$ decreases the solubility of sorbates in aqueous phase due to salting-out effect (C. Wu et al., 2016). This phenomenon highlights the presence of electrostatic interactions in governing the sorption of these sorbates.

A positive correlation was observed between the log K_{ow} value of the pesticides/PAHs and their sorption percentages and a cut-off value of log K_{ow} (between 3 and 4) seems to exist below which the sorption is non-existent (Fig. 3). Log K_{ow}, also known as the octanol-water partition coefficient, is an important parameter as it reflects the degree of hydrophobicity of the compound, which in turn would determine its interaction with the microplastic particle.

Another important factor that would affect the process of sorption is the ageing of the plastic polymer in the environment during its application life cycle. In a realistic scenario, before the production of microplastics from the plastic mulch film, the film would be exposed to various environmental factors that facilitate its ageing such as temperature and UV rays that might alter the superficial characteristics including formation of oxygenated groups such as hydroxyl, carbonyl and carbon-oxygen bonds (Sorasan et al., 2021). This cumulative phenomenon could in turn increase the sorption capacities as a consequence of the generated functional groups on the surface.

3.3. Kinetics of sorption

The results are shown in (Fig. 4) and the calculated model parameters are listed in Table S (2) for the sorption process at 5 μg/L and in Fig. S (3) and Table S (3) for sorption at 200 μg/L. As observed previously, only pyridate, fenazaquin, pyridaben, bifenthrin, etofenprox, and pyridalyl showed considerable sorption, while acetamiprid, azoxystrobin, carbendazim, and fluxapyroxad did not. In all cases of sorption, taking into account the R^2 and χ^2 values, pseudo-first order and pseudo-second order were found to be the best fit models while Elovich and intraparticle diffusion models show lower values of R^2 in the range of [0.72–0.90] and [0.65–0.85] respectively. At 5 μg/L, R^2 values ranging, between 0.98 and 0.87, were higher for the pseudo-first order model except for etofenprox. In the case of pyridaben and fenazaquin, the R^2 values for both pseudo-first and pseudo-second order models were very close, with smaller χ^2 values for pseudo-second order. For

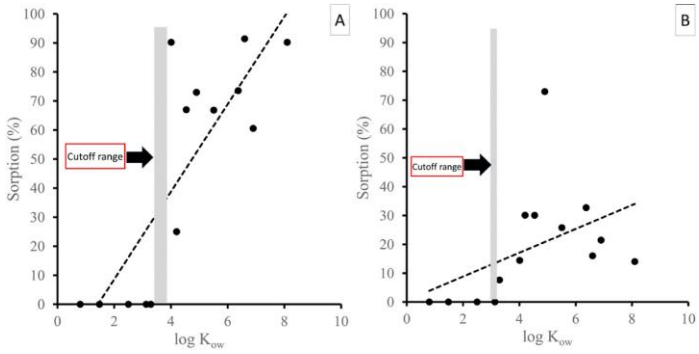

Fig. 3. Log K_{ow} versus Sorption (%) in Agri-PE in the case of pesticides and PAHs; initial concentration 5 μg/L (A) and 200 μg/L (B); in distilled water.

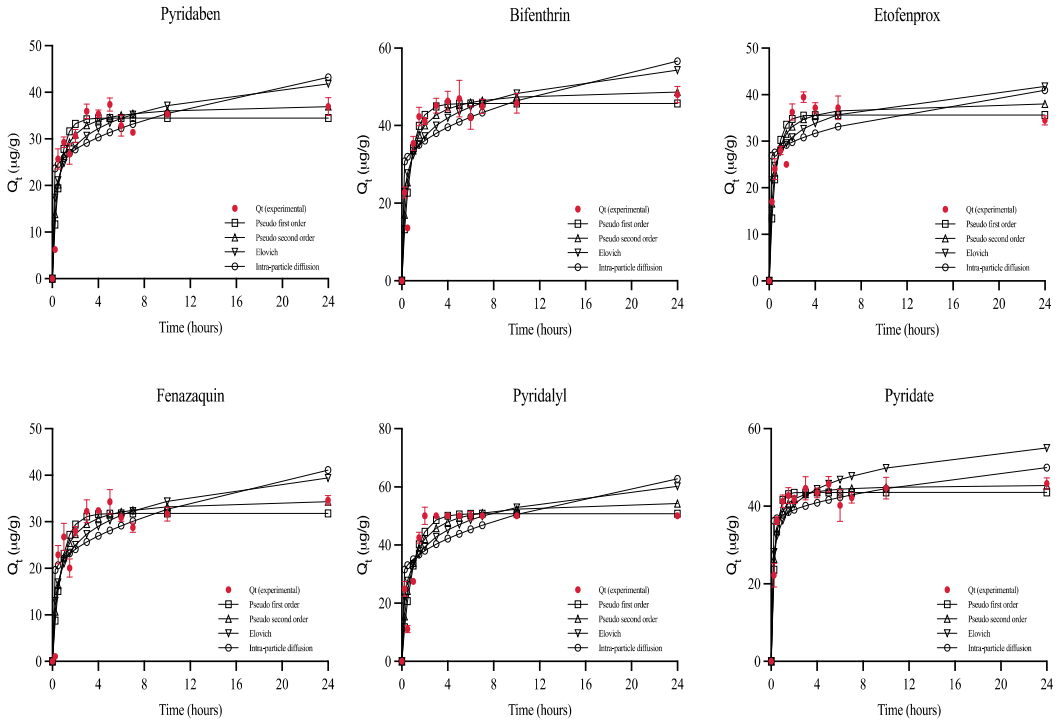

Fig. 4. Sorption kinetics of pesticides onto Agri-PE at 5 μg/L initial concentration level.

etofenprox, R^2 values were slightly higher for pseudo-second order (R^2 = 0.93) than those for pseudo-first order (R^2 = 0.91). At 200 μg/L concentration level, pseudo-first order model was found to be the best fit for all the pesticides (R^2 between 0.88 and 0.94).

Pseudo-first order model being the best fit, and taking into account that Elovich equation is used to describe adsorption processes that are of a chemical nature (Aharoni and Tompkins, 1970; F.-C. Wu et al., 2009), our data suggests that, in our case, physi-sorption plays an important role in determining how these pesticides interact with Agri-PE microplastics. This is in conformity with the idea that sorbate-MP interactions are predominantly surface level adsorption processes through non-specific van der Waals and electrostatic forces for crystalline and semi-crystalline plastics such as PE while predominantly hydrophobic partitioning for amorphous plastic types (Hüffer and Hofmann, 2016; Velez et al., 2018). Furthermore, lower R^2 values for intra-particle diffusion model suggest that intra-particle diffusion was not the sole rate limiting step in our case.

Q_e, calculated from the model, ranged, approximately, between 30 and 50 μg/g at 5 μg/L and between 800 and 2500 μg/g at 200 μg/L initial concentration level. Again, as observed during preliminary studies, a positive correlation was observed between the log K_{ow} values of the pesticides and Q_e calculated using the model. However, caution must be taken before extrapolating this correlation onto other compounds with similar log K_{ow} values to predict their sorption behavior. This is because other factors that would be specific to a particular compound such as molecular structure, functional groups and presence of charge can play a role in determining their behavior and influence this correlation. Additionally, the equilibrium time for sorption at 5 μg/L concentration level was found to be between 2 and 10 h, while at 200 μg/L level, it was found to be between 24 and 48 h (Table S (4)). The difference between the equilibrium times at the two concentrations could be explained by the fact that at 5 μg/L, the number of pesticide molecules available for interaction reduces rapidly upon initial sorption. This creates a situation where there is not enough probability of pesticide molecules being within the interactive field of the microplastic particle at a given time and therefore further sorption ceases even though the active sites on the MP are not saturated. However, at 200 μg/L, there are sufficient pesticide molecules available for the interaction to occur even after extended periods of time.

The initial sorption rate denoted by h (μg g^{-1} h^{-1}), which helps us to determine the pace of sorption is calculated using the equation , and was found to be higher at 200 μg/L with values between 249 and 2112 μg g^{-1} h^{-1} than at 5 μg/L with values between 62 and 250 μg g^{-1} h^{-1} (Table S (4)). Here k_2 (g $\mu g^{-1} h^{-1}$) is the second order rate constant while Q_e (μg/g) represents the amount of pesticide sorbed onto MP at equilibrium.

3.4. Sorption isotherms

As demonstrated in Fig. 5 and Table S (5), in the case of all the sorbed pesticides, Dubinin-Radushkevich model was found to best explain the process with R^2 values ranging between 0.92 and 0.99. The maximum sorption capacity (Q_{max}) ranged between 1003 μg/g for fenazaquin and 2420 μg/g for etofenprox. This model implies the presence of a micropore volume filling mechanism (Hutson and Yang, 1997). This mechanism has been previously reported in the case of sorption by other porous materials (Balarak et al., 2017; Sakurovs et al., 2007) and in microporous active carbonaceous material (Stoeckli, 1993). Our results

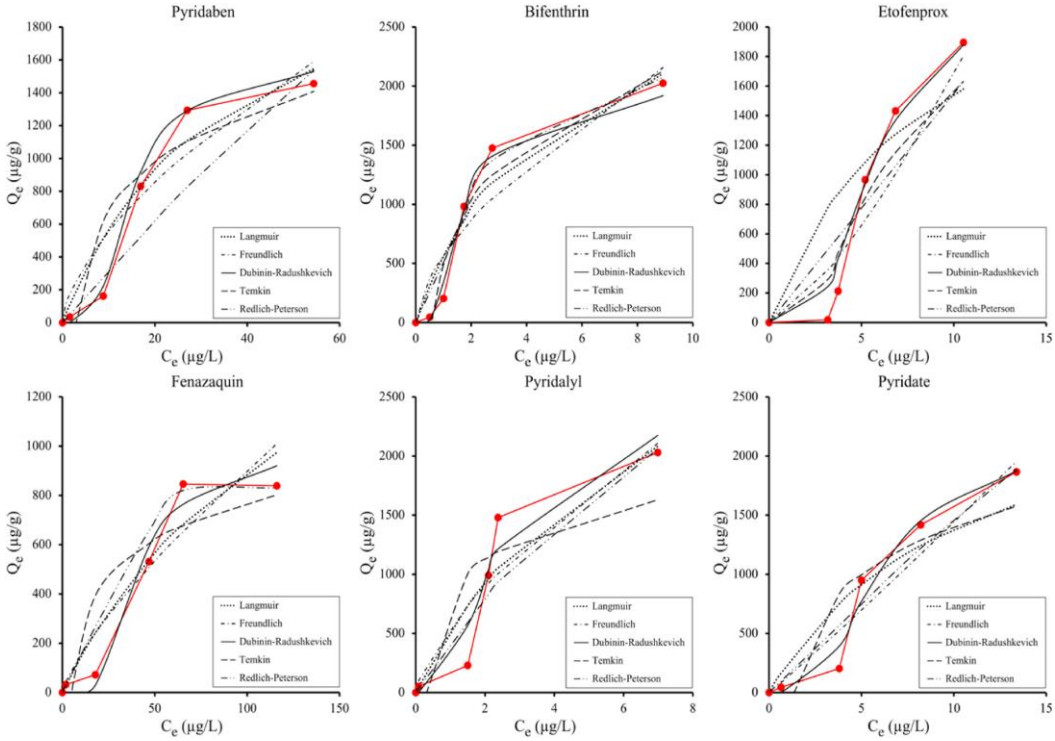

Fig. 5. Isotherms for sorption process of pesticides onto Agri-PE; Data points in red colour correspond to the Q_e values calculated using their respective experimental C_e value

differ from those of some previous findings wherein multilayer adsorption mechanism was reported in the case of agricultural microplastics (Lan et al., 2021; Wang et al., 2020), but it is important to note that, upon SEM analysis, the surface of the Agri-PE samples was found to be rough and porous and full of cracks which would provide increased surface area and micropores for sorption. This model also presumes the presence of a multilayer character to the mechanism involving van der Waals forces (Ayawei et al., 2017).

3.5. Desorption of pesticides from Agri-PE mulch film

After 10 days of incubation, 5 out of 9 pesticides including bifenthrin, etofenprox, fenazaquin, pyridalyl, and pyridate, that were sprayed onto the piece of agricultural mulch film did not show any desorption, while pyridaben showed slight desorption [< 5 µg/L] with no significant differences over the period of 2, 6 and 10 days (Kruskal-Wallis $p \geq 0.05$). On the other hand, azoxystrobin, acetamiprid and carbendazim showed high amounts of desorption after 10 days with the desorption amounts significantly increasing over 2, 6 and 10 days (Kruskal-Wallis $p \leq 0.05$). Pesticides with lower log K_{ow} were the most desorbed while the ones with high log K_{ow} values were retained in the plastic films even after 10 days of incubation. The results are demonstrated in Fig. 6.

It is interesting to observe that the pesticides that did not show any significant sorption earlier were also the ones that were the most desorbed. The results suggest that in the case of pyridaben (which has a relatively high log K_{ow} value and demonstrated a high degree of sorption earlier) was desorbed to its maximum possible extent in the first 2 days

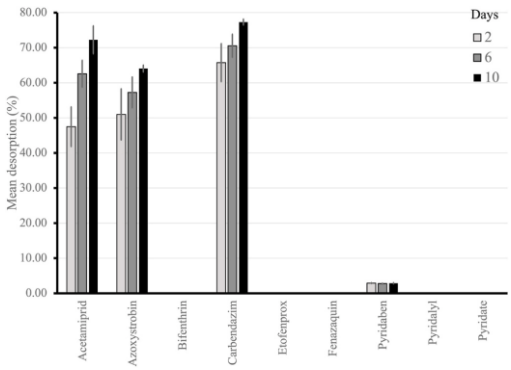

Fig. 6. Mean desorption % of pesticides over 2, 6 and 10 days.

and then over the next period of time until 10 days, did not show an increase in desorption amount. On the other hand, azoxystrobin, acetamiprid and carbendazim (pesticides with lower log K_{ow} values and no observed sorption) were slowly desorbed over a period of 10 days. Our results suggest that mulch films could rapidly desorb certain pesticides that come in contact with them after a spraying event, which would then

be leached into the surrounding agricultural soils, where they could be resorbed and concentrated by either the microplastics present in the soil or come in contact with the crop rhizosphere. However, it is interesting to note that these films, to a certain extent, could also act as sinks for pesticides with a high degree of hydrophobicity. This cumulative process leads to a situation of selective sorption and retention in the mulch film which further highlights the need for contaminant-specific research on its interactions with microplastics in the agricultural ecosystem and even more so, the need for proper collection and removal of the mulch films from the fields after application and subsequent storage, handling and disposal or recycling.

4. Conclusions

The presence of microplastics in the agricultural ecosystem reflects a big concern, the magnitude of which remains largely un-investigated and the extent of the issue is expected to increase if necessary steps are not taken for its mitigation. This study looked into the sorption of different PAHs as well as the sorption and desorption of various pesticides onto pure model microspheres and microplastic samples produced from commercial agricultural mulch films. Agri-PE samples used in this study, were found to be more realistic and comparable to the actual microplastic particles expected in the agricultural environments. Sorption percentages in all cases were found to be higher in case of Agri-PE samples as opposed to Pure-PE samples with the sorption increasing by 2%–91% for the investigated compounds. Our results demonstrate that even at realistic environmental concentration of 5 μg/L, pesticide residues could be sorbed to a high degree onto microplastics generated from mulch films in the agricultural ecosystem. Additionally, the process of sorption would be case-specific to each contaminant depending on it log K_{ow} value with compounds with high hydrophobicity being sorbed onto the microplastics to a high degree. The fact that sorption capacities were found to be influenced by the ionic strength of the reaction media, highlights the role of electrostatic forces in the process and thus implies that the process would be different in different agricultural scenarios depending on the properties of the irrigation water or soil.

For the type of microplastic sample investigated, pseudo-first order was found to be the best fitting kinetic model for all pesticides (R^2: 0.90–0.98) thereby implying the dominant role of physi-sorption and limited role of chemical bond formation in our case. Furthermore, the fact that Dubinin-Radushkevich was the best fitting isotherm model (R^2: 0.92–0.99), implied the presence of a micropore volume filling mechanism over the heterogeneous and rough surfaced MPs derived from mulch films. These results should however be considered for polyethylene polymer type as the process of sorption is influenced by the cumulative effect of the polymer, contaminant and media properties and can be specific to each polymer composition. Results from the desorption experiments furthermore highlight the role of mulch films acting as an additional source for the release of pesticide residues to the agricultural environment while serving as sinks for other specific contaminants.

Our study puts into focus the capacity of microplastics generated from the plastic films used for the process of mulching, to act as carries or vectors of transport of pesticide residues and certain PAHs in the agricultural ecosystem. This phenomenon could influence the ultimate fate and availability of these residual contaminants and could expose the surrounding agricultural environment to elevated levels of such residues.

Credit author statement

Harshit Sahai: Conceptualization, Investigation, Methodology, Formal analysis, Writing – Original Draft, Visualization. Mar García Valverde: Investigation, Methodology. María Murcia Morales: Investigation, Methodology. María Dolores Hernando: Supervision, Project administration, Funding acquisition, Conceptualization, Writing – Review & Editing. Ana M. Aguilera del Real: Conceptualization, Investigation, Methodology, Formal analysis, Writing – Review & Editing, Validation. A.R. Fernández- Alba: Supervision, Conceptualization, Validation, Resources, Writing – Review & Editing.

Declaration of competing interest

The authors declare that they have no known competing financial interests or personal relationships that could have appeared to influence the work reported in this paper.

Data availability

Data will be made available on request.

Acknowledgements

Authors are very grateful to the Spanish Ministry of Science and Innovation for the financial support given to the project "CERTAIN" (PID 2020-116230RB-I00 and Project PLEC 2021- 007693. H. Sahai acknowledges the support of "FoodTraNet" MSCA-ITN project and the funding received from the European Union's Horizon 2020 research and innovation programme under the Marie Skłodowska-Curie grant agreement No. 956265. M. García-Valverde acknowledges the Spanish Ministry of Science, Innovation and Universities for the pre-doctoral Training Research Staff (FPI) fellowship program (PRE 2018-087072). Experimental facilities and support were provided by the European Union Reference Laboratory for Residues of Pesticides in Fruits and Vegetables (EURL-FV) at the University of Almeria, Spain. Open Access funding provided thanks to the CSIC-CRUE agreement with Elsevier.

Appendix A. Supplementary data

Supplementary data to this article can be found online at https://doi.org/10.1016/j.chemosphere.2023.138959.

References

Aharoni, C., Tompkins, F.C., 1970. Kinetics of adsorption and desorption and the Elovich equation. Adv. Catal. 21, 1–49. https://doi.org/10.1016/S0360-0564(08)60563-5. Elsevier.

Alimi, O.S., Farner Budarz, J., Hernandez, L.M., Tufenkji, N., 2018. Microplastics and nanoplastics in aquatic environments: aggregation, deposition, and enhanced contaminant transport. Environ. Sci. Technol. 52 (4), 1704–1724. https://doi.org/10.1021/acs.est.7b05559.

Astner, A.F., Hayes, D.G., O'Neill, H., Evans, B.R., Pingali, S.V., Urban, V.S., Young, T.M., 2019. Mechanical formation of micro- and nano-plastic materials for environmental studies in agricultural ecosystems. Sci. Total Environ. 685, 1097–1106. https://doi.org/10.1016/j.scitotenv.2019.06.241.

Atugoda, T., Vithanage, M., Wijesekara, H., Bolan, N., Sarmah, A.K., Bank, M.S., You, S., Ok, Y.S., 2021. Interactions between microplastics, pharmaceuticals and personal care products: implications for vector transport. Environ. Int. 149, 106367 https://doi.org/10.1016/j.envint.2020.106367.

Ayawei, N., Ebelegi, A.N., Wankasi, D., 2017. Modelling and interpretation of adsorption isotherms. J. Chem., e3039817 https://doi.org/10.1155/2017/3039817, 2017.

Bakir, A., Rowland, S.J., Thompson, R.C., 2012. Competitive sorption of persistent organic pollutants onto microplastics in the marine environment. Mar. Pollut. Bull. 64 (12), 2782–2789. https://doi.org/10.1016/j.marpolbul.2012.09.010.

Balarak, D., Mostafapour, F.K., Azarpira, H., Joghataei, A., 2017. Langmuir, Freundlich, Temkin and dubinin–radushkevich isotherms studies of equilibrium sorption of ampicilin unto montmorillonite nanoparticles. J. Pharmaceutical Res. Inter. 1 https://doi.org/10.9734/JPRI/2017/38056. –9.

Brahney, J., Hallerud, M., Heim, E., Hahnenberger, M., Sukumaran, S., 2020. Plastic rain in protected areas of the United States. Science 368 (6496), 1257–1260. https://doi.org/10.1126/science.aaz5819.

Brdar, M., Šćiban, M., Takači, A., Došenović, T., 2012. Comparison of two and three parameters adsorption isotherm for Cr(VI) onto Kraft lignin. Chem. Eng. J. 183, 108–111. https://doi.org/10.1016/j.cej.2011.12.036.

Brennecke, D., Duarte, B., Paiva, F., Caçador, I., Canning-Clode, J., 2016. Microplastics as vector for heavy metal contamination from the marine environment. Estuar. Coast Shelf Sci. 178, 189–195. https://doi.org/10.1016/j.ecss.2015.12.003.

Brooks, A.L., Wang, S., Jambeck, J.R., 2018. The Chinese import ban and its impact on global plastic waste trade. Sci. Adv. 4 (6) https://doi.org/10.1126/sciadv.aat0131.

Bueno, M.J.M., Gomez, M.J., Herrera, S., Hernando, M.D., Agüera, A., Fernández-Alba, A.R., 2012. Occurrence and persistence of organic emerging contaminants and priority pollutants in five sewage treatment plants of Spain: two years pilot survey monitoring. Environ. Pollut. 164, 267–273. https://doi.org/10.1016/j.envpol.2012.01.038.

Camacho, M., Herrera, A., Gómez, M., Acosta-Dacal, A., Martínez, I., Henríquez-Hernández, L.A., Luzardo, O.P., 2019. Organic pollutants in marine plastic debris from Canary Islands beaches. Sci. Total Environ. 662, 22–31. https://doi.org/10.1016/j.scitotenv.2018.12.422.

Chen, S.G., Yang, R.T., 1994. Theoretical basis for the potential theory adsorption isotherms. The dubinin-radushkevich and dubinin-astakhov equations. Langmuir 10 (11), 4244–4249. https://doi.org/10.1021/la00023a054.

Cole, M., Lindeque, P., Halsband, C., Galloway, T.S., 2011. Microplastics as contaminants in the marine environment: a review. Mar. Pollut. Bull. 62 (12), 2588–2597. https://doi.org/10.1016/j.marpolbul.2011.09.025.

Dada, A.O., Olalekan, A.P., Olatunya, A.M., Dada, O., 2012. Langmuir, Freundlich, Temkin and dubinin–radushkevich isotherms studies of equilibrium sorption of Zn 2 + unto phosphoric acid modified rice husk. IOSR J. Appl. Chem. 3 (1), 38–45. https://doi.org/10.9790/5736-0313845.

De-la-Torre, G.E., 2020. Microplastics: an emerging threat to food security and human health. J. Food Sci. Technol. 57 (5), 1601–1608. https://doi.org/10.1007/s13197-019-04138-1.

Díaz-Galiano, F.J., Gómez-Ramos, M.J., Beraza, I., Murcia-Morales, M., Fernández-Alba, A.R., 2023. Cooking food in microwavable plastic containers: in situ formation of a new chemical substance and increased migration of polypropylene polymers. Food Chem. 417, 135852 https://doi.org/10.1016/j.foodchem.2023.135852.

FAO, 2021. Assessment of Agricultural Plastics and Their Sustainability: A Call for Action. FAO. https://doi.org/10.4060/cb7856en.

Huang, Y., Liu, Q., Jia, W., Yan, C., Wang, J., 2020. Agricultural plastic mulching as a source of microplastics in the terrestrial environment. Environ. Pollut. 260, 114096 https://doi.org/10.1016/j.envpol.2020.114096.

Hüffer, T., Hofmann, T., 2016. Sorption of non-polar organic compounds by micro-sized plastic particles in aqueous solution. Environ. Pollut. 214, 194–201. https://doi.org/10.1016/j.envpol.2016.04.018.

Hutson, N.D., Yang, R.T., 1997. Theoretical basis for the Dubinin-Radushkevitch (D-R) adsorption isotherm equation. Adsorption 3 (3), 189–195. https://doi.org/10.1007/BF01650130.

Jiménez-Morillo, N.T., Cabrita, M.J., Dias, C.B., González-Vila, F.J., González-Pérez, J.A., 2020. Pyrolysis-compound-specific hydrogen isotope analysis (δ2H Py-CSIA) of Mediterranean olive oils. Food Control 110, 107023. https://doi.org/10.1016/j.foodcont.2019.107023.

Lan, T., Wang, T., Cao, F., Yu, C., Chu, Q., Wang, F., 2021. A comparative study on the adsorption behavior of pesticides by pristine and aged microplastics from agricultural polyethylene soil films. Ecotoxicol. Environ. Saf. 209, 111781 https://doi.org/10.1016/j.ecoenv.2020.111781.

Li, H., Wang, F., Li, J., Deng, S., Zhang, S., 2021. Adsorption of three pesticides on polyethylene microplastics in aqueous solutions: kinetics, isotherms, thermodynamics, and molecular dynamics simulation. Chemosphere 264, 128556. https://doi.org/10.1016/j.chemosphere.2020.128556.

Mo, Q., Yang, X., Wang, J., Xu, H., Li, W., Fan, Q., Gao, S., Yang, W., Gao, C., Liao, D., Li, Y., Zhang, Y., 2021. Adsorption mechanism of two pesticides on polyethylene and polypropylene microplastics: DFT calculations and particle size effects. Environ. Pollut. 291, 118120 https://doi.org/10.1016/j.envpol.2021.118120.

Ng, E.-L., Huerta Lwanga, E., Eldridge, S.M., Johnston, P., Hu, H.-W., Geissen, V., Chen, D., 2018. An overview of microplastic and nanoplastic pollution in agroecosystems. Sci. Total Environ. 627, 1377–1388. https://doi.org/10.1016/j.scitotenv.2018.01.341.

Nizzetto, L., Futter, M., Langaas, S., 2016. Are agricultural soils dumps for microplastics of urban origin? Environ. Sci. Technol. 50 (20), 10777–10779. https://doi.org/10.1021/acs.est.6b04140.

PlasticsEurope, 2021. Plastics – the Facts 2021: an Analysis of European Plastics Production, Demand and Waste Data. Available at: https://plasticseurope.org/knowledge-hub/plastics-the-facts-2021/. (Accessed 22 January 2023).

Sakurovs, R., Day, S., Weir, S., Duffy, G., 2007. Application of a modified Dubinin−Radushkevich equation to adsorption of gases by coals under supercritical conditions. Energy Fuel. 21 (2), 992–997. https://doi.org/10.1021/ef0600614.

SANTE/11312/2021, European Commission Directorate-General for Health and Food Safety, 2021. Guidance Document on Analytical Quality Control and Method Validation Procedures for Pesticides Residues Analysis in Food and Feed. https://www.eurl-pesticides.eu/docs/public/tmplt_article.asp?CntID=727&LabID=100&Lang=EN. (Accessed 22 January 2023).

Sarkar, D.J., Barman, M., Bera, T., De, M., Chatterjee, D., 2018. Agriculture: Polymers in Crop Production Mulch and Fertilizer. https://doi.org/10.1201/9781351019422-140000083.

Scarascia-Mugnozza, G., Sica, C., Russo, G., 2011. Plastic materials in EUROPEAN agriculture: actual use and perspectives. J. Agricul. Eng. 42 (3) https://doi.org/10.4081/jae.2011.3.15. Article 3.

Simon, M., van Alst, N., Vollertsen, J., 2018. Quantification of microplastic mass and removal rates at wastewater treatment plants applying Focal Plane Array (FPA)-based Fourier Transform Infrared (FT-IR) imaging. Water Res. 142, 1–9. https://doi.org/10.1016/j.watres.2018.05.019.

Sohn, S., Kim, D., 2005. Modification of Langmuir isotherm in solution systems—definition and utilization of concentration dependent factor. Chemosphere 58 (1), 115–123. https://doi.org/10.1016/j.chemosphere.2004.08.091.

Sorasan, C., Edo, C., González-Pleiter, M., Fernández-Piñas, F., Leganés, F., Rodríguez, A., Rosal, R., 2021. Generation of nanoplastics during the photoageing of low-density polyethylene. Environ. Pollut. 289, 117919 https://doi.org/10.1016/j.envpol.2021.117919.

Sorasan, C., Edo, C., González-Pleiter, M., Fernández-Piñas, F., Leganés, F., Rodríguez, A., Rosal, R., 2022. Ageing and fragmentation of marine microplastics. Sci. Total Environ. 827, 154438 https://doi.org/10.1016/j.scitotenv.2022.154438.

Steinmetz, Z., Wollmann, C., Schaefer, M., Buchmann, C., David, J., Tröger, J., Muñoz, K., Frör, O., Schaumann, G.E., 2016. Plastic mulching in agriculture. Trading short-term agronomic benefits for long-term soil degradation? Sci. Total Environ. 550, 690–705. https://doi.org/10.1016/j.scitotenv.2016.01.153.

Stoeckli, F., 1993. Dubinin's theory for the volume filling of micropores: an historical approach. Adsorpt. Sci. Technol. 10 (1–4), 3–16. https://doi.org/10.1177/026361749901000l-402.

Tourinho, P.S., Kočí, V., Loureiro, S., van Gestel, C.A.M., 2019. Partitioning of chemical contaminants to microplastics: sorption mechanisms, environmental distribution and effects on toxicity and bioaccumulation. Environ. Pollut. 252, 1246–1256. https://doi.org/10.1016/j.envpol.2019.06.030.

Trouvé, G., Ngo, C., Almouallem, W., Joyeux, C., Dorge, S., Michel, J., Nouen, D.L., 2022. Development of a liquid/liquid extraction method and GC/MS analysis dedicated to the quantitative analysis of PAHs and O-PACs in groundwater from contaminated sites and soils. Polycycl. Aromat. Comp. 42 (7), 4000–4018. https://doi.org/10.1080/10406638.2021.1880449.

van den Berg, P., Huerta-Lwanga, E., Corradini, F., Geissen, V., 2020. Sewage sludge application as a vehicle for microplastics in eastern Spanish agricultural soils. Environ. Pollut. 261, 114198 https://doi.org/10.1016/j.envpol.2020.114198.

Velez, J.F.M., Shashoua, Y., Syberg, K., Khan, F.R., 2018. Considerations on the use of equilibrium models for the characterisation of HOC-microplastic interactions in vector studies. Chemosphere 210, 359–365. https://doi.org/10.1016/j.chemosphere.2018.07.020.

Velzeboer, I., Kwadijk, C.J.A.F., Koelmans, A.A., 2014. Strong sorption of PCBs to nanoplastics, microplastics, carbon nanotubes, and fullerenes. Environ. Sci. Technol. 48 (9), 4869–4876. https://doi.org/10.1021/es405721v.

Wang, J., Liu, X., Liu, G., Zhang, Z., Wu, H., Cui, B., Bai, J., Zhang, W., 2019. Size effect of polystyrene microplastics on sorption of phenanthrene and nitrobenzene. Ecotoxicol. Environ. Saf. 173, 331–338. https://doi.org/10.1016/j.ecoenv.2019.02.037.

Wang, F., Gao, J., Zhai, W., Liu, D., Zhou, Z., Wang, P., 2020. The influence of polyethylene microplastics on pesticide residue and degradation in the aquatic environment. J. Hazard Mater. 394, 122517 https://doi.org/10.1016/j.jhazmat.2020.122517.

Wang, T., Yu, C., Chu, Q., Wang, F., Lan, T., Wang, J., 2020. Adsorption behavior and mechanism of five pesticides on microplastics from agricultural polyethylene films. Chemosphere 244, 125491. https://doi.org/10.1016/j.chemosphere.2019.125491.

Wang, X., Bolan, N., Tsang, D.C.W., Sarkar, B., Bradney, L., Li, Y., 2021. A review of microplastics aggregation in aquatic environment: influence factors, analytical methods, and environmental implications. J. Hazard Mater. 402, 123496 https://doi.org/10.1016/j.jhazmat.2020.123496.

Wu, F.-C., Tseng, R.-L., Juang, R.-S., 2009. Characteristics of Elovich equation used for the analysis of adsorption kinetics in dye-chitosan systems. Chem. Eng. J. 150 (2–3), 366–373. https://doi.org/10.1016/j.cej.2009.01.014.

Wu, C., Zhang, K., Huang, X., Liu, J., 2016. Sorption of pharmaceuticals and personal care products to polyethylene debris. Environ. Sci. Pollut. Control Ser. 23 (9), 8819–8826. https://doi.org/10.1007/s11356-016-6121-7.

Xu, B., Liu, F., Brookes, P.C., Xu, J., 2018. Microplastics play a minor role in tetracycline sorption in the presence of dissolved organic matter. Environ. Pollut. 240, 87–94. https://doi.org/10.1016/j.envpol.2018.04.113.

Yang, C., 1998. Statistical mechanical study on the Freundlich isotherm equation. J. Colloid Interface Sci. 208 (2), 379–387. https://doi.org/10.1006/jcis.1998.5843.

Yang, Y., Li, Z., Yan, C., Chadwick, D., Jones, D.L., Liu, E., Liu, Q., Bai, R., He, W., 2022. Kinetics of microplastic generation from different types of mulch films in agricultural soil. Sci. Total Environ. 814, 152572 https://doi.org/10.1016/j.scitotenv.2021.152572.

Zhang, C., Lei, Y., Qian, J., Qiao, Y., Liu, J., Li, S., Dai, L., Sun, K., Guo, H., Sui, G., Jing, W., 2021. Sorption of organochlorine pesticides on polyethylene microplastics in soil suspension. Ecotoxicol. Environ. Saf. 223, 112591 https://doi.org/10.1016/j.ecoenv.2021.112591.

3.2 Publication 2

Title: Evaluation of the sorption/desorption processes of pesticides in biodegradable mulch films used in agriculture

Harshit Sahai[a,b,c], María Dolores Hernando[a], María Jesús Martínez Bueno[b], Ana M. Aguilera del Real[b,*], Amadeo R. Fern´ andez- Alba[b]

a) Experimental Station of Arid Zones, The Spanish National Research Council (CSIC-EEZA), Ctra. de Sacramento s/n, La Cañada de San Urbano, 04120, Almería, Spain
b) Agrifood Campus of International Excellence (ceiA3), European Union Reference Laboratory for Pesticide Residues in Fruit & Vegetables. Department of Chemistry and Physics, University of Almería, La Ca˜ nada de San Urbano, 04120, Almería, Spain
c) Jožef Stefan International Postgraduate School, Jamova 39, 1000, Ljubljana, Slovenia

Biodegradable polymers, such as PBAT, are intentionally formulated to degrade rapidly when exposed to environmental conditions. This characteristic has led to an increasing worldwide inclination towards their manufacturing and application as agricultural mulch films, displacing conventional non-degradable alternatives. Nonetheless, uncertainties persist regarding the possible interactions between these biodegradable films and pesticides within agricultural environments.

The primary focus of this paper revolves around addressing the ecological apprehensions associated with deploying biodegradable plastic mulch films in agricultural practices. Although traditional polyethylene mulch films have been widely favored due to their advantageous traits in soil upkeep and safeguarding crops, they also play a substantial role in contributing to the contamination stemming from microplastics. Biodegradable mulch films like PBAT have emerged as a greener option in this context; nevertheless, they have been associated with forming MNPs owing to incomplete degradation within the agricultural setting. By undertaking a comparative evaluation of the behaviors related to pesticide retention and release in standard PE films in contrast to biodegradable PBAT mulch films, coupled with in-depth scrutiny of the sorption mechanisms of specific pesticides on PE and PBAT mulch microplastics, the primary objective of this study is to confront this prevailing issue. By highlighting the differences in pesticide retention and release dynamics between biodegradable and conventional mulch films, the paper aims to furnish invaluable insights into the environmental efficacy exhibited by these materials. Despite endorsing biodegradable mulch films as an environmentally friendly choice, it is crucial to acknowledge that they might potentially retain elevated concentrations of pesticides, possibly impacting their environmental fate and transport.

Chemosphere 351 (2024) 141183

Contents lists available at ScienceDirect

Chemosphere

journal homepage: www.elsevier.com/locate/chemosphere

Evaluation of the sorption/desorption processes of pesticides in biodegradable mulch films used in agriculture

Harshit Sahai [a,b,c], María Dolores Hernando [a], María Jesús Martínez Bueno [b], Ana M. Aguilera del Real [b,*], Amadeo R. Fernández- Alba [b]

[a] Experimental Station of Arid Zones, The Spanish National Research Council (CSIC-EEZA), Ctra. de Sacramento s/n, La Cañada de San Urbano, 04120, Almería, Spain
[b] Agrifood Campus of International Excellence (ceiA3), European Union Reference Laboratory for Pesticide Residues in Fruit & Vegetables. Department of Chemistry and Physics, University of Almería, La Cañada de San Urbano, 04120, Almería, Spain
[c] Jozef Stefan International Postgraduate School, Jamova 39, 1000, Ljubljana, Slovenia

HIGHLIGHTS

- Biodegradable mulch films retained higher amounts of pesticides than PE films.
- Higher temperature increased pace of desorption in conventional mulch films.
- Sorption in biodegradable MP explained by Elovich and pseudo-second order models.
- Chemical bonding governed the sorption process and was the rate-limiting step.
- Log K_{ow} cutoff value was lower for biodegradable than conventional plastic.

GRAPHICAL ABSTRACT

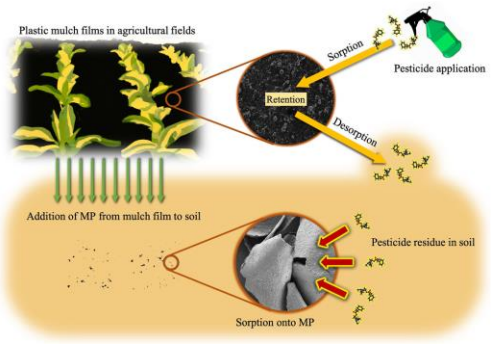

ARTICLE INFO

Handling Editor: Yongmei Li

Keywords:
Biodegradable
Mulch films
Pesticides
Microplastics
Sorption
Desorption

ABSTRACT

Microplastics from mulch films can be a source of chemical contamination to agricultural soils. In this context, biodegradable films have been widely positioned as a greener choice. However, their sorption/desorption capabilities, in contrast to the conventional plastic types remain understudied. It is for this reason that objective evaluation of their interactions with residual agricultural contaminants becomes important. Our findings reveal that polyethylene (PE) mulch films retained lower amounts of pesticide residues and demonstrated a higher desorption/release [median desorption = 71.86 μg/L or about 50%], while polybutylene adipate terephthalate (PBAT) mulch films retained higher amounts of pesticide residues onto their surface and demonstrated a much lower desorption [median desorption = 24.27 μg/L or about 17%] after a spraying event. A higher ambient temperature had no significant effect on final desorption amounts in both PE [median = 65.27 μg/L at 20 °C and 74.23 μg/L at 40 °C] and PBAT [median = 24.26 μg/L at 20 °C and 24.78 μg/L at 40 °C] mulch films. However, it

* Corresponding author.
E-mail address: aaguiler@ual.es (A.M. Aguilera del Real).

https://doi.org/10.1016/j.chemosphere.2024.141183
Received 26 October 2023; Received in revised form 15 December 2023; Accepted 9 January 2024
Available online 9 January 2024

did favour a faster desorption pace in PE films. Desorption in PBAT and PE plastic types was correlated with the log K_{ow} value [Spearman's correlation: 0.857 and 0.837 respectively, $p < 0.05$]. However, only a moderate correlation with pKa was observed in PBAT [Spearman's correlation: 0.478, $p < 0.05$], while none for PE plastic type. Sorption of pesticides onto biodegradable PBAT microplastics were best explained by Elovich [R^2: 0.937–0.959] and pseudo-second order kinetics [R^2: 0.942–0.987], suggesting the presence of chemisorption. Furthermore, Weber Morris plots suggested the presence of a multi-step process and Boyd plots indicated that film diffusion or chemical bond formation was the rate-limiting step governing this phenomenon.

1. Introduction

A plastic material is defined as a bioplastic if it is either biodegradable, bio-based (wholly or partially), or a combination of both of these properties (European Bioplastics, 2021). The current global production of bioplastics stands at 2.42 million tonnes in 2021with Asia being the largest producer (≈50%), Europe at the second spot (≈24%) and North America at the third spot (≈17%). However, this production capacity is projected to reach 7.59 million tonnes by 2026 (European Bioplastics, 2021). Of these, the top three materials currently employed for bioplastics are polybutylene adipate terephthalate or PBAT (19.2%), poly-lactic acid or PLA (18.9%) and starch-blends (16.4%). At the same time, an estimated 14% of the total biodegradable plastic production is used by the agricultural and horticultural markets (European Bioplastics, 2021).

Polymers such as PBAT, PLA, and other starch-based bioplastics are widely used in commercial agricultural mulch films and other agricultural practices. However, despite the numerous benefits that mulch films provide to the agricultural production systems such as protection from harsh climatic conditions, suppression of weeds, increased soil temperatures, reduced moisture loss, and reduced nutrient runoff (Guerrini et al., 2019; Scarascia-Mugnozza et al., 2011), they are also one of the major contributors of microplastics in the agricultural fields (Huang et al., 2020), and have been reported to be present in the agricultural environments across various regions of the globe (Kasa et al., 2022). According to recent estimates, depending on the type of polymer, 147 to 475 microplastic particles could be produced on average per cm^2 of the mulch film due to various degradative forces in the environment (Yang et al., 2022).

In this context, bioplastics have been widely positioned as sustainable, greener alternatives to conventional, non-degradable plastics because they can be naturally degraded into end products such as CO_2, H_2O and biomass and thus have a significantly less persistence in the environment than a non-degradable plastic waste. However, these bioplastics are often modified using several compounds (additives) that provide chemical, physical, and structural properties to the polymer, making them commercially useable. These modifications can affect the degradability of such bioplastics (Lambert and Wagner, 2017) and can also lead to the addition of micro-bioplastics to agricultural ecosystems owing to incomplete degradation (Qin et al., 2021; Shruti and Kutralam-Muniasamy, 2019). Furthermore, as reported previously, bioplastics could be responsible for the production of higher amounts of microplastics in the agricultural environment than a conventional plastic mulch film (Yang et al., 2022).

In an agricultural scenario, mulch films are expected to interact with pesticide residues through two major routes amongst others: (1) Firstly, during the application life cycle of the mulch film, it is expected to receive multiple exposures to pesticides during each spraying event. Due to this repeated exposure, pesticides might be adsorbed on to the plastic film and over time, these adsorbed pesticide residues could either be leached into the surrounding soil or be retained onto the mulch film for longer durations. (2) Secondly, over time and application life cycle and under the influence of various environmental degradative forces, these mulch films break down into microplastics and these microplastics might ultimately interact with the surrounding pesticide residues and adsorb them.

Due to their high specific surface area, microplastics have been known to interact with surrounding contaminants in the aquatic environment and affect the fate and bioavailability of such contaminants (Yang et al., 2022). The process of sorption of contaminants onto microplastics is expected to be governed by a number of underlying forces such as hydrophobic partitioning, electrostatic forces, van der Waals forces, H-bonding, π-π interactions, etc, and could be affected by the polymer properties such as hydrophobicity, particle size, surface area, crystallinity, surface roughness, surface charge and aggregation amongst others; sorbate properties such as octanol-water partition coefficient (log K_{ow}), molecule size, functional group content; and environmental factors such ambient pH, temperature, ionic strength, the presence of organic matter/co-existing solids, and other competing sorbates. Additionally, according to a recent study, biodegradable microplastics may have more harmful impacts than regular MPs and a greater affinity for interacting with particular environmental contaminants. (Qin et al., 2021). Yet, very few studies have investigated the presence and impact of these biodegradable microplastics in the environment and even fewer in the agricultural ecosystems (Qin et al., 2021).

The aim of this study was to investigate the interaction of biodegradable mulch films and microplastics derived from biodegradable mulch films with agricultural pesticide residues by simulating the two pathways mentioned previously. Here, to reproduce the first situation, we mimic the spraying of pesticides onto two types of mulch films: conventional PE and biodegradable PBAT, and highlight the trends of desorption and retention of various selected pesticides in the two plastic types. The results in the case of PE mulch film are contrasted with those for the biodegradable mulch film and the effect of temperature over the process is explored. Subsequently, experiments were conducted to study the process of sorption in microplastics produced from such biodegradable mulch films and mathematical equations were utilized to model the process.

2. Materials and methods

2.1. Analytical standards and microplastic samples

Analytical standards for the pesticides bifenthrin, pyridate, fenazaquin, lufenuron, pyriproxifen, spiromesifen and acetamiprid were obtained from Dr. Ehrenstorfer GmbH (Germany), while pyridaben, pyridalyl, etofenprox, carbendazim, azoxystrobin, chlorantraniliprole, cyprodinil, difenoconazole, fluopyram, flutriafol, myclobutanil and fluxapyroxad were obtained from Sigma-Aldrich (United States). All pesticides were chosen to represent a wide range of physicochemical properties across a broad range of log K_{ow} that are detailed in Table S (1). Agricultural plastic films labelled as conventional (sample: Agri-PE) and biodegradable (sample: Agri-BP) were purchased from commercial vendors in Almeria, Spain. In order to produce the microplastic samples, pieces of both plastic films were cut and exposed to liquid nitrogen for freezing. These frozen bits were then processed into microplastics using a grinder (Retsch GM 200, Retsch GmbH, Germany) at 10,000 rpm and multiple repetitions of grinding cycles lasting 30 s each. In order to prevent heating of the plastic film, which would lessen its brittleness and subsequently prevent the creation of microplastics, the period of each grinding cycle was maintained brief. To obtain particles with a size

range of 50–200 μm, the resulting particles were subsequently sieved through a stainless-steel mesh.

2.2. Analytical methods

2.2.1. Pyrolysis-GC/MS

Analytical pyrolysis (Py-GC/MS) was performed using 0.1 mg of microplastic sample at 400 °C (1 min) in a micro furnace pyrolysis system (Frontier Lab. model 3030D, Fukushima, Japan) as per the methodology described elsewhere (Jiménez-Morillo et al., 2020). In brief, the pyrolizer was coupled with a GC/MS system (Agilent 6890) equipped with a low polar-fused silica capillary column (HP5MS-UI; 30 m × 250 μm × 0.25 μm). The GC was equipped with an Agilent 5973 MSD mass selective detector, and mass spectra were collected at 70 eV. Chromatographic conditions were as follows: He carrier gas (flow rate: 1 mL/min); the oven was preheated to 50 °C for 1 min and then increased to 100 °C at 30 °C min^{-1}, from 100 to 300 °C at 10 °C min^{-1}, and then constant at 300 °C for the last 10 min. The samples were identified using single-ion monitoring (SIM) and mass spectra libraries (NIST11 and Wiley7).

2.2.2. FTIR-ATR characterization

Spectroscopic characterization of plastic films was performed using Fourier Transform Infrared Spectroscopy- Attenuated Total Reflectance (FTIR-ATR). The spectra were recorded with an Alpha I Bruker spectrometer coupled with a model ECO Alpha ATR (Ge crystal) with a resolution of 4 cm^{-1} and were averaged over 32 scans. The spectral readout was in the range of 4000 to 600 wavenumber (cm^{-1}). The instrument was connected to a computer and controlled using OPUS Version 6.5 software.

2.2.3. LC-MS/MS analysis

Pesticide concentrations were analysed using Sciex Exion HP-LC coupled to Sciex 6500+ triple quad-LC-MS/MS equipped with a Zorbax Eclipse Plus C8 column (1.8 μm × 2.1 mm x 100 mm) at T = 35 °C. Two mobile phases used were as follows: (A) 0.1% formic acid and 5 mM ammonium formate in MeOH/water (98/2 v/v) and (B) 0.1% formic acid and 5 mM ammonium formate in water/MeOH (98/2 v/v). The gradient program used was as follows: (0–1 min) - 100% A; (1–2 min) - 100% A to 70% A; (2–3 min) - 70% A to 50% A; (3–11 min) - 50% A to 0% A; (11–14 min) −100% B; (14–14.1 min) - 0% A to 100% A and (14.1–17 min) - 100% A. Flow rate was set at 0.3 mL/min and injection volume at 5 μL. Ionization temperature was set at 300 °C and ion spray voltages were 5550 V in positive mode and −4500 V in negative mode. Total run time was 17 min for each sample. Method validation was carried out following quality control standards described previously (SANTE/11312/2021). To control the performance of sample injection, 10 μg/L solution of dimethoate-d6 was used as internal injection standard and the subsequent analysis was monitored.

In addition to the above-mentioned techniques, electron microscopy (Zeiss Sigma 300 VP Field Emission High Resolution Scanning Electron Microscope) was also utilized to examine the microplastic particles and learn more about their surface characteristics.

2.3. Experimental design

2.3.1. Desorption/retention experiments

Desorption experiments were conducted based on the methodology described elsewhere (Díaz-Galiano et al., 2023) and Commission Regulation (EU) No 10/2011 of 14 January 2011 on plastic materials and articles intended to come into contact with food. Using methanol as the solvent, a mixture containing all selected pesticides (acetamiprid, azoxystrobin, bifenthrin, carbendazim, chlorantraniliprole, cyprodinil, difenoconazole, etofenprox, fenazaquin, fluopyram, flutriafol, fluxapyroxad, lufenuron, myclobutanil, pyridaben, pyridalyl, pyridate, pyriproxyfen and spiromesifen) was prepared and 2 mL of this solution was sprayed onto a 10 × 10 cm piece of conventional and biodegradable mulch film using a spray bottle in order to mimic the spraying of pesticides in the agricultural field. Spiked plastics were then left overnight to completely dry at room temperatures. The spiked concentration over the plastic films was analysed using LC-MS/MS as mentioned previously and calculated to be 142 μg/L. Subsequently, the films were transferred into polytetrafluoroethylene (PTFE) tubes and 35 mL of 10% ethanol solution was added to it. Two separate batches were incubated at 20 °C and 40 °C ambient temperature conditions. Subsequently, 1 mL samples of the media were extracted from these bottles at 2, 6, and 10 days and analysed using LC-MS/MS in order to detect the concentration of the released pesticides. The 10th day of sampling was chosen based on the previously reported methodology (Díaz-Galiano et al., 2023) and the Commission Regulation (EU) No 10/2011. The 2nd day of sampling was chosen since in our preliminary experiments, all of the compounds studied reached their sorption equilibrium within 48 h, while the 6th day of sampling was chosen as a mid-point between 2 and 10 days.

2.3.2. Sorption experiments

Sorption experiments were conducted in batches using glass Erlenmeyer flasks. To the flasks, 100 mL of 0.0018 mol/L $CaCl_2$ solution [pH ≈ 6] was added (to set the ionic strength of solution at environmentally comparable levels) and spiked with the pesticides (acetamiprid, azoxystrobin, carbendazim, bifenthrin, fenazaquin, pyridaben, pyridalyl, pyridate and fluxapyroxad) to achieve 5 μg/L initial pesticide concentration. Subsequently, 10 mg of Agri-BP microplastics were added to this solution and the entire setup placed on a rotary shaker. Flask tops were sealed using aluminium foil and low light conditions were maintained in order to prevent any photolysis. Rotary speed was set at 120 rpm. and ambient temperature was set at 25 °C. During the experimental period, 1 mL samples of the media were extracted from this solution at 0.25, 0.75, 1, 1.5, 2, 3, 4, 5, and 24 h and further analysed using LC-MS/MS as detailed in the previous section. All experiments were carried out in triplicates, and the coefficient of variation for all the replicates was less than 20%.

To monitor any potential degradation of pesticides over the course of the experiment, control samples comprising all chosen pesticides were set up in both the sorption and desorption experiments, without any plastics introduced. In order to prevent pesticide degradation, extra precautions were taken, such as correctly sealing the sorption experiment flasks and placing the setup in a dark area to inhibit photolysis. Regarding the desorption experiments, the process was conducted using opaque, sealed, PTFE tubes without any exposure to outside light or air. Upon analysis of the pesticide concentrations in the control groups, no significant decrease in pesticide concentrations was found at the end of the experiment.

2.4. Kinetic modelling and data analysis

Kinetics of the sorption process were fitted to non-linear forms of the mathematical models namely: pseudo-first order, pseudo-second order, Elovich and intra-particle diffusion model. Kinetic plots were generated by plotting Q_t (μg/g) (amount of pesticide sorbed onto unit mass of MP against time (t)). All kinetic models were fitted onto the experimental data using the Solver tool in MS Excel by changing the model parameters with the aim of achieving the least SSR (sum of square of residues). The best fit models were chosen based on goodness of fit parameter (R^2) and chi-square parameter (χ^2). In addition, Boyd and Weber Morris plots were also generated from the data to explore the mechanism of sorption in our case. A description of each model used in this study is included in the supplementary material.

Data were statistically processed using SPSS statistical software (IBM Corp, USA). All the variables available were tested to check if the data confirmed to normal distribution. Since our data was found to be non-normally distributed, non-parametric statistics were utilized and the tests used have been specified along with the results.

3. Results and discussions

3.1. Characterization of plastic samples

Results of the Pyrolysis-GC-MS analysis show that the Agri-BP sample (and thus in turn, the biodegradable mulch film) was a blend of polybutylene adipate terephthalate (PBAT) polymer with 1,6 Diisocyanatohexane present as an additive (Figure S (1)). According to the information received from the vendor, a certain percentage of starch was also present in Agri-BP films. PBAT and starch do not mix well, rendering the resulting polymer blend unsuitable for film applications. (Jun, 2000). In order to overcome this issue, 1,6 Diisocyanatohexane is used as an additive to promote cross-linking which increases the miscibility of such blends (Xiong et al., 2013), thus in turn increasing elongation capacity and tensile strength of the resultant polymer (Jun, 2000). Furthermore, the conventional mulch film utilized in this study was confirmed to be a polyethylene polymer. Pyrolysis-GC-MS analysis also revealed the presence of 2,4-Di-*tert*-butylphenol (Antioxidant No. 33) in PE mulch film samples (Fig. S (1)), a compound added to commercial plastic films as an intermediate to provide resistance against oxidation.

Using FTIR-ATR spectral analysis (Fig. S (2)), characteristic absorption bands for both PBAT and PE films were observed. For PBAT, the strong band at 1720 cm^{-1} is due to the stretching vibration of the C═O bond of the ester group. C–H bending of the aromatic ring is found at 728 cm^{-1}, while the peaks at 1267 and 1107 cm^{-1} correspond to C–O and C–O–C stretching vibrations respectively. In the case of PE, the characteristic peaks observed were as follows: the stretching vibrations of $–CH_2$ at 2917 and 2849 cm^{-1}, the bending mode of the $–CH_2$ at 1462 cm^{-1} and the $–CH_2$ rocking vibration at 721 cm^{-1}.

Upon inspection under a scanning electron microscope, Agri-BP surfaces were found to be compact with fewer visible irregularities including cracks and pores than Agri-PE samples (Fig. 1). In addition to this, PBAT plastic surface presented several granular/filamentous projections which have been previously reported in PLA/PBAT/Starch blend films (Bilck et al., 2021; Farsetti et al., 2011). These granular projections are primarily residual starch granules that did not completely melt and incorporate into the polymer matrix during the plastic production process (Olivato et al., 2013). Furthermore, microplastic particles were found to be irregular in appearance and comprising of varied shapes and sizes.

3.2. Desorption/retention of pesticides in mulch films

The data for the desorbed/retained pesticides in the case of both plastic types did not conform to normality (Kolmogorov-Smirnov, $p \leq$

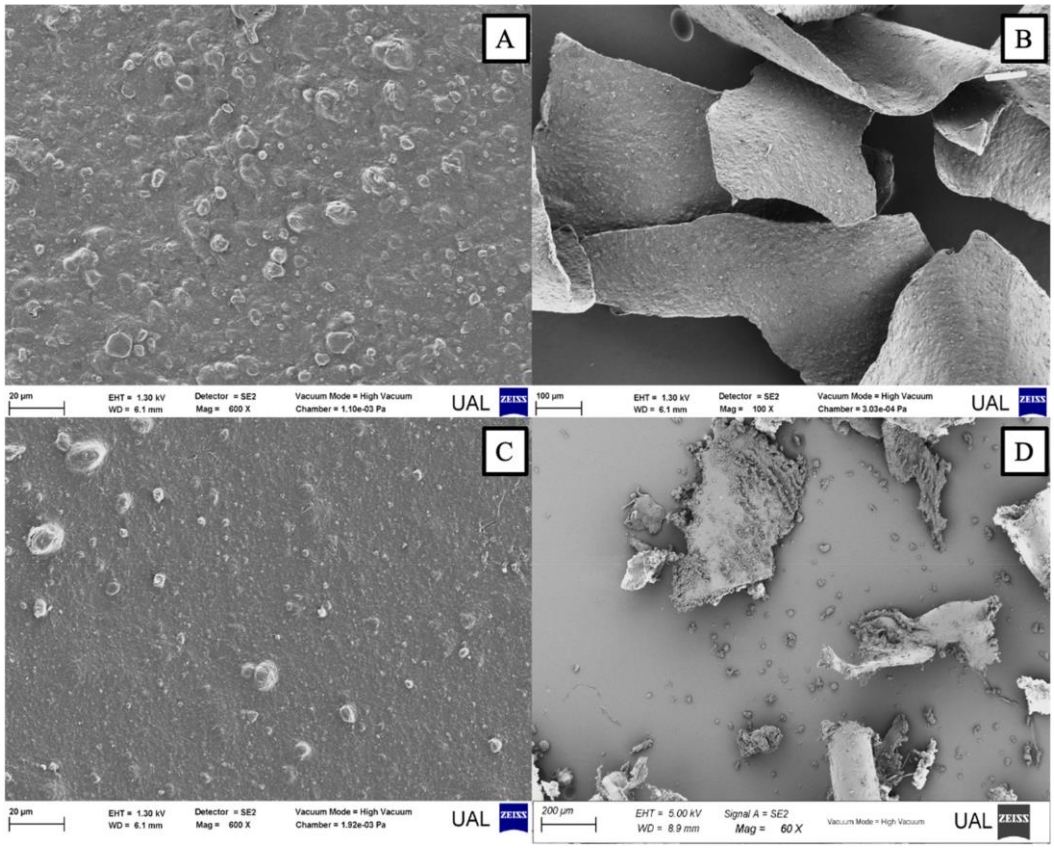

Fig. 1. SEM images of PBAT mulch film surface texture (A), PBAT microplastics sample (B), PE mulch film surface texture (C) and PE microplastics (D).

0.05) and therefore, non-parametric analysis was conducted. The results of desorption experiments have been depicted in Fig. 2 and explained below.

3.2.1. Effect of plastic type

At 20 °C, the mean desorbed concentration of pesticides in the case of PBAT film was 41.28 μg/L [95% C.I.: 33.45–49.10 μg/L], while for the PE film, it was 57.26 μg/L [95% C.I.: 51.12–63.41 μg/L]. Similarly at 40 °C, the mean desorbed concentration for all pesticides in the case of PBAT film was 35.92 μg/L [95% C.I.: 28.45–43.40 μg/L] and for PE film, it was 60.68 μg/L [95% C.I.: 54.18–67.18 μg/L]. Statistical analysis of the data revealed that for the pesticides that exhibited desorption, the overall desorption amounts were significantly different in the case of PBAT mulch film [median = 24.27 μg/L, n = 170] and were lower than PE mulch films [median = 71.86 μg/L, n = 234], [Mann-Whitney U = 13040.5, z = −5.91, $p < 0.05$], thus proving that under all experimental conditions, pesticides were desorbed to a greater extent in the case of PE mulch film while the PBAT mulch film was better at retaining higher amounts of the same pesticides.

Out of the 19 pesticides studied, 7 including pyridate, pyriproxifen, fenazaquin, pyridaben, bifenthrin, etofenprox and pyridalyl did not show any significant desorption [<5%] in the case of PE mulch film and were thus mostly retained in the plastic. While in the case of PBAT mulch film, 11 pesticides including azoxystrobin, fluxapyroxad, cyprodinil, difenoconazole, pyridate, pyriproxifen, fenazaquin, pyridaben, bifenthrin, etofenprox and pyridalyl did not show any significant desorption [<5%] indicating the retention of a greater number of pesticides in the biodegradable PBAT mulch film and desorption of a greater number of pesticides in conventional PE mulch film.

3.2.2. Effect of temperature

In order to investigate the effect of temperature over the desorption amounts, the desorbed concentrations at both 20 °C and 40 °C were compared for each plastic type. At the end of 10 days, in the case of PBAT film, there was no significant difference in the final desorption amounts of pesticides at 20 °C [median = 24.26 μg/L, n = 80] and 40 °C [median = 24.78 μg/L, n = 90], [Mann-Whitney U = 3250, z = −1.09, p = 0.275]. Similarly in the case of PE mulch film, there was no significant difference in the final desorption amounts at 20 °C [median = 65.27 μg/L, n = 117] and 40 °C [median = 74.23 μg/L, n = 117] [Mann-Whitney U = 6358.5, z = −0.94, p = 0.348].

Interestingly, it was observed that the desorption in the case of PE films at 20 °C increased significantly between 2, 6 and 10 days [Friedman test: $\chi^2 = 42.00$, df = 2, $p < 0.05$]. Wilcoxon signed-rank tests were used in post hoc analysis, and with the application of the Bonferroni correction, the significance level was set at p = 0.017. Upon post-hoc analysis it was observed that in the case of PE film at 20 °C, desorption increased significantly from 2 days [median: 54.23 μg/L] to 6 days [median: 75.27 μg/L] [Wilcoxon signed-rank: z = −4.640, $p < 0.017$] and then, from 6 days to 10 days [median: 82.38 μg/L] [Wilcoxon signed-rank: z = −4.689, $p < 0.017$]. In contrast to this, in the case of PE mulch film at 40 °C, the desorption increased significantly from the 2nd day [median: 72.99 μg/L] to the 6th day [median: 81.48 μg/L] [Wilcoxon signed-rank: z = −3.210, $p < 0.017$] but not from the 6th day to the 10th day [median: 81.18 μg/L] [Wilcoxon signed-rank: z = −0.628, $p > 0.017$]. This demonstrated that, while temperature had no effect on

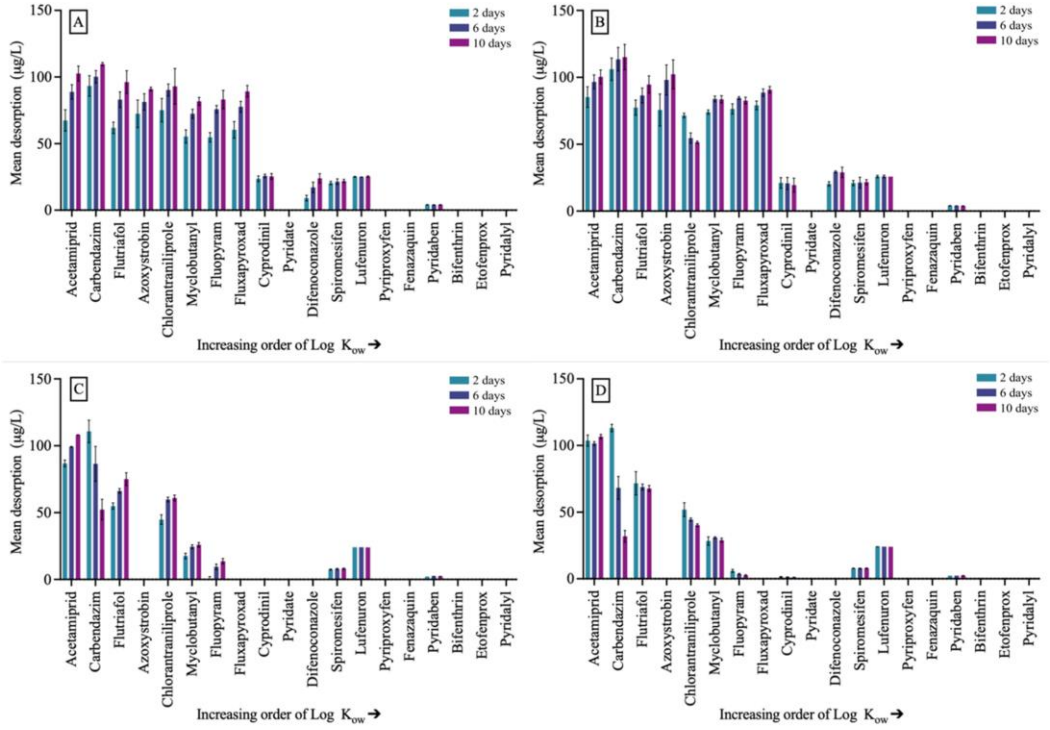

Fig. 2. Pesticide desorption amounts in PE mulch film at 20 °C (A) and at 40 °C (B) and pesticide desorption amounts in PBAT mulch film at 20 °C (C) and at 40 °C (D).

the final desorption amounts of the pesticides, a higher temperature (40 °C) resulted in the desorption process reaching its equilibrium time in around 6 days as opposed to the same film at 20 °C, where desorption increased until the 10th day.

On the other hand, in the case of PBAT films, desorption increased significantly over the experimental duration at both 20 °C [Friedman test: $\chi^2 = 9.920$, df = 2, $p < 0.05$] and at 40 °C [Friedman test: $\chi^2 = 9.731$, df = 2, $p < 0.05$], however, the increase was only significant between 2 and 6 days [Wilcoxon signed-rank: $p < 0.017$] and not between 6 and 10 days [Wilcoxon signed-rank: $p > 0.017$]. This suggests that in the case of biodegradable PBAT mulch film at 20 °C, the desorption reached its peak at a faster rate (around the 6th day) than PE mulch film (around the 10th day). These findings indicate that in the case of PBAT films, temperature had no apparent effect over the final desorption amounts as well as the time period.

3.2.3. *Effect of log K_{ow}*

The mean desorbed concentrations in both plastic types, accounting for all desorbed pesticides and at both temperature conditions combined at the end of 10 days, was found to be correlated with the log K_{ow} value of the respective pesticide [Spearman's correlation: 0.857 for PBAT and 0.837 for PE, p value < 0.05]. This relation for both plastic types at both temperatures is visualized in Fig. 3. Additionally, the value of log K_{ow} above which pesticides were majorly retained by the plastic film (cut-off point), was observed to be around 3.3 for PE film and around 2.8 for PBAT film.

In the case of PE mulch film at both temperature conditions, pesticides with log K_{ow} value $\leq$ 3.3 showed a high degree of desorption [84.38 ± 16.61 μg/L], while pesticides with log K_{ow} value above this point showed either no desorption or moderate desorption [29.32 ± 24.91 μg/L]. Furthermore, in the case of PBAT mulch film at both temperature conditions, pesticides with log K_{ow} value $\leq$ 2.8 showed a high degree of desorption [81.86 ± 23.48 μg/L], while pesticides with log K_{ow} value above this point showed either no desorption or moderate desorption [18.23 ± 17.13 μg/L]. This suggests affinity for a broader range of pesticides (broader range of log K_{ow}) in the case of biodegradable PBAT films.

Interestingly, azoxystrobin, which has a lower log K_{ow} value (2.5) and exhibited a high degree of desorption in PE mulch film, did not show any desorption in PBAT film probably due to differences in surface functional groups. This is also in contrast to our sorption experiments in the subsequent sections at 5 μg/L concentration levels, where azoxystrobin was not adsorbed at all for PBAT microplastic samples. One of the possible reasons for this contrasting behaviour could be the high

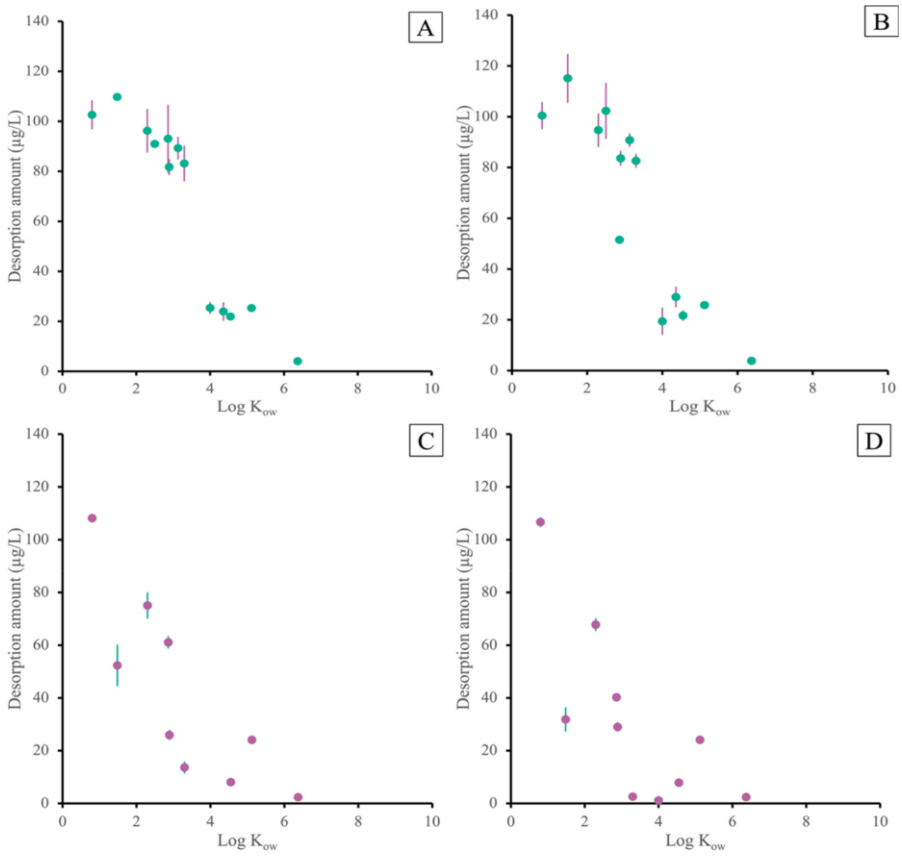

Fig. 3. log K_{ow} versus mean desorption amounts of pesticides at the end of 10 days in PE mulch film at 20 °C (A) and 40 °C (B) and in biodegradable PBAT mulch film at 20 °C (C) and 40 °C (D).

pesticide concentration and long exposure time used for the desorption experiments which are factors that could alter the process of sorption.

In addition to this, desorption amounts were moderately correlated with the pKa value of respective pesticides in the case of PBAT mulch films [Spearman's correlation: 0.478, $p < 0.05$]. However, no such correlation was reported in the case for PE mulch films. This relation however is specific for a solution pH of around 6 in our case, and might change for different ambient pH values.

3.3. Sorption of pesticides onto biodegradable microplastics

Out of the 9 pesticides studied for sorption, only 6 including bifenthrin, fenazaquin, pyridaben, pyridalyl, pyridate and fluxapyroxad exhibited sorption onto Agri-BP samples. On the other hand, acetamiprid, azoxystrobin and carbendazim did not show any significant sorption. It must be noted that azoxystrobin and carbendazim have been previously reported to exhibit sorption onto microplastics, however, that was either in the case of polyethylene and polypropylene microplastics and/or at relatively higher concentration levels which might not be realistic in the environment (Mo et al., 2021; Wang et al., 2020). All three of these pesticides that did not show any significant sorption have lower log K_{ow} values (between 0.8 and 2.5) compared to the others that have higher log K_{ow} values. The relationship between Q_e values (amount of pesticide sorbed at equilibrium) of the pesticides and their respective log K_{ow} values is depicted in Supplementary Fig. S (3). As can be seen in this figure, again, a cut-off value of log K_{ow} was observed below which there is no visible sorption. A similar cut-off value was also observed in one of our previous works, wherein the sorption of pesticide residues was studied in the case of microplastics derived from conventional polyethylene films under similar experimental and analytical conditions (Sahai et al., 2023). However, in that case, the cut-off was observed to be between the log K_{ow} values 3 and 4, which is higher than the one observed for biodegradable microplastics in this study (2.8). Fluxapyroxad (log $K_{ow} = 3.31$) which exhibited some degree of sorption in the case of Agri-BP samples, was not sorbed onto polyethylene film microplastics previously. These differences suggest that microplastics derived from biodegradable mulch films could adsorb a greater range of pesticide residues with even lower log K_{ow} values (i.e., greater hydrophilicity) than the ones derived from polyethylene films at environmentally realistic concentration levels.

3.4. Kinetics of sorption

Due to the problems that arise upon linearization of models while fitting experimental data (Lima et al., 2015), the data for those pesticides that showed sorption onto Agri-BP microplastics was fitted onto non-linear forms of pseudo-first order, pseudo-second order, Elovich and Intra-particular diffusion models. The results are depicted below in Fig. 4 and their respective calculated model parameters are detailed in Table 1.

As observed from our results, the best-fitting kinetic model in the case of bifenthrin and pyridalyl was found to be the Elovich kinetic model [R^2: 0.959 and 0.937 respectively]. Furthermore, for these pesticides, pseudo-second-order kinetic model was the second-best fitting scenario. While for pyridate, pyridaben, fenazaquin and fluxapyroxad, the pseudo-second-order model was found to be the best fitting scenario [R^2: 0.987, 0.980, 0.978 and 0.942 respectively]. The initial sorption rate denoted by h (μg g^{-1} h^{-1}), which helps us to determine the pace of

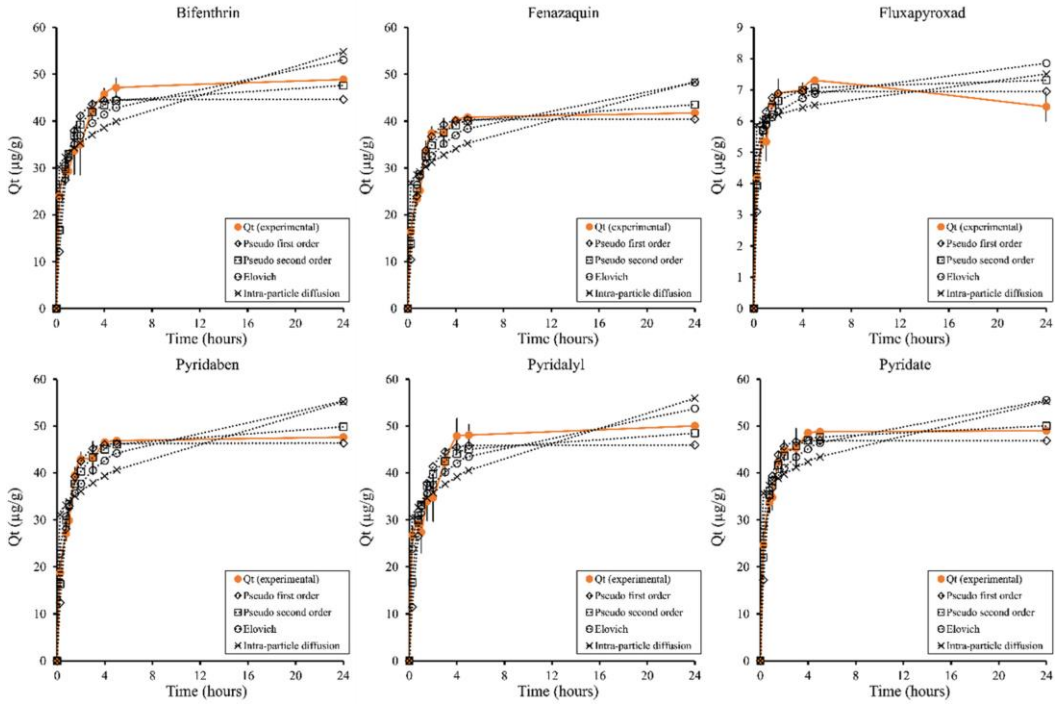

Fig. 4. Kinetic models for the sorption of pesticides onto PBAT (Agri-BP) microplastics at 5 μg/L initial pesticide concentration levels.

Table 1
Calculated parameters of kinetic models for sorption of pesticides onto biodegradable PBAT microplastic samples Agri-BP.

Pesticide	Pseudo-first order		Pseudo-second order		Elovich		Intra-particular diffusion	
Bifenthrin	K_1	1.27	K_2	0.04	**α**	956.19	K_i	5.59
	Q_e	44.62	Q_e	48.54	b	0.15	C_i	27.40
	R^2	0.893	R^2	0.945	R^2	0.959	R^2	0.882
Fenazaquin	K_1	1.20	K_2	0.04	**α**	553.52	K_i	4.92
	Q_e	40.40	Q_e	44.51	b	0.16	C_i	24.24
	R^2	0.973	R^2	0.978	R^2	0.924	R^2	0.795
Pyridaben	K_1	1.24	K_2	0.04	**α**	708.49	K_i	5.47
	Q_e	46.31	Q_e	50.94	b	0.14	C_i	28.37
	R^2	0.977	R^2	0.980	R^2	0.921	R^2	0.792
Pyridalyl	K_1	1.15	K_2	0.04	**α**	995.27	K_i	5.79
	Q_e	45.95	Q_e	49.44	b	0.15	C_i	27.57
	R^2	0.855	R^2	0.905	R^2	0.937	R^2	0.873
Pyridate	K_1	1.83	K_2	0.06	**α**	3237.79	K_i	4.46
	Q_e	46.86	Q_e	50.70	b	0.17	C_i	33.43
	R^2	0.960	R^2	0.987	R^2	0.947	R^2	0.856
Fluxapyroxad	K_1	2.36	K_2	0.62	**α**	7702.30	K_i	0.37
	Q_e	6.95	Q_e	7.37	b	1.60	C_i	5.68
	R^2	0.925	R^2	0.942	R^2	0.878	R^2	0.807

initial sorption was calculated using the equation $h = k_2 Q_e^2$ and was found to be between 33 and 102 μg g^{-1} h^{-1} for all the investigated pesticides. In this equation, k_2 represents the second order rate constant (g μg^{-1} h^{-1}), while Qe is the amount of pesticide sorbed onto MP at equilibrium (μg/g).

In general, the process of sorption can be divided into steps: (1) migration of sorbate from bulk solution to the surface of sorbent (bulk diffusion); (2) diffusion through boundary layer to the surface of sorbent (film diffusion); (3) diffusion from surface to interior pores (intraparticle diffusion or pore diffusion) and (4) adsorption at an active site on the surface of sorbent through chemical reaction (Nethaji et al., 2013). Elovich and pseudo-second-order models have been widely applied to describe adsorption processes that follow the second order kinetics and correspond to sorption processes that are chemical in nature (Aharoni and Tompkins, 1970; Ebelegi et al., 2020; Wu et al., 2009). Furthermore, the Elovich kinetic model assumes that the system involves energetically heterogeneous surfaces (Ebelegi et al., 2020). This suggests the presence of chemisorption over the surface in the case of biodegradable PBAT mulch film microplastic samples.

A possible reason for the retention of higher amounts of pesticides in the case of PBAT films as compared to PE films, as discussed in previous sections, could be this difference in the mechanism of sorption between the two plastic types, which we observe here using modelling. As mentioned, in the case of PBAT films, the sorption process was governed by the formation of chemical bonds between the pesticide and plastic particle (chemisorption). This contrasts with the findings of our earlier investigation on polyethylene microplastics, which indicated physisorption as the predominant process (Sahai et al., 2023). The forces of attraction that govern physisorption include weak van der Waals forces and electrostatic attraction, however, during chemisorption, chemical bond formation takes place through covalent or ionic bonding and has a higher adsorption enthalpy than physisorption. This implies that forces involved in chemical bond formation are stronger and the energy required to release the pesticide molecule from the surface of the PBAT plastic is higher than PE plastic. This reason also explains our finding that a higher ambient temperature of 40 °C was able to reduce desorption times for the PE mulch film by providing the required energy for quick desorption, while having no effect over desorption times in the case of PBAT film.

Using the Weber and Morris plot, the representation of Q_t versus $t^{1/2}$ can be linear or multilinear, indicating if only intra-particle diffusion is dominating in the adsorption process (if the plot passes through origin) or if two or more steps control the adsorption process (if the plot does not pass through origin) (Qiu et al., 2009; Svilović et al., 2010). As is depicted in Fig. S (4), these plots for the adsorbed pesticides in our case did not pass through origin. Additionally, the lower R^2 values for the intra-particle diffusion model in all cases [R^2: 0.792 to 0.882] suggested that intra-particle diffusion was not the rate limiting step. Furthermore, Boyd plots for the adsorbed pesticides (Fig. S (5)) did not pass through origin as well, thus proving, that in our case, film diffusion or chemisorption was the rate limiting step (Agboola and Benson, 2021; Cáceres-Jensen et al., 2013).

Now, the sorption of certain agricultural contaminants has been previously reported in the case of biodegradable microplastics and the best fitting kinetic models were either pseudo-first order or pseudo-second order (Gong et al., 2019; Jiang et al., 2020; Ni et al., 2023). However, these results correspond to either environmentally high concentrations of the contaminants and/or different polymer types. Here, it must be taken into account that the concentration of pesticide residues in the environment, which is an important factor that would govern the dynamics of sorption, is expected to be in the range of ng/L to a few μg/L (Bueno et al., 2012). In this context, our results from this study highlight that even at very low environmentally relevant residual concentrations (5 μg/L), microplastics produced from biodegradable mulch films could easily adsorb pesticides to a high degree.

It is important to point out that before extrapolating these results to additional compounds with comparable log K_{ow} values to forecast their sorption behavior, care must be exercised. This is due to the possibility that other variables that would be unique to a particular compound, such as its molecular structure, functional groups and/or the presence of charge, could affect this relationship and have an impact on how that compound behaves.

4. Conclusions

The extensive application of mulch films in farming areas gives rise to grave worries about the introduction of microplastics into the soil and the interplay between these films and microplastics with residual on-field contaminants like pesticides. With a particular focus on the interactions of biodegradable PBAT mulch films and highlighting the distinctions between PBAT and traditional PE mulch films and microplastics, this study aims to close this knowledge gap. From our finding we observe that biodegradable PBAT mulch films exhibited a higher retention of pesticides onto their surface [median desorption = 24.27 μg/L or about 17%], while PE mulch films exhibited a higher desorption or release of pesticides to the surrounding media after a spraying event [median desorption = 71.86 μg/L or about 50%]. This could have implications for the ultimate fate and availability of these pesticide residues in the agricultural ecosystem. Even though a higher ambient temperature did not affect the final desorption amounts in both plastic types, the pace of desorption of pesticides from the mulch film surfaces, appears to be temperature dependent for PE films, wherein, an ambient

temperature of 40 °C, appeared to reduce the desorption times from 10 days at 20 °C to 6 days at 40 °C, while having no significant effect on PBAT mulch films. This variation, due to changes in ambient temperature, could result in a seasonal effect over the process in natural, on-field conditions; suggesting a faster release of pesticides from PE mulch films surfaces to the surrounding media during warm seasons or in warmer climatic regions.

Our findings further revealed that both the processes of desorption in mulch films and sorption in microplastics were influenced by the log K_{ow} value of the pesticides [Spearman's correlation: 0.857 for PBAT and 0.837 for PE, $p < 0.05$], however, the effect of pKa was not found to be as strong. A cut-off value of log K_{ow} was identified for both plastic types below which the sorption in microplastics was negligible and desorption in mulch films was the maximum. This log K_{ow} cut-off value was found to be around 2.8 for biodegradable PBAT mulch films and around 3.3 for conventional PE mulch films. Additionally, through the modelling of the process, the adsorption of pesticide residues onto biodegradable PBAT microplastics appeared to follow Elovich [R^2: 0.937–0.959] and pseudo-second order kinetics [R^2: 0.942–0.987], and was facilitated by chemical interaction and bond formation as opposed to physical adsorption that has been demonstrated previously for PE microplastic type (Sahai et al., 2023). Sorption in PBAT was found to be a multi-step process, however, the rate limiting step was film diffusion or chemical bond formation. This difference in the interaction mechanism (chemisorption versus physisorption) could possibly explain the higher retention of pesticide residues in PBAT plastic types as opposed to PE film as mentioned above.

This study not only emphasizes the function of microplastics and mulch films as pesticide transport vectors in agricultural settings, but also offers empirical proof of the capacity of biodegradable PBAT microplastics and mulch films to adsorb and retain a broader range of pesticides and higher amounts of the same pesticides than conventional PE mulch films. Given their increased retention capacity, PBAT films could potentially operate as pesticide residue sinks, decreasing their release into the surrounding soil. On the one hand, this could protect the soil from excessive residual contamination, but it also emphasizes the importance of proper collection, decontamination, and recycling of such films after their usage life cycle.

Disclaimer

The contents of this publication and the opinions expressed are those of the author(s) only and this document should not be considered as representative of CSIC's official position and it does not involve CSIC in liability of any kind.

CRediT authorship contribution statement

Harshit Sahai: Conceptualization, Formal analysis, Investigation, Methodology, Visualization, Writing - original draft. **María Dolores Hernando:** Conceptualization, Funding acquisition, Project administration, Supervision, Writing - review & editing. **María Jesús Martínez Bueno:** Conceptualization, Resources, Writing - review & editing. **Ana M. Aguilera del Real:** Conceptualization, Formal analysis, Investigation, Methodology, Validation, Writing - review & editing. **Amadeo R. Fernández- Alba:** Conceptualization, Funding acquisition, Resources, Supervision, Validation, Writing - review & editing.

Declaration of competing interest

The authors declare that they have no known competing financial interests or personal relationships that could have appeared to influence the work reported in this paper.

Data availability

Data will be made available on request.

Acknowledgements

Authors acknowledge the support of "FoodTraNet" MSCA-ITN project, and the funding received from the European Union's Horizon 2020 research and innovation programme under the Marie Skłodowska-Curie grant agreement No. 956265, as well as to the Spanish Ministry of Science, Innovation and Universities (MICINN) for the financial support given to the projects TED2021-131609B–C31, "CERTAIN" (PID2020-116230RB-I00) and project PLEC2021-007693.

Appendix A. Supplementary data

Supplementary data to this article can be found online at.https://doi.org/10.1016/j.chemosphere.2024.141183.

References

Agboola, O.D., Benson, N.U., 2021. Physisorption and chemisorption mechanisms influencing micro (Nano) plastics-organic chemical contaminants interactions: a review. Front. Environ. Sci. 9, 678574 https://doi.org/10.3389/fenvs.2021.678574.
Aharoni, C., Tompkins, F.C., 1970. Kinetics of adsorption and desorption and the Elovich equation. In: Advances in Catalysis, vol. 21. Elsevier, pp. 1–49. https://doi.org/10.1016/S0360-0564(08)60563-5.
Bilck, A.P., Yamashita, F., Marzano-Barreda, L.A., 2021. Characterization and application of starch/polyester packaging produced by blown extrusion. Carbohydrate Polymer Technologies and Applications 2, 100088. https://doi.org/10.1016/j.carpta.2021.100088.
Bueno, M.J.M., Gomez, M.J., Herrera, S., Hernando, M.D., Agüera, A., Fernández-Alba, A.R., 2012. Occurrence and persistence of organic emerging contaminants and priority pollutants in five sewage treatment plants of Spain: two years pilot survey monitoring. Environ. Pollut. 164, 267–273. https://doi.org/10.1016/j.envpol.2012.01.038.
Cáceres-Jensen, L., Rodríguez-Becerra, J., Parra-Rivero, J., Escudey, M., Barrientos, L., Castro-Castillo, V., 2013. Sorption kinetics of diuron on volcanic ash derived soils. J. Hazard Mater. 261, 602–613. https://doi.org/10.1016/j.jhazmat.2013.07.073.
Díaz-Galiano, F.J., Gómez-Ramos, M.J., Beraza, I., Murcia-Morales, M., Fernández-Alba, A.R., 2023. Cooking food in microwavable plastic containers: in situ formation of a new chemical substance and increased migration of polypropylene polymers. Food Chem. 417, 135852 https://doi.org/10.1016/j.foodchem.2023.135852.
European Bioplastics, 2021. Bioplastics Facts and Figures. https://www.european-bioplastics.org/bioplastics-facts-figures/. (Accessed 10 June 2023).
Ebelegi, A.N., Ayawei, N., Wankasi, D., 2020. Interpretation of adsorption thermodynamics and kinetics. Open J. Phys. Chem. 10 (3), 3 https://doi.org/10.4236/ojpc.2020.103010.
Farsetti, S., Cioni, B., Lazzeri, A., 2011. Physico-mechanical properties of biodegradable rubber toughened polymers. Macromol. Symp. 301, 82–89. https://doi.org/10.1002/masy.201150311.
Gong, W., Jiang, M., Han, P., Liang, G., Zhang, T., Liu, G., 2019. Comparative analysis on the sorption kinetics and isotherms of fipronil on nondegradable and biodegradable microplastics. Environ. Pollut. 254, 112927 https://doi.org/10.1016/j.envpol.2019.07.095.
Guerrini, S., Yan, C., Malinconico, M., Mormile, P., 2019. Agronomical overview of mulch film systems. In: Gutiérrez, T.J. (Ed.), Polymers for Agri-Food Applications. Springer International Publishing, pp. 241–264. https://doi.org/10.1007/978-3-030-19416-1_13.
Huang, Y., Liu, Q., Jia, W., Yan, C., Wang, J., 2020. Agricultural plastic mulching as a source of microplastics in the terrestrial environment. Environ. Pollut. 260, 114096 https://doi.org/10.1016/j.envpol.2020.114096.
Jiang, M., Hu, L., Lu, A., Liang, G., Lin, Z., Zhang, T., Xu, L., Li, B., Gong, W., 2020. Strong sorption of two fungicides onto biodegradable microplastics with emphasis on the negligible role of environmental factors. Environ. Pollut. 267, 115496 https://doi.org/10.1016/j.envpol.2020.115496.
Jiménez-Morillo, N.T., Cabrita, M.J., Dias, C.B., González-Vila, F.J., González-Pérez, J.A., 2020. Pyrolysis-compound-specific hydrogen isotope analysis (δ2H Py-CSIA) of Mediterranean olive oils. Food Control 110, 107023. https://doi.org/10.1016/j.foodcont.2019.107023.
Jun, C.L., 2000. Reactive blending of biodegradable polymers: PLA and starch. J. Polym. Environ. 8 (1), 33–37. https://doi.org/10.1023/A:1010172112118.
Kasa, V.P., Mondal, A., Cheela, Vrs, Dubey, B.K., 2022. Occurrences, impacts, and characterization of microplastics in terrestrial ecosystem to aid policy. Current Opinion in Environmental Science & Health 27, 100361. https://doi.org/10.1016/j.coesh.2022.100361.
Lambert, S., Wagner, M., 2017. Environmental performance of bio-based and biodegradable plastics: the road ahead. Chem. Soc. Rev. 46 (22), 6855–6871. https://doi.org/10.1039/C7CS00149E.
Lima, É.C., Adebayo, M.A., Machado, F.M., 2015. Kinetic and equilibrium models of adsorption. In: Bergmann, C.P., Machado, F.M. (Eds.), Carbon Nanomaterials as Adsorbents for Environmental and Biological Applications. Springer International Publishing, pp. 33–69. https://doi.org/10.1007/978-3-319-18875-1_3.
Mo, Q., Yang, X., Wang, J., Xu, H., Li, W., Fan, Q., Gao, S., Yang, W., Gao, C., Liao, D., Li, Y., Zhang, Y., 2021. Adsorption mechanism of two pesticides on polyethylene and

polypropylene microplastics: DFT calculations and particle size effects. Environ. Pollut. 291, 118120 https://doi.org/10.1016/j.envpol.2021.118120.
Nethaji, S., Sivasamy, A., Mandal, A.B., 2013. Adsorption isotherms, kinetics and mechanism for the adsorption of cationic and anionic dyes onto carbonaceous particles prepared from Juglans regia shell biomass. Int. J. Environ. Sci. Technol. 10 (2), 231–242. https://doi.org/10.1007/s13762-012-0112-0.
Ni, N., Shi, R., Meng, J., Guo, X., Shi, M., Zhang, X., Yao, S., Nkoh, J.N., Wang, F., Song, Y., Wang, N., 2023. Comparative analysis of the sorption behaviors and mechanisms of amide herbicides on biodegradable and nondegradable microplastics derived from agricultural plastic products. Environ. Pollut. 318, 120865 https://doi.org/10.1016/j.envpol.2022.120865.
Olivato, J.B., Grossmann, M.V.E., Bilck, A.P., Yamashita, F., Oliveira, L.M., 2013. Starch/polyester films: simultaneous optimisation of the properties for the production of biodegradable plastic bags. Polímeros 23, 32–36. https://doi.org/10.1590/S0104-14282013005000017.
Qin, M., Chen, C., Song, B., Shen, M., Cao, W., Yang, H., Zeng, G., Gong, J., 2021. A review of biodegradable plastics to biodegradable microplastics: another ecological threat to soil environments? J. Clean. Prod. 312, 127816 https://doi.org/10.1016/j.jclepro.2021.127816.
Qiu, H., Lv, L., Pan, B., Zhang, Q., Zhang, W., Zhang, Q., 2009. Critical review in adsorption kinetic models. J. Zhejiang Univ. - Sci. 10 (5), 716–724. https://doi.org/10.1631/jzus.A0820524.
Sahai, H., García Valverde, M., Murcia Morales, M., Hernando, M.D., Aguilera del Real, A.M., Fernández- Alba, A.R., 2023. Exploring sorption of pesticides and PAHs in microplastics derived from plastic mulch films used in modern agriculture. Chemosphere 333, 138959. https://doi.org/10.1016/j.chemosphere.2023.138959.
SANTE/11312/2021, European Commission Directorate-General for Health and Food Safety, 2021. Guidance document on analytical quality control and method validation procedures for pesticides residues analysis in food and feed. https://www.eurl-pesticides.eu/docs/public/tmplt_article.asp?CntID=727&LabID=100&Lang=EN. (Accessed 10 June 2023).
Scarascia-Mugnozza, G., Sica, C., Russo, G., 2011. Plastic materials in EUROPEAN agriculture: actual use and perspectives. Journal of Agricultural Engineering 42 (3), 3. https://doi.org/10.4081/jae.2011.3.15.
Shruti, V.C., Kutralam-Muniasamy, G., 2019. Bioplastics: missing link in the era of microplastics. Sci. Total Environ. 697, 134139 https://doi.org/10.1016/j.scitotenv.2019.134139.
Svilović, S., Rušić, D., Bašić, A., 2010. Investigations of different kinetic models of copper ions sorption on zeolite 13X. Desalination 259 (1), 71–75. https://doi.org/10.1016/j.desal.2010.04.033.
Wang, T., Yu, C., Chu, Q., Wang, F., Lan, T., Wang, J., 2020. Adsorption behavior and mechanism of five pesticides on microplastics from agricultural polyethylene films. Chemosphere 244, 125491. https://doi.org/10.1016/j.chemosphere.2019.125491.
Wu, F.-C., Tseng, R.-L., Juang, R.-S., 2009. Characteristics of Elovich equation used for the analysis of adsorption kinetics in dye-chitosan systems. Chem. Eng. J. 150 (2), 366–373. https://doi.org/10.1016/j.cej.2009.01.014.
Xiong, Z., Zhang, L., Ma, S., Yang, Y., Zhang, C., Tang, Z., Zhu, J., 2013. Effect of castor oil enrichment layer produced by reaction on the properties of PLA/HDI-g-starch blends. Carbohydr. Polym. 94 (1), 235–243. https://doi.org/10.1016/j.carbpol.2013.01.038.
Yang, X.-D., Gong, B., Chen, W., Qian, C., Du, M., Yu, H.-Q., 2022. In-situ quantitative monitoring the organic contaminants uptake onto suspended microplastics in aquatic environments. Water Res. 215, 118235 https://doi.org/10.1016/j.watres.2022.118235.
Yang, Y., Li, Z., Yan, C., Chadwick, D., Jones, D.L., Liu, E., Liu, Q., Bai, R., He, W., 2022. Kinetics of microplastic generation from different types of mulch films in agricultural soil. Sci. Total Environ. 814, 152572 https://doi.org/10.1016/j.scitotenv.2021.152572.

3.3 Publication 3

Title: Quantification of nanoplastic uptake and distribution in the root, stem and leaves of the edible herb *Lepidium sativum*

Harshit Sahai[a,c], María Jesús Martínez Bueno[b], María del Mar Gomez-Ramos[b], Amadeo R. Fernandez-Alba[b], María Dolores Hernando[a,*]

a) Experimental Station of Arid Zones, The Spanish National Research Council (CSIC-EEZA), Ctra. de Sacramento s/n, La Cañada de San Urbano, 04120, Almería, Spain
b) Agrifood Campus of International Excellence (ceiA3), European Union Reference Laboratory for Pesticide Residues in Fruit & Vegetables. Department of Chemistry and Physics, University of Almería, La Ca˜ nada de San Urbano, 04120, Almería, Spain
c) Jožef Stefan International Postgraduate School, Jamova 39, 1000, Ljubljana, Slovenia

A comprehensive review of the existing body of literature indicates that despite the gradual increase in attention towards the effects and presence of MNPs in agricultural settings, there remains a relatively nascent understanding of their interactions with terrestrial plants, particularly crops. The accumulation of these plastic particles in crops poses a significant risk to the ecosystem and human health. Current estimations suggest that agricultural soils receive a considerable annual influx of microplastics from various sources, including composts, biosolids, plastic mulch films, and irrigation with treated wastewater. Although a few recent investigations have demonstrated the ability of plant species to uptake MNPs, the mechanisms and quantitative aspects of this phenomenon remain largely unexplored.

This publication addresses the mounting apprehensions regarding MNP contamination in agricultural environments and its potential repercussions on food safety. The primary objective was to bridge the knowledge gap by quantitatively evaluating the uptake and dispersion of PS nanoplastics in *Lepidium sativum* using CLSM and fluorescence image analysis. The experimental procedure involved subjecting plants to varying concentrations of fluorescently labeled PS NPs and examining their distribution within the root, stem, and leaves. Moreover, a novel approach was employed to analyze the fluorescent images to estimate the quantity of NPs accumulated in different plant tissues. The study's outcomes indicate that plants can absorb even environmentally relevant concentrations of nanoplastics, thereby accentuating concerns regarding their presence within the food chain. Furthermore, the paper assesses the effects of NP exposure on plant health by examining biophysical parameters such as germination rate, fresh weight, root length, root weight, number of lateral roots, and shoot weight. The significance of this work lies in its potential implications for agricultural food safety and health, as it offers a quantitative insight into nanoplastic uptake in crops, underscoring the necessity for further exploration into the ramifications of nanoplastics on plants and crops.

Science of the Total Environment 912 (2024) 168903

Contents lists available at ScienceDirect

Science of the Total Environment

journal homepage: www.elsevier.com/locate/scitotenv

Quantification of nanoplastic uptake and distribution in the root, stem and leaves of the edible herb *Lepidum sativum*

Harshit Sahai [a,c], María Jesús Martínez Bueno [b], María del Mar Gómez-Ramos [b], Amadeo R. Fernández-Alba [b], María Dolores Hernando [a,*]

[a] Experimental Station of Arid Zones, The Spanish National Research Council (CSIC-EEZA), Ctra. de Sacramento s/n, La Cañada de San Urbano 04120, Almería, Spain
[b] Agrifood Campus of International Excellence (ceiA3), European Union Reference Laboratory for Pesticide Residues in Fruit & Vegetables, Department of Chemistry and Physics, University of Almería, La Cañada de San Urbano 04120, Almería, Spain
[c] Jozef Stefan International Postgraduate School, Jamova 39, 1000 Ljubljana, Slovenia

HIGHLIGHTS

- Quantification and distribution of PS NPs in root, stem and leaf of the model plant *Lepidum sativum*.
- 13 to 18 % of the NPs were transferred to aerial parts compared to the root.
- Bioaccumulation was characterised by aggregation and heterogenous distribution.
- NPs present in intercellular spaces suggesting the role of apoplastic uptake.
- NPs significantly affected plant health only at high exposure concentrations.

GRAPHICAL ABSTRACT

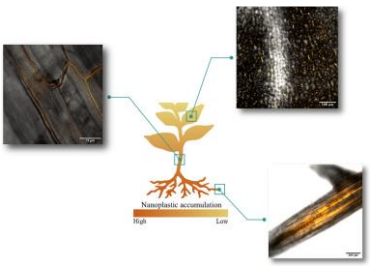

ARTICLE INFO

Editor: Dimitra A Lambropoulou

Keywords:
Nanoplastic uptake
Bioaccumulation
Translocation
Quantification
Food safety

ABSTRACT

This study confirms the uptake, translocation and bioaccumulation of 100 nm polystyrene nanoplastics in the root, stem and leaves of the plant *Lepidum sativum* at exposure concentrations ranging from environmentally realistic 10 μg/L up to a high of 100 mg/L. Accumulation in plant tissues was characterised by aggregation in the intercellular spaces and heterogeneous distribution. Nanoplastic presence was confirmed in the root tips, root surface and stele, lateral roots, root hairs, stem vascular bundles, leaf veins and mesophyll, as well as leaf epidermis including stomatal sites. Quantification results show that majority of the particles were retained in the root and accumulation in stem and leaves was only 13 to 18 % of the median value in roots. There was a reduction of 38.89 ± 9.62 % in the germination rate, 55 % in plant fresh weight, as well as in root weight (> 80 %), root length (> 60 %), shoot weight (51 to 78 %) and number of lateral roots (> 28 %) at exposure concentrations at and above 50 mg/L. However, lower, environmentally probable exposure concentrations did not affect the plant health significantly. Our results highlight the urgent need for further exploration of this issue from the point of view of food safety and security.

Statement of environmental implication: Micro and nanoplastics have been reported in agricultural environments across the globe and reports regarding their hazardous effects over agricultural and plant health call for an urgent

* Corresponding author.
E-mail address: hernando.dolores@eeza.csic.es (M.D. Hernando).

https://doi.org/10.1016/j.scitotenv.2023.168903
Received 12 October 2023; Received in revised form 14 November 2023; Accepted 24 November 2023
Available online 25 November 2023

exploration of this issue. This work demonstrates the uptake, bioaccumulation and distribution of nanoplastics in an edible plant at an environmentally realistic concentration and raises serious concerns regarding the possible implications for food safety and security. It presents a novel approach which addresses the quantification of nanoplastic accumulation in plant tissues and helps identify the mechanism and trends behind this phenomenon which has been a challenge up until now.

1. Introduction

In recent years there has been a growing concern regarding the presence and effects of micro and nano plastics in the agricultural ecosystem and its implications for food safety and security. The current annual input of microplastics to agricultural soils is estimated to be 63,000–430,000 and 44,000–300,000 t to European and North American farmlands, respectively (Nizzetto et al., 2016). The major identified sources of micro and nano plastics in the agricultural ecosystem include the use of plastic material such as plastic mulch films, soil amendments such as composts and bio solids, repurposed sewage sludge, wastewater from treatment plants for irrigation and atmospheric deposition (Tian et al., 2022). There have been studies reporting the presence of this contaminant in agricultural lands from all across the globe (Büks and Kaupenjohann, 2020). At the same time, numerous studies have reported the deleterious effects of microplastics to soil ecosystems including changes to soil bulk density, structure, aggregation, moisture retention, nutrient mobilization as well as effects to the soil biota and negative impacts to plant health amongst others (Tian et al., 2022). One of the most important concerns regarding this issue in recent years has been the possible uptake, translocation and bioaccumulation of these micro and nano plastics in crops.

Research regarding the uptake and bioaccumulation of micro and nano plastics in plants and agricultural crops is still at its infancy. Few studies have demonstrated the uptake of plastic particles ranging from about 25 nm to about a micron in plants including *Triticum aestivum* (wheat), *Lactuva sativa* (lettuce), *Arabidopsis thaliana* (cress), *Pisum sativum* (pea), *Oryza sativa* (rice), *Daucus carota* (carrot), *Murraya exotica* (orange jasmine), *Raphanus sativus* (raddish), *Zea mays* (maize), *Allium cepa* (onion) seeds, *Cucumis sativum* (cucumber) and *Vicia faba* (fava bean or broad bean) (Li et al., 2020; Kim et al., 2022; Liu et al., 2022; Dong et al., 2021; Zhang et al., 2019; Gong et al., 2021; Sun et al., 2021; Lian et al., 2021; Sun et al., 2020; Giorgetti et al., 2020; Li et al., 2021; Jiang et al., 2019; Zhou et al., 2021). However, the mechanisms and trends behind this phenomenon remain unexplored.

The uptake of micro and nano plastics in crops is a complex phenomenon possibly governed by factors such as plant anatomy, properties of the plastic polymer such as charge (Sun et al., 2020) and characteristics of the ambient media such as soil. A set of physical, chemical and physiological barriers that regulate the size exclusion limits (SELs) must be overcome by these micro and nano plastics for their possible uptake and translocation in plants (Li et al., 2020). From what we know, the uptake might be possible through the roots via a crack entry mode (Li et al., 2020) and its upward translocation could be facilitated by the transpiration stream through intercellular spaces or the apoplastic pathway (Li et al., 2020; Liu et al., 2022). Additionally, the symplastic pathway which involves endocytosis through the plasmodesmatal openings and subsequent movement of nanoparticles through cell membranes has also been speculated as a possible uptake mechanism (Taylor et al., 2020; Bandmann et al., 2012). Other than the entry through roots, nanoplastic uptake has been shown to also occur through the stomatal entry route followed by its downward translocation from leaves to the root (Sun et al., 2021; Lian et al., 2021). From the point of view of food safety and security, these findings suggest an urgent need for further exploration of this issue and efforts to investigate its mechanism, possible extent, impact and solutions.

Some of the techniques that have been employed in the recent past to study the uptake and accumulation of nano plastics in plants include confocal laser scanning microscopy (CLSM) (Li et al., 2020; Kim et al., 2022; Liu et al., 2022; Gong et al., 2021; Sun et al., 2020; Li et al., 2021; Jiang et al., 2019; Zhou et al., 2021; Taylor et al., 2020; Bandmann et al., 2012; Bosker et al., 2019), X-Ray computed nano-tomography (nano-CT) clubbed with dark-field hyperspectral imaging (DF-HIS) (Avellan et al., 2017), transmission electron microscopy (TEM) (Dong et al., 2021; Lian et al., 2021; Sun et al., 2020; Giorgetti et al., 2020), time resolved optical imaging/fluorescence imaging (Zhang et al., 2019; Luo et al., 2022) and scanning electron microscopy (SEM) (Lian et al., 2021). However, even though these techniques allow us to study the uptake and accumulation of micro and nano plastics qualitatively, the quantitative aspect still remains a challenge.

In this study we aim to suggest a step towards the exploration of the quantitative nature of nano plastic uptake by plants. From all the techniques that have been utilized previously, confocal laser scanning microscopy remains the most prominently used one till date. Our approach builds upon this already used analytical technique and presents a way of uptake quantification without the need for any separate analytical requirement. In this work, different concentration solutions of fluorescent polystyrene (PS) nano particles were imaged under a confocal laser-scanning microscope and their fluorescence intensities were recorded in order to calculate the mean fluorescence intensity of a single nano particle. In order to study the qualitative aspect, plant samples exposed to fluorescently labelled polystyrene nano spheres were imaged using CLSM and nano particles accumulated in the plant tissues were visualised using their fluorescence signals. Subsequently, using image analysis, information regarding the fluorescence intensity of detected nano particles in plant tissues was extracted from the same images and the calculated mean fluorescence of a single nano particle was used to estimate the number of particles present per unit volume in the plant.

Here we study the uptake and accumulation of polystyrene nanoplastics in the plant *Lepidum sativum* both qualitatively and quantitatively and provide visual evidence for the accumulation of nanoplastics in plant tissues as well as highlight the trends observed. Using image analysis, we quantify the nanoplastics inside plant tissues and highlight their distribution between the root, stem and leaves of the plant. In addition, we also report the effects of different nanoplastic exposure concentrations over the biophysical parameters of the plant including effects to both root and shoot regions.

2. Materials and methods

2.1. Materials

Red fluorescent polystyrene nanosphere stock solutions were purchased from Applied Microspheres (Applied Microspheres BV, Netherlands) that were supplied in aqueous suspension form (1 % solid content). According to the supplier information, the solutions also contained <0.1 % undisclosed surfactants and < 0.05 % preservatives. Additionally, the particles were neutrally charged and devoid of any surface functionalization. The nominal diameter was 0.100 μm (100 nm) and the mean diameter was 0.098 μm (CV < 5 %). The particles demonstrated a fluorescence excitation between 490 and 560 nm with a peak around 530 nm and fluorescence emission between 535 and 610 nm with a peak close to 570 nm. There was no reported leaching of fluorescent dye from the particles. Hoagland plant nutrient mix was purchased from Sigma-Aldrich (United States) in powder form and diluted as per the supplier information to prepare hydroponic nutrient

solution for plant growth. *Lepidum sativum* seeds were purchased from a commercial agricultural supplier (Rocalba S.A., Spain) and germinated in aluminium germination trays lined with moist cotton cloth before use.

2.2. Plant exposure experiments

Lepidum sativum plant was selected as a model plant for this study due to its relatively simpler morphology, small size, short growing period and minimal maintenance requirements. In order to study the uptake of PS nanoplastics by plants, exposure experiments were setup. From our preliminary experiments, it was observed that the plant germinated successfully in about 3 days which in our case was defined by the emergence of the radicle and two green leaves. Therefore, 3 days old healthy *Lepidum sativum* plants were selected and transplanted into glass pots and supported with the help of stainless-steel mesh. Complete care was taken to avoid any use of plastic apparatus for the setup and all experimental steps were conducted using glass apparatus (including the preparation of stock solutions, growth of plant samples, as well as storage, transport and processing of all samples) to eliminate any ambient as well as cross contamination. For microscopic and image analysis, 6 groups of 3 plants each were chosen for different exposure concentrations. 5 of these groups were exposed to 25 mL of Hoagland nutrient solution containing 10 μg/L, 100 μg/L, 1 mg/L, 50 mg/L and 100 mg/L fluorescent polystyrene nanoparticles while the sixth group (containing 25 mL Hoagland solution without nanoparticles) was treated as the control. The total exposure time for the plants was 12 days. During this period, the plants were placed in an incubator at a constant ambient temperature of 24 °C, relative humidity of 80 % and a photoperiod of 12 h. The nutrient solution was re-filled every second day in order to maintain a constant solution volume of 25 mL.

Furthermore, 24 individual seeds of the plant were selected and divided into two groups of 12 seeds each. The seeds were placed in aluminium germination trays over a cotton cloth and Hoagland solution was added to each group to create moist conditions for germination. One of the groups was exposed to a nutrient solution containing 100 mg/L nanoplastic particles and the number of germinated seeds was counted at the end of 2 days. Three separate runs of the experiment were conducted for surety.

In a separate experimental setup, 3 days old plants were selected and categorized into 5 groups of 9 plants each and an additional group of 9 plants as the control. The groups were exposed to hydroponic nutrient solution containing nanoplastic particles at concentrations of 10 μg/L, 100 μg/L, 1 mg/L, 50 mg/L and 100 mg/L for a period of 12 days in order to investigate the effect of nanoplastic exposure over the biophysical parameters of the plant including plant fresh weight, root length, root weight, total number of lateral roots, shoot height and shoot weight.

2.3. Confocal laser scanning microscopy

After exposure to fluorescent polystyrene nanoplastics, plant samples were collected for CLSM analysis. Each plant was divided into root, stem and leaf and rinsed using distilled water in order to remove any superficial nanoparticles that were not adhered to the tissues. Randomly selected regions from each plant part were subsequently sectioned and mounted on a glass slide using distilled water and cover slip. The sectioned tissues were analysed using a confocal laser scanning microscope (Leica TCS SP8, Leica Microsystems) and image acquisition was done using the software LAS X 3.5.6.21594 (Leica Microsystems). The analysis was carried out at the excitation/emission wavelength of 530/580 nm. The objective utilized had a 10× magnification (HC PL APO CS 10x/0.40 DRY) and the zoom factor was set at 0.75 in order to accommodate a larger sample region within the analysis area. Z step size was set to 1 μm, scanning mode was set in the xyz direction and scan speed at 400 Hz. Signals were collected using a HyD detector under standard mode with a gain factor of 117.1 % and time gating was utilized from 6.72 to 12 ns in order to minimize any autofluorescence collection. Additionally, control plant samples were also analysed under the same conditions in order to detect the presence of any residual background autofluorescence which would be utilized in the quantification step. For the estimation of fluorescence intensity of a single nanoparticle, 200 μL of nanoparticle solutions (at different concentrations) were placed in an 8-well setup (μ-Slide 8 well, Ibidi GmbH, Germany) and analysed using the microscope under the exact same conditions as the plant samples in order for the fluorescence intensities to be comparable.

QA/QC were performed under UNE-EN ISO 9001 guidelines. In order to obtain reproducible and relevant measurements, quality assessments of detectors and laser status were performed. The power and alignment of the lasers, as well as, the optimal detection of the microscope was checked by performing average intensity measurements of a standard sample of TetraSpeck™ Microspheres beads 1.0 μm fluorescent in blue/green/orange/dark red (ThermoFisher T7282). Additionally, laser power was measured directly using an optical power meter (PM 160-Thorlabs) to ensure proper functionality.

2.4. Image analysis

Analysis of the acquired images was carried out using the freely available and open-source software Fiji widely used in the field of scientific imaging (Schindelin et al., 2012). Output images from the microscope were comprised of multiple layers of individual 2-dimensional slice-by-slice images stacked on top of each other to produce a 3-dimensional stack. Each of these constituent layers was made up of individual pixels containing information of the detected fluorescence intensity at that region of the sample. For the quantification of fluorescence intensities, only the red channel of the stack (which contains the fluorescence information) was required and thus selected. Firstly, the image stack was z-projected using the "sum of slices" method under the stack project option in Fiji. This merges all the individual layers into a single 2-dimensional image where each pixel represents the sum of fluorescence intensities from all the corresponding pixels in the individual layers of the original stack. The next step was to set a threshold level for quantification, which is one of the most important parameters of this approach. This selects all the objects of interest (single or multi pixel) in the sample image whose fluorescence intensity values fall within the threshold range. Since the range in the case of 16-bit images is between 0 and 65,535, the lower threshold was set at 1 and the upper threshold was set at its maximum, thereby including the whole range of fluorescence that was detected. In order for the results to be comparable and the quantification to be accurate, it is important to use the same thresholding for all the steps including calculation of single particle fluorescence, calculation of residual autofluorescence in control samples as well as the calculation of NP fluorescence from positive plant samples. After setting up the threshold levels, the "Analyze particles" tool in Fiji was used to calculate the fluorescence intensities of the pixels constituting the z-projected image. This function outputs a table of all detected pixels or objects of interest along with their fluorescence intensity values under the parameter "RawIntDen". In the case of the object being a single pixel in dimension, this value corresponds to the fluorescence intensity of that individual pixel and in case of objects spanning across multiple pixels, it gives the cumulative value of all constituent pixels.

For the preparation of figures highlighting the nanoplastic accumulation in plant tissues, the images were brightness and contrast corrected and visualised using the "Orange Hot" option under the "Lookup Tables" section in Fiji for better visualization.

2.5. Data analysis

Data were statistically processed using SPSS (Statistical Package for the Social Sciences) Statistical software for Windows, IBM Corp, version 29.0.0.0 (241) (IBM Corp, US). All the variables available were tested to check whether data trespassing the assumptions for regular parametric

tests to report valid results. Since the data did not follow normal distribution, non-parametric approach was applied in order to explore the data.

3. Results and discussions

3.1. Visualization of accumulated particles

In order to qualitatively study the uptake and accumulation of nanoplastics by *Lepidum sativum* plants, 3 days old saplings were transplanted in to glass jars containing 25 mL nutrient solution with 10 μg/L, 100 μg/L, 1 mg/L, 50 mg/L and 100 mg/L fluorescent polystyrene nanoparticles (neutrally charged, size: 100 nm) for a period of 12 days. Sections of root, stem and leaf from control plants with no exposure to nanoparticles showed no significant fluorescence when analysed under a laser confocal scanning microscope (Fig. 1). Now it is common to observe some amount of autofluorescence at different ranges of the spectrum in plant samples due to the presence of various pigments and metabolites (Donaldson, 2020). This however, was significantly reduced or eliminated in our case by the selection of nanoparticles that emitted fluorescence in a specific wavelength range where autofluorescence was not significant and the application of time gating to the microscope detector. On the other hand, all exposed samples exhibited clear concentration dependent fluorescence across the whole range of exposure concentration (Fig. S.1). Accumulation of nanoplastics was also observed at the lowest exposure concentration of 10 μg/L (Fig. S.2) confirming the possibility of nanoplastic uptake by crops even at very low environmentally realistic concentrations. For higher exposure concentrations, nanoparticle fluorescence was detected throughout the plant including the root, stem and leaves, however, the fluorescence was much higher in roots compared to stem or leaf samples. Images of samples showed accumulation of nanoparticles along the root tip and areas of lateral root emergence (Fig. 2), surface of the root and root hairs and the stele of the root (Fig. 3) which is how they would be translocated upwards along the transpiration stream. At the locations where lateral root primordia form, the overlying tissues undergo cell separation, resulting in gaps between the epidermal cells which act as an entry point for the nanoparticles (Li et al., 2020). It was interesting to observe that nanoparticles were not homogenously dispersed within the root tissues, but showed aggregations at different sites. The formation of aggregates within root tissues leads to blockage of the translocation pathways thus in turn hindering further upward translocation, which is why the fluorescence in stem and leaves were much lower than the roots. Magnified images of the samples showed the particles majorly accumulated in the intercellular spaces and evidence of cellular uptake was not present (Fig. 4). However, in some studies, the possibility of cellular uptake has been reported previously (Bandmann et al., 2012). Within the stem samples, particles were mainly detected along the stele and rarely in the cortical or epidermal regions except occasional aggregations emerging from the stele and expanding into the cortical and epidermal regions (Fig. 5). Furthermore, in the leaves, the particles seemed to be present in the intercellular spaces of leaf veins but also detected along the epidermal regions, mesophyll tissue as well as around stomatal sites including spaces around the guard cells and stomatal pore (Fig. 6). The presence of chloroplast in the leaf cells often produces a strong autofluorescence in red spectral region between the 680 to 720 nm emission range which can interfere with the NP signals. However, in our case, the emission peak of the NPs was much lower thus eliminating this interference. A composite image contrasting the autofluorescence from the chloroplasts with the signal from the accumulated NPs at the same region of a leaf sample is illustrated in Fig. S.3 for our readers. It has been speculated previously that majority of the nanoplastic uptake occurs via the crack-entry mode at the sites of lateral root emergence (Li et al., 2020). The particles are subsequently carried to the stele of the root via the apoplastic pathway and translocated further to aerial parts with the help of the transpiration stream. However, the possibility of cellular uptake and transfer through the symplastic pathway cannot be dismissed at this point, as that would depend on the SEL of the plant tissue and size of the nanoplastic in question. It is important to keep in mind that the uptake can also be influenced by the charge present on the nanoplastic particle as has been reported previously (Sun et al., 2021; Sun et al., 2020). This could lead to selective uptake and accumulation of particles in different regions based on interactions with different biological compartments. Since our nanoplastics were neutral in nature, therefore, no specific pattern was observed from our samples in this context.

3.2. Quantification methodology

Conceptually, the quantification of nanoplastics within plant tissues is based on the fact that the fluorescence intensity that is detected in the samples is directly proportional to the number of nanoparticles present in them (Torrano et al., 2013). The self-quenching of fluorescence due to aggregation of the nanoparticles has been proven to be negligible for small aggregates and thus would have minimal effect on the quantification if any (Torrano et al., 2013). This approach requires the calculation of the fluorescence intensity of a single nanoparticle as observed through the confocal fluorescence microscope, calculation of the mean residual autofluorescence present in the control plant samples and calculation of fluorescence intensities of detected NPs in positive samples. Here, the mean residual autofluorescence value is subtracted from each positive sample image so that the final fluorescence intensity would correspond to only the accumulated nanoparticles. Finally, the fluorescence of a single NP is used to estimate the number of NPs present per unit volume in a plant sample.

3.2.1. Calculation of single NP fluorescence intensity

For the calculation of the fluorescence intensity of a single nanoparticle, particle solutions were imaged using CLSM at different concentrations of 10 μg/L, 100 μg/L, 1 mg/L, 50 mg/L and 100 mg/L in order to rule out any concentration dependent effect on the fluorescence of a single nanoparticle. Each nanoparticle was shown as an individual pixel in the resultant image which was subsequently analysed using Fiji as described previously. Thresholding was applied from 1 to 65,535 range in order to select all individual nanoparticles within the frame. Using these settings, it was observed that at all solution concentrations, our approach was successfully able to distinguish and select individual pixels representing individual nanoparticles. Confocal images of the nanoparticle solutions are shown in the Fig. S.4. Upon calculation of the fluorescence intensity of each selected pixel, it was observed that the intensities were similar for each such pixel at all concentration levels (15.22 ± 0.12), thereby proving that what we were quantifying were in fact individual nanoparticles. Few selected pixels or groups of pixels were also observed with different intensities in multiples of the unit intensity, proving the presence of a few aggregates (primarily dimers) in the solution. Since the calculated fluorescence intensity of each individual pixel (and thus in turn individual NPs) was the same at all concentrations, it proved that our method was able to calculate the fluorescence of a single NP precisely and accurately. Using this approach, the calculated fluorescence of a single NP including all the detected particles at all solution concentrations was 15.22 ± 0.12.

3.2.2. Calculation of residual background autofluorescence

In order to calculate the residual background autofluorescence in the plant tissues, control plant samples were analysed using CLSM under the exact same settings as before. Processing of the images in Fiji was also done using the same threshold range and steps as detailed in the methods section above. Images of control root, stem and leaves were analysed in replicates to determine the mean autofluorescence intensity for each part separately. The mean residual autofluorescence in the root, stem and leaf samples from control plants was calculated to be 186.47, 253.48 and 436.04 respectively.

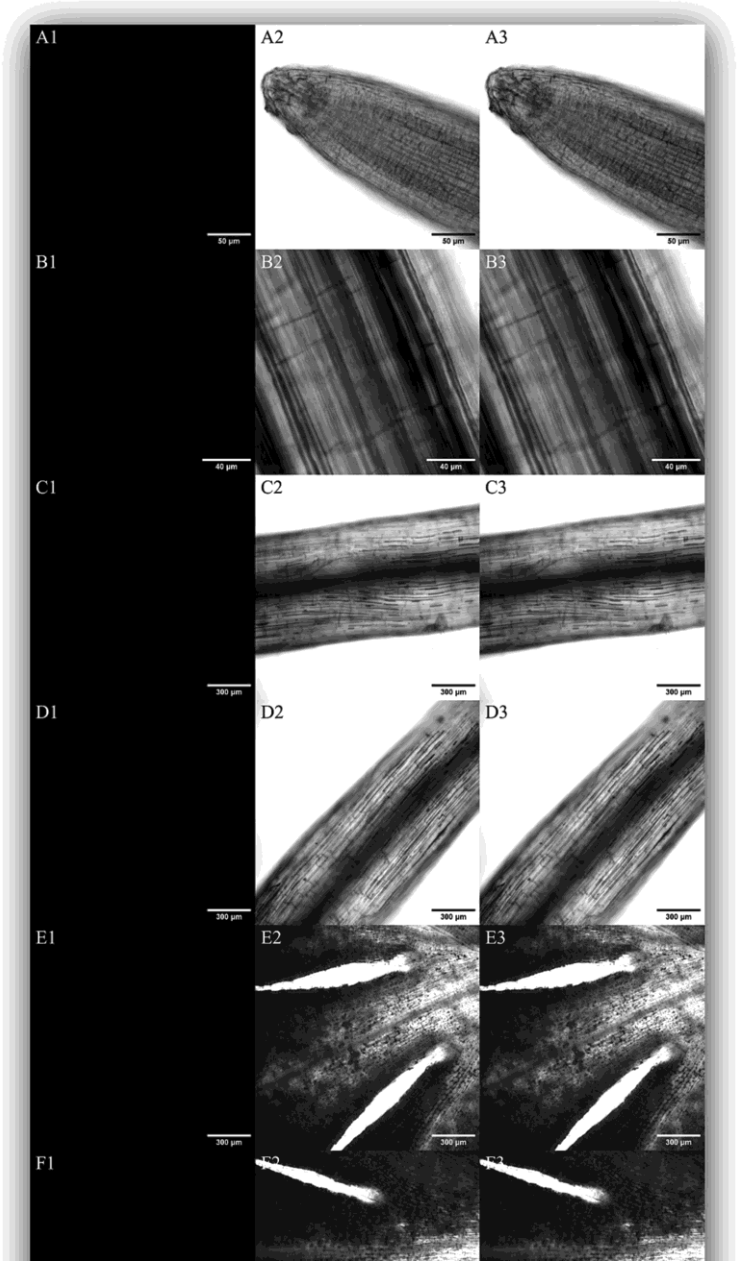

Fig. 1. Confocal images of control root (A and B), stem (C and D) and leaf (E and F) samples highlighting the absence PS nanoparticles and any significant detected autofluorescence. Column 1 shows the dark-field fluorescence channel, column 2 shows the brightfield image of the sample and column 3 is the overlay or composite image of the dark-field and bright-field image.

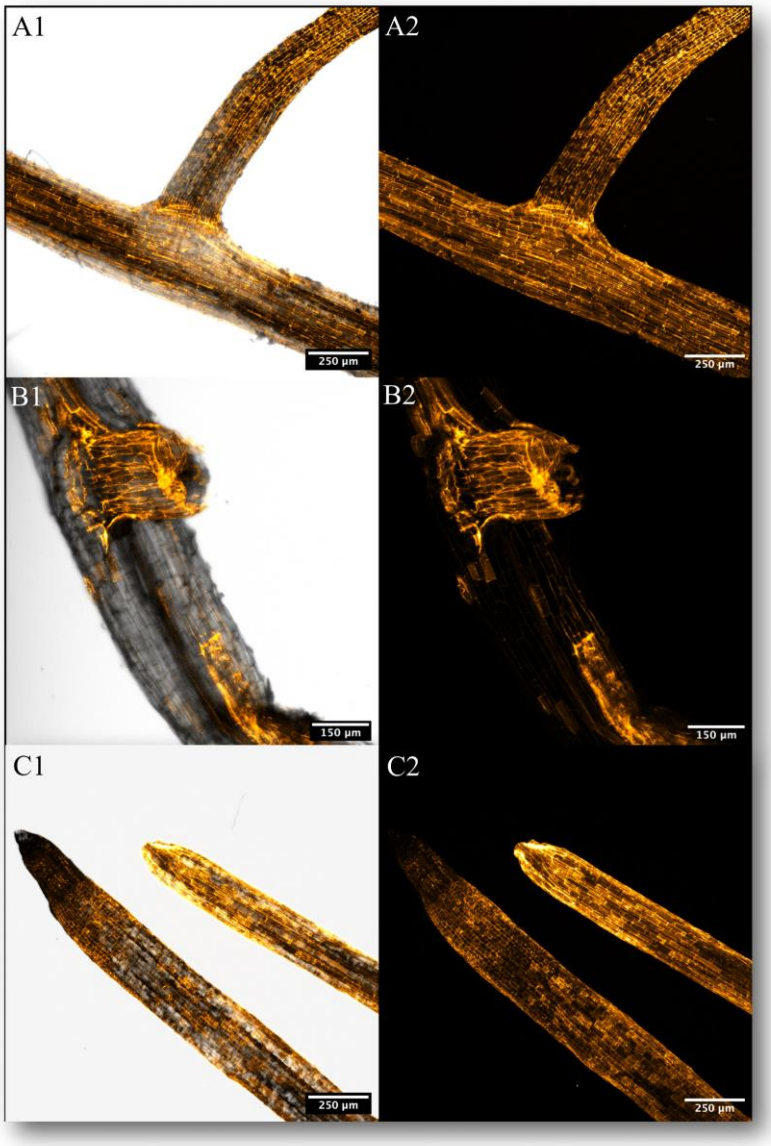

Fig. 2. Highlighting the presence and accumulation of NPs in the lateral roots (A1 and A2) areas of lateral root emergence (B1 and B2) and root tips (C1 and C2). Composite of brightfield and darkfield images (A1, B1 and C1) and just the darkfield image showing the NP fluorescence (A2, B2 and C2). Yellow-orange fluorescence signal corresponds to the accumulated NPs.

3.2.3. Estimation of NPs in positive plant tissues

5 Confocal fluorescence images of root, stem and leaves separately from positive plant samples at 10 µg/L, 100 µg/L, 1 mg/L, 50 mg/L and 100 mg/L nanoplastic exposure concentrations were analysed. Here before the thresholding step, the "subtract" function in Fiji was utilized in order to subtract the calculated residual autofluorescence from root, stem and leaf images respectively. This eliminates the residual auto-fluorescence from positive images and thus the resultant fluorescence values correspond to just the accumulated nanoparticles. Subsequently, thresholding was done using the same settings as before and "Analyze

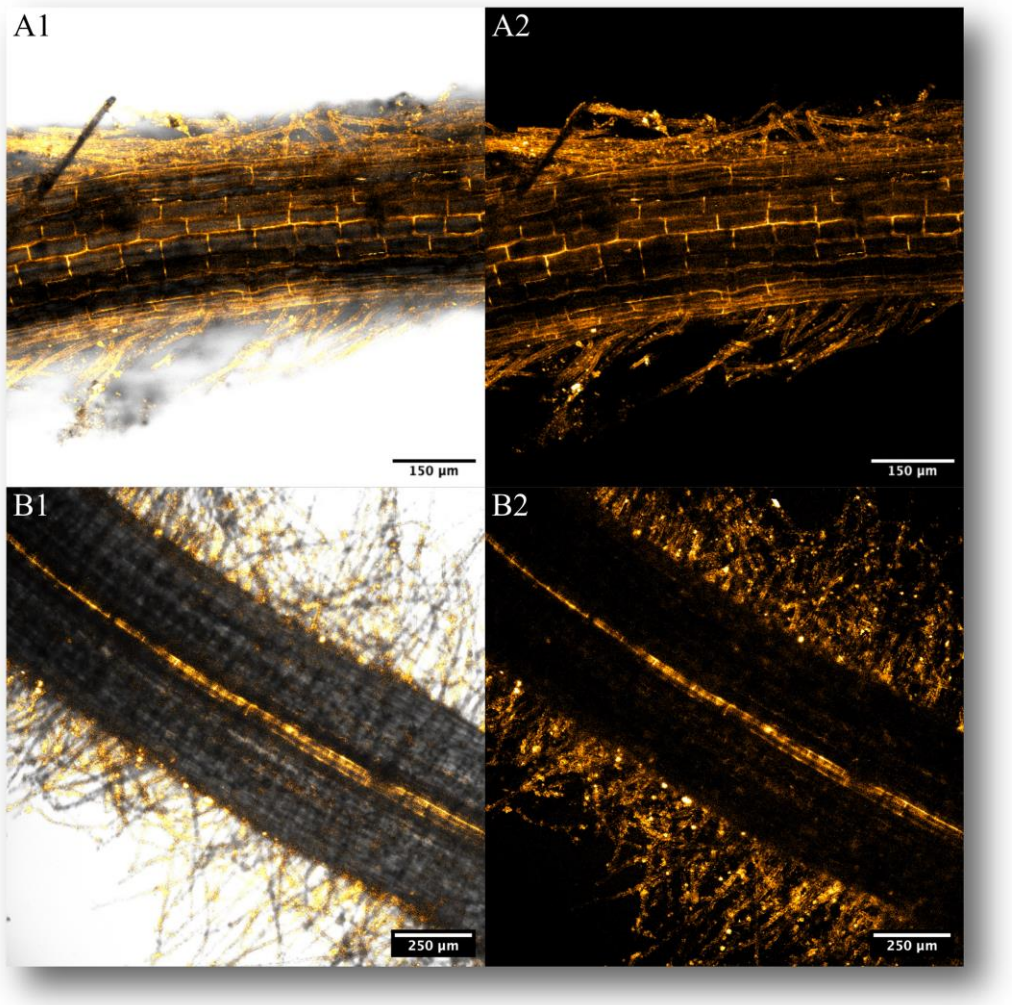

Fig. 3. Highlighting the accumulation of nanoplastics over the root surface and root hairs (A) and within the central stele of the root (B). Composite of the brightfield and darkfield images (A1 and B1) and just the darkfield image with NP fluorescence (A2 and B2). Yellow-orange fluorescence signal corresponds to the accumulated NPs.

particles" tool was used to calculate the fluorescence of each detected object of interest (nanoparticle) within the sample tissue. Finally, all fluorescence intensities were summed up together and the resultant value was divided by the calculated intensity of a single nanoparticle to estimate the number of nanoparticles present in the plant part.

Area of the plant tissue in an image was measured for each sample image and multiplied by the scan thickness (number of z steps of 1 µm each) to calculate the volume of the sample that was analysed. This volume is in voxels (μm^3) and is constituted of 3 dimensional volumetric pixels. Finally, the total amount of NP estimated in each sample image in the previous step was divided by the respective sample volume to achieve the final number of NPs present per unit μm^3 of the plant tissue. This step also normalizes any differences in the scanned sample area and thickness (z steps) between the analysed samples thereby giving results that are comparable.

3.3. Quantification and distribution of NPs in plant tissue

Using the approach described above, the calculated nanoplastic particles per unit volume (μm^3) in positive plant samples at different concentrations were as follows: at 10 µg/L – median 0.019 [IQR: 0.033], at 100 µg/L – median 0.023 [IQR: 0.297], at 1 mg/L – median 0.098 [IQR: 1.373], at 50 mg/L – median 0.382 [IQR: 1.121], at 100 mg/L – median 0.910 [IQR: 3.118]. As can be seen from the IQR values here, the dispersion within the samples at each concentration is quite large. This is because the values include images from root, stem and leaves together.

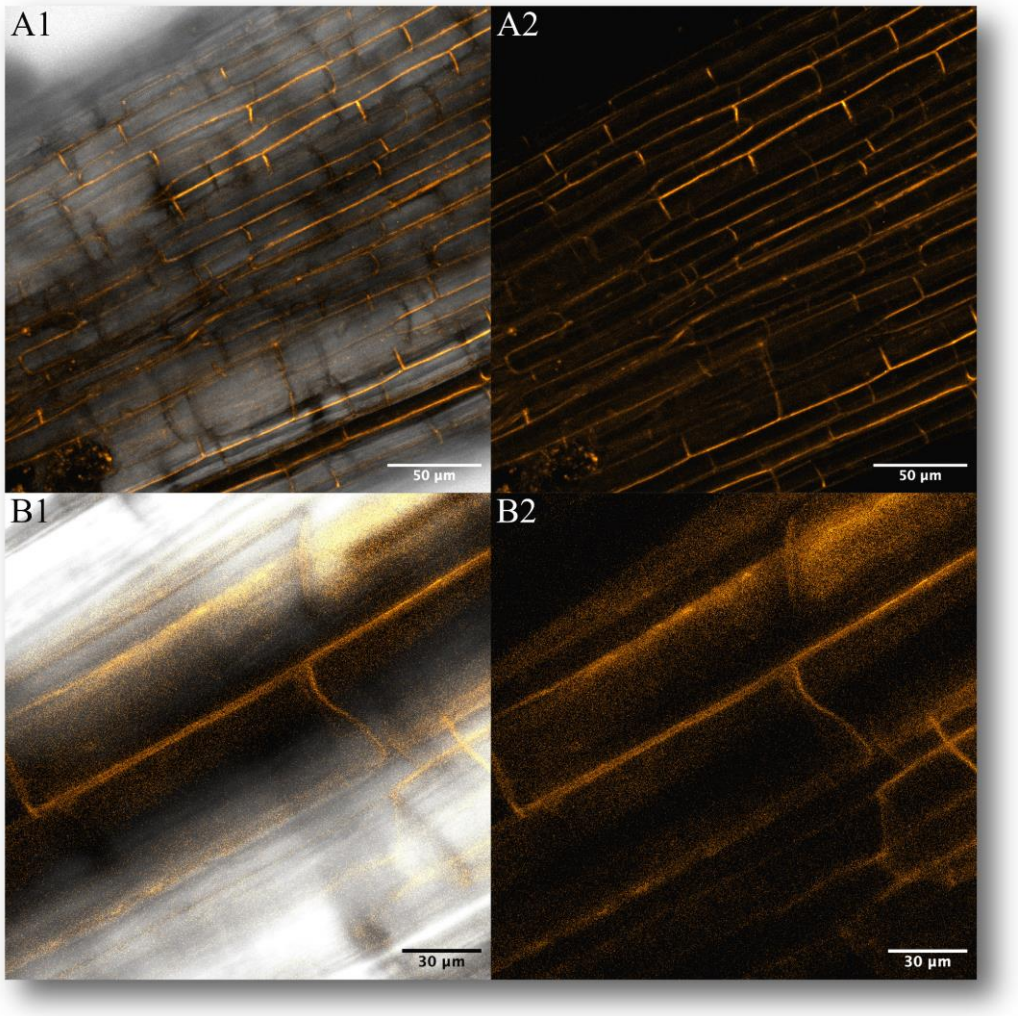

Fig. 4. Accumulation of 100 nm polystyrene nanoplastics in the intercellular spaces of *Lepidum sativum* root. Composite of brightfield and darkfield images (A1 and B1) and darkfield image of NP fluorescence (A2 and B2). Yellow-orange fluorescence signal corresponds to the accumulated NPs.

As was visualised from the confocal fluorescence images previously, the number of nanoparticles translocated to stem and leaves was much lower than in the roots, which were in direct contact with the nanoplastic solution. Another contributing factor to this high dispersion is the aggregation of nanoplastic particles within plant tissues, which results in heterogenous accumulation in different parts, as well as different regions of the same plant part. Out of all the different parts of the plant, root samples had the highest median concentration of calculated nanoparticles which were 0.023/μm^3 at 10 µg/L, 0.302/μm^3 at 100 µg/L, 1.727/μm^3 at 1 mg/L, 1.264/μm^3 at 50 mg/L and 3.936/μm^3 at 100 mg/L exposure concentrations. Similarly for stem samples, the median concentrations were 0.020/μm^3 at 10 µg/L, 0.019/μm^3 at 100 µg/L, 0.093/μm^3 at 1 mg/L, 0.228/μm^3 at 50 mg/L and 0.732/μm^3 at 100 mg/L exposure concentrations. While for the leaf samples, the concentrations were 0.003/μm^3 at 10 µg/L, 0.037/μm^3 at 100 µg/L, 0.009/μm^3 at 1 mg/L, 0.488/μm^3 at 50 mg/L and 0.683/μm^3 at 100 mg/L exposure concentrations.

These results confirmed the concentration dependent accumulation of NPs in the plant tissues. As was observed, majority of the nanoplastics were retained in the root tissues at all exposure concentrations. Since the roots were directly in contact with the NP solutions, they were able to accumulate particles both within the tissues as well as on the root surface (Fig. 3). The median number of NPs found in the stem samples was only 18.04 % of the amount calculated in roots while for the leaf samples, this median was just 13.04 %. There was no clear statistical difference between the NP concentrations in the stem and leaf tissues.

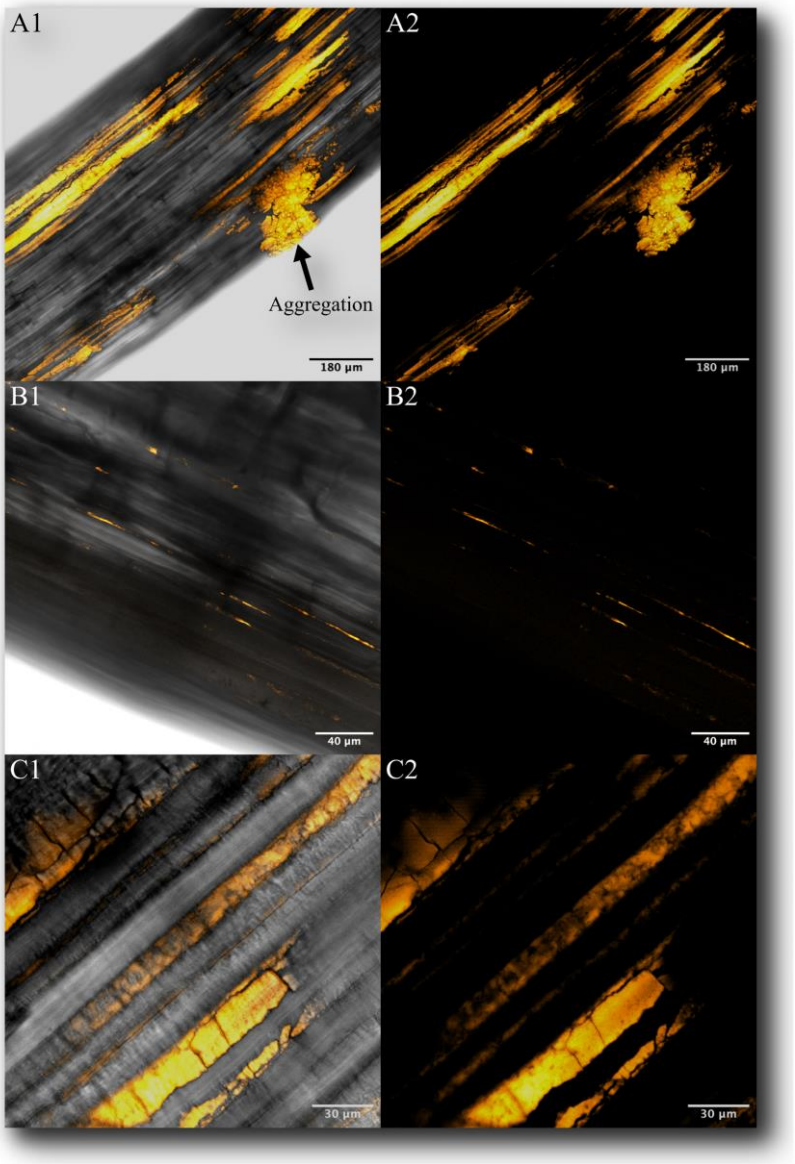

Fig. 5. Accumulation of NPs in *Lepidum sativum* stem. Highlighting an aggregate emerging from the stele and spanning across cortical and epidermal region (A), accumulation in the intercellular spaces of the epidermal region (B) and presence of NPs in the vascular channels (C). Composite images (left) and darkfield images of NP fluorescence (right). Yellow-orange fluorescence signal corresponds to the accumulated NPs.

3.4. Effect on biophysical parameters of the plant

As an additional proof, in this work we also investigated the effect of nanoplastic exposure over the germination of *Lepidum sativum* seeds and the growth of the plant. The rate of germination in the case of the control group was 94.44 ± 4.81 %. However, in the exposure groups, only 55.55 ± 12.73 % of the seeds were able to germinate successfully. This amounted to a reduction of 38.89 ± 9.62 % in the overall germination rate of the plant seeds. This however was only tested at an exposure concentration of 100 mg/L and therefore could be different for lower

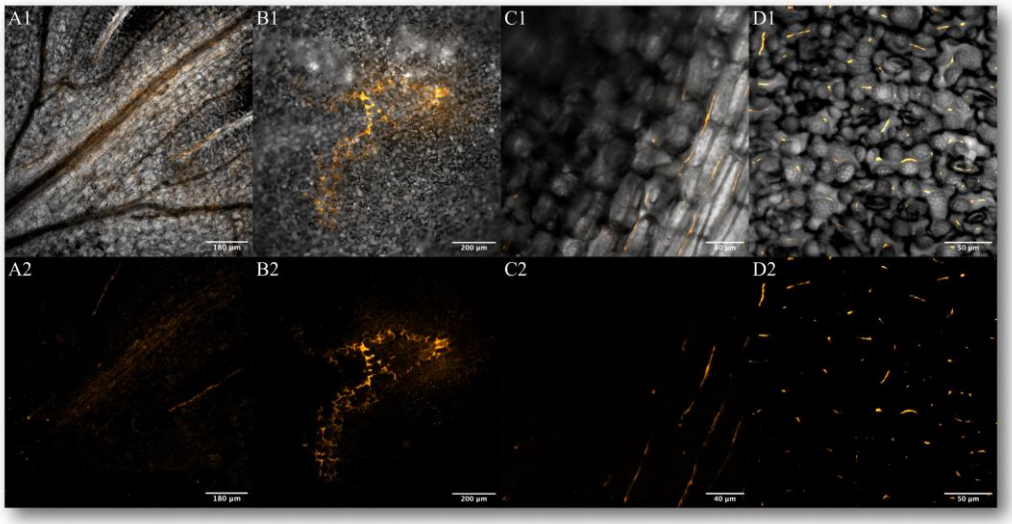

Fig. 6. Accumulation of nanoplastics in *Lepidium sativum* leaf tissue. Surface scan of a leaf showing NP fluorescence in and around the central vein (A), accumulation in the epidermal intercellular spaces (B), NP fluorescence in the intercellular spaces of the central vein (C) and presence in the stomatal region including spaces between guard cells and stomatal pore (D). Composite images with plant tissue (above) and darkfield images with only the NP fluorescence (below). Yellow-orange fluorescence signal corresponds to the accumulated NPs.

concentrations. There was no significant effect of nanoplastic exposure to plant biophysical parameters at lower exposure concentrations of 10 μg/L, 100 μg/L and 1 mg/L (Fig. 7 and Fig. S.5). However, plant fresh weight, root length, root weight, number of lateral roots and shoot weight were significantly affected at 50 mg/L and 100 mg/L exposure concentrations (Kruskal-Wallis $p < 0.05$) (Fig. 7 and Fig. S.5). Interestingly, shoot height was not significantly affected by nanoplastic exposure in our experiments. In brief, the overall plant fresh weight was reduced by 55.17 % at the higher exposure concentrations of 50 mg/L and 100 mg/L. Similarly at 50 mg/L and 100 mg/L, root length was reduced by 62.56 and 63.08 % respectively, root weight was reduced by 80.95 and 80.95 % respectively, number of lateral roots were reduced by 51.35 and 78.38 % respectively and finally the shoot weight was reduced by 28.12 % at both exposure concentrations. As was observed in these results, there seems to be a greater impact of nanoplastic exposure over the root health while the impact over shoot health seems to be lesser. A possible explanation of this could be the direct contact of roots with the nanoplastic particles and the higher accumulation of nanoplastics in root tissues as demonstrated in the previous section.

4. Conclusions

From our findings we conclude that 100 nm polystyrene nanoplastics were taken up by the roots of the edible herb *Lepidum sativum* and successfully translocated to aerial parts of the plant including both stem and leaves. Nanoplastic particles were up taken through the root surface and sites such as regions of lateral root emergence. Detection of NPs in the intercellular spaces suggested the translocation through the apoplastic route and accumulation of nanoplastics within the plant tissues was characterised by aggregation and heterogenous distribution. In our experiments, the presence of cellular uptake and accumulation could not be confirmed. A clear concentration dependent bioaccumulation of nanoplastics was demonstrated and the accumulation of nanoplastics in plant tissues at very low and environmentally realistic exposure concentration of 10 μg/L was confirmed raising concerns about the uptake in the natural environment.

As evidence for the uptake of micro and nano plastics by agricultural crops emerges, it becomes increasingly important for us to be able to explore the quantitative nature of this phenomenon. In this work, an approach to quantification of nanoplastic uptake by plants using confocal laser scanning microscopy and subsequent image analysis was presented which uses a single instrument and a single data collection step with minimal sample preparation steps and pre-processing requirements for the plant. It was shown that our approach was able to successfully estimate the number of nanoplastics present per unit μm^3 of plant samples and as observed from our results, majority of the nanoplastics were retained in the root tissues while only about 13 to 18 % of the NPs were translocated to aerial parts compared to the median root accumulation. The accumulation of NPs in root, stem and leaves was directly proportional to the exposure concentration. However, no clear difference was observed between the accumulated amount in stem and leaves of the plant. Using this approach, we were successfully able to study the spatial distribution of nanoplastics in plant tissues and compare the accumulation in different plant parts. At this point in time, it might not be appropriate to project this methodology as perfect but it certainly seems to be a step in the right direction. Its scope includes quantification of NP accumulation and comparison between different plant samples (inter-sample) but also intra-sample comparisons such as different parts of the same plant or different regions of the same plant part.

In addition to bioaccumulation, in this work, it was also observed that nanoplastic exposure affected the germination rate and health of the plant with effects on the biophysical parameters. The overall plant weight was reduced by about 55 % at higher exposure concentrations and similar effects were observed in root length, root weight, number of lateral roots as well as shoot weight. However, the effects were only significant at exposure concentrations at and above 50 mg/L which as less probable environmentally. Lower exposure concentrations of 10 μg/

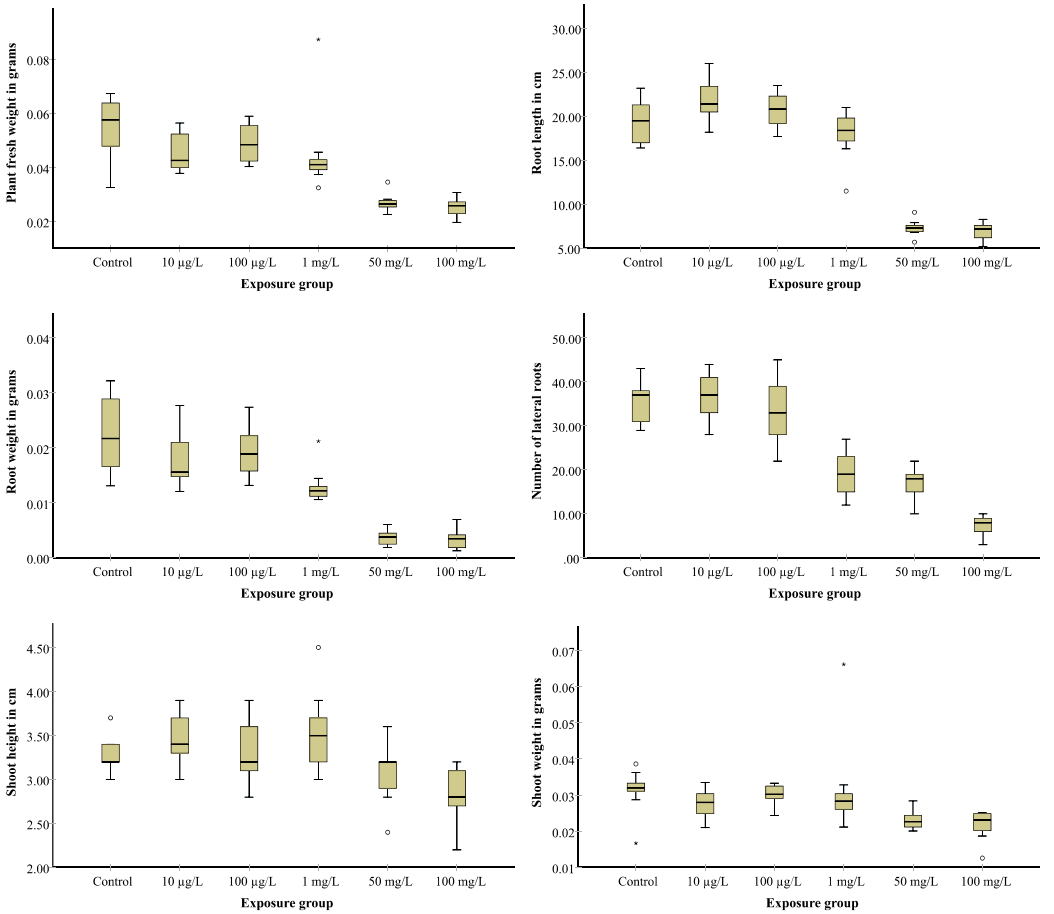

Fig. 7. Effect of 100 nm polystyrene nanoplastic exposure over the biophysical parameters of the plant *Lepidum sativum.*

L, 100 µg/L and 1 mg/L were not able to affect the plant health significantly. This again highlights the need to study this issue at environmentally realistic concentrations in order to get an accurate idea of the real world phenomenon. In addition, the effect seems to be more direct and severe in the roots than the shoot. Here it is important to keep in mind that even if lower concentrations did not affect the plant health significantly, uptake and accumulation was still confirmed at these concentrations, raising concerns for food safety. Our work adds to the emerging knowledge about the impacts of micro and nano plastics over our agricultural ecosystems and highlights the need of a focussed effort to investigate this issue.

CRediT authorship contribution statement

Harshit Sahai: Conceptualization, Investigation, Methodology, Formal analysis, Writing – original draft, Visualization. **María Jesús Martínez Bueno:** Conceptualization, Investigation, Resources, Writing – review & editing. **María del Mar Gómez-Ramos:** Formal analysis, Investigation. **Amadeo R. Fernández-Alba:** Conceptualization, Investigation, Supervision, Validation, Resources, Writing – review & editing. **María Dolores Hernando:** Conceptualization, Supervision, Investigation, Methodology, Project administration, Funding acquisition, Validation, Writing – review & editing.

Declaration of competing interest

The authors declare that they have no known competing financial interests or personal relationships that could have appeared to influence the work reported in this paper.

Data availability

Data will be made available on request.

Acknowledgements

Authors acknowledge the support of the projects "FoodTraNet" MSCA-ITN, the funding received from the European Union's Horizon 2020 - Research and Innovation Framework Programme under the Marie Skłodowska-Curie grant agreement No. 956265 and the funding

received for the REVEAL project, Ref TED2021-131609B-C31. We would like to thank Ana Oña and Gianluca D'Agostino at the Advanced Light Microscopy unit of the National Centre for Biotechnology (CNB-CSIC), Spain for their help and support with the microscopic analysis. Open Access funding provided thanks to the CSIC-CRUE agreement with Elsevier.

Disclaimer

The contents of this publication and the opinions expressed are those of the author(s) only and this document should not be considered as representative of CSIC's official position and it does not involve CSIC in liability of any kind.

Appendix A. Supplementary data

Supplementary data to this article can be found online at https://doi.org/10.1016/j.scitotenv.2023.168903.

References

Avellan, A., et al., 2017. Nanoparticle uptake in plants: gold nanomaterial localized in roots of Arabidopsis thaliana by X-ray computed nanotomography and hyperspectral imaging. Environ. Sci. Technol. 51, 8682–8691.
Bandmann, V., Müller, J.D., Köhler, T., Homann, U., 2012. Uptake of fluorescent nano beads into BY2-cells involves clathrin-dependent and clathrin-independent endocytosis. FEBS Lett. 586, 3626–3632.
Bosker, T., Bouwman, L.J., Brun, N.R., Behrens, P., Vijver, M.G., 2019. Microplastics accumulate on pores in seed capsule and delay germination and root growth of the terrestrial vascular plant Lepidium sativum. Chemosphere 226, 774–781.
Büks, F., Kaupenjohann, M., 2020. Global concentrations of microplastics in soils – a review. Soil 6, 649–662.
Donaldson, L., 2020. Autofluorescence in plants. Molecules 25, 2393.
Dong, Y., Gao, M., Qiu, W., Song, Z., 2021. Uptake of microplastics by carrots in presence of As (III): combined toxic effects. J. Hazard. Mater. 411, 125055.
Giorgetti, L., et al., 2020. Exploring the interaction between polystyrene nanoplastics and Allium cepa during germination: internalization in root cells, induction of toxicity and oxidative stress. Plant Physiol. Biochem. 149, 170–177.
Gong, W., et al., 2021. Species-dependent response of food crops to polystyrene nanoplastics and microplastics. Sci. Total Environ. 796, 148750.
Jiang, X., et al., 2019. Ecotoxicity and genotoxicity of polystyrene microplastics on higher plant Vicia faba. Environ. Pollut. 250, 831–838.
Kim, D., et al., 2022. Translocation and chronic effects of microplastics on pea plants (Pisum sativum) in copper-contaminated soil. J. Hazard. Mater. 436, 129194.
Li, L., et al., 2020. Effective uptake of submicrometre plastics by crop plants via a crack-entry mode. Nat. Sustain. 3, 929–937.
Li, Z., Li, Q., Li, R., Zhou, J., Wang, G., 2021. The distribution and impact of polystyrene nanoplastics on cucumber plants. Environ. Sci. Pollut. Res. 28, 16042–16053.
Lian, J., et al., 2021. Foliar-applied polystyrene nanoplastics (PSNPs) reduce the growth and nutritional quality of lettuce (Lactuca sativa L.). Environ. Pollut. 280, 116978.
Liu, Y., Guo, R., Zhang, S., Sun, Y., Wang, F., 2022. Uptake and translocation of nano/microplastics by rice seedlings: evidence from a hydroponic experiment. J. Hazard. Mater. 421, 126700.
Luo, Y., et al., 2022. Quantitative tracing of uptake and transport of submicrometre plastics in crop plants using lanthanide chelates as a dual-functional tracer. Nat. Nanotechnol. 17, 424–431.
Nizzetto, L., Futter, M., Langaas, S., 2016. Are agricultural soils dumps for microplastics of urban origin? Environ. Sci. Technol. 50, 10777–10779.
Schindelin, J., et al., 2012. Fiji: an open-source platform for biological-image analysis. Nat. Methods 9, 676–682.
Sun, H., Lei, C., Xu, J., Li, R., 2021. Foliar uptake and leaf-to-root translocation of nanoplastics with different coating charge in maize plants. J. Hazard. Mater. 416, 125854.
Sun, X.-D., et al., 2020. Differentially charged nanoplastics demonstrate distinct accumulation in Arabidopsis thaliana. Nat. Nanotechnol. 15, 755–760.
Taylor, E., S., et al., 2020. Polystyrene nano- and microplastic accumulation at Arabidopsis and wheat root cap cells, but no evidence for uptake into roots. Environ. Sci. Nano 7, 1942–1953.
Tian, L., Jinjin, C., Ji, R., Ma, Y., Yu, X., 2022. Microplastics in agricultural soils: sources, effects, and their fate. Curr. Opin. Environ. Sci. Health 25, 100311.
Torrano, A.A., et al., 2013. A fast analysis method to quantify nanoparticle uptake on a single cell level. Nanomedicine 8, 1815–1828.
Zhang, T.-R., et al., 2019. Uptake and translocation of styrene maleic anhydride nanoparticles in Murraya exotica plants as revealed by noninvasive, real-time optical bioimaging. Environ. Sci. Technol. 53, 1471–1481.
Zhou, C.-Q., et al., 2021. Response of rice (Oryza sativa L.) roots to nanoplastic treatment at seedling stage. J. Hazard. Mater. 401, 123412.

Chapter 4

Conclusions

The use of plastics in nearly every facet of our daily lives underscores its significance. The constant increase in global plastic production and consumption and future growth projections highlight its pivotal role in human society and emphasize the need for a sustainable future. The characteristics of plastic that make it a remarkable material, including its malleability, longevity, and non-degradable nature, are the attributes that make it detrimental to the environment if not managed properly. More importantly, the potential environmental repercussions of MNPs should not be overlooked. Their ubiquity across ecosystems and documented effects on their living organisms and non-living components highlight the extent of the problem and the need for mitigative actions.

Until recently, most studies reporting the presence and impacts of MNPs on the environment have focused on aquatic ecosystems. However, there is a growing interest and concern regarding the presence and interactions of MNPs in the terrestrial domain, specifically within agricultural soils, and the term "plasticulture" is now used to describe the extensive use of plastic materials in agriculture. This practice includes using plastic products like mulch films, tunnels, irrigation equipment, silage, greenhouses, and other on-field infrastructure in the pre-harvest phase, crates, packaging materials, and bags in the post-harvest phase. Improper management of these materials can potentially result in the introduction of MNPs into the agricultural ecosystem.

MNP and mulch film interactions with pesticide residues

One of the key sources of MNPs in agricultural soils is plastic mulch films. Numerous studies have highlighted the generation of MNPs from plastic mulch films in agricultural areas and have demonstrated the link between mulch film usage and MNPs concentration. A predominant polymer commonly used for traditional mulch film applications is PE. Nevertheless, this polymer is non-biodegradable and forms MNPs due to various degradative factors acting on it throughout its application lifespan. This problem has led to the increasing use of biodegradable mulch films, positioned as eco-friendlier options. However, these films are also modified with numerous additives that enhance properties like cross-linking and strength yet may cause issues like poor degradation and interactions within the agricultural setting. The use of these biodegradable mulch films may result in even higher levels of MNPs due to inadequate degradation in the field.

The occurrence of MNPs in agricultural soil significantly affects the physicochemical and biological properties. Furthermore, it may lead to interactions between MNP particles and other agricultural contaminants like pesticide residues. Although the interactions of MNPs with contaminants and their uptake have been extensively researched in aquatic environments, their presence in agricultural systems is not well-explored. This study

focused on investigating the adsorption of pesticide residues onto microplastics obtained from agricultural mulch films. The study used traditional PE and biodegradable PBAT mulch films to compare the sorption mechanisms and desorption of pesticide residues from the mulch film samples.

In my work, I found that biodegradable PBAT mulch films have a heightened capacity for retaining pesticides on their surface. Conversely, PE mulch films displayed greater desorption or discharge of pesticides into the surrounding environment following a spraying event. The implications of this observation extend to the eventual destiny and accessibility of these pesticide remnants within the agricultural ecosystem. Even though increased ambient temperatures did not impact the final desorption quantities in both types of plastics, the rate of pesticide desorption from the mulch film surfaces is influenced by temperature, particularly for PE films. At an ambient temperature of 40°C, the desorption duration decreased from 10 days at 20°C to 6 days for PE films, while PBAT mulch films exhibited no significant alteration. This temperature-dependent trend in desorption, influenced by fluctuations in ambient temperature, may introduce a seasonal dimension to the process under natural, on-field conditions. It also suggests a more rapid release of pesticides from the surfaces of PE mulch films into the surrounding environment during warmer seasons or in regions with higher temperatures. Therefore, my work confirms the hypothesis H3: Biodegradable PBAT mulch films exhibit a higher pesticide adsorption capacity, with a higher retention and reduced desorption rate than conventional PE mulch films.

Regarding the sorption of pesticide residues onto mulch film microplastics samples, I demonstrated that even at environmental concentrations (5 µg/L), pesticide residues could be sorbed to a high degree onto microplastics generated from mulch films. In the case of PE microplastic samples, the process of sorption would be case-specific to each contaminant depending on its log K_{ow} value, with compounds with high hydrophobicity being sorbed onto the microplastics to a high degree. The fact that sorption capacities were influenced by the ionic strength of the reaction media highlights the role of electrostatic forces in the process. It thus implies that the process would be different in different agricultural scenarios depending on the properties of the irrigation water or soil. For the PE type of microplastic sample investigated, pseudo-first order was the best-fitting kinetic model for all pesticides (R^2: 0.90 - 0.98), implying the dominant role of physisorption and the limited role of chemical bond formation. The fact that Dubinin-Radushkevich was the best-fitting isotherm model (R^2: 0.92 - 0.99) implies the presence of a micropore volume filling mechanism over the heterogeneous and rough-surfaced MPs derived from mulch films.

Sorption on microplastics derived from PBAT films was influenced by the log Kow value of the pesticides, with a Spearman's correlation of 0.857 for PBAT and 0.837 for PE ($p < 0.05$), while the impact of pKa was comparatively weaker. A specific log Kow cut-off point was determined for both types of plastic, below which sorption in microplastics became insignificant, and desorption in mulch films reached its peak. This critical log Kow value was approximately 2.8 for biodegradable PBAT mulch films and 3.3 for conventional PE mulch films.

Furthermore, modeling revealed that the adsorption of pesticide residues onto biodegradable PBAT microplastics adhere to Elovich (R2: 0.937-0.959) and pseudo-second-order kinetics (R2: 0.942-0.987), primarily driven by chemical interaction and bond formation rather than the physical adsorption characteristic of PE microplastics as indicated above. Sorption in PBAT is a multi-step process, with film diffusion or chemical bond formation being the rate-limiting step. As mentioned earlier, this variation in the interaction mechanisms (chemisorption *vs.* physisorption) may potentially elucidate the enhanced retention of pesticide residues on PBAT compared to PE films. From this, I was

able to confirm the hypotheses H1: Microplastics derived from mulch films can be shown to adsorb agricultural pesticide residues and H2: The sorption mechanism of pesticides on conventional petroleum-based PE microplastic particles differs from that on biodegradable PBAT microplastic particles.

My work not only highlights the role of microplastics and mulch films in transporting pesticides within agricultural environments but also provides concrete evidence of the ability of biodegradable PBAT microplastics and mulch films to absorb and hold a wider variety of pesticides and in higher amounts compared to traditional PE mulch films. With their enhanced capacity for retaining pesticides, PBAT films have the potential to act as reservoirs for pesticide residues, thereby reducing the amount of these chemicals released into the surrounding soil. This dual function not only safeguards the soil from excessive contamination by pesticide residues but also underscores the significance of appropriately managing the collection, decontamination, and recycling of such films at the end of their life cycle. Properly handling these films post-usage can minimize environmental impact and promote sustainable agricultural practices.

Uptake and bioaccumulation of MNPs in plants

Another crucial factor to consider regarding MNPs in agricultural soils pertains to the intricate relationships they establish with plants, particularly regarding the potential uptake of MNPs by plants and subsequent bioaccumulation processes. For this reason, my research also focused on investigating the bioaccumulation of 100nm PS nanoplastics within *Lepidium sativum* plants. This study delved into the intricate mechanisms underlying the interaction between MNPs and plant species, shedding light on the potential implications for environmental and agricultural systems.

Based on the outcomes of my investigations, I deduce that 100 nm PS nanoplastics managed to enter the roots of the edible herb *Lepidium sativum* and were effectively transported to the above-ground sections of the plant, encompassing both the stem and the leaves. The uptake of nanoplastic particles was observed to occur *via* the root surface and specific locations, such as at lateral root emergence. The presence of NPs in the intercellular spaces indicated the translocation process through the apoplastic pathway, while the accumulation of nanoplastics within plant tissues exhibited aggregation and non-uniform distribution. However, I could not validate the existence of cellular absorption and accumulation. Notably, a distinct relationship between nanoplastics' bioaccumulation and concentration levels was illustrated, emphasizing the accumulation of nanoplastics in plant tissues even at trace and environmental exposure levels (10 µg/L), prompting concerns regarding uptake in the natural surroundings. These findings confirm the hypothesis H4: Nanoplastics can bioaccumulate in the model crop *Lepidium sativum* and translocate from the roots to aerial/edible parts.

In this work, alongside bioaccumulation, I observed that exposure to nanoplastics impacted germination rate and overall plant health, leading to alterations in various biophysical parameters. The plant's total weight experienced a reduction of approximately 55% at elevated exposure levels, and similar consequences were observed in metrics such as root length, root weight, number of lateral roots, and shoot weight. Nonetheless, these impacts were deemed statistically significant solely at exposure concentrations equal to or exceeding 50 mg/L, a scenario less likely to occur in the environment. Lower exposure levels of 10 µg/L, 100 µg/L, and 1 mg/L did not substantially affect plant health. Moreover, I observed that the effects were more pronounced in the roots and shoots. However, even though lower concentrations did not significantly impact plant health, their uptake and accumulation were confirmed, raising concerns regarding food safety.

Quantification of MNP uptake in the plant

As the emergence of evidence regarding the uptake of MNPs by crops unfolds, it is becoming increasingly critical for researchers to investigate the quantitative aspects of this phenomenon. My thesis has introduced an innovative method for quantifying the uptake of nanoplastics by plants, utilizing CLSM and subsequent image analysis. The method uses a single instrument and data collection step, requiring minimal sample preparation procedures and pre-processing steps for the plant specimens. The findings demonstrate the efficacy of my approach in estimating the quantity of nanoplastics per unit μm^3 of plant samples. The results indicate that a significant portion of the nanoplastics is retained in the root tissues, with only approximately 13 to 18 % of the NPs being translocated to the aerial parts compared to the median root accumulation. The distribution of NPs in the root, stem, and leaves is directly correlated with the exposure concentration. However, there is no distinct variance in the accumulated amount between the stem and leaves of the plant. Through this innovative methodology, I successfully examined the spatial dispersion of nanoplastics in plant tissues and conducted comparisons of the accumulation in various plant components. While it may be premature to characterize this approach as flawless at this juncture, it undeniably signifies a progressive stride in the right direction within this field of study. The scope of this methodology encompasses not only the quantification of NP accumulation and inter-sample comparisons among different plant samples but also intra-sample evaluations, such as contrasting different segments of the same plant or diverse regions within the same plant part. Overall, I can confirm the hypothesis H5: Fluorescence-based confocal laser-scanning microscopy with image analysis can quantify nanoplastics uptake and bioaccumulation in plants.

Chapter 5

Future Perspectives

As emerging evidence continues to surface regarding the presence and impacts of MNPs in the agricultural ecosystem, there is a pressing and specific need for an immediate and focused exploration of this issue. The research presented in my thesis effectively showcases the intricate interactions of MNPs originating from mulch films with pesticide residues; however, the implications of these interactions on the final fate and accessibility of absorbed pesticide residues are yet to be firmly established. The study underscores that microplastics originating from agricultural mulch films can serve as carriers for the transportation and fate of pesticides. The repercussions of this phenomenon on both biotic and abiotic elements in the agricultural domain, encompassing crops, necessitate assessment grounded on direct empirical proof, which is currently lacking. Moreover, despite highlighting the significance of biodegradable PBAT mulch films as reservoirs for pesticide residues, it remains to assess whether they mitigate pesticide residue contamination in real-field conditions or inadvertently exacerbate it. This evaluation would hinge on various factors, such as the efficient collection, decontamination, and recycling of these mulch films after their usage, their capability to generate secondary MNPs, and the influence of environmental factors.

In my thesis, I further showcased the efficient uptake, accumulation, and translocation of 100 nm PS nanoplastics within the consumable herb known as *Lepidium sativum*. It is crucial to highlight that the outcomes and deductions are rooted in observations made on a model plant characterized by its small size, simplistic morphological and anatomical composition, and rapid growth rate. Nonetheless, it is imperative to underscore the necessity for additional investigations involving a diverse array of plant species, encompassing a broad spectrum of plant varieties with varying morphological and anatomical structures and longer life spans, subjected to diverse exposure conditions and durations. Such a comprehensive approach would provide a greater understanding of the extent of this phenomenon in real-world scenarios, facilitating an assessment of the likelihood and magnitude of this issue. Moreover, it is essential to emphasize the significance of conducting experiments using a broad range of polymer types with differing surface morphologies that mimic real-world conditions. These experiments should ideally be carried out in field settings to enhance the ecological relevance of the findings.

This dissertation also puts forward an innovative methodology for quantifying the absorption of nanoplastics in plant tissues utilizing fluorescence-based CLSM combined with image analysis. This method can quantify MNPs in various plant components; nevertheless, there remains room for improvement. Further investigation is needed to comprehend the suitability of this methodology across diverse plant matrices since factors such as the plant's anatomy and the presence of metabolites and pigments could potentially influence the method. Therefore, further research is needed to optimize this approach for various plant species, specific types of nanoplastic particles, and analytical parameters. Additionally, it is crucial to establish its effectiveness and suitability for large-scale monitoring and analysis. Nonetheless, this new work represents a significant advancement in MNP research.

References

[1] R. Geyer, 'A Brief History of Plastics', in *Mare Plasticum - The Plastic Sea: Combatting Plastic Pollution Through Science and Art*, M. Streit-Bianchi, M. Cimadevila, and W. Trettnak, Eds., Cham: Springer International Publishing, 2020, pp. 31–47. doi: 10.1007/978-3-030-38945-1_2.

[2] R. Geyer, J. R. Jambeck, and K. L. Law, 'Production, use, and fate of all plastics ever made', *Sci. Adv.*, vol. 3, no. 7, p. e1700782, Jul. 2017, doi: 10.1126/sciadv.1700782.

[3] F. Bauer *et al.*, 'Plastics and climate change—Breaking carbon lock-ins through three mitigation pathways', *One Earth*, vol. 5, no. 4, pp. 361–376, Apr. 2022, doi: 10.1016/j.oneear.2022.03.007.

[4] 'Plastics – the fast Facts 2023 • Plastics Europe', Plastics Europe. Accessed: Jun. 10, 2024. [Online]. Available: https://plasticseurope.org/knowledge-hub/plastics-the-fast-facts-2023/

[5] 'The Circular Economy for Plastics – A European Analysis 2024 • Plastics Europe', Plastics Europe. Accessed: Jun. 10, 2024. [Online]. Available: https://plasticseurope.org/knowledge-hub/the-circular-economy-for-plastics-a-european-analysis-2024/

[6] OECD, 'Global Plastics Outlook: Policy Scenarios to 2060', oecd-ilibrary.org. Accessed: Jun. 10, 2024. [Online]. Available: https://read.oecd-ilibrary.org/environment/global-plastics-outlook_aa1edf33-en

[7] 'Production, use, and fate of synthetic polymers', pp. 13–32, Jan. 2020, doi: 10.1016/B978-0-12-817880-5.00002-5.

[8] 'Plastic waste management, a matter for the "community".', *Microb. Biotechnol.*, vol. 12, no. 1, pp. 66–68, Jan. 2019, doi: 10.1111/1751-7915.13328.

[9] 'Plastic Management and Sustainability: A Data-Driven Study', *Sustainability*, vol. 15, no. 9, pp. 7181–7181, Apr. 2023, doi: 10.3390/su15097181.

[10] J. Zalasiewicz *et al.*, 'The geological cycle of plastics and their use as a stratigraphic indicator of the Anthropocene', *Anthropocene*, vol. 13, pp. 4–17, Mar. 2016, doi: 10.1016/j.ancene.2016.01.002.

[11] M. Cole, P. Lindeque, C. Halsband, and T. S. Galloway, 'Microplastics as contaminants in the marine environment: A review', *Mar. Pollut. Bull.*, vol. 62, no. 12, pp. 2588–2597, Dec. 2011, doi: 10.1016/j.marpolbul.2011.09.025.

[12] K. W. Kenyon and E. Kridler, 'Laysan Albatrosses Swallow Indigestible Matter', *The Auk*, vol. 86, no. 2, pp. 339–343, Apr. 1969, doi: 10.2307/4083505.

[13] J. B. Colton, B. R. Burns, and F. D. Knapp, 'Plastic Particles in Surface Waters of the Northwestern Atlantic', *Science*, vol. 185, no. 4150, pp. 491–497, Aug. 1974, doi: 10.1126/science.185.4150.491.

[14] E. J. Carpenter and K. L. Smith, 'Plastics on the Sargasso Sea Surface', *Science*, vol. 175, no. 4027, pp. 1240–1241, Mar. 1972, doi: 10.1126/science.175.4027.1240.

[15] I. E. Napper and R. C. Thompson, 'Plastic Debris in the Marine Environment: History and Future Challenges', *Glob. Chall.*, vol. 4, no. 6, p. 1900081, Apr. 2020, doi: 10.1002/gch2.201900081.

[16] Y. Wang *et al.*, 'The Global Trend of Microplastic Research in Freshwater Ecosystems', *Toxics*, vol. 11, no. 6, Art. no. 6, Jun. 2023, doi: 10.3390/toxics11060539.

[17] M. C. Rillig and A. Lehmann, 'Microplastic in terrestrial ecosystems', *Science*, vol. 368, no. 6498, pp. 1430–1431, Jun. 2020, doi: 10.1126/science.abb5979.

[18] A. Rossatto, M. Z. F. Arlindo, M. S. de Morais, T. D. de Souza, and C. S. Ogrodowski, 'Microplastics in aquatic systems: A review of occurrence, monitoring and potential environmental risks', *Environ. Adv.*, vol. 13, p. 100396, Oct. 2023, doi: 10.1016/j.envadv.2023.100396.

[19] U. Surendran, M. Jayakumar, P. Raja, G. Gopinath, and P. V. Chellam, 'Microplastics in terrestrial ecosystem: Sources and migration in soil environment', *Chemosphere*, vol. 318, p. 137946, Mar. 2023, doi: 10.1016/j.chemosphere.2023.137946.

[20] G. Sathyamohan, M. Sewwandi, B. Ambade, and M. Vithanage, 'Sources and Circulation of Microplastics in the Aerosphere – Atmospheric Transport of Microplastics', in *Microplastics in the Ecosphere*, John Wiley & Sons, Ltd, 2023, pp. 125–146. doi: 10.1002/9781119879534.ch8.

[21] M. Bergmann *et al.*, 'High Quantities of Microplastic in Arctic Deep-Sea Sediments from the HAUSGARTEN Observatory', *Environ. Sci. Technol.*, vol. 51, no. 19, pp. 11000–11010, Oct. 2017, doi: 10.1021/acs.est.7b03331.

[22] M. Bergmann, S. Mützel, S. Primpke, M. B. Tekman, J. Trachsel, and G. Gerdts, 'White and wonderful? Microplastics prevail in snow from the Alps to the Arctic', *Sci. Adv.*, vol. 5, no. 8, p. eaax1157, Aug. 2019, doi: 10.1126/sciadv.aax1157.

[23] A. L. Lusher, V. Tirelli, I. O'Connor, and R. Officer, 'Microplastics in Arctic polar waters: the first reported values of particles in surface and sub-surface samples', *Sci. Rep.*, vol. 5, no. 1, p. 14947, Oct. 2015, doi: 10.1038/srep14947.

[24] A. R. Aves *et al.*, 'First evidence of microplastics in Antarctic snow', *The Cryosphere*, vol. 16, no. 6, pp. 2127–2145, Jun. 2022, doi: 10.5194/tc-16-2127-2022.

[25] C. L. Waller *et al.*, 'Microplastics in the Antarctic marine system: An emerging area of research', *Sci. Total Environ.*, vol. 598, pp. 220–227, Nov. 2017, doi: 10.1016/j.scitotenv.2017.03.283.

[26] A. Kaliszewicz *et al.*, 'First Evidence of Microplastic Occurrence in the Marine and Freshwater Environments in a Remote Polar Region of the Kola Peninsula and a Correlation with Human Presence', *Biology*, vol. 12, no. 2, p. 259, Feb. 2023, doi: 10.3390/biology12020259.

[27] B. Eyheraguibel, A. T. Halle, Y. Ourmieres, J.-F. Ghiglione, and P. Amato, 'High debit sampling of airborne micro and nanoplastics in remote sea', Copernicus Meetings, EGU23-6536, Feb. 2023. doi: 10.5194/egusphere-egu23-6536.

[28] D. Materić *et al.*, 'Presence of nanoplastics in rural and remote surface waters', *Environ. Res. Lett.*, vol. 17, no. 5, p. 054036, May 2022, doi: 10.1088/1748-9326/ac68f7.

[29] S. Allen *et al.*, 'Atmospheric transport and deposition of microplastics in a remote mountain catchment', *Nat. Geosci.*, vol. 12, no. 5, pp. 339–344, May 2019, doi: 10.1038/s41561-019-0335-5.

[30] S. Padha, R. Kumar, A. Dhar, and P. Sharma, 'Microplastic pollution in mountain terrains and foothills: A review on source, extraction, and distribution of microplastics in remote areas', *Environ. Res.*, vol. 207, p. 112232, May 2022, doi: 10.1016/j.envres.2021.112232.

[31] V. Godoy *et al.*, 'The human connection: First evidence of microplastics in remote high mountain lakes of Sierra Nevada, Spain', *Environ. Pollut.*, vol. 311, p. 119922, Oct. 2022, doi: 10.1016/j.envpol.2022.119922.

[32] J. Brahney, M. Hallerud, E. Heim, M. Hahnenberger, and S. Sukumaran, 'Plastic rain in protected areas of the United States', *Science*, vol. 368, no. 6496, pp. 1257–1260, Jun. 2020, doi: 10.1126/science.aaz5819.

[33] M. Mistri *et al.*, 'Microplastic Contamination in Protected Areas of the Gulf of Venice', *Water. Air. Soil Pollut.*, vol. 232, no. 9, p. 379, Sep. 2021, doi: 10.1007/s11270-021-05323-9.

[34] F. Büks and M. Kaupenjohann, 'Global concentrations of microplastics in soils – a review', *SOIL*, vol. 6, no. 2, pp. 649–662, Dec. 2020, doi: 10.5194/soil-6-649-2020.
[35] J. C. Prata, J. P. da Costa, I. Lopes, A. C. Duarte, and T. Rocha-Santos, 'Effects of microplastics on microalgae populations: A critical review', *Sci. Total Environ.*, vol. 665, pp. 400–405, May 2019, doi: 10.1016/j.scitotenv.2019.02.132.
[36] Q. Li, Z. Feng, T. Zhang, C. Ma, and H. Shi, 'Microplastics in the commercial seaweed nori', *J. Hazard. Mater.*, vol. 388, p. 122060, Apr. 2020, doi: 10.1016/j.jhazmat.2020.122060.
[37] S. L. Wright and F. J. Kelly, 'Plastic and Human Health: A Micro Issue?', *Environ. Sci. Technol.*, vol. 51, no. 12, pp. 6634–6647, Jun. 2017, doi: 10.1021/acs.est.7b00423.
[38] M. Revel, A. Châtel, and C. Mouneyrac, 'Micro(nano)plastics: A threat to human health?', *Curr. Opin. Environ. Sci. Health*, vol. 1, pp. 17–23, Feb. 2018, doi: 10.1016/j.coesh.2017.10.003.
[39] G. E. De-la-Torre, 'Microplastics: an emerging threat to food security and human health', *J. Food Sci. Technol.*, vol. 57, no. 5, pp. 1601–1608, May 2020, doi: 10.1007/s13197-019-04138-1.
[40] L. Qiu *et al.*, 'Evidence of Microplastics in Bronchoalveolar Lavage Fluid among Never-Smokers: A Prospective Case Series', *Environ. Sci. Technol.*, vol. 57, no. 6, pp. 2435–2444, Feb. 2023, doi: 10.1021/acs.est.2c06880.
[41] W. Lu *et al.*, 'New Evidence of Microplastics in the Lower Respiratory Tract: Inhalation through Smoking', *Environ. Sci. Technol.*, vol. 57, no. 23, pp. 8496–8505, Jun. 2023, doi: 10.1021/acs.est.3c00716.
[42] I. Goßmann *et al.*, 'Occurrence and backtracking of microplastic mass loads including tire wear particles in northern Atlantic air', *Nat. Commun.*, vol. 14, no. 1, p. 3707, Jun. 2023, doi: 10.1038/s41467-023-39340-5.
[43] W. Fan, J. A. Salmond, K. N. Dirks, P. Cabedo Sanz, G. M. Miskelly, and J. D. Rindelaub, 'Evidence and Mass Quantification of Atmospheric Microplastics in a Coastal New Zealand City', *Environ. Sci. Technol.*, vol. 56, no. 24, pp. 17556–17568, Dec. 2022, doi: 10.1021/acs.est.2c05850.
[44] R. A. Romarate *et al.*, 'Breathing plastics in Metro Manila, Philippines: presence of suspended atmospheric microplastics in ambient air', *Environ. Sci. Pollut. Res.*, vol. 30, no. 18, pp. 53662–53673, Mar. 2023, doi: 10.1007/s11356-023-26117-y.
[45] S. Kacprzak and L. D. Tijing, 'Microplastics in indoor environment: Sources, mitigation and fate', *J. Environ. Chem. Eng.*, vol. 10, no. 2, p. 107359, Apr. 2022, doi: 10.1016/j.jece.2022.107359.
[46] L. Nizzetto, M. Futter, and S. Langaas, 'Are Agricultural Soils Dumps for Microplastics of Urban Origin?', *Environ. Sci. Technol.*, vol. 50, no. 20, pp. 10777–10779, Oct. 2016, doi: 10.1021/acs.est.6b04140.
[47] D. Nandan and Dr. P. Kumar, 'Plasticulture for Vegetable Production: A Review', *Int. J. Innov. Res. Eng. Manag.*, pp. 410–414, Feb. 2022, doi: 10.55524/ijirem.2022.9.1.86.
[48] 'The World of Plasticulture', pp. 1–21, Jan. 2017, doi: 10.1007/978-3-662-54130-2_1.
[49] C. Nnamdi and A. Hajihassani, 'Effect of Different Rates, Application Timing, and Combination of Nonfumigant Nematicides in Control of Meloidogyne incognita in Watermelon', *Plant Health Prog.*, vol. 24, no. 3, pp. 375–379, Jan. 2023, doi: 10.1094/PHP-01-23-0005-RS.
[50] C. A. Weber, 'Performance of Strawberry Varieties Developed for Perennial Matted-Row Production in Annual Plasticulture in a Cold Climate Region', *Agronomy*, vol. 11, no. 7, Art. no. 7, Jul. 2021, doi: 10.3390/agronomy11071407.

[51] C. A. Weber, 'Strawberry Crown Plugs Provide Flexibility and Improved Performance in Cold Climate Plasticulture Production', *Agronomy*, vol. 11, no. 8, Art. no. 8, Aug. 2021, doi: 10.3390/agronomy11081635.

[52] C. J. Land, G. E. Vallad, J. Desaeger, E. Van Santen, J. Noling, and K. Lawrence, 'Supplemental Fumigant Placement Improves Root Knot and Fusarium Wilt Management for Tomatoes Produced on a Raised-Bed Plasticulture System in Florida's Myakka Fine Sand', *Plant Dis.*, vol. 106, no. 1, pp. 73–78, Jan. 2022, doi: 10.1094/PDIS-03-21-0543-RE.

[53] 'Irrigation, Fertigation, and Plasticulture Increase Yield and Quality while Reducing Carcinogen Formation in Burley Tobacco'. Accessed: Apr. 30, 2024. [Online]. Available: https://doi.org/10.13031/2013.29953

[54] F. D. Gioia, E. Simonne, D. Jarry, and M. Dukes, 'Real-time Drip-irrigation Scheduling of Watermelon Grown with Plasticulture'.

[55] E. Simonne, B. Hochmuth, J. Simons, E. Vinson, and A. Caylor, 'Evaluation of New Okra Cultivars for Bare Ground and Plasticulture Production', *HortTechnology*, vol. 12, no. 3, pp. 470–476, Jan. 2002, doi: 10.21273/HORTTECH.12.3.470.

[56] FAO, *Assessment of agricultural plastics and their sustainability: A call for action*. FAO, 2021. doi: 10.4060/cb7856en.

[57] 'Plasticulture: economy of resources', no. 1252, pp. 121–130, Sep. 2019, doi: 10.17660/ACTAHORTIC.2019.1252.17.

[58] 'Agriculture • Plastics Europe', Plastics Europe. Accessed: Apr. 13, 2024. [Online]. Available: https://plasticseurope.org/sustainability/sustainable-use/sustainable-agriculture/

[59] D. Yang, S. Sun, J. Chen, and X. Liu, 'Analysis for the spatial and temporal patterns of plasticulture in Shandong province, China with remotely sensed data', in *2016 Fifth International Conference on Agro-Geoinformatics (Agro-Geoinformatics)*, Jul. 2016, pp. 1–4. doi: 10.1109/Agro-Geoinformatics.2016.7577663.

[60] D. Briassoulis, 'Agricultural plastics as a potential threat to food security, health, and environment through soil pollution by microplastics: Problem definition', *Sci. Total Environ.*, vol. 892, p. 164533, Sep. 2023, doi: 10.1016/j.scitotenv.2023.164533.

[61] H. Y. Sintim and M. Flury, 'Is Biodegradable Plastic Mulch the Solution to Agriculture's Plastic Problem?', *Environ. Sci. Technol.*, vol. 51, no. 3, pp. 1068–1069, Feb. 2017, doi: 10.1021/acs.est.6b06042.

[62] K. Jabran, 'Use of Mulches in Agriculture: Introduction and Concepts', in *Role of Mulching in Pest Management and Agricultural Sustainability*, K. Jabran, Ed., Cham: Springer International Publishing, 2019, pp. 1–14. doi: 10.1007/978-3-030-22301-4_1.

[63] R. R. Raju, P. M. D'souza, R. N. Aalam
, and S. C. Moses, 'Formulation and Utilization of Bio Degradable Mulch Films and A Design Considerations of Mulch Film Laying Machine – A Review', *Int. J. Curr. Microbiol. Appl. Sci.*, vol. 11, no. 11, pp. 187–199, Nov. 2022, doi: 10.20546/ijcmas.2022.1111.022.

[64] Z. Xu, R. Wallach, J. Song, and X. Mao, 'Effect of Plastic Film Colours and Perforations on Energy Distribution, Soil Temperature, and Evaporation', *Agronomy*, vol. 13, no. 3, Art. no. 3, Mar. 2023, doi: 10.3390/agronomy13030926.

[65] P. S. Jayswal, N. S. Joshi, Junagadh Agricultural University, K. N. Sondarva, and Navsari Agricultural University, 'EFFECT OF PLASTIC MULCH ON COTTON YIELD AND ITS ECONOMICS', *Gujarat J. Ext. Educ.*, vol. 2022, no. 1, pp. 170–172, Nov. 2022, doi: 10.56572/gjoee.2022.si.0033.

[66] J. Xu, Y. Wang, Y. Chen, W. He, X. Li, and J. Cui, 'Identifying the Influencing Factors of Plastic Film Mulching on Improving the Yield and Water Use Efficiency

of Potato in the Northwest China', *Water*, vol. 15, no. 12, Art. no. 12, Jan. 2023, doi: 10.3390/w15122279.

[67] M. Shi *et al.*, 'Effects of plastic film mulching and legume rotation on soil nutrients and microbial communities in the Loess Plateau of China', *Chem. Biol. Technol. Agric.*, vol. 10, no. 1, p. 38, May 2023, doi: 10.1186/s40538-023-00411-w.

[68] M. Samphire, D. R. Chadwick, and D. L. Jones, 'Biodegradable plastic mulch films increase yield and promote nitrogen use efficiency in organic horticulture', *Front. Agron.*, vol. 5, May 2023, doi: 10.3389/fagro.2023.1141608.

[69] C. Ashman *et al.*, 'Developing Miscanthus seed plug establishment protocols with mulch film for commercial upscaling', *GCB Bioenergy*, vol. 15, no. 6, pp. 746–764, 2023, doi: 10.1111/gcbb.13044.

[70] E. Standards, 'CSN EN 13655 - Plastics - Thermoplastic mulch films recoverable after use, for use in agriculture and horticulture', https://www.en-standard.eu. Accessed: Apr. 19, 2024. [Online]. Available: https://www.en-standard.eu/csn-en-13655-plastics-thermoplastic-mulch-films-recoverable-after-use-for-use-in-agriculture-and-horticulture/

[71] S. Hann *et al.*, 'Relevance of Conventional and Biodegradable Plastics in Agriculture', European Commission DG Environment, Jul. 2021. Accessed: May 15, 2024. [Online]. Available: https://environment.ec.europa.eu/system/files/2021-09/Agricultural%20Plastics%20Final%20Report.pdf

[72] M. B. Anunciado *et al.*, 'Effect of Environmental Weathering on Biodegradation of Biodegradable Plastic Mulch Films under Ambient Soil and Composting Conditions', *J. Polym. Environ.*, vol. 29, no. 9, pp. 2916–2931, Sep. 2021, doi: 10.1007/s10924-021-02088-4.

[73] Z. Mansoor *et al.*, 'Polymers Use as Mulch Films in Agriculture—A Review of History, Problems and Current Trends', *Polymers*, vol. 14, no. 23, Art. no. 23, Jan. 2022, doi: 10.3390/polym14235062.

[74] M. Velandia, S. Galinato, and A. Wszelaki, 'Economic Evaluation of Biodegradable Plastic Films in Tennessee Pumpkin Production', *Agronomy*, vol. 10, no. 1, Art. no. 1, Jan. 2020, doi: 10.3390/agronomy10010051.

[75] A. I. Marí, G. Pardo, A. Cirujeda, and Y. Martínez, 'Economic Evaluation of Biodegradable Plastic Films and Paper Mulches Used in Open-Air Grown Pepper (Capsicum annum L.) Crop', *Agronomy*, vol. 9, no. 1, Art. no. 1, Jan. 2019, doi: 10.3390/agronomy9010036.

[76] M. Menossi, M. Cisneros, V. A. Alvarez, and C. Casalongué, 'Current and emerging biodegradable mulch films based on polysaccharide bio-composites. A review', *Agron. Sustain. Dev.*, vol. 41, no. 4, p. 53, Jul. 2021, doi: 10.1007/s13593-021-00685-0.

[77] Y. Yang *et al.*, 'Kinetics of microplastic generation from different types of mulch films in agricultural soil', *Sci. Total Environ.*, vol. 814, p. 152572, Mar. 2022, doi: 10.1016/j.scitotenv.2021.152572.

[78] F. Ding *et al.*, 'Consequences of 33 Years of Plastic Film Mulching and Nitrogen Fertilization on Maize Growth and Soil Quality', *Environ. Sci. Technol.*, vol. 57, no. 25, pp. 9174–9183, Jun. 2023, doi: 10.1021/acs.est.2c08878.

[79] C. Monkley, M. Reay, R. Evershed, and C. Lloyd, 'Characterising the Chemical Additive Content of Agricultural Plastic Mulch Film', Copernicus Meetings, EGU23-9039, Feb. 2023. doi: 10.5194/egusphere-egu23-9039.

[80] C. Scopetani, S. Selonen, A. Cincinelli, and J. Pellinen, 'Chemical leaching from polyethylene mulching films to soil in strawberry farming', *Front. Environ. Sci.*, vol. 11, Feb. 2023, doi: 10.3389/fenvs.2023.1129336.

[81] S. Lambert and M. Wagner, 'Environmental performance of bio-based and biodegradable plastics: the road ahead', *Chem. Soc. Rev.*, vol. 46, no. 22, pp. 6855–6871, 2017, doi: 10.1039/C7CS00149E.

[82] M. Qin *et al.*, 'A review of biodegradable plastics to biodegradable microplastics: Another ecological threat to soil environments?', *J. Clean. Prod.*, vol. 312, p. 127816, Aug. 2021, doi: 10.1016/j.jclepro.2021.127816.

[83] V. C. Shruti and G. Kutralam-Muniasamy, 'Bioplastics: Missing link in the era of Microplastics', *Sci. Total Environ.*, vol. 697, p. 134139, Dec. 2019, doi: 10.1016/j.scitotenv.2019.134139.

[84] N. R. Maddela, B. Ramakrishnan, T. Kadiyala, K. Venkateswarlu, and M. Megharaj, 'Do Microplastics and Nanoplastics Pose Risks to Biota in Agricultural Ecosystems?', *Soil Syst.*, vol. 7, no. 1, Art. no. 1, Mar. 2023, doi: 10.3390/soilsystems7010019.

[85] W. Shi, N. Wu, Z. Zhang, Y. Liu, J. Chen, and J. Li, 'A global review on the abundance and threats of microplastics in soils to terrestrial ecosystem and human health', *Sci. Total Environ.*, vol. 912, p. 169469, Feb. 2024, doi: 10.1016/j.scitotenv.2023.169469.

[86] G. S. Zhang and Y. F. Liu, 'The distribution of microplastics in soil aggregate fractions in southwestern China', *Sci. Total Environ.*, vol. 642, pp. 12–20, Nov. 2018, doi: 10.1016/j.scitotenv.2018.06.004.

[87] S. Zhang, A. Bao, X. Lin, G. Jia, and Q. Zhang, 'Microplastic Accumulation in Agricultural Soils with Different Mulching Histories in Xinjiang, China', *Sustainability*, vol. 15, no. 6, Art. no. 6, Jan. 2023, doi: 10.3390/su15065438.

[88] F. Radford, A. Horton, M. Hudson, P. Shaw, and I. Williams, 'Agricultural soils and microplastics: Are biosolids the problem?', *Front. Soil Sci.*, vol. 2, Jan. 2023, doi: 10.3389/fsoil.2022.941837.

[89] S. Y. Park and C. G. Kim, 'A comparative study on the distribution behavior of microplastics through FT-IR analysis on different land uses in agricultural soils', *Environ. Res.*, vol. 215, p. 114404, Dec. 2022, doi: 10.1016/j.envres.2022.114404.

[90] I. A. Leitão, L. van Schaik, A. J. D. Ferreira, N. Alexandre, and V. Geissen, 'The spatial distribution of microplastics in topsoils of an urban environment - Coimbra city case-study', *Environ. Res.*, vol. 218, p. 114961, Feb. 2023, doi: 10.1016/j.envres.2022.114961.

[91] J. Crossman, R. R. Hurley, M. Futter, and L. Nizzetto, 'Transfer and transport of microplastics from biosolids to agricultural soils and the wider environment', *Sci. Total Environ.*, vol. 724, p. 138334, Jul. 2020, doi: 10.1016/j.scitotenv.2020.138334.

[92] B. Thakur, J. Singh, J. Singh, D. Angmo, and A. P. Vig, 'Identification and characterization of extracted microplastics from agricultural soil near industrial area: FTIR and X-ray diffraction method', *Environ. Qual. Manag.*, vol. 33, no. 1, pp. 173–181, 2023, doi: 10.1002/tqem.22035.

[93] C. J. Weber, J.-E. Bastijans, and C. Heller, 'Spatial and temporal variance of microplastics in agricultural soils', Copernicus Meetings, EGU23-77, Feb. 2023. doi: 10.5194/egusphere-egu23-77.

[94] C. J. Weber, A. Santowski, and P. Chifflard, 'Investigating the dispersal of macro- and microplastics on agricultural fields 30 years after sewage sludge application', *Sci. Rep.*, vol. 12, no. 1, p. 6401, Apr. 2022, doi: 10.1038/s41598-022-10294-w.

[95] L. Chen *et al.*, 'Spatial Distributions, Compositional Profiles, Potential Sources, and Intfluencing Factors of Microplastics in Soils from Different Agricultural Farmlands in China: A National Perspective', *Environ. Sci. Technol.*, vol. 56, no. 23, pp. 16964–16974, Dec. 2022, doi: 10.1021/acs.est.2c07621.

[96] E. A. Isari, D. Papaioannou, I. K. Kalavrouziotis, and H. K. Karapanagioti, 'Microplastics in Agricultural Soils: A Case Study in Cultivation of Watermelons and

Canning Tomatoes', *Water*, vol. 13, no. 16, Art. no. 16, Jan. 2021, doi: 10.3390/w13162168.

[97] M. Rezaei, S. Abbasi, H. Pourmahmood, P. Oleszczuk, C. Ritsema, and A. Turner, 'Microplastics in agricultural soils from a semi-arid region and their transport by wind erosion', *Environ. Res.*, vol. 212, p. 113213, Sep. 2022, doi: 10.1016/j.envres.2022.113213.

[98] Md. N. Hossain, Md. M. Rahman, S. Afrin, Md. A. Akbor, Md. A. B. Siddique, and G. Malafaia, 'Identification and quantification of microplastics in agricultural farmland soil and textile sludge in Bangladesh', *Sci. Total Environ.*, vol. 858, p. 160118, Feb. 2023, doi: 10.1016/j.scitotenv.2022.160118.

[99] D. Bi *et al.*, 'Occurrence and distribution of microplastics in coastal plain soils under three land-use types', *Sci. Total Environ.*, vol. 855, p. 159023, Jan. 2023, doi: 10.1016/j.scitotenv.2022.159023.

[100] S. Piehl, A. Leibner, M. G. J. Löder, R. Dris, C. Bogner, and C. Laforsch, 'Identification and quantification of macro- and microplastics on an agricultural farmland', *Sci. Rep.*, vol. 8, no. 1, p. 17950, Dec. 2018, doi: 10.1038/s41598-018-36172-y.

[101] H. Fakour *et al.*, 'Quantification and Analysis of Microplastics in Farmland Soils: Characterization, Sources, and Pathways', *Agriculture*, vol. 11, no. 4, Art. no. 4, Apr. 2021, doi: 10.3390/agriculture11040330.

[102] B. van Schothorst, N. Beriot, E. Huerta Lwanga, and V. Geissen, 'Sources of Light Density Microplastic Related to Two Agricultural Practices: The Use of Compost and Plastic Mulch', *Environments*, vol. 8, no. 4, Art. no. 4, Apr. 2021, doi: 10.3390/environments8040036.

[103] Z. Xu *et al.*, 'Distribution characteristics of plastic film residue in long-term mulched farmland soil', *Soil Ecol. Lett.*, vol. 5, no. 3, p. 220144, Dec. 2022, doi: 10.1007/s42832-022-0144-4.

[104] K. Chouchene, T. Nacci, F. Modugno, V. Castelvetro, and M. Ksibi, 'Soil contamination by microplastics in relation to local agricultural development as revealed by FTIR, ICP-MS and pyrolysis-GC/MS', *Environ. Pollut.*, vol. 303, p. 119016, Jun. 2022, doi: 10.1016/j.envpol.2022.119016.

[105] F. Corradini, F. Casado, V. Leiva, E. Huerta-Lwanga, and V. Geissen, 'Microplastics occurrence and frequency in soils under different land uses on a regional scale', *Sci. Total Environ.*, vol. 752, p. 141917, Jan. 2021, doi: 10.1016/j.scitotenv.2020.141917.

[106] Y. R. Choi, Y.-N. Kim, J.-H. Yoon, N. Dickinson, and K.-H. Kim, 'Plastic contamination of forest, urban, and agricultural soils: a case study of Yeoju City in the Republic of Korea', *J. Soils Sediments*, vol. 21, no. 5, pp. 1962–1973, May 2021, doi: 10.1007/s11368-020-02759-0.

[107] Y. Huang, Q. Liu, W. Jia, C. Yan, and J. Wang, 'Agricultural plastic mulching as a source of microplastics in the terrestrial environment', *Environ. Pollut.*, vol. 260, p. 114096, May 2020, doi: 10.1016/j.envpol.2020.114096.

[108] A. Hooge *et al.*, 'Fate of microplastics in sewage sludge and in agricultural soils', *TrAC Trends Anal. Chem.*, vol. 166, p. 117184, Sep. 2023, doi: 10.1016/j.trac.2023.117184.

[109] P. van den Berg, E. Huerta-Lwanga, F. Corradini, and V. Geissen, 'Sewage sludge application as a vehicle for microplastics in eastern Spanish agricultural soils', *Environ. Pollut.*, vol. 261, p. 114198, Jun. 2020, doi: 10.1016/j.envpol.2020.114198.

[110] R.-T. Wu, Y.-F. Cai, Y.-X. Chen, Y.-W. Yang, S.-C. Xing, and X.-D. Liao, 'Occurrence of microplastic in livestock and poultry manure in South China', *Environ. Pollut.*, vol. 277, p. 116790, May 2021, doi: 10.1016/j.envpol.2021.116790.

[111] K. Adhikari *et al.*, 'Accumulation of microplastics in soil after long-term application of biosolids and atmospheric deposition', *Sci. Total Environ.*, vol. 912, p. 168883, Feb. 2024, doi: 10.1016/j.scitotenv.2023.168883.
[112] P. U. Iyare, S. K. Ouki, and T. Bond, 'Microplastics removal in wastewater treatment plants: a critical review', *Environ. Sci. Water Res. Technol.*, vol. 6, no. 10, pp. 2664–2675, 2020, doi: 10.1039/D0EW00397B.
[113] H. Zhang *et al.*, 'Occurrence of Microplastics from Plastic Fragments in Cultivated Soil of Sichuan Province: The Key Controls', *Water*, vol. 14, no. 9, Art. no. 9, Jan. 2022, doi: 10.3390/w14091417.
[114] J. A. Conesa and N. Ortuño, 'Reuse of Water Contaminated by Microplastics, the Effectiveness of Filtration Processes: A Review', *Energies*, vol. 15, no. 7, Art. no. 7, Jan. 2022, doi: 10.3390/en15072432.
[115] J. Worek, X. Badura, A. Białas, J. Chwiej, K. Kawoń, and K. Styszko, 'Pollution from Transport: Detection of Tyre Particles in Environmental Samples', *Energies*, vol. 15, no. 8, Art. no. 8, Jan. 2022, doi: 10.3390/en15082816.
[116] 'Recent Advances on Multilevel Effects of Micro(Nano)Plastics and Coexisting Pollutants on Terrestrial Soil-Plants System', *Sustainability*, vol. 15, no. 5, pp. 4504–4504, Mar. 2023, doi: 10.3390/su15054504.
[117] 'How Do Microplastics Affect Physical Properties of Silt Loam Soil under Wetting–Drying Cycles?', *Agronomy*, vol. 13, no. 3, pp. 844–844, Mar. 2023, doi: 10.3390/agronomy13030844.
[118] A. A. de Souza Machado *et al.*, 'Impacts of Microplastics on the Soil Biophysical Environment', *Environ. Sci. Technol.*, vol. 52, no. 17, pp. 9656–9665, Sep. 2018, doi: 10.1021/acs.est.8b02212.
[119] 'Microplastics reduce soil microbial network complexity and ecological deterministic selection.', *Environ. Microbiol.*, vol. 24, no. 4, pp. 2157–2169, Mar. 2022, doi: 10.1111/1462-2920.15955.
[120] 'Microplastic fibers affect dynamics and intensity of CO2 and N2O fluxes from soil differently', *Microplastics Nanoplastics*, vol. 1, no. 1, pp. 1–11, Dec. 2021, doi: 10.1186/S43591-021-00004-0.
[121] 'Polyester microplastic fibers affect soil physical properties and erosion as a function of soil type', *Soil*, vol. 8, no. 1, pp. 421–435, Jun. 2022, doi: 10.5194/soil-8-421-2022.
[122] H. Mai, N. D. Thien, N. T. Dung, and C. Valentin, 'Impacts of microplastics and heavy metals on the earthworm Eisenia foetida and on soil organic carbon, nitrogen and phosphorus'. Sep. 29, 2022. doi: 10.21203/rs.3.rs-2054147/v1.
[123] H. Zang, J. Zhou, M. R. Marshall, D. R. Chadwick, Y. Wen, and D. L. Jones, 'Microplastics in the agroecosystem: Are they an emerging threat to the plant-soil system?', *Soil Biol. Biochem.*, vol. 148, p. 107926, Sep. 2020, doi: 10.1016/j.soilbio.2020.107926.
[124] Y. Yu *et al.*, 'Minimal Impacts of Microplastics on Soil Physical Properties under Environmentally Relevant Concentrations', *Environ. Sci. Technol.*, vol. 57, no. 13, pp. 5296–5304, Apr. 2023, doi: 10.1021/acs.est.2c09822.
[125] Z. Wang, W. Li, W. Li, W. Yang, and S. Jing, 'Effects of microplastics on the water characteristic curve of soils with different textures', *Chemosphere*, vol. 317, p. 137762, Mar. 2023, doi: 10.1016/j.chemosphere.2023.137762.
[126] E. Daghighi, T. Shah, R. Chia, J.-Y. Lee, J. Shang, and A. Rodríguez-Seijo, 'The forgotten impacts of plastic contamination on terrestrial micro- and mesofauna: A call for research', *Environ. Res.*, vol. 231, p. 116227, Aug. 2023, doi: 10.1016/j.envres.2023.116227.

[127] M. Liu, J. Feng, Y. Shen, and B. Zhu, 'Microplastics effects on soil biota are dependent on their properties: A meta-analysis', *Soil Biol. Biochem.*, vol. 178, p. 108940, Mar. 2023, doi: 10.1016/j.soilbio.2023.108940.

[128] B. Boots, 'Implication of microplastics on soil faunal communities — identifying gaps of knowledge', *Emerg. Top. Life Sci.*, vol. 6, no. 4, pp. 403–409, Sep. 2022, doi: 10.1042/ETLS20220023.

[129] L. Wan, H. Cheng, Y. Liu, Y. Shen, G. Liu, and X. Su, 'Global meta-analysis reveals differential effects of microplastics on soil ecosystem', *Sci. Total Environ.*, vol. 867, p. 161403, Apr. 2023, doi: 10.1016/j.scitotenv.2023.161403.

[130] A. Jemec Kokalj *et al.*, 'Effects of microplastics from disposable medical masks on terrestrial invertebrates', *J. Hazard. Mater.*, vol. 438, p. 129440, Sep. 2022, doi: 10.1016/j.jhazmat.2022.129440.

[131] J. Shen, B. Liang, and H. Jin, 'The impact of microplastics on insect physiology and the indication of hormesis', *TrAC Trends Anal. Chem.*, vol. 165, p. 117130, Aug. 2023, doi: 10.1016/j.trac.2023.117130.

[132] S. Guo *et al.*, 'Ecological risk of microplastic toxicity to earthworms in soil: A bibliometric analysis', *Front. Environ. Sci.*, vol. 11, Jan. 2023, doi: 10.3389/fenvs.2023.1126847.

[133] Z. Sobhani, L. Panneerselvan, C. Fang, R. Naidu, and M. Megharaj, 'Chronic and transgenerational effects of polyethylene microplastics at environmentally relevant concentrations in earthworms', *Environ. Technol. Innov.*, vol. 25, p. 102226, Feb. 2022, doi: 10.1016/j.eti.2021.102226.

[134] Q. Shang, M. Tan, and J. Chi, 'Effect of Microplastics on Gut Bacterial Community of the Earthworm Pheretima guillelmi', presented at the The International Conference on Biomedical Engineering and Bioinformatics, May 2024, pp. 260–264. Accessed: May 02, 2024. [Online]. Available: https://www.scitepress.org/Link.aspx?doi=10.5220/0011199300003443

[135] K. Adhikari *et al.*, 'Earthworms Exposed to Polyethylene and Biodegradable Microplastics in Soil: Microplastic Characterization and Microbial Community Analysis', *ACS Agric. Sci. Technol.*, vol. 3, no. 4, pp. 340–349, Apr. 2023, doi: 10.1021/acsagscitech.2c00333.

[136] S. Barili *et al.*, 'Long term influences of PVC microplastics on soil chemical and microbiological parameters', Copernicus Meetings, EGU23-15971, Feb. 2023. doi: 10.5194/egusphere-egu23-15971.

[137] S. Kublik, S. Gschwendtner, T. Magritsch, V. Radl, M. C. Rillig, and M. Schloter, 'Microplastics in soil induce a new microbial habitat, with consequences for bulk soil microbiomes', *Front. Environ. Sci.*, vol. 10, Aug. 2022, doi: 10.3389/fenvs.2022.989267.

[138] O. D. Agboola and N. U. Benson, 'Physisorption and Chemisorption Mechanisms Influencing Micro (Nano) Plastics-Organic Chemical Contaminants Interactions: A Review', *Front. Environ. Sci.*, vol. 9, p. 678574, May 2021, doi: 10.3389/fenvs.2021.678574.

[139] A. Turner and L. A. Holmes, 'Adsorption of trace metals by microplastic pellets in fresh water', *Environ. Chem.*, vol. 12, no. 5, pp. 600–610, Apr. 2015, doi: 10.1071/EN14143.

[140] J. Li, K. Zhang, and H. Zhang, 'Adsorption of antibiotics on microplastics', *Environ. Pollut.*, vol. 237, pp. 460–467, Jun. 2018, doi: 10.1016/j.envpol.2018.02.050.

[141] N. N. Phuong, A. Zalouk-Vergnoux, T. T. Duong, T. P. Q. Le, and L. Poirier, 'Sorption of alkylphenols and estrogens on microplastics in marine conditions', *Open Chem.*, vol. 21, no. 1, Jan. 2023, doi: 10.1515/chem-2022-0315.

[142] M. Yang, D. Zhang, and W. Chu, 'Adsorption of highly toxic chlorophenylacetonitriles on typical microplastics in aqueous solutions: Kinetics, isotherm, impact factors and mechanism', *Sci. Total Environ.*, vol. 880, p. 163261, Jul. 2023, doi: 10.1016/j.scitotenv.2023.163261.

[143] X. Kong *et al.*, 'Insights into adsorption mechanisms of nitro polycyclic aromatic hydrocarbons on common microplastic particles: Experimental studies and modeling', *Chemosphere*, vol. 320, p. 138050, Apr. 2023, doi: 10.1016/j.chemosphere.2023.138050.

[144] C. Lim, N. Kim, J. Lee, and Y. Yoon, 'Potential of Adsorption of Diverse Environmental Contaminants onto Microplastics', *Water*, vol. 14, no. 24, Art. no. 24, Jan. 2022, doi: 10.3390/w14244086.

[145] M. Llorca, G. Schirinzi, M. Martínez, D. Barceló, and M. Farré, 'Adsorption of perfluoroalkyl substances on microplastics under environmental conditions', *Environ. Pollut.*, vol. 235, pp. 680–691, Apr. 2018, doi: 10.1016/j.envpol.2017.12.075.

[146] K. Y. Yap and M. C. Tan, 'Oil adsorption onto different types of microplastic in synthetic seawater', *Environ. Technol. Innov.*, vol. 24, p. 101994, Nov. 2021, doi: 10.1016/j.eti.2021.101994.

[147] Q. Liu *et al.*, 'Adsorption mechanism of trace heavy metals on microplastics and simulating their effect on microalgae in river', *Environ. Res.*, vol. 214, p. 113777, Nov. 2022, doi: 10.1016/j.envres.2022.113777.

[148] J. Lu, J. Wu, J. Wu, C. Zhang, and Y. Luo, 'Adsorption and Desorption of Steroid Hormones by Microplastics in Seawater', *Bull. Environ. Contam. Toxicol.*, vol. 107, no. 4, pp. 730–735, Oct. 2021, doi: 10.1007/s00128-020-02784-2.

[149] Y. Zhang *et al.*, 'Mechanistic insight into different adsorption of norfloxacin on microplastics in simulated natural water and real surface water', *Environ. Pollut.*, vol. 284, p. 117537, Sep. 2021, doi: 10.1016/j.envpol.2021.117537.

[150] A. Tubić *et al.*, 'Adsorption mechanisms of chlorobenzenes and trifluralin on primary polyethylene microplastics in the aquatic environment', *Environ. Sci. Pollut. Res.*, vol. 28, no. 42, pp. 59416–59429, Nov. 2021, doi: 10.1007/s11356-020-11875-w.

[151] H. Wang, W. Huang, Y. Zhang, C. Wang, and H. Jiang, 'Unique metalloid uptake on microplastics: The interaction between boron and microplastics in aquatic environment', *Sci. Total Environ.*, vol. 800, p. 149668, Dec. 2021, doi: 10.1016/j.scitotenv.2021.149668.

[152] P. D. Dissanayake *et al.*, 'Effects of microplastics on the terrestrial environment: A critical review', *Environ. Res.*, vol. 209, p. 112734, Jun. 2022, doi: 10.1016/j.envres.2022.112734.

[153] Z. Li, L. Sun, and H. Wang, 'Adsorption behaviour and mechanism of polycyclic aromatic hydrocarbons onto typical microplastics in a soil solution', *Int. J. Environ. Anal. Chem.*, pp. 1–16, doi: 10.1080/03067319.2022.2128791.

[154] X. Chen, X. Gu, L. Bao, S. Ma, and Y. Mu, 'Comparison of adsorption and desorption of triclosan between microplastics and soil particles', *Chemosphere*, vol. 263, p. 127947, Jan. 2021, doi: 10.1016/j.chemosphere.2020.127947.

[155] B. Hu *et al.*, 'Influence of microplastics occurrence on the adsorption of 17β-estradiol in soil', *J. Hazard. Mater.*, vol. 400, p. 123325, Dec. 2020, doi: 10.1016/j.jhazmat.2020.123325.

[156] N. Khalid, M. Aqeel, A. Noman, S. M. Khan, and N. Akhter, 'Interactions and effects of microplastics with heavy metals in aquatic and terrestrial environments', *Environ. Pollut.*, vol. 290, p. 118104, Dec. 2021, doi: 10.1016/j.envpol.2021.118104.

[157] F. Wang, X. Zhang, S. Zhang, S. Zhang, C. A. Adams, and Y. Sun, 'Effects of Co-Contamination of Microplastics and Cd on Plant Growth and Cd Accumulation', *Toxics*, vol. 8, no. 2, Art. no. 2, Jun. 2020, doi: 10.3390/toxics8020036.

[158] Y. Dong, Q. Bao, M. Gao, W. Qiu, and Z. Song, 'A novel mechanism study of microplastic and As co-contamination on indica rice (Oryza sativa L.)', *J. Hazard. Mater.*, vol. 421, p. 126694, Jan. 2022, doi: 10.1016/j.jhazmat.2021.126694.

[159] X. Feng, Q. Wang, Y. Sun, S. Zhang, and F. Wang, 'Microplastics change soil properties, heavy metal availability and bacterial community in a Pb-Zn-contaminated soil', *J. Hazard. Mater.*, vol. 424, p. 127364, Feb. 2022, doi: 10.1016/j.jhazmat.2021.127364.

[160] S. Nethaji, A. Sivasamy, and A. B. Mandal, 'Adsorption isotherms, kinetics and mechanism for the adsorption of cationic and anionic dyes onto carbonaceous particles prepared from Juglans regia shell biomass', *Int. J. Environ. Sci. Technol.*, vol. 10, no. 2, pp. 231–242, Mar. 2013, doi: 10.1007/s13762-012-0112-0.

[161] W. Stroberg and S. Schnell, 'On the validity and errors of the pseudo-first-order kinetics in ligand–receptor binding', *Math. Biosci.*, vol. 287, pp. 3–11, May 2017, doi: 10.1016/j.mbs.2016.09.010.

[162] A. R. Conrad, H. A. Hassanin, M. J. Tubergen, I. Fábián, and N. E. Brasch, 'The effects of ligand decomposition on the pseudo first-order profile of a ligand substitution reaction: a "silent killer" in the background', *New J. Chem.*, vol. 36, no. 6, p. 1408, 2012, doi: 10.1039/c2nj40055c.

[163] A. N. Ebelegi, N. Ayawei, and D. Wankasi, 'Interpretation of Adsorption Thermodynamics and Kinetics', *Open J. Phys. Chem.*, vol. 10, no. 3, Art. no. 3, Aug. 2020, doi: 10.4236/ojpc.2020.103010.

[164] L. Largitte and R. Pasquier, 'A review of the kinetics adsorption models and their application to the adsorption of lead by an activated carbon', *Chem. Eng. Res. Des.*, vol. 109, pp. 495–504, May 2016, doi: 10.1016/j.cherd.2016.02.006.

[165] X. Guo, Y. Liu, and J. Wang, 'Sorption of sulfamethazine onto different types of microplastics: A combined experimental and molecular dynamics simulation study', *Mar. Pollut. Bull.*, vol. 145, pp. 547–554, Aug. 2019, doi: 10.1016/j.marpolbul.2019.06.063.

[166] M. Musah, Y. Azeh, J. Mathew, M. Umar, Z. Abdulhamid, and A. Muhammad, 'Adsorption Kinetics and Isotherm Models: A Review', *Caliphate J. Sci. Technol.*, vol. 4, no. 1, pp. 20–26, Feb. 2022, doi: 10.4314/cajost.v4i1.3.

[167] J. Debord, K. H. Chu, M. Harel, S. Salvestrini, and J.-C. Bollinger, 'Yesterday, Today, and Tomorrow. Evolution of a Sleeping Beauty: The Freundlich Isotherm', *Langmuir*, vol. 39, no. 8, pp. 3062–3071, Feb. 2023, doi: 10.1021/acs.langmuir.2c03105.

[168] C.-C. Qiu, G.-X. Li, Q.-S. Li, and C.-Z. Yan, 'Effects of Polystyrene Nanoplastics (PS-NPs) on the Physiology of Allium sativum L', *Huan Jing Ke Xue Huanjing Kexue*, vol. 43, no. 8, pp. 4387–4393, Aug. 2022, doi: 10.13227/j.hjkx.202110021.

[169] M. Kaur, M. Xu, and L. Wang, 'Cyto–Genotoxic Effect Causing Potential of Polystyrene Micro-Plastics in Terrestrial Plants', *Nanomaterials*, vol. 12, no. 12, p. 2024, Jun. 2022, doi: 10.3390/nano12122024.

[170] M. A. Urbina, F. Correa, F. Aburto, and J. P. Ferrio, 'Adsorption of polyethylene microbeads and physiological effects on hydroponic maize', *Sci. Total Environ.*, vol. 741, p. 140216, Nov. 2020, doi: 10.1016/j.scitotenv.2020.140216.

[171] J. Lian *et al.*, 'Impact of polystyrene nanoplastics (PSNPs) on seed germination and seedling growth of wheat (*Triticum aestivum* L.)', *J. Hazard. Mater.*, vol. 385, p. 121620, Mar. 2020, doi: 10.1016/j.jhazmat.2019.121620.

[172] J. Lian *et al.*, 'Foliar-applied polystyrene nanoplastics (PSNPs) reduce the growth and nutritional quality of lettuce (Lactuca sativa L.)', *Environ. Pollut.*, vol. 280, p. 116978, Jul. 2021, doi: 10.1016/j.envpol.2021.116978.

[173] T. Bosker, L. J. Bouwman, N. R. Brun, P. Behrens, and M. G. Vijver, 'Microplastics accumulate on pores in seed capsule and delay germination and root growth of the terrestrial vascular plant Lepidium sativum', *Chemosphere*, vol. 226, pp. 774–781, Jul. 2019, doi: 10.1016/j.chemosphere.2019.03.163.

[174] S. Pignattelli, A. Broccoli, and M. Renzi, 'Physiological responses of garden cress (*L. sativum*) to different types of microplastics', *Sci. Total Environ.*, vol. 727, p. 138609, Jul. 2020, doi: 10.1016/j.scitotenv.2020.138609.

[175] I. Colzi *et al.*, 'Impact of microplastics on growth, photosynthesis and essential elements in *Cucurbita pepo* L.', *J. Hazard. Mater.*, vol. 423, p. 127238, Feb. 2022, doi: 10.1016/j.jhazmat.2021.127238.

[176] X. Jiang, H. Chen, Y. Liao, Z. Ye, M. Li, and G. Klobučar, 'Ecotoxicity and genotoxicity of polystyrene microplastics on higher plant Vicia faba', *Environ. Pollut.*, vol. 250, pp. 831–838, Jul. 2019, doi: 10.1016/j.envpol.2019.04.055.

[177] Z. Li, Q. Li, R. Li, Y. Zhao, J. Geng, and G. Wang, 'Physiological responses of lettuce (Lactuca sativa L.) to microplastic pollution', *Environ. Sci. Pollut. Res.*, vol. 27, no. 24, pp. 30306–30314, Aug. 2020, doi: 10.1007/s11356-020-09349-0.

[178] A. Lehmann, E. F. Leifheit, L. Feng, J. Bergmann, A. Wulf, and M. C. Rillig, 'Microplastic fiber and drought effects on plants and soil are only slightly modified by arbuscular mycorrhizal fungi', *Soil Ecol. Lett.*, vol. 4, no. 1, pp. 32–44, Mar. 2022, doi: 10.1007/s42832-020-0060-4.

[179] Y. Qi *et al.*, 'Macro- and micro- plastics in soil-plant system: Effects of plastic mulch film residues on wheat (Triticum aestivum) growth', *Sci. Total Environ.*, vol. 645, pp. 1048–1056, Dec. 2018, doi: 10.1016/j.scitotenv.2018.07.229.

[180] X. Wu *et al.*, 'Metabolomics revealing the response of rice (Oryza sativa L.) exposed to polystyrene microplastics', *Environ. Pollut.*, vol. 266, p. 115159, Nov. 2020, doi: 10.1016/j.envpol.2020.115159.

[181] C.-Q. Zhou, C.-H. Lu, L. Mai, L.-J. Bao, L.-Y. Liu, and E. Y. Zeng, 'Response of rice (Oryza sativa L.) roots to nanoplastic treatment at seedling stage', *J. Hazard. Mater.*, vol. 401, p. 123412, Jan. 2021, doi: 10.1016/j.jhazmat.2020.123412.

[182] B. Li *et al.*, 'Effects of plastic particles on germination and growth of soybean (*Glycine max*): A pot experiment under field condition', *Environ. Pollut.*, vol. 272, p. 116418, Mar. 2021, doi: 10.1016/j.envpol.2020.116418.

[183] L. Wang, Y. Liu, M. Kaur, Z. Yao, T. Chen, and M. Xu, 'Phytotoxic Effects of Polyethylene Microplastics on the Growth of Food Crops Soybean (Glycine max) and Mung Bean (Vigna radiata)', *Int. J. Environ. Res. Public. Health*, vol. 18, no. 20, Art. no. 20, Jan. 2021, doi: 10.3390/ijerph182010629.

[184] Z. Li, Q. Li, R. Li, J. Zhou, and G. Wang, 'The distribution and impact of polystyrene nanoplastics on cucumber plants', *Environ. Sci. Pollut. Res.*, vol. 28, no. 13, pp. 16042–16053, Apr. 2021, doi: 10.1007/s11356-020-11702-2.

[185] Z. Li, R. Li, Q. Li, J. Zhou, and G. Wang, 'Physiological response of cucumber (Cucumis sativus L.) leaves to polystyrene nanoplastics pollution', *Chemosphere*, vol. 255, p. 127041, Sep. 2020, doi: 10.1016/j.chemosphere.2020.127041.

[186] J. Lian *et al.*, 'Do polystyrene nanoplastics affect the toxicity of cadmium to wheat (Triticum aestivum L.)?', *Environ. Pollut.*, vol. 263, p. 114498, Aug. 2020, doi: 10.1016/j.envpol.2020.114498.

[187] A. A. de Souza Machado *et al.*, 'Microplastics Can Change Soil Properties and Affect Plant Performance', *Environ. Sci. Technol.*, vol. 53, no. 10, pp. 6044–6052, May 2019, doi: 10.1021/acs.est.9b01339.

[188] F. Meng, X. Yang, M. Riksen, M. Xu, and V. Geissen, 'Response of common bean (*Phaseolus vulgaris L.*) growth to soil contaminated with microplastics', *Sci. Total Environ.*, vol. 755, p. 142516, Feb. 2021, doi: 10.1016/j.scitotenv.2020.142516.

[189] X. Ren, J. Tang, L. Wang, and Q. Liu, 'Microplastics in soil-plant system: effects of nano/microplastics on plant photosynthesis, rhizosphere microbes and soil properties in soil with different residues', *Plant Soil*, vol. 462, no. 1, pp. 561–576, May 2021, doi: 10.1007/s11104-021-04869-1.

[190] R. Shi, W. Liu, Y. Lian, Q. Wang, A. Zeb, and J. Tang, 'Phytotoxicity of polystyrene, polyethylene and polypropylene microplastics on tomato (*Lycopersicon esculentum* L.)', *J. Environ. Manage.*, vol. 317, p. 115441, Sep. 2022, doi: 10.1016/j.jenvman.2022.115441.

[191] C. Yang and X. Gao, 'Impact of microplastics from polyethylene and biodegradable mulch films on rice (Oryza sativa L.)', *Sci. Total Environ.*, vol. 828, p. 154579, Jul. 2022, doi: 10.1016/j.scitotenv.2022.154579.

[192] X.-D. Sun *et al.*, 'Differentially charged nanoplastics demonstrate distinct accumulation in Arabidopsis thaliana', *Nat. Nanotechnol.*, vol. 15, no. 9, Art. no. 9, Sep. 2020, doi: 10.1038/s41565-020-0707-4.

[193] Y. Yue *et al.*, 'Recent Advances on Multilevel Effects of Micro(Nano)Plastics and Coexisting Pollutants on Terrestrial Soil-Plants System', *Sustainability*, vol. 15, no. 5, Art. no. 5, Jan. 2023, doi: 10.3390/su15054504.

[194] L. Li *et al.*, 'Effective uptake of submicrometre plastics by crop plants via a crack-entry mode', *Nat. Sustain.*, vol. 3, no. 11, pp. 929–937, Nov. 2020, doi: 10.1038/s41893-020-0567-9.

[195] D. Kim *et al.*, 'Translocation and chronic effects of microplastics on pea plants (Pisum sativum) in copper-contaminated soil', *J. Hazard. Mater.*, vol. 436, p. 129194, Aug. 2022, doi: 10.1016/j.jhazmat.2022.129194.

[196] Y. Luo *et al.*, 'Quantitative tracing of uptake and transport of submicrometre plastics in crop plants using lanthanide chelates as a dual-functional tracer', *Nat. Nanotechnol.*, vol. 17, no. 4, Art. no. 4, Apr. 2022, doi: 10.1038/s41565-021-01063-3.

[197] W. Gong *et al.*, 'Species-dependent response of food crops to polystyrene nanoplastics and microplastics', *Sci. Total Environ.*, vol. 796, p. 148750, Nov. 2021, doi: 10.1016/j.scitotenv.2021.148750.

[198] A. Avellan *et al.*, 'Nanoparticle Uptake in Plants: Gold Nanomaterial Localized in Roots of Arabidopsis thaliana by X-ray Computed Nanotomography and Hyperspectral Imaging', *Environ. Sci. Technol.*, vol. 51, no. 15, pp. 8682–8691, Aug. 2017, doi: 10.1021/acs.est.7b01133.

[199] Y. Liu, R. Guo, S. Zhang, Y. Sun, and F. Wang, 'Uptake and translocation of nano/microplastics by rice seedlings: Evidence from a hydroponic experiment', *J. Hazard. Mater.*, vol. 421, p. 126700, Jan. 2022, doi: 10.1016/j.jhazmat.2021.126700.

[200] Y. Dong, M. Gao, W. Qiu, and Z. Song, 'Uptake of microplastics by carrots in presence of As (III): Combined toxic effects', *J. Hazard. Mater.*, vol. 411, p. 125055, Jun. 2021, doi: 10.1016/j.jhazmat.2021.125055.

[201] T.-R. Zhang *et al.*, 'Uptake and Translocation of Styrene Maleic Anhydride Nanoparticles in Murraya exotica Plants As Revealed by Noninvasive, Real-Time Optical Bioimaging', *Environ. Sci. Technol.*, vol. 53, no. 3, pp. 1471–1481, Feb. 2019, doi: 10.1021/acs.est.8b05689.

[202] H. Sun, C. Lei, J. Xu, and R. Li, 'Foliar uptake and leaf-to-root translocation of nanoplastics with different coating charge in maize plants', *J. Hazard. Mater.*, vol. 416, p. 125854, Aug. 2021, doi: 10.1016/j.jhazmat.2021.125854.

[203] Z. Yu, X. Xu, L. Guo, R. Jin, and Y. Lu, 'Uptake and transport of micro/nanoplastics in terrestrial plants: Detection, mechanisms, and influencing factors', *Sci. Total Environ.*, vol. 907, p. 168155, Jan. 2024, doi: 10.1016/j.scitotenv.2023.168155.

[204] D. Kim *et al.*, 'Translocation and chronic effects of microplastics on pea plants (Pisum sativum) in copper-contaminated soil', *J. Hazard. Mater.*, vol. 436, p. 129194, Aug. 2022, doi: 10.1016/j.jhazmat.2022.129194.

[205] Y. Liu, R. Guo, S. Zhang, Y. Sun, and F. Wang, 'Uptake and translocation of nano/microplastics by rice seedlings: Evidence from a hydroponic experiment', *J. Hazard. Mater.*, vol. 421, p. 126700, Jan. 2022, doi: 10.1016/j.jhazmat.2021.126700.

[206] S. E. Taylor *et al.*, 'Polystyrene nano- and microplastic accumulation at Arabidopsis and wheat root cap cells, but no evidence for uptake into roots', *Environ. Sci. Nano*, vol. 7, no. 7, pp. 1942–1953, 2020, doi: 10.1039/D0EN00309C.

[207] V. Bandmann, J. D. Müller, T. Köhler, and U. Homann, 'Uptake of fluorescent nano beads into BY2-cells involves clathrin-dependent and clathrin-independent endocytosis', *FEBS Lett.*, vol. 586, no. 20, pp. 3626–3632, Oct. 2012, doi: 10.1016/j.febslet.2012.08.008.

[208] L. Giorgetti *et al.*, 'Exploring the interaction between polystyrene nanoplastics and Allium cepa during germination: Internalization in root cells, induction of toxicity and oxidative stress', *Plant Physiol. Biochem.*, vol. 149, pp. 170–177, Apr. 2020, doi: 10.1016/j.plaphy.2020.02.014.

[209] S. E. Taylor *et al.*, 'Polystyrene nano- and microplastic accumulation at Arabidopsis and wheat root cap cells, but no evidence for uptake into roots', *Environ. Sci. Nano*, vol. 7, no. 7, pp. 1942–1953, 2020, doi: 10.1039/D0EN00309C.

[210] A. E. P. del Real *et al.*, 'Assessing implications of nanoplastics exposure to plants with advanced nanometrology techniques', *J. Hazard. Mater.*, vol. 430, p. 128356, May 2022, doi: 10.1016/j.jhazmat.2022.128356.

[211] W. Li, Y. Luo, and X. Pan, 'Identification and Characterization Methods for Microplastics Basing on Spatial Imaging in Micro-/Nanoscales', in *Microplastics in Terrestrial Environments: Emerging Contaminants and Major Challenges*, D. He and Y. Luo, Eds., Cham: Springer International Publishing, 2020, pp. 25–37. doi: 10.1007/698_2020_446.

[212] P. Gao and G. U. Nienhaus, 'Confocal laser scanning microscopy with spatiotemporal structured illumination', *Opt. Lett.*, vol. 41, no. 6, p. 1193, Mar. 2016, doi: 10.1364/OL.41.001193.

[213] K. Vidot, C. Gaillard, C. Rivard, R. Siret, and M. Lahaye, 'Cryo-laser scanning confocal microscopy of diffusible plant compounds', *Plant Methods*, vol. 14, no. 1, p. 89, Oct. 2018, doi: 10.1186/s13007-018-0356-x.

[214] P. Xi, Y. Liu, and Q. Ren, 'Scanning and Image Reconstruction Techniques in Confocal Laser Scanning Microscopy', in *Laser Scanning, Theory and Applications*, IntechOpen, 2011. doi: 10.5772/14545.

[215] L. Donaldson, 'Autofluorescence in Plants', *Molecules*, vol. 25, no. 10, Art. no. 10, Jan. 2020, doi: 10.3390/molecules25102393.

[216] P. Deore, S. J. T. M. Ching, D. R. Brumley, M. J. H. van Oppen, E. Hinde, and L. L. Blackall, 'Cutting through host autofluorescence: fluorescence lifetime imaging microscopy for visualising intracellular bacteria in Symbiodiniaceae'. bioRxiv, p. 2024.01.16.575970, Jan. 18, 2024. doi: 10.1101/2024.01.16.575970.

[217] M. J. Huber *et al.*, 'Physicochemical characterization and quantification of nanoplastics: applicability, limitations and complementarity of batch and fractionation methods', *Anal. Bioanal. Chem.*, vol. 415, no. 15, pp. 3007–3031, Jun. 2023, doi: 10.1007/s00216-023-04689-5.

[218] M. R. Karimi Estahbanati, S. Rostami, M. Ghasemian, M. Kiendrebeogo, P. Drogui, and R. D. Tyagi, 'Chapter 5 - Quantitative and qualitative identification, characterization, and analysis of microplastics and nanoplastics in water', in *Current Developments in Biotechnology and Bioengineering*, R. D. Tyagi, A. Pandey, P.

Drogui, B. Yadav, and S. Pilli, Eds., Elsevier, 2023, pp. 99–123. doi: 10.1016/B978-0-323-99908-3.00020-8.

[219] B. C. Keys *et al.*, 'New Methods for the Quantification of Ingested Nano- and Ultrafine Plastics in Seabirds', *Environ. Sci. Technol.*, vol. 57, no. 1, pp. 310–320, Jan. 2023, doi: 10.1021/acs.est.2c06973.

[220] P. Wu *et al.*, 'Determination of Environmental Micro(Nano)Plastics by Matrix-Assisted Laser Desorption/Ionization–Time-of-Flight Mass Spectrometry', *Anal. Chem.*, vol. 92, no. 21, pp. 14346–14356, Nov. 2020, doi: 10.1021/acs.analchem.0c01928.

[221] C. E. Enyoh *et al.*, 'New Analytical Approaches for Effective Quantification and Identification of Nanoplastics in Environmental Samples', *Processes*, vol. 9, no. 11, Art. no. 11, Nov. 2021, doi: 10.3390/pr9112086.

[222] R. Molenaar, S. Chatterjee, B. Kamphuis, I. M. J. Segers-Nolten, M. M. A. E. Claessens, and C. Blum, 'Nanoplastic sizes and numbers: quantification by single particle tracking', *Environ. Sci. Nano*, vol. 8, no. 3, pp. 723–730, Mar. 2021, doi: 10.1039/D0EN00951B.

[223] Y. Lai *et al.*, 'Counting Nanoplastics in Environmental Waters by Single Particle Inductively Coupled Plasma Mass Spectroscopy after Cloud-Point Extraction and In Situ Labeling of Gold Nanoparticles', *Environ. Sci. Technol.*, vol. 55, no. 8, pp. 4783–4791, Apr. 2021, doi: 10.1021/acs.est.0c06839.

[224] Y. Dan, W. Zhang, R. Xue, X. Ma, C. Stephan, and H. Shi, 'Characterization of Gold Nanoparticle Uptake by Tomato Plants Using Enzymatic Extraction Followed by Single-Particle Inductively Coupled Plasma–Mass Spectrometry Analysis', *Environ. Sci. Technol.*, vol. 49, no. 5, pp. 3007–3014, Mar. 2015, doi: 10.1021/es506179e.

[225] A. A. Keller, Y. Huang, and J. Nelson, 'Detection of nanoparticles in edible plant tissues exposed to nano-copper using single-particle ICP-MS', *J. Nanoparticle Res.*, vol. 20, no. 4, p. 101, Apr. 2018, doi: 10.1007/s11051-018-4192-8.

[226] X.-X. Zhou *et al.*, 'Quantitative Analysis of Polystyrene and Poly(methyl methacrylate) Nanoplastics in Tissues of Aquatic Animals', *Environ. Sci. Technol.*, vol. 55, no. 5, pp. 3032–3040, Mar. 2021, doi: 10.1021/acs.est.0c08374.

[227] B. Nguyen, D. Claveau-Mallet, L. M. Hernandez, E. G. Xu, J. M. Farner, and N. Tufenkji, 'Separation and Analysis of Microplastics and Nanoplastics in Complex Environmental Samples', *Acc. Chem. Res.*, vol. 52, no. 4, pp. 858–866, Apr. 2019, doi: 10.1021/acs.accounts.8b00602.

[228] J. Schindelin *et al.*, 'Fiji: an open-source platform for biological-image analysis', *Nat. Methods*, vol. 9, no. 7, Art. no. 7, Jul. 2012, doi: 10.1038/nmeth.2019.

[229] C. Souchier, C. Brisson, B. Batteux, M. Robert-Nicoud, and P.-A. Bryon, 'Data reproducibility in fluorescence image analysis', *Methods Cell Sci.*, vol. 25, no. 3, pp. 195–200, Jan. 2004, doi: 10.1007/s11022-004-2383-4.

Bibliography

Publications related to the thesis

Sahai, H., García Valverde, M., Murcia Morales, M., Hernando, M. D., Aguilera del Real, A. M., & Fernández- Alba, A. (2023). Exploring sorption of pesticides and PAHs in microplastics derived from plastic mulch films used in modern agriculture. *Chemosphere*, *333*, 138959. https://doi.org/10.1016/j.chemosphere.2023.138959

Sahai, H., Hernando, M. D., Martínez Bueno, M. J., Aguilera del Real, A. M., & Fernández- Alba, A. R. (2024). Evaluation of the sorption/desorption processes of pesticides in biodegradable mulch films used in agriculture. *Chemosphere*, *351*, 141183. https://doi.org/10.1016/j.chemosphere.2024.141183

Sahai, H., Bueno, M. J. M., Del Mar Gómez-Ramos, M., Fernández-Alba, A. R., & Hernando, M. D. (2024). Quantification of nanoplastic uptake and distribution in the root, stem and leaves of the edible herb *Lepidium sativum*. *Science of The Total Environment*, *912*, 168903. https://doi.org/10.1016/j.scitotenv.2023.168903

Biography

Short Biography

The candidate, Harshit Sahai, obtained his Bachelor of Science in Life Sciences from the University of Lucknow in 2018 and a Master of Science in Environmental Studies from the University of Delhi in 2020. Since then, he has been a doctoral candidate in the Ecotechnologies program at the Josef Stefan International Postgraduate School in Ljubljana, Slovenia. Harshit has held several notable research positions, including a Pre-Doctoral Marie Curie Researcher at the CSIC-EEZA in Spain, a researcher on Secondment at the Jožef Stefan Institute, and the European Union Reference Laboratory for Pesticide Residues in Fruit & Vegetables. He has been actively involved in the MSCA-ITN FoodTraNet project, focusing on microplastics in water and their reuse in crops, funded by the European Union's Horizon 2020 program. Harshit has presented his research at numerous international conferences and has been recognized with several awards, including the Marie-Curie PhD Fellowship and the Best Presentation Award at the XVII Maratón Científico held at CSIC-EEZA. Through his research and professional development, Harshit Sahai remains committed to advancing the understanding of environmental contaminants and their impacts.

Long biography

Education and Academic Background

2015-2018: Bachelor of Science in Life Sciences at the University of Lucknow
2018-2020: Master of Science in Environmental Studies from the University of Delhi

2021-present: PhD candidate at the Josef Stefan International Postgraduate School in Ljubljana, Slovenia, within the Ecotechnologies program.

Thesis title: Micro and Nano Plastics in Agriculture: Interactions with Pesticide Residues and Bioaccumulation in Plants

Professional Experience

The candidate has accumulated extensive research experience through the following positions:

- **Pre-Doctoral Marie Curie Researcher** at the Experimental Station of Arid Zones, Spanish National Research Council (CSIC-EEZA) in Almería, Spain (2023 – present).

- **Researcher on Secondment** at the Jožef Stefan Institute in Ljubljana, Slovenia (June – July 2024).
- **Non-Academic Researcher Secondment** at Labcolor - Coexphal, Almería, Spain (April – May 2024), where they received training in mass spectrometry-based analytical techniques for routine analysis of contaminants in fruits and vegetables.
- **Researcher on Secondment** at the European Union Reference Laboratory for Pesticide Residues in Fruit & Vegetables (EURL-FV) in Almería, Spain (January – July 2022).
- **Pre-Doctoral Marie Curie Researcher** at the National Institute for Agricultural and Food Research and Technology, Spanish National Research Council (CSIC-INIA) in Madrid, Spain (December 2021 – December 2022).
- **Project Linked Person** at the Indian Statistical Institute, North-East Centre in Tezpur, Assam, India (December 2020 – August 2021).

Research and Projects

The candidate has been actively involved in the MSCA-ITN FoodTraNet project, focusing on the alternative exploitation of waste, specifically microplastics in water and their reuse in crops. This project has been funded by the European Union's Horizon 2020 research and innovation program under the Marie Sklodowska-Curie grant agreement no. 956265.

Previous projects include an assessment of atmospheric particulate matter (PM2.5) and associated elemental carbon, organic carbon, and water-soluble organic carbon in Tezpur, Assam, India.

Awards and Recognitions

The candidate's dedication to research has been recognized through several awards:

- **Best Poster Presentation Award** at the 5th International Conference on Risk Assessment of Pharmaceuticals in Environment held on 24th – 25th June 2024 at Anacapri (NA).
- **Best Presentation Award** at the XVII Maratón Científico in December 2023 for their presentation on the uptake and bioaccumulation of nano-plastics in plants.
- **Marie-Curie PhD Fellowship** under the European Union H2020 Programme (2021).
- **GATE 2020** qualification from the Indian Institute of Technology, Delhi.
- **UGC-NET/JRF Exam** qualification from the University Grants Commission, India (June 2020).

Conferences and Presentations

During his research, the candidate actively participated in numerous conferences and seminars, presenting his findings on nanoplastics, organic microcontaminants, and microplastic pollution. Notable presentations include:

- Poster presentation at the 5th International Conference on Risk Assessment of Pharmaceuticals in Environment held on 24th – 25th June 2024 at Anacapri (NA).
- Poster presentations at the SETAC Europe 34th Annual Meeting in Seville, Spain (May 2024)

- Oral presentation at the XVII Maratón Científico in Almería, Spain (December 2023)
- Participation in the European Researchers' Night 2023 in Almería, Spain.
- Poster presentation at the UNESCO-EU-H2020 LIMNOPLAST Conference in Paris, France (March 2023)
- Poster presentation at the 12th Micropol and Ecohazard Conference in Santiago de Compostela, Spain (June 2022)
- Presentations at various national and international conferences in India

Training and Professional Development

In addition to his research, the candidate also participated in the following advanced training programs:

- Winter School on "Advanced Solutions in Food Production and Safety" at the Aristotle University of Thessaloniki, Greece (March 2024)
- Summer School on food quality, authenticity, and traceability in Trento, Italy (June 2022), and the Summer School on advanced solutions in food production and safety in Almería, Spain (June 2023)

Committed to advancing the understanding of environmental contaminants and their impacts, Harshit Sahai continues to contribute to environmental science through his research and active participation in the scientific community.